Silver complexes having potential as precursors for metal film deposition

Ogrodnik, Virginie

Award date:
1998

Awarding institution:
University of Bath

SILVER COMPLEXES HAVING POTENTIAL AS PRECURSORS FOR METAL FILM DEPOSITION.

Submitted by Virginie Ogrodnik

For the degree of PhD
of the University of Bath
1998

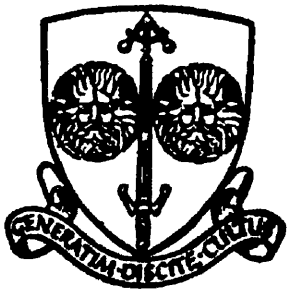

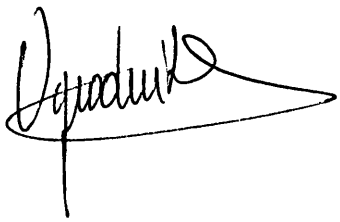

ProQuest LLC
789 East Eisenhower Parkway
P.O. Box 1346
Ann Arbor, MI 48106-1346

Dedication

To my mother and my grandparents

ABSTRACT

The work described in this thesis involves the synthesis and characterisation of three different groups of compounds that have been investigated as precursors for the Chemical Vapour Deposition (CVD) of silver films. The classes of precursors described are (a) unsaturated silver(I) carboxylates and their adducts, (b) silver(I) alkoxides and aryloxides and their triphenylphosphine adducts and (c) silver(I) complexes containing sulfur ligands.

Compounds from all three different classes have been synthesised and characterised by micro-analysis, infrared, ^{1}H, ^{13}C and ^{31}P NMR spectroscopy. Mass spectrometry (ES and FAB) and thermogravimetric analysis (TGA) studies have also been carried out on selected compounds.

For each class, several compounds have been tested as silver CVD precursors using aerosol-assisted methodology. The resulting films have been characterised by EDXS, SEM, reflectivity and conductivity measurements. A nucleation study has also been carried out for the compounds $[Ag\{O_2C(CH_3)C{=}CHCH_3\}(PPh_3)_2]$ and $[Ag\{O_2C(CH_2)_2CH{=}CH_2\}(PPh_3)_2]$.

The structure of $[Ag\{O_2C(CH_3)C{=}CHCH_3\}]$ as determined by XRD is also described. The polymeric structure of silver(I) tiglate is based on bis(carboxylato-O,O') dimers. The silver atoms of the asymmetric unit are included in eight-membered $(Ag\text{-}O\text{-}C\text{-}O)_2$ rings. The overall geometry around each silver atom is distorted octahedral, the crystal structure showing in addition (a) an intermolecular interaction between the silver atom and the vinyl moiety of the residue, and (b) another interaction between Ag(1) and O(2) of the adjacent $(Ag\text{-}O\text{-}C\text{-}O)_2$ unit.

The structures of $[Ag(O_2CCH_2CN)(PPh_3)_2]$, $[Ag\{O_2C(CH_2)_2CH{=}CH_2\}(PPh_3)_2]$ and $[Ag\{O_2C(CH_3)C{=}CHCH_3\}(PPh_3)_2]$ have been determined. All complexes form monomers with a bidentate carboxylate group and two triphenylphosphine ligands in which the silver atom has a distorted tetrahedral arrangement.

The crystal structure of $[Ag(OC_6H_4CH_3\text{-}2)(PPh_3)_3]\cdot[2\text{-}CH_3C_6H_4OH]$ has been characterised by X-ray crystallography. The asymmetric unit in this crystal structure contains one molecule of (o-cresolato-O)*tris*(triphenylphosphine)silver(I), one molecule of o-cresol and one disordered toluene solvent molecule. The silver atom is bonded to the

oxygen of the o-cresolato ligand and to three phosphorus atoms from the triphenylphosphine ligands, giving a distorted tetrahedral arrangement. The additional o-cresol molecule in the lattice is strongly hydrogen-bonded to the coordinated cresolate anion.

The crystal structure of $[Ag(SOCCH_3)(PPh_3)]_4 \cdot 2CH_2Cl_2$ has been characterised by X-ray crystallography. The structure consists of a discrete eight-membered ring of alternating Ag and S atoms, Ag_4S_4, arranged as a chair or a step structure. The sulfur atoms act as bridging ligands. The silver atoms are bonded to two sulfurs from monothioacetate groups and to one phosphorus atom from a triphenylphosphine ligand giving a distorted trigonal geometry.

A brief conclusion summarises the comparisons between the three groups of compounds studied and includes some suggestions for further work. Appendices provide information regarding the starting materials, instrumentation, crystallographic data and details of the CVD reactor.

ACKNOWLEDGEMENTS

I would like to thank my supervisors Dr Dennis Edwards and Dr Kieran Molloy for their guidance throughout the project and their support during the writing of my thesis. I would like also to thank Dr Mary Mahon for the crystallographic data included in this thesis, for the time she spent teaching me crystallography (which I enjoyed very much) and also for her support during the past three years. Many thanks to Dr David Sheel, Dr Kevin Sanderson and Simon Hurst from Pilkington Plc, for their help in the CVD part of my work. Financial support from the University of Bath and Pilkington Plc is gratefully acknowledged.

I would like to thank the technical staff, Robert Stevens, Ahmed Sheibani and Sheila Osborne for their help during the laboratory work, Alan Carver for the microanalyses and to Dave Wood and Harry Hartell for assistance with NMR spectroscopy. Many thanks to Dr Glyn Love and Hugh Perrott for the EDXS and SEM analysis, the mass spectrometry service at the University of Wales, Swansea, for the mass spectrometry studies performed.

I also thank all my laboratory colleagues in particular Tim Paget, Veronica Paget, Chris Rainford, Mike Maxwell, Joanne Stanley, Dave Smith, Phil Wright, Mike Hill, Paul Williams, Anthony Swain, Tom Hibbert, Claire Beddows and Harish Patel, who made my time enjoyable.

I would like to thank my family for all the support and encouragement throughout the last three years. Special thanks to my mother, grandparents, Angélique, Romain and Claude for their support and belief in my ability to succeed. I also want to thank Marielle and Christian Buche for their support during the past few years. Finally, I would like to thank Silvain Buche, my partner, for his support, patience and encouragements throughout this work.

ABBREVIATIONS

2,2'-bipy = 2,2'-bipyridine

AES = Auger Electron Microscopy

br = Broad

CVD = Chemical Vapour Deposition

d = Doublet

dd = Doublet of doublets

DMF = Dimethylformamide

DMSO = Dimethylsulfoxide

EDX = Energy Dispersive X-ray

Et = Ethyl

IPA = Isopropyl alcohol

IR = Infrared

ITO = Indium Tin Oxide

m = Medium

Me = Methyl

MOCVD = Metal Organic Chemical Vapour Deposition

NMR = Nuclear Magnetic Resonance

Ph = Phenyl

PMe_3 = Trimethylphosphine

PPh_3 = Triphenylphosphine

ppm = Parts per million

py = Pyridine

s = Singlet

s = Strong

t-Bu = Tertiary Butyl

THF = Tetrahydrofuran

w = Weak

XRD = X-ray Diffraction

CONTENTS

Chapter One

Introduction

1.1 APPLICATIONS OF SILVER FILMS.

Silver films have useful properties such as very high reflectivities and high conductivities. Depending on the properties, silver films have a wide range of industrial applications. (Fig. 1.1)

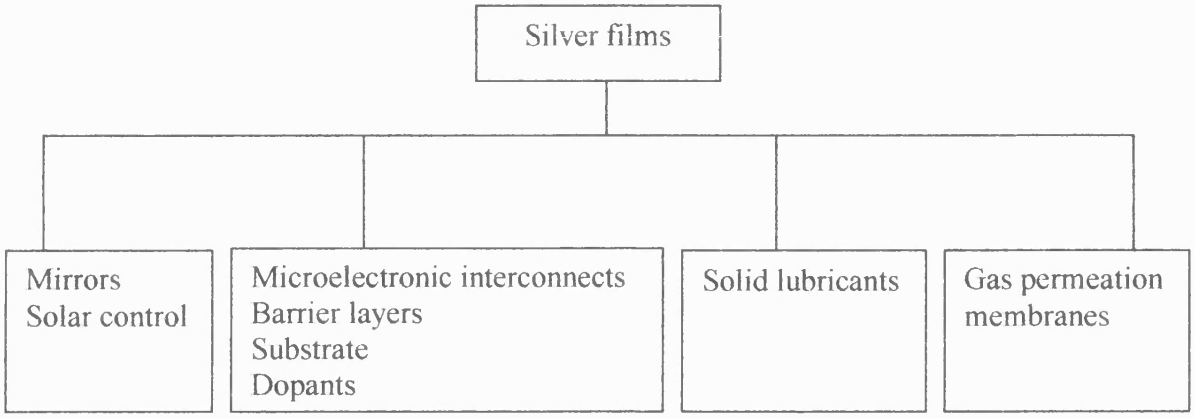

Figure 1.1 Applications of silver films.

1.1.1 Optical properties.

Because of its high reflectivity (97% between 250-2500 nm in the range of the solar spectrum), silver is a metal of choice for a reflecting material.

Silver films have been used in the fabrication of mirrors.[1] There are three different techniques used to produce silver mirrors. These are chemical reduction, electroless plating and electrodeposition.[2,3]

In the chemical reduction technique, the substrate is in direct contact with a silver salt and the reducing agent (sucrose, hydrazine, formaldehyde or sodium potassium tartrate commonly called Rochelle salt). Reduction of the silver salt to silver metal occurs resulting in a thin film on the substrate.

The electroless plating technique also involves chemical reduction of metal salts. The metal salt and the reducing agent react to deposit a metal film on catalytic sites of the substrate, which then serves as a catalyst to ensure the growth of the metal film.

The electrodeposition technique is a process where a potential is applied across a solution containing a silver salt. The metal film is deposited on the cathode. The rate of deposition is directly proportional to the current that passes through the solution.

Unfortunately, by using these techniques, mirrors degrade slowly after a few months reducing their desirable optical properties. The reflectivity can also be affected by some impurities like sulphur and chloride ion. Diffusion between component layers and delamination from the substrate also alter the mirror-like properties. Due to such problems, new processes for producing silver mirrors are of interest.

Recently there has been interest in silvered polymer films.[4,5] Because of their high reflectivity and excellent radiation resistance properties, they can be used in space or on earth as antennas and reflectors. These metallized polymeric films are made in a two-stage process. The first stage involves the preparation of the polymeric film and the second stage the deposition of the metal on the film by various techniques such as chemical vapour deposition, sputtering, electrodeposition or electroless chemical reduction.

Thin silver films have been found to have useful properties when deposited on glass substrates. The properties allow control of reflection and transmission of light from or through the glass and also permit visible light to transmit through the glass while reflecting IR radiation. Thin silver films have also found use as heat reflecting systems for automotive glazing. Special layer systems (e.g.: SnO_2/Ag/SnO_2,[6] ITO/Ag/ITO,[7] Ta_2O_5/Ni-Cr/Ag/Ni-Cr/Ta_2O_5[8,9]) have been developed which both reflect heat radiation and also have high visible transmission.

1.1.2 Microelectronic applications.

With a low resistivity (1.59μΩcm) silver has found applications in microelectronics. However, the use of silver is limited due to the rapid diffusion into silicon substrates and the tendency to be corroded easily.[10] Nevertheless Ag/Pd thick film conductors have found use in electronic packaging.[11]

Silver has also found specific applications in superconducting devices as electrical contacts, passivation barriers and as a dopant. One of the problems encountered during CVD of silver for use in superconducting devices, is the interaction between the substrate

and the superconductor. This interaction can lead to a reduction in device performance. To solve the problem, it was found that deposition of a thin silver film between the superconductor and the substrate limited interactions between the substrate and the superconductor. For superconducting wire applications silver films have found use as electrical contacts when deposited over the superconductor and as a passive barrier when deposited between the substrate and the superconductor.[12]

Silver has been found to be an attractive dopant in high T_c superconductors because it promotes crystallisation and c-axis orientation, strengthens intergranular coupling and improves surface morphology.[13] It was found that addition of silver to a superconductor increased the T_c values (T_c = critical temperature, temperature at which a pure metal or a metal alloy becomes a superconductor), reduced resistivity and increased J_c values (J_c = critical current density). For example YBCO ($YBa_2Cu_3O_{7-x}$) with 10% silver decreased resistivity (1.5mΩ) and increased T_c to 82 K when compared with undoped films (resistivity: 60mΩ, and T_c<50 K).[14] Other superconducting materials such as TBCCO (Tl-Ba-Ca-Cu-O)[15,16], BSCCO (Bi-Sr-Ca-Cu-O)[17] and BPSCCO (Bi-Pb-Sr-Ca-Cu-O)[18] have been doped with silver.

The purity of silver films in microelectronic applications is very important. Contamination by, for example, phosphorus or sulfur may affect the properties because oxidation to phosphate or sulphate will affect the superconductivity.

1.1.3 Other applications.

Soft metal films (including silver) are ideal solid lubricants where liquid-based systems cannot be used. They have low shear strength, high chemical inertness, good lubricity, high thermal conductivity and a moderately high melting point (962°C for silver). For example silver-alkaline earth metal fluoride composites can act as lubricants from room temperature to 900°C.[1] Silver films are used as lubricants in advanced transport systems, heat engines and space technology where in air or vacuum, high temperatures are involved. They are especially used at high temperature in air because they do not form oxides and are much softer under these conditions.

Surface qualities, porosity, tribological properties (wear and friction), and substrate adhesion, are important properties for the application of silver films as lubricants. Under severe conditions and high temperature, metal films may fail by oxidation of the substrate base metal through holes in the thin noble metal film followed by eventual spalling off of the film. Film adhesion may be increased by the use of ion bombardment during deposition or by the use of intermediate bond layers such as Cu, Cr or Ti.[1] Silver films have been grown by ion beam assisted deposition, sputtering and laser surface cladding.[1]

Silver is known to be more permeable to oxygen than to other gases and this has led to studies of silver as a gas permeable membrane.[19] Oxygen transport through silver is thought to proceed normally by the following sequence:

- Dissociative adsorption of molecular O_2 at the upstream surface.
- Dissolution of the atomic O into the bulk.
- Migration of the atoms between octahedral sites of the metal lattice.
- Arrival at the vacuum interface downstream where recombination to O_2 occurs with subsequent desorption to the gas phase.

Direct current glow discharge technology is known to increase the transfer rate of O_2.

Hydrogen separation has also been achieved using a Pd/Ag alloy membrane on a porous alumina tube support.[20] Reducing film thickness increases the permeation rate. A spray pyrolysis technique has been used to grow such films and it was shown that reducing film thickness increases the permeation rate.[20]

1.2 METHODS OF FILM DEPOSITION.

There are several processes like PVD (Physical Vapour Deposition), CVD, wet chemical or electrodeposition, which have been developed to apply silver to a substrate. Due to the nature of the work described in this thesis only Chemical Vapour Deposition (CVD) will be discussed in detail and other methods will be briefly mentioned.

1.2.1 Chemical Vapour Deposition.

CVD is a chemical decomposition process, which takes place in gas phase near the substrate or on the substrate so that a reaction product is deposited onto the substrate. The major requirement is for a volatile precursor, which decomposes after transport to a reaction zone where deposition occurs. The decomposition may be a fundamental breakdown process leading to a metal or metal oxide but may involve oxidation, reduction, hydrolysis or disproportionation.

The CVD technique dates from 1880 in the production of carbon filaments for the incandescent lamp industry.[21] Since then many metal-containing molecules have been used for CVD. Chemical vapour deposition has become an important deposition technique and has found a wide range of applications. A large number of reviews in the literature explain the process in detail.[3,10,21-24] However there are a few fundamental steps involved in a CVD process irrespective of the nature of the film being deposited (Fig. 1.2):

i. *Transport of the precursor into the reactor.*
ii. *Gas phase reactions leading to film formation and by-products.*
iii. *Transport of the precursor to the substrate surface where adsorption occurs.*
iv. *Reaction of the adsorbed species on the substrate.*
v. *Surface diffusion of the adsorbed species.*
vi. *Nucleation and growth of the film.*
vii. *Desorption of by-products.*
viii. *Mass transport of by-products out of the reactor.*

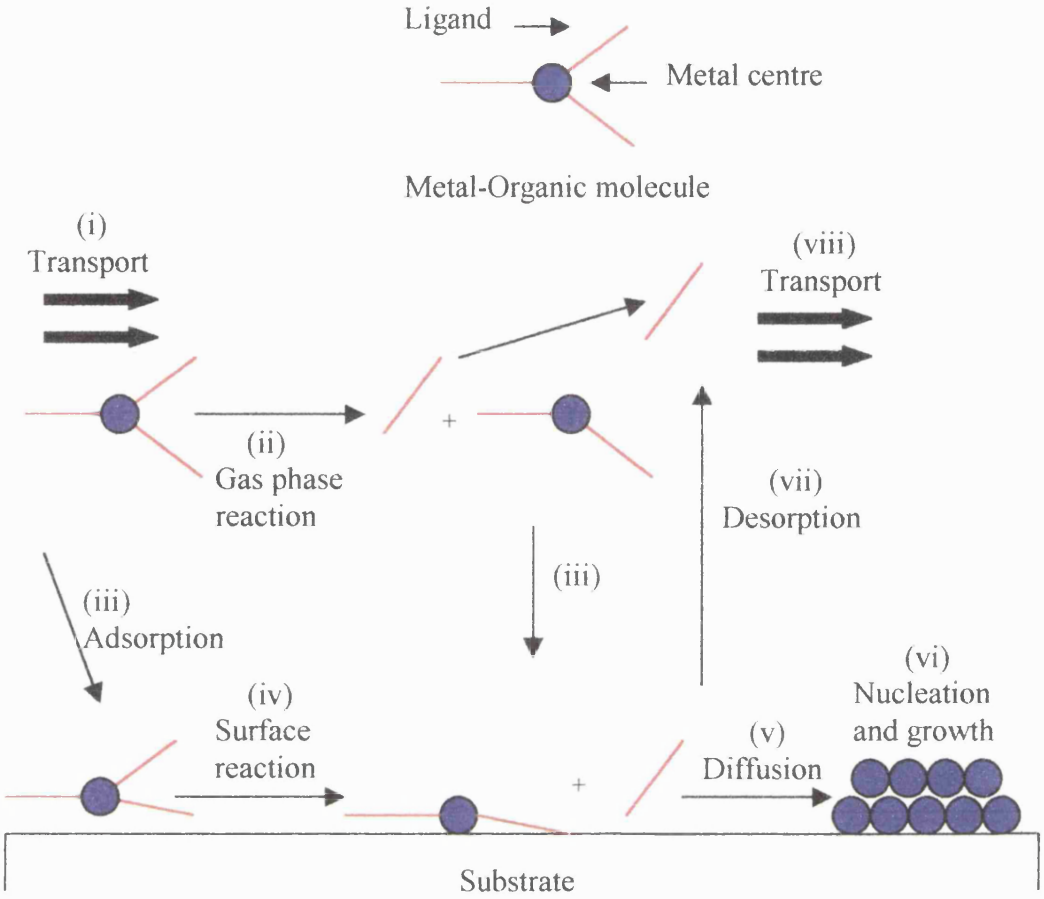

Figure 1.2 Key steps involved in CVD.[23]

Gas phase transport rates and surface reaction rates are important factors for CVD because they can be rate limiting. If the temperature of the substrate is high enough, the surface reaction rate will be faster than the rate at which the material is delivered. This leads to a mass-transport limiting process. Conversely, if the mass-transport is fast then the deposition rate is limited by the surface reaction rate. In this case it is feed rate limited. Mass transport and feed rate limiting conditions are independent of the temperature and are dependent on factors such as the delivery system and gas flow rates whereas in the surface reaction process, the rate increases exponentially with temperature according to the Arrhenius relationship.[10]

Gas-phase reactions can influence the growth and the quality of the film. It is important that the precursor does not decompose in such a manner as to give additional species, which can contaminate the film.[10]

To be useful, a CVD process must produce thin films with reproducible and controllable properties including purity, composition, thickness, adhesion, microstructure and surface morphology.

1.2.2 Film growth mechanisms.

Film growth takes place when the precursor is adsorbed on the surface of a substrate and then diffuses to a growth site. The growth mode is dependent on the nature of the interaction between the growing film and the substrate, the thermodynamics of adsorption, the kinetics of crystal growth and the substrate temperature.[21]

The growth of metal-containing films on a surface follows one of three classical modes (A, B, C) each of which are illustrated in Figure 1.3.[21] They are:

(A) The layer or Francke –van der Merwe growth (Fig.1.3.A). A complete monolayer is formed on the substrate with the deposited atoms more strongly bonded to the substrate than to each other. This monolayer is then covered by further layers. This growth is referred to as simultaneous multilayer growth and its occurrence depends on the relative rates of nucleation and growth of the deposition.

(B) The layer plus-island or Stranski-Krastanov growth mode (Fig. 1.3.B). Initially a layer type growth occurs but after several layers have been deposited continued layer growth is unfavourable and islands are formed on the previously deposited layers.

(C) The island or Volmer-Weber growth mode (Fig. 1.3.C). Small droplets or clusters initially nucleate on the substrate to form islands and subsequent growth occurs on these island sites, the islands subsequently coalescing to give a film. This growth mode occurs when the depositing atoms bind more strongly to each other than to the substrate.

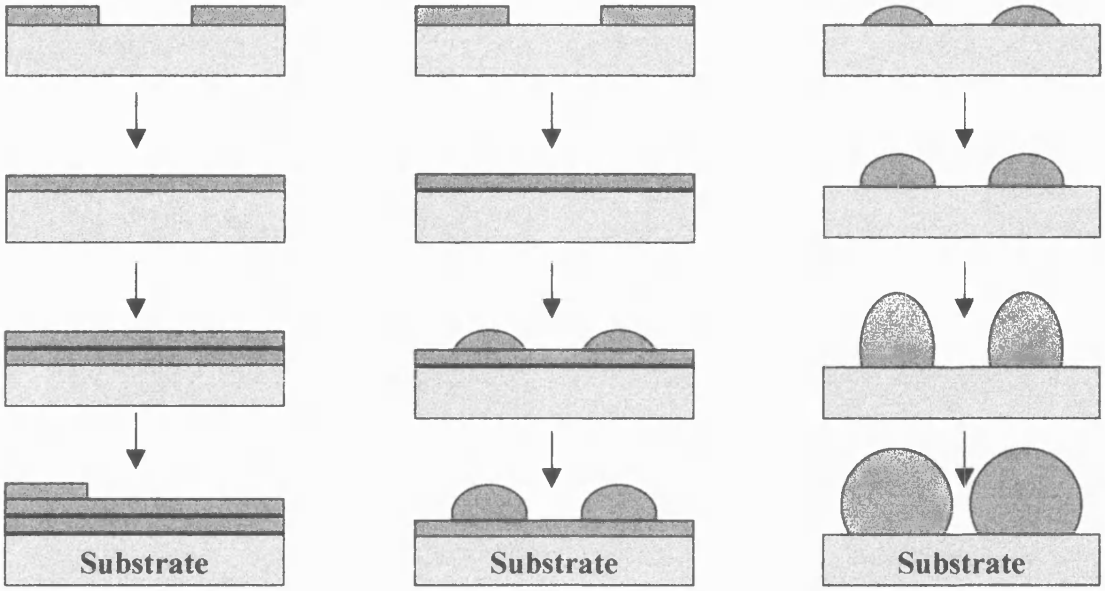

Figure 1.3 Modes of film growth.[21]

1.2.3 Reactor design.

Design of the CVD reactor is very important because it can affect the nature and the quality of the material deposited. They are two general types of reactors (a) hot wall reactors and (b) cold wall reactors.[23]

Hot wall reactors use an external heat source, which surrounds the reaction chamber, and cold wall reactors maintain the reactor walls at cool temperatures.

Hot wall reactors are simple to use, they can operate at different ranges of temperature and pressure and can accommodate several substrates. The major problem with hot wall reactors is that deposition not only occurs on the substrate but also on the walls. These deposits can fall and contaminate the film or the substrate. The consumption of precursor is extensive due to a large deposition area.

In cold wall reactors deposition is much more controlled. However they are much more sensitive to secondary-flow effects and turbulence than hot wall reactors.

1.2.4 Advantages of CVD.

CVD has a number of advantages in depositing thin films when compared to other techniques. These advantages include:

- Conformal coverage, i.e. the ability to coat a surface with a uniform thickness.
- Selective deposition, i.e. the ability to deposit a coating on a specific area.
- Low deposition temperatures, which is important for thermally sensitive substrates.
- High deposition rates.
- Formation of high purity materials.
- Facility of large-scale production.
- Low cost.

1.2.5 Precursor design.

Choosing a precursor is very important. The choice usually depends on the particular applications. The most important precursor qualities can be summarised as follows:[23]

- High vapour pressure, i.e. to achieve high transport rate.
- Careful precursor design, i.e. to control the surface reaction of the precursor to give high purity films.
- Thermally inert precursors at the delivery temperature, i.e. to avoid premature decomposition.
- Liquid precursors, i.e. to reproduce delivery rates if standard delivery methods are used.

1.2.6 Other deposition techniques.

Chemical Vapour Deposition has been an area of great interest for depositing thin films for copper and gold but only a few reports on silver CVD have been reported. The major problem for silver CVD is the lack of stable, volatile silver complexes. However there are a number of alternative techniques available for the deposition of silver thin films. The methods mentioned below are the most common.

1.2.6.1 Physical Vapour Deposition (PVD).

PVD of silver is a relatively well-developed method of deposition. PVD can be achieved by evaporation[25] or sputtering.[26,27]

In the evaporation process the bulk metal is heated by an electron beam or by induction under high vacuum giving metal vapour, which then condenses to give a film.

In the sputtering process, the surface atoms of the material are bombarded by high-energy ions created from a glow discharge. The sputtered atoms are then transported to the substrate surface where they condense to form a film.

Unfortunately this technique cannot produce films with a uniform thickness.

1.2.6.2 Laser Assisted Chemical Vapour Deposition (LACVD).[28]

The precursor is transported to an evacuated cell containing the substrate. The substrate is illuminated with a focused laser beam resulting in deposition. By using UV light between 250-350 nm the precursor undergoes photolysis in the gas phase and on the substrate surface. By using UV light between 475-525 nm or IR radiation of 10.6 μm, the substrate is heated to a temperature sufficient to pyrolyse the precursor. By moving the laser, fine lines can be written directly on to the substrate, thus allowing selective area deposition. As a potentially low temperature process, substrates sensitive to high temperatures may be used. This technique has potential applications in the microelectronics industry. It can be used to repair interconnects on integrated circuits. LACVD of gold for circuit repair has already been used in industry.[29]

1.2.6.3 Plasma Enhanced Chemical Vapour Deposition (PECVD).[30]

PECVD is also a low temperature deposition method. It operates at around 200-300°C or below. A glow discharge produces high-energy electrons in the vapour above the substrate. These high-energy electrons collide with the precursor molecules to produce active radical and ionic species. Another effect of the glow discharge is to bathe the substrate in a flux of high-energy particles, having the effect of radically altering the surface chemistry as the deposition proceeds. Because of this, films grown by this technique have different properties to those grown by conventional CVD. High growth

rates can be obtained using the PECVD technique. However pure films are difficult to obtain due to the slow desorption of the by-products and hence the presence of impurities.

1.2.6.4 Low Pressure Chemical Vapour Deposition (LPCVD).

The difference between thermal CVD and LPCVD is that for the latter the total pressure in the system is decreased. With this technique, quite involatile precursors having low partial pressures may be used. As a result, diffusion of precursor to the surface becomes much easier. Growth rates are limited by the rate of surface reaction rather than by the mass transport. Desorption of by-products is much easier. Films have improved uniform thickness and properties, better step coverage and conformality and superior structural integrity. Thin films of palladium have been grown using the LPCVD technique.[31]

1.2.6.5 Aerosol Assisted Chemical Vapour Deposition (AACVD).

Very often, metal-containing precursors having low volatility and low thermal stability produce poor quality films by conventional CVD. Therefore a number of alternative precursor transport methods have been developed. They include liquid delivery, supercritical fluid transport (SCT) CVD, spray-metal organic (MO) CVD and aerosol assisted (AA) CVD.[32]

Aerosol delivery requires the precursor to be soluble in a solvent that does not decompose on the substrate during deposition of the film. The process involves a number of steps (Fig. 1.4):

i. *The precursor is dissolved in a solvent.*

ii. *It passes through an aerosol generator to form micro-sized aerosol droplets.*

iii. *These droplets evaporate partially or completely to give the precursor and solvent vapours.*

iv. *These vapours or aerosol droplets are transported to the substrate.*

v. *Adsorption and surface reaction occur with formation of the film and removal of volatile by-products.*

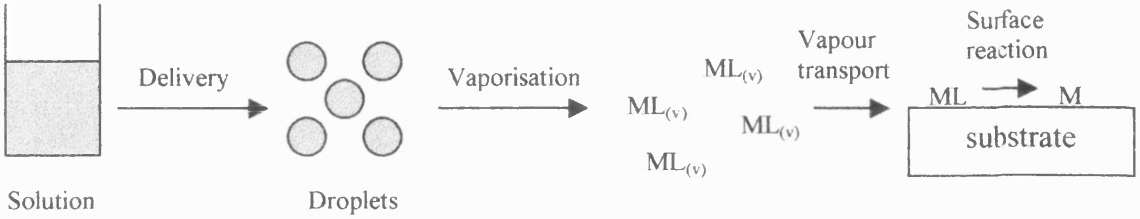

Figure 1.4 Key steps involved in AACVD.

AACVD has several advantages. They are:

- High mass transport rate and therefore high deposition rate.
- Precursors need not be highly volatile or be of high thermal stability.
- Reproducible films can be produced.

AACVD should be distinguished from spray pyrolysis where the precursor dissolved in a solvent is sprayed onto the heated substrate. In this case solvent evaporation and reaction occur on the surface whereas in AACVD gas phase molecules are responsible for the deposition.

There are different methods of nebulisation i.e. formation of the aerosol. Examples include: the pneumatic jet nebulisation, which uses a gas stream to atomise the solution into an aerosol, the electrospray technique which uses an electrostatic field to produce droplets and ultrasonic nebulisation which uses a piezoelectric transducer vibrating at high frequencies to atomise the solution. The latter has been used for this study and will therefore be discussed later.

A large amount of work has been carried out with aerosols for the generation of advanced materials.[33] However, only a few papers have reported the use of AACVD for copper[34] and silver alloys.[32,35,36] Recently, thin films of gallium sulfide,[37] zinc sulfide,[38] cadmium sulfide,[38] zinc-cadmium sulfide,[38,39] and zinc-cadmium sulfide:manganese[39] have been deposited using AACVD technology.

1.3 SURVEY OF THIN SILVER FILMS.

Silver film precursors can be classified into four different groups: silver(I) halides, silver(I) carboxylates, silver(I) β-diketonates and organosilver compounds. Silver(I) halides are known to be non-volatile and organometallic silver compounds are light, air and moisture sensitive and have a low thermal stability. Nevertheless both types have been explored as silver CVD precursors.

1.3.1 Silver(I) halides.

Deposition of silver from silver(I) halides was first reported in 1972 during a study of silver(I) fluoride (AgF) vapour on silicon.[40] AgF was evaporated onto a silicon substrate from a graphite crucible at 10^{-6} Torr with a temperature ranging from 80°C to 600°C. The deposition proceeds via etching of the silicon substrate forming SiF_4. Smooth silver films, which adhered well to the substrate, were obtained.

More recently, silver(I) iodide (AgI) was tested as a potential precursor for silver films.[12] AgI was deposited on an Al_2O_3 substrate at 300-900°C in an Ar/H_2 atmosphere at 20-30 Torr using a powder feed delivery system. Smooth and continuous silver films were obtained at 800°C and 22.8 Torr. It was found that the quantity of H_2 used affected the thickness of deposited film.

1.3.2 Silver(I) carboxylates.

Silver(I) trifluoroacetate was the first precursor of this type to be tested. Two different methods were carried out. The first study was carried out in 1986 using laser assisted CVD.[41] The second study was carried out in 1992 using thermal CVD.[12] Uniform films were deposited at 600°C and 30 Torr and in a presence of H_2. XRD and AES were used to detect any impurities. Once again it was found that thickness of the film was proportional to the H_2 flow rate.

Recently, a wide range of silver(I) carboxylate and fluorocarboxylate complexes $[Ag(O_2CR)L_x]$ (RCO_2 = acetate, pivalate, mesitylate, perfluorobutyrate, perfluoroheptanoate, perfluorooctanoate. L = PPh_3 or PMe_3. x = 2 or 3) have been studied

using an Aerosol Assisted CVD (AACVD) technique.[1] The precursors were dissolved in THF. Films were grown onto glass substrates at 310°C and 750 Torr pressure in a N_2 atmosphere. It was found that precursors containing PPh_3 limited the growth rate but the resulting films had reasonable reflectivity. Precursors with PMe_3 ligands had much faster growth rates but gave poor quality films. Use of the fluorocarboxylate precursors generated films of limited quality.

1.3.3 Silver(I) β-diketonates.

Since 1992, silver(I) β-diketonates probably have been the most common CVD precursors for silver film production. They are usually represented by the formula [Ag(β-diketonate)L] where L is a neutral donor ligand such as an olefin, phosphine, isocyanide or thioether.

The first silver β-diketonate precursor was tested in 1992 by thermal CVD.[42] The precursor [Ag(hfac)(COD)] (hfac = 1,1,1,5,5,5-hexafluoroacetylacetonate, COD = 1,5-cyclooctadiene) was heated to 60°C. Films were grown at 250°C using H_2/He as carrier gas. Shiny films of high purity (>95%) were obtained. Further studies of [Ag(hfac)(alkene)] showed that sublimation was accompanied by decomposition. These complexes lose the alkene ligand at or below the sublimation temperature giving a non-volatile polymeric complex $[Ag(hfac)]_n$.

More recently, [Ag(hfac)(VTES)] (VTES = vinyltriethylsilane) was tested as a silver CVD precursor.[43] The precursor was heated to 30°C and films were grown between 160-280°C at 10^{-1} Torr on silicon(100) coated with silica substrates. Continuous silver films were obtained. AES showed the films consist mainly of silver (96%) with a trace of oxygen contamination.

New complexes such as $[Ag(hfac)(PR_3)_n]$ (R = Me or Et and n = 1 or 2) have been synthesised.[44] These compounds were found to be stable to air, moisture and light. $[Ag(hfac)(PMe_3)]$ was heated to 95°C at 5×10^{-2} Torr and films were grown at 310°C onto a glass substrate. EDX analysis showed the presence of Ag and C (5-10%) but no sign of O, F or P. $[Ag(hfac)(PEt_3)]$ was heated to 50-70°C at 5×10^{-2} Torr and films were grown onto a

glass substrate between 250-350°C. Matte or smooth mirror silver films were obtained from both precursors.

[Ag(hfac)(PMe_3)] and [Ag(hfac)(PMe_3)$_2$] were also used to grow films between 200-245°C on glass, silicon, copper, tungsten, aluminium and nickel in a presence of H_2.[45] Under vacuum (10^{-4} Torr) silver films were obtained only on the copper substrate. Less than 1% C, O and F contaminants were found in the films.

Similar experiments were carried out using [Ag(fod)L] (fod = 2,2-dimethyl-6,6,7,7,8,8,8-heptafluorocta-3,5-dionate and L = PMe_3 or PEt_3).[46] Poor quality films were obtained at 370-380°C and 10^{-4} Torr. High levels of impurities of C, O, P and F were detected. However in the presence of dry or moist H_2, at 230-300°C and 10^{-1} Torr, good quality silver films were obtained. Only traces of C (0-9%) and O (0-5%) could be detected.

Recently the Aerosol Assisted CVD (AACVD) technique has been used to grow silver[35] and silver alloy.[32,35,36] The first precursor used with this technique was [Ag(hfac)SEt_2].[35] This precursor was found to have a low volatility therefore conventional CVD could not be used. The precursor was dissolved in toluene and nebulised, using N_2 in a heated tube at 80°C when vaporisation took place. Silver deposition occurred on a copper coated silicon substrate at 120-250°C. No impurities were detected. More recently the same precursor has been used to grow alloy films. The precursor was again dissolved in toluene, nebulised and carried to the reaction zone through a pre-heated zone (70-80°C). The carrier gas used in this study was argon with 10% H_2. Films were grown onto a SiO_2 substrate heated at 250°C and held at atmospheric pressure.

A number of silver precursors containing different β-diketonate and β-ketoiminate groups have been studied by AACVD. Examples are [Ag(acac)PPh_3], [Ag(dpm)PPh_3], [Ag_3(fod)$_3$(PPh_3)$_5$], [Ag(tfac)PPh_3], [Ag(hfac)PPh_3], [Ag(hfacNhex)PPh_3] and [Ag(hfacNchex)PPh_3] (acac = pentane-2,4-dionate, dpm = 2,2,6,6-tetramethyl-3,5-heptanedionate, tfac = 1,1,1-trifluoro-2,4-pentanedionate, hfacNhex = 1,1,1,5,5,5-hexafluoro-4-(hexylimino)-2-pentanoate, hfacNchex = 1,1,1,5,5,5-hexafluoro-4-(cyclohexylimino)-2-pentanoate).[1] These precursors were dissolved in THF. Depending on the precursor used, fairly smooth silver films were deposited onto glass substrates at 310°C

and at atmospheric pressure. The EDX analysis detected mainly silver with some carbon impurities and trace of P in the case of [Ag(hfac)PPh_3].

Based on reports that Pt and Au complexes containing methyl isocyanide groups can easily be isolated and characterised, [Ag(hfac)(C≡NMe)] was tested as a potential precursor for silver CVD.[47] Pure silver films were obtained by thermal CVD in a presence of H_2 at 250°C and 10^{-1} Torr.

Complexes of the type [Ag(hfac)(alkyne)] (alkyne = diphenylacetylene, bis(trimethylsilyl)acetylene, 2-butyne, 2-hexyne, 3-hexyne and 4-octyne) have been synthesised and characterised as precursors for silver CVD.[48] [Ag(hfac)($Me_3SiC{\equiv}CSiMe_3$)] was found to be volatile and can be sublimed at 40°C under reduced pressure (100 mTorr). However the CVD of this compound appears not to have been reported.

1.3.4 Organometallic silver(I) compounds.

The organosilver complexes [Ag(η-C_5H_5)PEt_3][49] and [$AgC(CF_3){=}CF(CF_3)]_n$ have been tested as precursors for silver CVD. No film growth details have been published for the cyclopentadienyl complex but perflouo-1-methylpropenylsilver has been tested using a plasma enhanced CVD technique.[50] Films were deposited on glass, quartz, silicon(100), tungsten, aluminium, alumina and polyimide substrates between 40-150°C and at 0.2 Torr in an Ar/H_2 atmosphere. The presence of hydrogen was found to be essential for the formation of good quality silver films. The same precursor was tested using thermal CVD.[12] Silver films were deposited onto alumina at 700°C, in a presence of an Ar/H_2 atmosphere at 30 Torr. Uniform films were obtained with no or little porosity. The presence or not of H_2 did not influence the film quality. No impurities were detected using AES. However, silver oxide was detected using XRD when little or no H_2 was used. In another thermal CVD technique experiment, the same precursor was tested.[13] The experiment was carried out at 275°C and at 10^{-4} Torr and films were grown onto borosilicate glass. The films contain only traces of F and O and no C. The film produced consisted of an agglomeration of particles with voids, as shown by SEM.

1.4 SOME ASPECTS OF THE CHEMISTRY OF SILVER.

Silver, copper and gold belong to the same group of the Periodic Table (group 11 or IB) but show few resemblances. They have same basic electronic configuration with a single s electron outside a completed d shell and have high ionisation potentials. The chemistry of silver differs quite markedly from copper and gold chemistry.

Silver displays three different oxidation states (+I) (+II) and (+III). Ag(+IV) seems to have been reported once in the form of $Cs_2[AgF_6]$.[51] Loss of one electron gives Ag(+I) ($4d^{10}$), the most stable and common oxidation state. Silver(I) forms complexes with coordination numbers from 2 to 6. Loss of further electrons from the d shell give Ag(+II) (d^9) and Ag(+III) (d^8), which are less common oxidation states. Ag(II) and Ag(III) can be obtained by chemical or electrochemical oxidation but are thermodynamically and kinetically unstable in aqueous solution.

Complexes of Ag(II) and Ag(III) are known to be stabilised by N-donor ligands. Based on the stability with N-donor ligands, Ag(II) and Ag(III) have been characterised as 'class A' or 'hard' Lewis acids. AgF_2, $[Ag(py)_4]^{2+}$and $[Ag(2,2'\text{-bipy})_2]^{2+}$ are examples of silver species having oxidation state (+II).[52,53] Silver(III) can be found in various oxides[54,55] (e.g. AgO, which is really $Ag^{I}Ag^{III}O_2$) and in a variety of compounds containing multidentate nitrogen ligands such as tetraazacycloalkanes, ethylenebis(guanidine) or porphyrins,[52,53,56] and cryptates.[57] Silver(III) can also be stabilised by perfluorinated methyl groups.[56,57] Thus, $[Ag(CF_3)_4]^-$ was first synthesised in 1986 and since then other complexes such as $[Ag(CF_2H)_4]^-$ and $[PPh_4][Ag(CF_3)_3(CH_3)]$ have been synthesised.[58,59] Silver(II) and silver(III) complexes usually adopt a 4-coordinate square planar geometry but can also take up 6-coordinated octahedral geometry, as in $[Ag^{II}(\text{pyridine-2,6-dicarboxylate})_2(H_2O)]$ or $[Ag^{III}F_6]^{3-}$.

Studies on Ag(I) exploring the reactivity and stability in combination with 'soft' Lewis bases, suggested that Ag(I) could be classified as a 'class B' or 'soft' Lewis acid. It was found that the stability of complexes involving phosphorus and sulfur donor ligands was greater than those formed using nitrogen and oxygen donors. Within group 15, the relative stabilities are N<<P>As>Sb and group 16, O<<S>Se>Te.[56] The stabilities between

these two groups can be combined as P>S>N>O.[56] The stability sequence for halide complexes is I>Br>Cl>F.[56]

The study of the coordination chemistry of silver probably began with the introduction of photography in 1800. The first studies of silver chemistry involved halides and N-donor ligands and was followed by P and S donor ligands, whilst O donor ligands have been studied in less detail. A short review of silver coordination chemistry is given here as a background to the structural discussions in the following chapters.

Silver(I) is known to show coordination numbers from two to six. The coordination geometries can be linear, trigonal or tetrahedral but complexes can also be found less commonly which are highly distorted five or six-coordinate. Examples of different geometries and coordination numbers of silver(I) complexes are presented in Table 1.1.

Coordination number	Geometry around silver	Examples	Ref
2	Linear	$[Ag(NH_3)_2]^+$	60
		$[Ag(CN)_2]^-$	60
		[AgBr(TMPP)]	61
		$[Ag(1,4\text{-pyrazine})](PF_6)_{0.5}(OH)_{0.5}$	62
3	Trigonal	$[Ag_2(dppm)_3](NO_3)_2$	63
	Distorted trigonal	$[Ag(HDPhF)(SO_3CF_3)]$	64
		$[Ag(PPh_3)I]_4$	65
		$[AgBr(PPh_3)_2]$	66
		$[Ag_2(\mu\text{-dppf})(dppf)_2](PF_6)_2$	67
		$[AgCN\{P(C_6H_{11})_3\}_2]$	68
		$[Ag(dppf)(PPh_3)](ClO_4)$	69
4	Tetrahedral	$[AgI(PPh_3)_3]$	65
		$[AgBr(PPh_3)_3]$	70
		$[Ag(dptpy)(MeCN)][BF_4]$	71
		$[Ag(dppp)_2]SCN$	72
	Trigonal pyramidal	$[Ag(1,3,5\text{-triazine})(CF_3SO_3)].H_2O$	62
		$[Ag(1,3,5\text{-tricyanobenzene})(CF_3SO_3)]$	62
	See-saw	$[Ag(1,4\text{-pyrazine})_{1.5}(CF_3SO_3)]$	62
5	Square pyramidal	[Ag(hfpd)(pmdien)]	73
	Trigonal bipyramidal	$[Ag_2(dmpqpy)_2][ClO_4]_2$	74
6	Octahedral	AgCl, AgBr, AgF	
	Highly distorted	$[Ag\{[15]aneS_2O_3\}]^+$	75
		$[Ag_n(mn\text{-}21S_2O_5)_n]^{n+}$	76

TMPP = tris(2,4,6-trimethoxyphenyl)phosphine, dppm = bis(diphenylphosphino)methane, HDPhF = N-N'-diphenylformamidine, dppf = 1,1'-bis(diphenylphosphino)ferrocene, dptpy = 6,6''-diphenyl-2,2':6',2''-terpyridine, dppp = 1,3-bis(diphenylphosphino)propane, hfdp = 1,1,1,5,5,5-hexafluoropentan-2,4-dionate, pmdien = $Me_2N(CH_2)_2NMe(CH_2)_2NMe_2$, dmpqpy = 6,6''''-dimethyl-4',4'''-diphenyl-2,2':6',2'':6'',2''':6''',2'''':6'''',2''''-quinquepyridine, $[15]aneS_2O_3$ = 1,4,7-trioxa-10,13-dithiacyclopentadecane, mn-$21S_2O_5$- = oxa crowned derivative of dithiomaleonitrile.

Table 1.1 Examples of different coordination number of Ag(I) complexes.

1.4.1 Coordination number 2.

Two-coordinate silver complexes adopt a linear structure. This linear geometry is produced by hybridisation of d_{z2}, s and p_z orbitals (Fig. 1.5).[60]

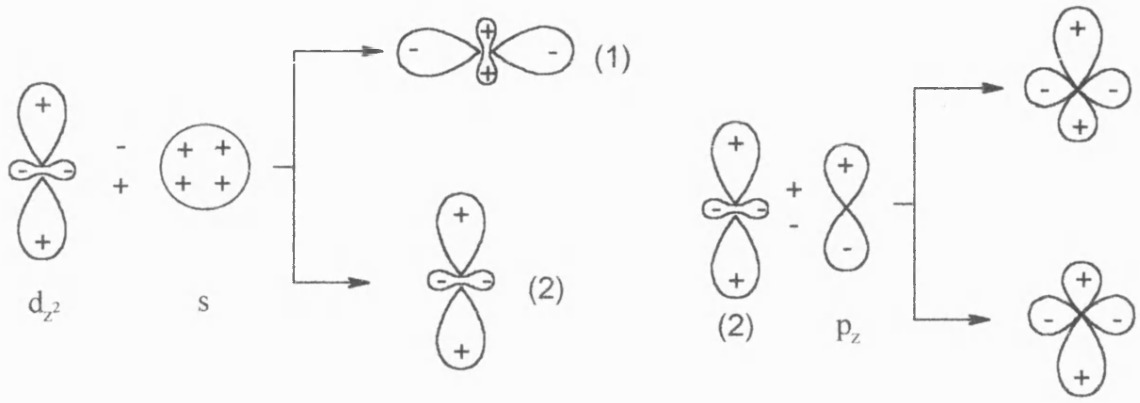

Figure 1.5 Hybridisation of d_{z2}, s and p_z orbitals resulting in covalent bonds.[60]

The d_{z2} and s orbitals of silver hybridise to form two hybrid orbitals (1) and (2). (1) is heavily populated with electrons therefore ligands will be repelled. (2) contains less electron density than (1). Following the hybridisation of (2) with p_z as shown in Figure 1.5 above, the two hybrid orbitals of the far right hand side of the figure can be used to form bonds with the incoming ligands.

The two-coordinate silver ion in Figure 1.6 adopts a linear geometry, the metal being bonded to two nitrogen lone pairs from the two ligands. The N-Ag-N angle is exactly 180°. The structure consists of infinite chains of alternating 1,4-pyrazine and silver(I) units.

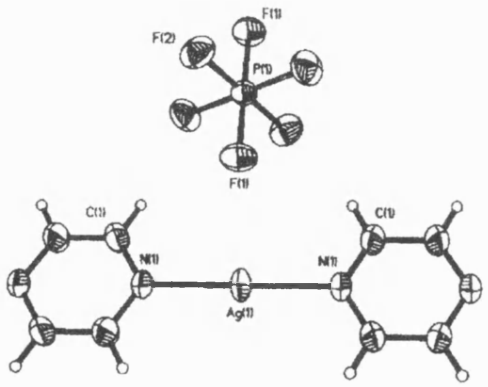

Figure 1.6 Structure of $[Ag(1,4\text{-pyrazine})](PF_6)_{0.5}(OH)_{0.5}$.[62]

Another example of a structure having a linear geometry is the complex $[Ag_2\{Bu^t_2P(CH_2)_3PBu^t_2\}_2][BF_4]_2 \cdot 2CH_2Cl_2$.[77] Silver atoms are bridged by two diphosphine ligands and have a linear P-Ag-P geometry.

1.4.2 Coordination number 3.

Silver complexes having a coordination number 3 adopt a trigonal or a distorted trigonal geometry.

Trigonal planar T-shaped

The cation $[Ag_2(dppm)_3]^{2+}$ (dppm = bis(diphenylphosphino)methane)[63] is an example showing ideal trigonal planar geometry. All P-Ag-P angles are equal to 120°. $[Ag(dppf)(PPh_3)](ClO_4)$[69] is another example of a 3-coordinate complex (Fig. 1.7). The silver atom is coordinated to two phosphorus lone pairs from the diphosphine ligand and to one phosphorus lone pair from the PPh_3 ligand. All angles are different, the P_1-Ag-P_2 angle being 109.63°, P_2-Ag-P_3 119.12° and P_1-Ag-P_3 131.19°.

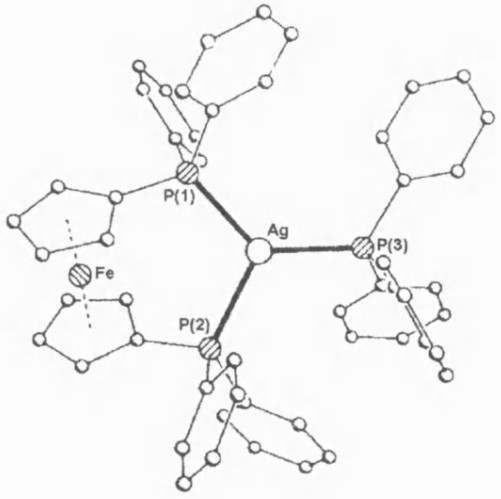

Figure 1.7 Structure of the cation of $[Ag(dppf)(PPh_3)]^+$.[69]

1.4.3 Coordination number 4.

Theoretically, there are four different geometries possible for 4-coordinate silver(I) complexes. Of these there are no known square planar examples.

Tetrahedral Trigonal pyramidal See-saw Square planar

Four coordinate complexes are probably the most common for silver(I) which usually adopts a tetrahedral or distorted tetrahedral geometry. Thus the 1:1 phosphine adducts of silver halides exist as tetrameric 'cubane' clusters in which the silver atoms are surrounded by one phosphine ligand and three triply bridging halide anions to form a distorted tetrahedral geometry. They may form also a 'step' tetramer in which two silver atoms adopt a distorted tetrahedral geometry and two other silvers are distorted trigonal (Fig. 1.8).

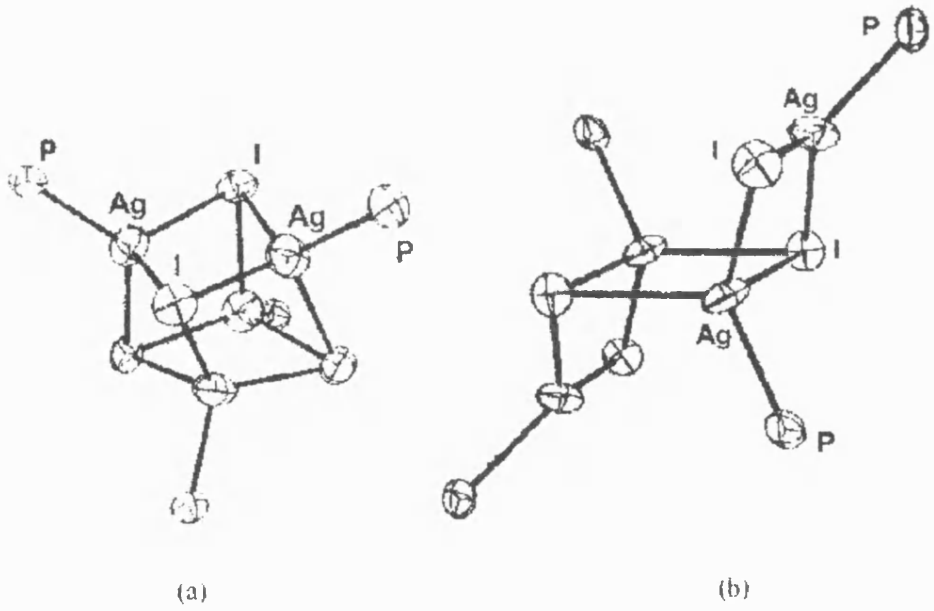

Figure 1.8 Structures of (triphenylphosphine)silver(I) iodide. (a) 'cubane' form and (b) 'step' form.[65]

Silver(I) complexes may also form dimers. $[Ag_2Cl_2(m\text{-}PP)_2]$[78] (m-PP = 1,3-bis[(diphenylphosphino)methyl]benzene) being one example. Figure 1.9 shows that the halide (Cl) is bridging between the silver atoms, each silver being bonded to two phosphorus from the ligand and to two chlorine atoms giving a distorted tetrahedral arrangement.

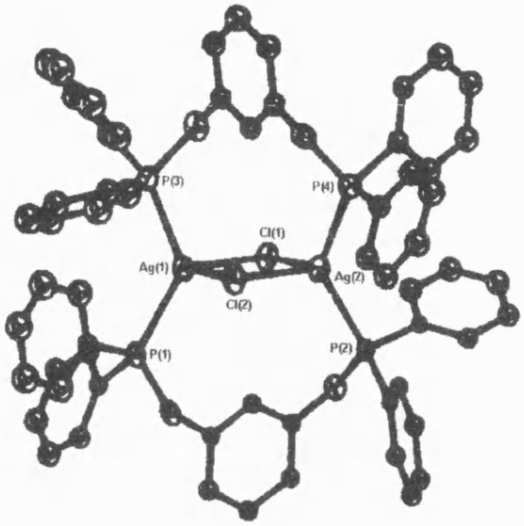

Figure 1.9 Structure of $[Ag_2Cl_2(m\text{-}PP)_2]$.[78]

The structure of $[Ag(1.4\text{-pyrazine})_{1.5}(CF_3SO_3)]$ involves a rather unusual geometry (Fig. 1.10). The silver atom is bonded to three nitrogen from the 1,4-pyrazine ligands and to one oxygen from the triflate giving a see-saw or a saw-horse geometry. The N-Ag-N angles are 173.2° and 87.3°.

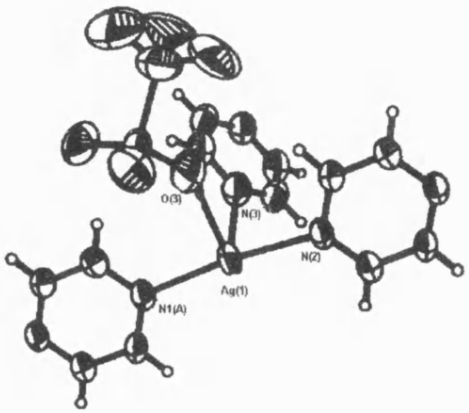

Figure 1.10 Structure of $[Ag(1,4\text{-pyrazine})_{1.5}(CF_3SO_3)]$.[62]

1.4.4 Coordination number 5.

Five-coordinate complexes are less common for silver(I). Idealised geometries are square based pyramidal[73] and trigonal bipyramidal.[74]

Square pyramidal Trigonal bipyramidal

Complexes of this coordination number are usually obtained by reaction of silver(I) with multidentate ligands. The complex $[AgL^1][PF_6]$[79] is mononuclear and has a nearly planar arrangement (Fig. 1.11). The complex also contains a helical twist around the silver atom. Other complexes with substituted quinquepyridine ligands form helical complexes and adopt a trigonal bipyramidal arrangement.[74]

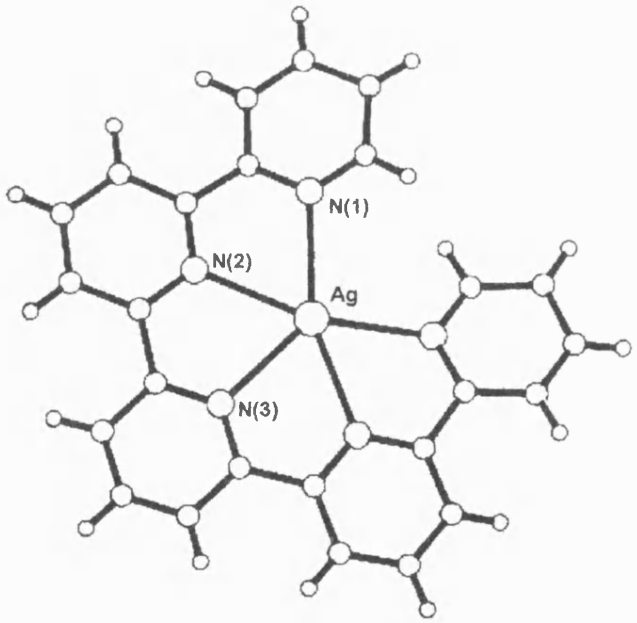

Figure 1.11 Structure of $[AgL^1][PF_6]$ (L^1: 2,2':6',2'':6'',2''':6''',2'''-quinquepyridine).[79]

1.4.5 Coordination number 6.

The highest coordination number for silver(I) is six, octahedral geometry usually being found.

AgCl, AgBr and AgF adopt the NaCl solid state structure with each silver surrounded by 6 halide ions. When reacted with some macrocyclic ligands such as crown ethers, silver(I) has a distorted octahedral arrangement. The silver ion in $[Ag([15]aneS_2O_3)]^+$ is bonded to all heteroatoms contained in the thioether oxa crown molecule and to a sulfur atom from a second molecule.[75] The geometry around silver is distorted octahedral (Fig. 1.12).

Silver(I) complexes of aza-thia macrocycles also exhibit a distorted octahedral geometry. The structure of $[Ag[18]N_4S_2]^+$ ($[18]N_4S_2$ = 1,10-dithia-4,7,13,16-tetra-azacyclo-octadecane) shows that all heteroatoms (S and N) from the ligand were bonded to silver.[80]

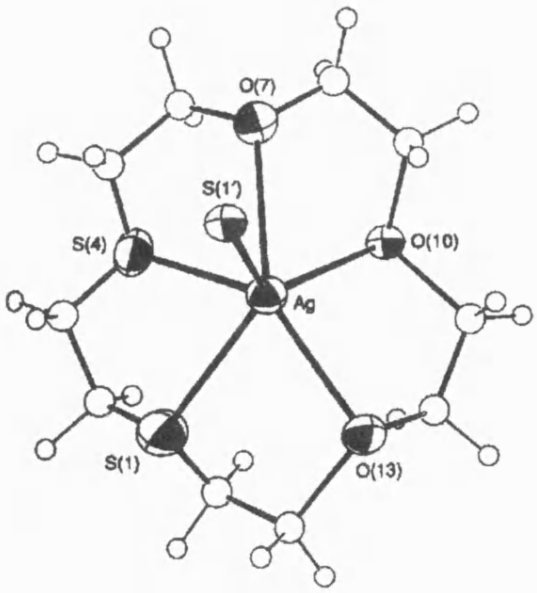

Figure 1.12 Structure of $[Ag([15]aneS_2O_3)]^+$.[75]

1.4.6 Relationships between coordination numbers, ligands and solvents.

Coordination numbers are sensitive to the nature of ligands used and any anions present. A perfect example to illustrate this observation is the pair of complexes $[Ag(NP_3)(NO_3)]$ and $[Ag(NP_3)(PF_6)]$ [NP_3 = tris{2-(diphenylphosphino)ethyl}amine].[81] Both complexes contain the same ligand but a different anion (Fig. 1.13). In $[Ag(NP_3)(NO_3)]$ the metal is coordinated to one oxygen from (NO_3) and to three P from the ligand giving a distorted tetrahedral arrangement. However, in $[Ag(NP_3)(PF_6)]$ the three phosphorus from the ligand coordinate to silver but the anion (PF_6^-) does not coordinate to the silver atom, which thereby adopts a distorted trigonal geometry.

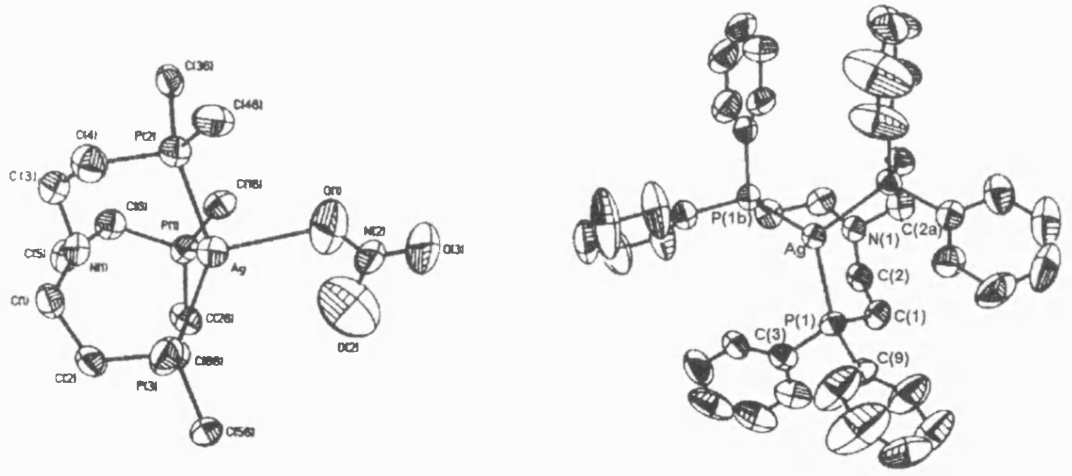

Figure 1.13 Structures of $[Ag(NP_3)PF_6]$ and $[Ag(NP_3)(NO_3)]$.[81]

The coordination number of a metal ion may also be sensitive to the solvent employed. In some cases the presence of solvent molecules in the product can change completely the structure of a complex. Thus, $[AgBr(PPh_3)_2]$ is an example where the solvent plays a role in the crystal structure (Fig. 1.14).[66] Unsolvated $[AgBr(PPh_3)_2]$ is a monomer, the silver ion having trigonal planar geometry. However, when solvated with chloroform the complex exists as a dimer, the silver atoms being bonded to two phosphorus from the phosphine ligands and to two bridging bromine anions. The geometry around silver is distorted tetrahedral.

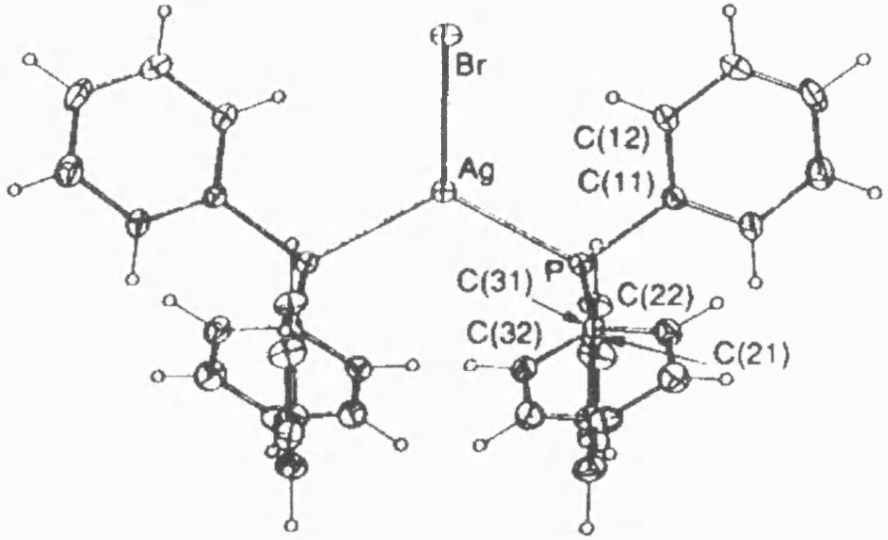

(a)

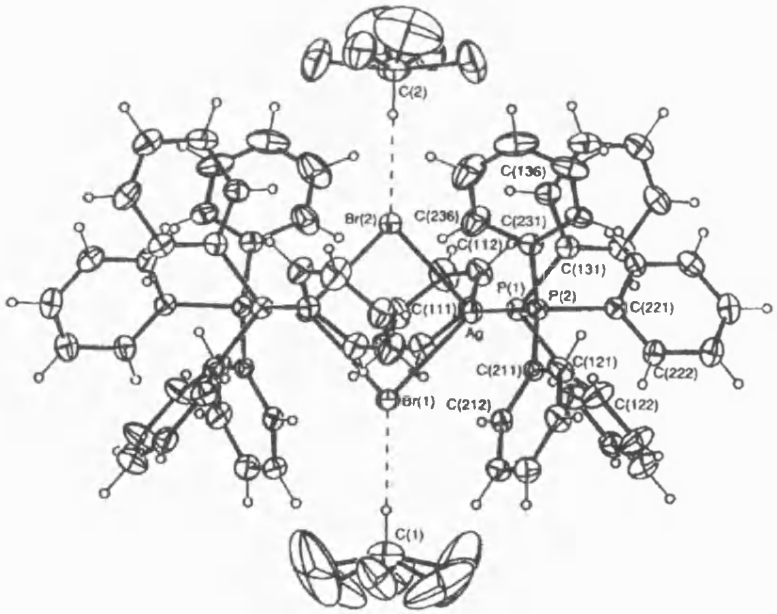

(b)

Figure 1.14 Structures of $[AgBr(PPh_3)_2]$: (a) unsolvated. (b) solvated with chloroform.[66]

1.5 CRYSTALLOGRAPHY AND SPECTROSCOPY OF SILVER(I) COMPOUNDS.

A large number of analytical techniques are available for the characterisation and structural classification of silver(I) complexes. Infrared, ^{1}H NMR and ^{13}C NMR spectroscopies are useful techniques for giving information concerning the ligand structure. For structural information concerning geometry around the silver atom in solid compounds, the technique of single crystal diffraction is necessary. ^{31}P NMR provides information concerning the phosphorus ligand but also around the silver atom via ^{107}Ag-^{31}P and ^{109}Ag-^{31}P spin-spin coupling observable when the spectra are recorded at low temperature. These techniques have been used in the work described in this thesis and therefore will be discussed in more detail.

1.5.1 X-ray crystallography.

The study of the growth, shape and geometric character of crystals is called crystallography. When conditions are favourable, each chemical element and many molecular compounds crystallise in a definite and characteristic form.

There are several steps, which are involved in crystallography. They include:

- *Recrystallisation.*
- *Crystal selection.*
- *Search for reflections.*
- *Indexation.*
- *Data collection.*
- *Data reduction.*
- *Solving the crystal structure.*

All steps will be discussed in more detail below.

5.1.1.1 Recrystallisation.

Like all techniques, X-ray crystallography is not without problems. The first hurdle is to obtain a suitable crystal, which may be dependent on the solvent used during the

recrystallisation process. In some cases, where solvent has been incorporated into the lattice, the crystal may lose this solvent when removed from solution and the crystal disintegrates. To overcome this difficulty, data can often be obtained at low temperature. The presence of solvent in the crystal may disrupt intermolecular interactions, thus modifying the system under study.

1.5.1.2 Crystal selection.

Choosing a suitable crystal is very important. The crystal must be single, which means it must possess a uniform internal structure (no fractures, no impurities, not twinned) and be of suitable size and shape. The crystal size should be approximately $0.5mm^3$ for a light atom structure and $0.3mm^3$ for an organometallic compound or other material containing a heavy atom. Once a crystal has been selected, it is mounted on a glass fibre using epoxy resin and placed on a goniometer head, which fits onto the diffractometer. The sample is then centred on the diffractometer using a telescope and cross hairs by making minor adjustments on the three axes of the goniometer.

1.5.1.3 Searching for reflections.

The description below is related to our particular Enraf-Nonius CAD 4 diffractometer. With the crystal in position, the diffractometer is programmed to search randomly for reflections in the crystal. There are three independent angles θ (Bragg angle), χ and ϕ on the diffractometer, and it is usual to begin a search with a θ value of 8° approximately. In most crystals there is a high density of strong reflections at this Bragg angle. ϕ is normally set to 100°, and χ varied between ±30°. When a reflection is located, the diffractometer automatically refines the associated angular positions and saves the refined angles to a file, for a maximum of 25 reflections. During the search, it is important to have reflections from different locations within the crystal, which is usually achieved by doing a number of searches at different χ values.

1.5.1.4 Indexation.

There is a mathematical relationship between the setting angles of reflections for a given crystal, and their Miller Indices with reference to the unit cell of that sample.

Therefore, once the 25 reflections are found, the software will attempt to index them. Miller Indices (*h*, *k*, and *l* are integers which determine the orientation of a crystal plane in relation to the three crystallographic axes. i.e. *h* is related to *a*, *k* to *b* and *l* to *c*) are assigned to each reflection and unit cell parameters *a*, *b*, *c*, α, β and γ are also output. These unit cell parameters dictate the crystal system (Table 1.2), while the Miller Indices help to indicate the lattice type (*P*, *C*, *I* or *F*) (*P* = primitive lattice, *C* = side-centred lattice, *I* = body-centred lattice, *F* = face-centred lattice) and hence the Bravais lattice for the crystal. The Bravais lattice (one of 14) indicates the locations and number of lattice points in the unit cell, where a lattice point may be defined as a repeating environment, by translation within a crystalline array. The volume of the unit cell is also calculated. By allowing approximately 20Å^3 for each non-hydrogen atom, the number of molecules contained in the unit cell can also be established at this stage, with reasonable certainty.

Crystal System	Bravais Lattices	Parameters
Cubic	P, I, F	a=b=c, α=β=γ=90°
Tetragonal	P, I	a=b≠c, α=β=γ=90°
Orthorhombic	P, I, C, F	a≠b≠c, α=β=γ=90°
Trigonal	P	a=b=c, α=β=γ≠90°
Hexagonal	P	a=b≠c, α=β=90°, γ=120°
Monoclinic	P, C	a≠b≠c, α=γ=90°, β≠90°
Triclinic	P	a≠b≠c, α≠β≠γ

Table 1.2 Crystal systems and Bravais lattices.

The indexation procedure also produces a 3×3 orientation matrix. This matrix relates the setting angles on the diffractometer to Miller indices for a given unit cell. Data collection depends on this matrix, therefore it needs to be as accurate as possible. To optimise the matrix, a quick data collection is performed at high Bragg angle (15-18°) to minimise background and noise, and from this data set 25 new evenly spread reflections

across all Miller Indices are selected and refined. A least squares refinement on these angles gives a refined non-biased orientation matrix and unit cell parameters with low errors.

1.5.1.5 Data collection.

Using this refined orientation matrix, diffraction data on all *h*, *k* and *l* values from approximately 0 to *a*, -*b* to *b* and –*c* to *c* (depending on the crystal system) can be obtained slowly. One reflection from the set of 25 is designated as a standard reflection. Its intensity is measured every 4800 seconds throughout the data collection to monitor possible crystal decomposition. The data collection may take between one day and two weeks depending on the complexity of the sample.

1.5.1.6 Data reduction.

Once the data collection is finished, the next step is the data reduction, which is performed using the NEWCAD4 program. This program calculates an intensity for each reflection in a format that the SHELX package for crystal solution and refinement can read. NEWCAD4 also makes corrections for polarisation of the X-ray beam, and the path length of the X-ray beam through the crystal for different diffraction spots. If a crystal has decayed during the collection, a correction factor for decay is also added to the data at this stage.

1.5.1.7 Lattice points and space group determination.

Lattice points have only 6 types of associated symmetry elements, namely, inversion centres, mirrors planes, rotation axes, rotary inversion axes, screw axes and glide planes. There are 230 unique combinations of all possible lattice point symmetries with the 14 Bravais lattices, called Space Groups. These Space Groups describe the only 230 ways in which the identical objects can be stacked together to fill 3-D space.

To determine the space group for a structure it is necessary to study the pattern of absent reflections in the data set. Absences arise because of destructive interference of the

diffracted X-ray beam from a set of Miller planes. There are two types of absences (a) general absences and (b) systematic absences.

General absences are related to the lattice type, while systematic absences are related to the symmetry of the lattice point. Each lattice type has characteristic absences (Table 1.3). The presence of glide planes or screw axes produce specific absences in the data set, as these symmetry elements contain a translational component. Examples are given in Table 1.4.

Lattice type.	**Absences when**
P	None
I	$h+k+l = 2n+1$
A	$k+l = 2n+1$
B	$h+l = 2n+1$
C	$h+k = 2n+1$
F	Reflections must all have odd or even indices to be observed. Mixed odd/even not allowed.

Table 1.3 Lattice types and absences.

Symmetry	**Absences when**
2_1 screw axis	
On *a*	*h*, 0, 0 *h*= odd (absent)
On *b*	0, *k*, 0 *k*= odd (absent)
On *c*	0, 0, *l* *l*= odd (absent)
Glide plane	*h*, 0, *l* When *l*= odd is absent we will have a *c* glide perpendicular to *b*. When *h*= odd is absent we will have an *a* glide perpendicular to *b*.

Table 1.4 Symmetry and absences.

Most space groups are completely defined by their absences and it is seldom difficult to assign a space group to a structure.

It is important to know the space group as it dictates the relative positions of objects within the lattice point, and consequently, within the unit cell. These relative locations are needed in order to solve the crystal structure, as the electron density is examined only in one specific location of the unit cell, called the asymmetric unit. Computer programs for solution and refinement must be told the relative positions for objects within the unit cell in order to determine the crystal structure successfully.

1.5.1.8 Solving the crystal structure from intensity data.

The corrected intensity (I_{hkl}^{corr}) for each Miller index is related to the observed structure factor for each *h k l* as follows:

$$I_{hkl}^{corr} = (F_{hkl}^{obs})^2 \quad \textbf{(1.1)}$$

Thus from the experimental data, the magnitude of each observed structure factor can be calculated but not its sign. This is referred to as the phase problem in crystallography.

The structure factor F_{hkl} is related to the atomic scattering factors (f_j) and the position x_j, y_j, z_j of the jth atom in a structure containing 'n' atoms by equation (**1.2**):

$$F_{hkl} = \sum_{j=1}^{j=n} f_j \cos 2\pi(hx_j + ky_j + lz_j) + i\sum_{j=1}^{j=n} f_j \sin 2\pi(hx_j + ky_j + lz_j) \quad \textbf{(1.2)}$$

These structure factors are in turn related to the electron density (e Å^{-3}) at any point *x*, *y*, and *z* given by equation (**1.3**):

$$\rho_{xyz} = \frac{1}{V}\sum_h \sum_k \sum_l (F_{hkl}) \cos 2\pi(hx + ky + lz) \quad \textbf{(1.3)}$$

However, to calculate electron density it is clear that some mechanism is required to overcome the phase problem.

1.5.1.9 Patterson synthesis.

Structures of organometallic and coordination compounds can be solved using the Patterson approach. Patterson series are based on F_{hkl}^2 rather than F_{hkl} and hence eliminate

the need to know the sign of the structure factor. The Fourier series for Patterson synthesis is given in equation (**1.4**).

$$P = \frac{1}{V}\sum_{h}\sum_{k}\sum_{l}(F_{hkl})^2 \cos 2\pi(hx + ky + lz) \quad \textbf{(1.4)}$$

The Patterson map consists of all interatomic vectors in a given structure, but has no physical meaning in itself. Peak intensities in a Patterson map are proportional to the square of the atomic number of the atoms involved. Thus, heavy atoms are much easier to recognise due to their relatively large $(Z)^2$ values. Once the heavy atom position is assigned, the scattering factor can be calculated for all *h, k, l* planes according to equation (**1.2**). These calculated values can be then inserted into equation (**1.3**) to produce an electron density map.

1.5.1.10 Crystal solution and refinement using SHELXS and SHELXL.[82,83]

The SHELXS program automatically produces Patterson maps for heavy atom structures and once the position of the heavy atom has been identified, SHELXS uses equation (**1.4**) to then produce an electron density map, where other atomic positions become obvious. These new atomic positions are input into the SHELXL program, which is used to refine the proposed crystal structure. This program takes all the atomic positions assigned and does least squares fits on them against the experimental data. Subsequently it recalculates the structure factors based on all input atoms, and produces a new electron density map where further atomic positions appear. This iterative procedure is repeated until all the atomic positions are assigned and all the electron density is accounted for.

The *R* factor measures the accuracy of the crystallographic structure proposed for the compound against the experimental data. When all the atomic positions are correctly assigned, the magnitude of the structure factor from the experimental data $\left|F_{hkl}^{obs}\right|$ should be similar to the calculated values $\left|F_{hkl}^{calc}\right|$, for all Miller Indices. At this point the *R* factor, defined in equation (**1.5**), should be low. Values in the range 0.01 to 0.07 are normally considered to be acceptable.

$$R = \frac{\sum(\left|F_{hkl}^{obs}\right| - \left|F_{hkl}^{calc}\right|)}{\sum\left|F_{hkl}^{obs}\right|} \quad \textbf{(1.5)}$$

1.5.2 ^{31}P NMR Spectroscopy.

Phosphorus has only one isotope ^{31}P with a 100% abundance and nuclear spin I = ½. This generally makes the acquisition of ^{31}P NMR spectra quite easy. The most common reference used for ^{31}P NMR chemical shifts is an external sample of 85% H_3PO_4 solution. The chemical shifts vary from about +250 ppm to about –450 ppm depending on the oxidation state of the phosphorus. Phosphorus(III) gives signals in the region from about +250 ppm to –450 ppm whereas phosphorus(V) chemical shifts are found between +100 ppm to –300 ppm (Fig. 1.15). There is thus no clearly defined chemical shift region for the individual oxidation states. ^{31}P can couple to other NMR active nuclei and the resulting spin-spin coupling can be measured. In this study, we are interested in Ag-P coupling.

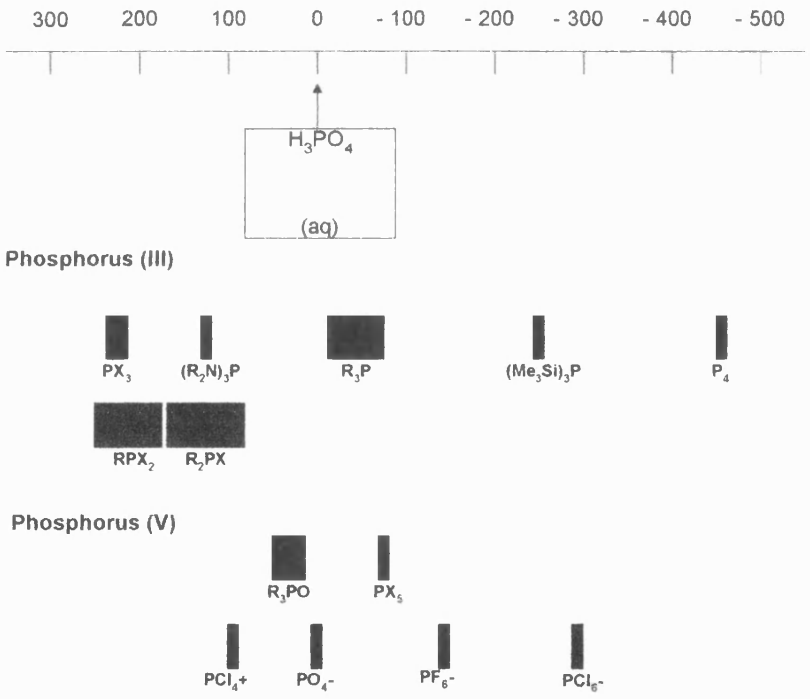

Figure 1.15 Chemical shifts of ^{31}P.[84]

Silver has two isotopes ^{107}Ag and ^{109}Ag. Although they both have a nuclear spin of ½ and high natural abundance (51.8% and 48.2% respectively), low receptivities and long relaxation times cause problems for NMR studies. The majority of coupling constants ^{1}J(Ag-P) have been reported via ^{31}P NMR. ^{1}J(Ag-P) is extremely sensitive to the coordination environment around the silver atom, but ^{1}J(Ag-P) of complexes cannot

usually be resolved at ambient temperature due to the kinetic lability of the Ag-P bond.[85] Therefore low temperature NMR experiments are necessary to obtain the coupling constant information. Figure 1.16 is an example of a ^{31}P NMR spectrum at low temperature. The spectrum exhibits a doublet of doublets. The inner doublet is the coupling between ^{107}Ag and ^{31}P and the outer doublet is the coupling between ^{109}Ag and ^{31}P.

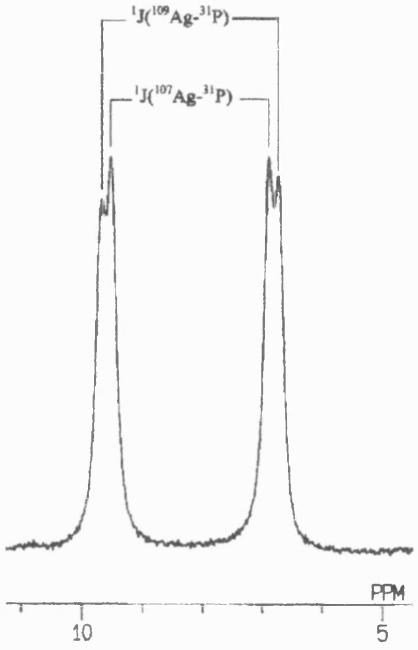

Figure 1.16 ^{31}P NMR spectrum of $[Ag(O_2CCH{=}CH_2)(PPh_3)_2]$.

Typical $^1J(^{107}Ag\text{-}P)$ values vary from 221 Hz in $[Ag(dppp)_2]^+$ [72] to 756 Hz in $[Ag(ClO_4)\{P(OEt)_3\}_2]$.[86]

^{107}Ag NMR or ^{109}Ag NMR spectroscopy is another method for the determination of $^1J(Ag\text{-}P)$ coupling constants. From such NMR spectra, $^1J(Ag\text{-}P)$ can be directly observed. For example, $^1J(^{109}Ag\text{-}^{31}P)$ of triphenylphosphine adducts of silver(I) carboxylates and fluorocarboxylates vary from 484 Hz to 524 Hz and $^1J(^{109}Ag\text{-}^{31}P)$ of triphenylphosphine adducts of silver(I) β-diketonate and β-ketoiminate range from 496 Hz to 831 Hz.[1]

1.6 AIMS AND SYNTHETIC STRATEGIES.

The major aim of the work describe in this thesis is the synthesis and characterisation of novel precursors for silver CVD. Syntheses of three different groups of compounds, namely unsaturated silver(I) carboxylates, silver(I) alkoxides or aryloxides and silver(I) complexes with sulfur donors, have been investigated as precursors for the chemical vapour deposition of silver films.

As mentioned earlier, the major problem for silver CVD is the lack of stable and volatile silver complexes. They often exist in polymeric forms, therefore volatility is low. Several strategies have been employed during this study in order to obtain stable and volatile complexes. They include:

- Use of unsaturated multidentate anions such as unsaturated carboxylates. These might increase the intramolecular bonding and volatility.
- Use of bulky species or species with additional donor atoms to reduce oligomerisation.
- Use of neutral donor molecules with sterically bulky groups such as phosphines. These might decrease polymerisation.

The use of fluorinated compounds should increase volatility, due to a decrease in van der Waals attractions, but the latter has not been explored during this thesis.

The precursors were designed to be potentially useful in an industrial context, as they should be:

- Prepared from relatively cheap starting materials. This allowed large-scale CVD trials, to be performed.
- Relatively easy to handle. i.e. stable in air and not moisture sensitive.

Apart from the synthesis of precursors, CVD experiments have been carried out in order to evaluate each compound as a potential precursor for silver CVD. Characterisation of several compounds using X-ray crystallography has also been carried out.

Chapter Two

Unsaturated silver(I) carboxylates and their adducts

2.1 INTRODUCTION.

Silver(I) carboxylates have found applications in several different areas. They are used in organic synthesis, for example in the Hunsdiecker reaction (decarboxylation), the Simonini reaction (ester synthesis) and the Prévot reaction (diol synthesis).[87] They have also found extensive use as catalysts in the manufacture of urethane polymers.[1]

Silver(I) carboxylates were chosen as a starting point for silver CVD precursors even though they are known to be light sensitive and insoluble in most organic solvents. However advantages include their ease of synthesis and their thermal stabilities at low temperatures.

Previous mass spectrometric studies on a range of silver(I) carboxylates showed that these compounds are usually dimeric in the vapour phase. Two fragmentation pathways were observed. The alkyl carboxylates initially lose $RCO_2\cdot$ from the radical ion $[Ag_2(O_2CR)_2]^+$, whereas the benzoate and perfluorocarboxylates also easily lose CO_2 from the radical ion leading to the formation of abundant organosilver ions (eqn. 2.1).[88]

$$RCO_2Ag \xrightarrow{\Delta} R\text{-}Ag + CO_2 \quad \textbf{(2.1)}$$

The major problem for silver CVD is the lack of stable volatile silver complexes. The phosphine adducts of silver(I) carboxylates and silver(I) fluorocarboxylates have already been tested as precursors for silver CVD and have produced silver films of reasonable quality.[1]

Silver(I) carboxylates containing unsaturated carboxylate anions were chosen as potential precursors for silver CVD because it was thought that in addition to the oxygen donation a carbon-carbon double bond may bond to the silver atom and perhaps increase the volatility. Although the sensitivity of silver(I) carboxylates to light and their insolubility in most organic solvents may cause some problems, reaction with triphenylphosphine is known to improve solubilisation and light sensitivity characteristics.

This chapter will describe the structural chemistry and various synthetic routes known for this class of compounds. The introduction will be followed by details of the synthesis, characterisation and CVD testing of new silver(I) unsaturated carboxylate complexes, prepared in this work.

2.2 STRUCTURAL CHEMISTRY.

The basic structural unit found in the majority of silver(I) carboxylates is the bis(carboxylato-O,O') dimer containing an eight-membered central $[Ag(O\text{-}C\text{-}O)]_2$ ring. As a result, silver(I) carboxylates exist as discrete dimers or as a variety of polymeric structures (Fig. 2.1). Polymerisation is achieved through additional bonds to silver atoms using other donor atoms from adjacent groups.

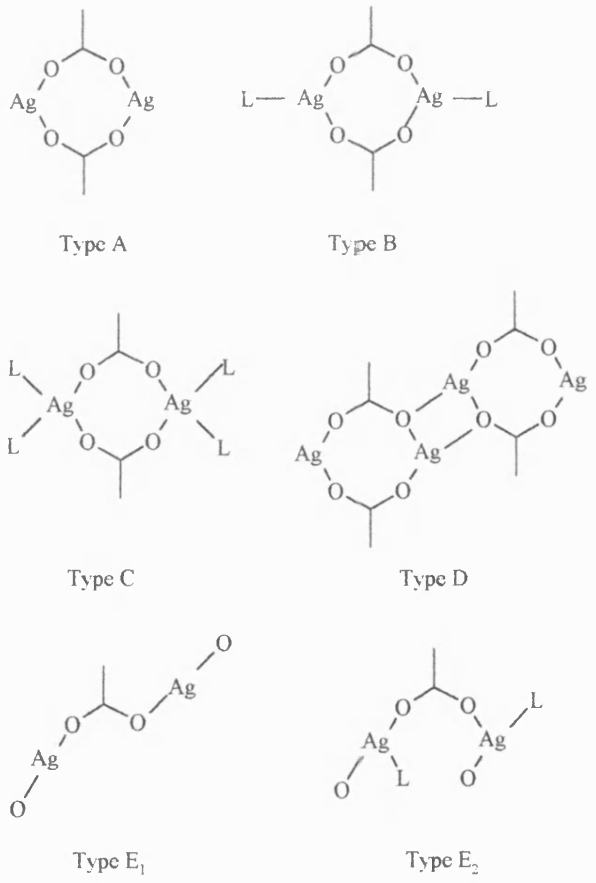

Figure 2.1 Structural types of silver(I) carboxylates.[89]

Table 2.1 summarises examples of silver(I) carboxylate complexes having established structures.

Compounds	C.N of silver atom	Structure type	Ref
$[Ag_2(C_6H_5CO_2)_2]$	3	Type A	90
$[Ag_2(HOC_6H_4CO_2)_2]\cdot H_2O$	3	Type A	90
$[Ag_2(C_6F_5OCH_2CO_2)_2]$	2	Type A	91
$[Ag_2(C_9H_8NO_3)_2(H_2O)_2]\cdot 2\ H_2O$	3	Type B	92
$[Sb_2Ag_2(C_6H_6O_7)_4]$	3	Dimeric Type B	93
$[Ag(C_5H_4NCO_2)]_n$	3	Polymeric Type B	92
$[Ag_2(sa)_2]_n$	3	Polymeric Type B	94
$[Ag_2(cis\text{-}C_4H_3O_4)_2]_n$	3	Polymeric Type B	95
$[Ag(O_2CCH_2CN)]_n$	4	Polymeric Type B	96
$[Ag_2(C_2O_4)]$	5	Dimeric Type C	97,102
$[Ag_2(HOCH_2CO_2)_2]_n\cdot nH_2O$	5	Polymeric Type C	98
$[Ag_2(CF_3(CF_2)_2CO_2)_2]$	5	Dimeric Type C	99
$[Ag(Et_3BET)_2(NO_3)_2]$	4	Dimeric Type C	100
$[NH_4][Ag_2(C_6H_5O_7)(H_2O)]_n$	4	Polymeric Type C	101
$[Ag_2(cis\text{-}C_4H_2O_4)]_n$	4	Polymeric Type C	95
$[Ag_2(C_3H_2O_4)]_n$	5	Polymeric Type C	102
$[Ag_2(O_2CCF_3)_2].C_6H_6$	3, 4	Polymeric Type D	103
$[Ag_2(C_5H_5N)(C_7H_5O_2)_2\}]$	4	Polymeric Type D	104
$[Ag_2(C_6H_5OCH_2CO_2)_2]_n$	3	Polymeric Type D	105
$[Ag(C_5H_3O_3)]$	5	Polymeric Type D	106
$[Ag_2(C_4H_2O_4)]$	3, 4	Polymeric Type D	107
$[Ag_2(4\text{-}FC_6H_4OCH_2CO_2)_2(H_2O)_2]_2$	3,4	Tetrameric Type D	105
$[Ag_4\{O_2C(CH_2)_3CO_2\}_2]_n$	3	Polymeric Type D	108
$[Ag_2(O_2CCF_3)_2]_n$	3	PolymericType D	109
$[\{Ag_2(O_2CCH_2OC_6H_4Cl\text{-}2)_2\cdot AgClO_4\}_n]$	3, 2	Polymeric Type D	110
$[\{Ag_2(L^1)\}_n][ClO_4]_{2n}$	3	Polymeric Type D	111
$[\{Ag_2(L^2)\}_n][ClO_4]_{2n}\cdot 2nH_2O$	3	Polymeric Type D	111
$[\{Ag_2(L^1)(NO_3)_2\}_n]$	4	Polymeric modified Type D	111
$[\{Ag_2(L^2)(NO_3)_2\}_n]$	5	Polymeric Type D	111
$[Ag(Et_3BET)_2]_n(ClO_4)_{2n}$	4	Polymeric Type D	100
$[\{Ag_2(L^3)_2)(NO_3)(H_2O)\}_n)](NO_3)_n$	4	Polymeric modified Type D	112
$[\{Ag(O_2CCH_2OC_6H_3Me\text{-}2,Cl\text{-}4)\}_n]$	2	Type E_1	110
$[\{Ag(O_2CCH_2OC_6H_3\text{-}Cl_2\text{-}2,4)\}_n]$	2	Type E_1	110

$[Ag(pyBET)(NO_3)]$	3	Type E_2	89
$[Ag(O_2CC_6H_4NO_2\text{-}2)]_n$	4, 5	Polymeric	113
$[Ag(O_3SCH_2CO_2)Ag]_n{\cdot}H_2O$	4, 6	Polymeric	114
$[(NH_4)\{Ag(C_5H_4NCO_2)_2\}{\cdot}H_2O]_n$	3	Polymeric	92
$[NH_4][\{Ag(C_7H_3NO_4)\}{\cdot}2\ H_2O]_n$	5	Polymeric	92
$[Ag(C_5H_4NCO_2)]_n$	4, 5	Polymeric	115
$[NH_4][Ag_5\{C_6H_3(CO_2)_3\}_2(NH_3)_2(H_2O)_2]{\cdot}H_2O$	2, 3, 4	Polymeric	116
$[Ag_4(trans\text{-}C_4H_2O_4)_2]_n$	2, 5	Polymeric	95
$[Ag_6(C_7H_4NO_4)_2(C_7H_3NO_4)_2(H_2O)_4]_n$	4, 5	Polymeric	115
$[Ag(O_2CCH_2SC_6H_5)]_n$	4	Polymeric	117
$[Ag_2((O_2C)_2C_6H_4)(C_8H_6N_2)_2(H_2O)]_n$	3, 4	Polymeric	118
$[\{Ag_4(L^4)_3\}_n](ClO_4)_{4n}{\cdot}\ 3nH_2O$	2, 3	Polymeric	112
$[NH_4][Ag\{C_4H_2N_2(CO_2)_2\}]_n$	3	Ribbon polymer	116
$[Ag_2(NO_2C_6H_4CO_2)_2(NH_3)]_n$	2, 3	Zigzag polymeric	119
$[Ag(C_{16}H_{21}O_3)_2]{\cdot}H_2O$	6	OH bridged dimers	120
$[Ag_6\{C_5H_3N(CO_2)_2\}_2\{C_5H_3N(CO_2)CO_2H)\}_2(H_2O)_4]$	5	Polymeric	121
$[Ag_2(C_7H_4NO_5)_2]_n$	3	Polymeric OH bridged	122

C.N. = Coordination number.

$C_9H_8NO_3$ = N-acetylanthranilate, $C_6H_6O_7$ = citrate (2-), $C_5H_4NCO_2$ = pyridine-3-carboxylate, sa = salicylamide-O-acetate, cis-$C_4H_3O_4$ = hydrogen maleate, C_2O_4 = oxalate, Et_3BET = triethyl betaine ($Et_3N^+CH_2CO_2^-$), pyBET = pyridine betaine ($C_5H_5N^+CH_2CO_2^-$), $C_6H_5O_7$ = citrate (3-), cis-$C_4H_2O_4$ = maleate, $C_3H_2O_4$ = malonate, C_5H_5N = pyridine, $C_7H_5O_2$ = benzoate, $C_5H_3O_3$ = furoate, $C_4H_2O_4$ = cis-butenedioate, L^1 = betaine ($O_2CCH(Me_3N^+)CH_2CH_2CH(Me_3N^+)CO_2^-$) L^2 = betaine ($O_2CCH(N^+C_5H_5)CH_2CH_2CH(N^+C_5H_5)CO_2^-$), L^3 = betaine ($p\text{-}Me_2NC_5H_4N^+CH_2CO_2^-$), $C_7H_3NO_4$ = pyridine-2,3-dicarboxylate, trans-$C_4H_2O_4$ = fumarate, $C_7H_4NO_4$ = pyridine-2,3-dicarboxylic acid, $C_8H_6N_2$ = phthalazine, L^4 = betaine ($O_2C(CH_2)_2N^+(CH_2CH_2)_3N^+(CH_2)_2CO_2^-$), $C_4H_2N_2(CO_2)_2$ = pyrazine-2,3-dicarboxylate, $C_{16}H_{21}O_3$ = bis(3-hydroxy-3-phenyl-2,2,3-trimethylcyclohexanecarboxylate), $C_7H_4NO_5$ = 2-hydroxy-4-nitrobenzoate

Table 2.1 Examples of silver(I) carboxylates and silver(I) betaines.

In metal carboxylates with bidentate bridging groups such as the above silver examples (Fig. 2.1), both oxygens of the carboxylate moiety are usually involved in forming the carboxylate bridges as follows (Fig. 2.2):

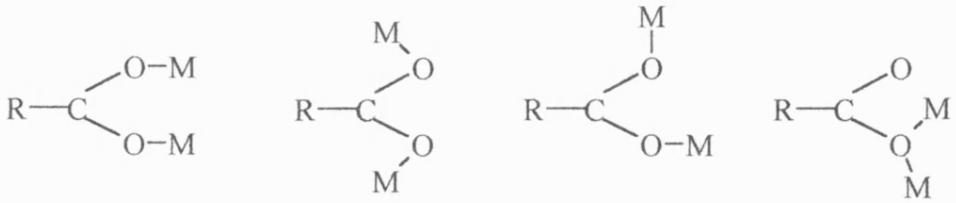

Figure 2.2 Examples of carboxylate bridges.[88]

The syn-syn geometry can bring the metal atoms close enough to form clustered structures with metal-metal bonds. The anti-anti and anti-syn configurations can only lead to polymeric structures. Silver(I) 2,4-dichlorophenoxyacetate and silver(I) 4-chloro-2-methylphenoxyacetate are examples having the anti-syn configuration.[110]

Type A structures have no additional donors on the axial positions of the dimer. Examples of silver(I) carboxylates having type A structures are silver(I) benzoate,[90] silver(I) p-hydroxybenzoate[90] and silver(I) glycylglycine·silver(I) nitrate.[1] The silver atom is bonded to two oxygen atoms from two carboxyl groups and to the other silver atom at a distance of around 2.9Å. Therefore each silver atom can be considered to be three-coordinate.

Type B structures form a polymer through an additional donor group on an adjacent ligand. The structure of silver(I) (2-carbamoylphenoxy)acetate, represented in Figure 2.3, is an example of a Type B structure.[94] The structure is described as a zigzag polymer chain. The Ag-O (axial) bond distance of 2.49 Å is a typical value for silver dimers or polymers. The Ag-Ag distance [3.001(1) Å], longer than those found in dimeric species of Type A, was still considered as an interaction. The silver atom therefore can be regarded as four-coordinate.

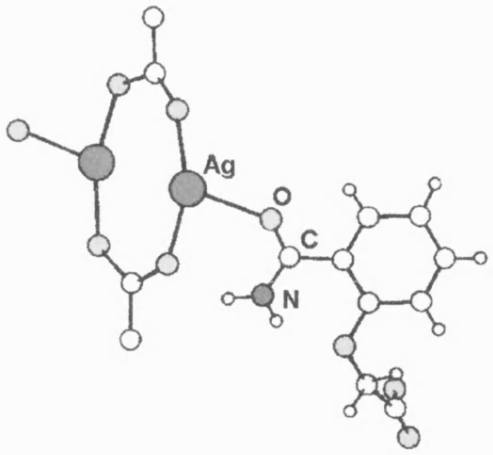

Figure 2.3 Structure of silver(I) (2-carbamoylphenoxy)acetate.[94]

Structures of Type C have two oxygens from adjacent carboxylate groups in the structure and these are located at the end of each dimer. The Ag-O bond distances are longer than in type B i.e. 2.50 Å to 2.71 Å. Other longer range Ag-O distances are common but are not considered as bonding interactions. Terminal oxygens may extend the dimer into a polymer structure through adjacent carboxylate groups. The geometry of the silver atom is usually tetrahedral. Figure 2.4 represents the structure of silver(I) oxalate, in which the silver atom is bonded to four oxygen atoms and to one silver atom giving a distorted trigonal bipyramidal geometry .[97,102]

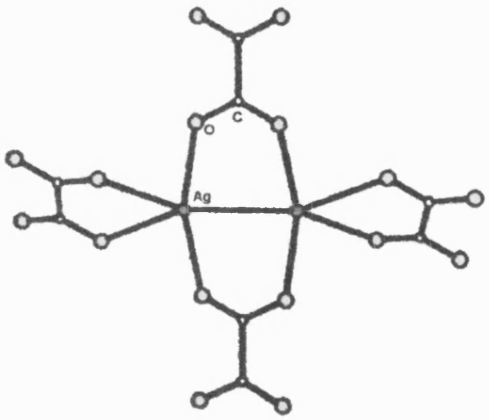

Figure 2.4 Structure of silver(I) oxalate.[102]

Type D structures take the form of step polymers. Every oxygen and silver atom is bonded to silver and oxygen atoms, respectively, of adjacent dimers. Examples include silver(I) phenoxyacetate[105] (Fig. 2.5), silver(I) betaine,[100,110,111] silver(I) trifluoroacetate,[109] silver(I) trifluoroacetate·benzene[1] and glycinesilver(I) nitrate[1]. The silver atoms adopt a trigonal geometry when bonded to three oxygen atoms from the carboxyl group.

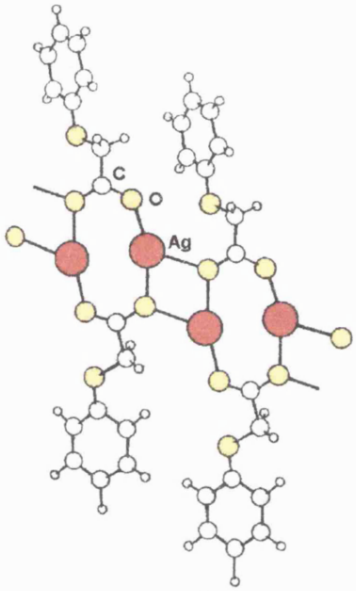

Figure 2.5 Structure of silver(I) phenoxyacetate.[105]

The structure of silver(I) 4-fluorophenoxyacetate hydrate [Ag(4-$FC_6H_4OCH_2CO_2$)(H_2O)] is a variation of a type D structure (Fig. 2.6).[105] The compound forms discrete bis-dimers, which have water molecules on each of the four silver atoms. The geometry around the silver atoms is either trigonal or tetrahedral.

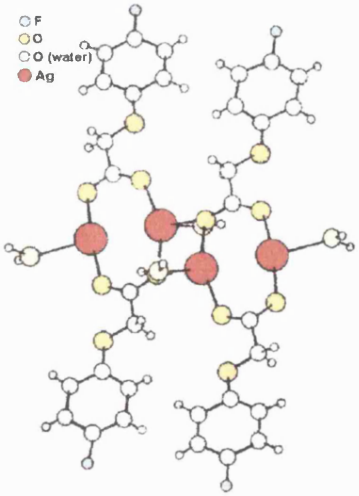

Figure 2.6 Structure of silver(I) 4-fluorophenoxyacetate.[105]

The structure of a silver(I) betaine $[\{Ag_3(Me_2N^+(CH_2CO_2^-)_2)\}_n][ClO_4]_n$ is not based on the dimeric subunits found in Type D.[123] The structure contains discrete ClO_4^- anions and a 2-D cationic polymer containing tetrakis(carboxylato-O,O') bridged trimeric subunits (Fig. 2.7). Each carboxylate group is syn-syn bridging. Within the trimer, six silver atoms are coordinated to four oxygen atoms giving a distorted tetrahedral geometry, the remaining three silver atoms being coordinated to only three oxygen atoms giving a T-shaped geometry. One oxygen atom of a carboxyl group bonds to one silver atom, while the other oxygen atom bonds to two silver atoms, the carboxylates thereby behaving as tridentate ligands.

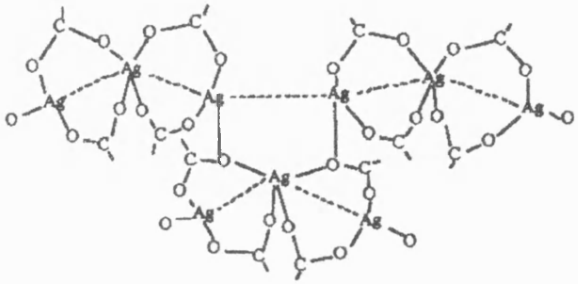

Figure 2.7 Core of the trimeric subunit contained in $[\{Ag_3(Me_2N^+(CH_2CO_2^-)_2)\}_n][ClO_4]_n$.[123]

There are examples of silver(I) carboxylates, which are not based on bis(carboxylato-O,O') dimers. They form different polymeric structures. For example, the structure of $[Ag_2(p\text{-}NO_2C_6H_4CO_2)_2(NH_3)]$ consists of a zigzag polymeric chain, where the silver atoms are bonded by a single syn-syn p-nitrobenzoate bridge. One silver atom is linearly coordinated, while the other is three-coordinate.

Other examples of complexes containing a zigzag structure are $[\{Ag(O_2CCH_2OC_6H_3Me\text{-}2,Cl\text{-}4)\}_n]$ and $[\{Ag(O_2CCH_2OC_6H_3Cl_2\text{-}2,4)\}_n]$.[110] Both structures are of Type E_1, the silver atoms possessing a linear geometry and the carboxylate groups showing an anti-syn configuration.

The structure of $[Ag(pyBET)(NO_3)]$ (pyBET = pyridine betaine, $C_5H_5N^+CH_2CO_2^-$) pyridine betaine is described as Type E_2, the silver atom being distorted trigonal planar with a syn-syn carboxylate group.[89]

The 3-D structure of silver(I) fumarate $[Ag_4(trans\text{-}C_4H_2O_4)_2]_n$ is based on an unusual figure-of-eight tetrameric unit.[95] One of the carboxylate groups forms one tetrameric ring while the other is part of an adjacent ring (Fig. 2.8). One silver atom is bonded to two oxygen atoms from each of two carboxyl groups giving a linear geometry, while the other silver atom is bonded to four oxygen atoms from carboxyl groups to produce a four coordinate arrangement.

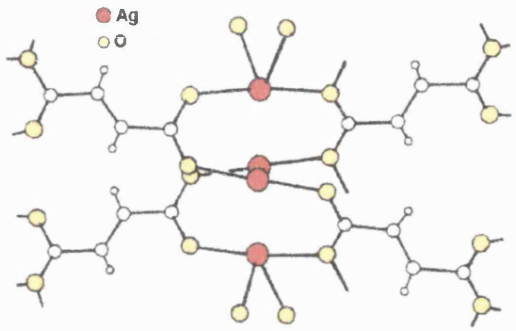

Figure 2.8 Structure of silver(I) fumarate.[95]

Structures containing carboxylates with additional donor atoms may not be based on the bis(carboxylato-O,O') dimer array containing the $(Ag\text{-}O\text{-}C\text{-}O)_2$ central ring but may involve the carboxylate acting as a multidentate ligand. For example, the structure of a silver(I) pyridine carboxylate anion in $[NH_4][Ag(C_5H_4NCO_2)_2]\cdot H_2O]_n$ can be described as a helical chain polymer.[92] Each silver atom is bonded to one oxygen atom from a carboxyl group and to two nitrogen atoms from two different nicotinate ligands giving distorted trigonal planar geometry.

Addition of neutral donor molecules to silver(I) carboxylates is likely to change the structural nature of the silver(I) carboxylate, due to a combination of steric and electronic effects. Thus the polymeric nature of the parent carboxylate may be simplified and at the extreme broken down to generate monomeric complexes. A wide range of adducts of silver(I) carboxylates have been characterised. These adducts were found to be more soluble in organic solvents than the parent carboxylate. Table 2.2 summarises examples of adducts of silver(I) carboxylates having established structures.

Compounds	C.N. of silver atom.	Structure type	Ref
$[Ag(O_2CCF_3)(PPh_3)_2]$	4	Monomeric	124
$[Ag_2(O_2CH)_2(dppf)_3] \cdot 2\ CH_2Cl_2$	4	Dimeric	125
$[Ag_2(O_2CCH_3)_2(dppf)]_2$	4	Tetrameric	125
$[Ag_2(O_2CC_6H_5)_2(dppf)]$	3	Dimeric	125
$[Ag_2(O_2CCH_3)_2(dppm)]_2 \cdot 2\ H_2O$	3	Tetrameric	126
$[Ag(O_2CCH_3)(dppm)]_2 \cdot 2\ CHCl_3$	4	Dimeric	126
$[Ag(O_2CCH_3)(PPh_3)]_4$	3, 4	Tetrameric	127
$[Ag(O_2CH)(PPh_3)_2]$	4	Monomeric	128
$[Ag(O_2CH)(PPh_3)_2] \cdot 2\ HCO_2H$	4	Monomeric	128
$[Ag(O_2CCH_3)(PPh_3)_2]$	4	Monomeric	1,129
$[Ag(O_2CCH_3)(PPh_3)_2] \cdot 1.5\ H_2O$	4	Monomeric	129
$[Ag(O_2CC_3F_7)(PPh_3)_2]$	4	Monomeric	1
$[Ag(O_2CC_6H_4COC_6H_4Cl)(NH_3)]$	2, 3	Monomeric	130
$[Ag(O_2CCH_3)(PPh_3)_2] \cdot H_2O$	3, 4	Dimeric	129
$[Ag(O_2CCH_3)(PPh_3)_2] \cdot 0.5\ H_2O$	3	Dimeric	129
$[Ag(O_2CCH_2Ph)(dppm)_2]$	3	Dimeric	63
$[(PPh_3Ag)_4(C_{10}H_6(CO_2)_2] \cdot 2\ C_6H_6$	4	Tetranuclear dimer	131
$[Ag(C_{20}H_{42}N_2S_2)(CH_3CO_2)] \cdot 2\ H_2O$	5	Monomeric	132
$[Ag(CH_3CO_2)(S\text{-alkyne})] \cdot 0.5\ CH_3CN$	3, 4	Polymeric	133
$[Ag_2(O_2CCCl_3)_2(HO_2CCCl_3)(IC_6H_5)]_n$	4	Polymeric	134,135
$[\{Ag_2(O_2CCF_3)_2(CH_2I_2)_2\}_n]$	4	Polymeric	134
$[\{Ag_2(O_2CCF_3)_2(1,2\text{-}I_2C_6H_4)_2\}_n]$	4	Polymeric	134
$[\{Ag_2(O_2CCF_3)_2(1,4\text{-}I_2C_6H_4)_2\}_n]$	4	Polymeric	134
$[\{Ag_2(O_2CCF_3)_2(IC_6H_5)\}_n]$	3, 4	Polymeric	134
$[\{Ag_4(O_2CCF_3)_4(H_2O)_2(p\text{-}IC_6H_4Me)_2\}_n]$	3, 4	Polymeric	134
$[\{Ag_2(O_2CCF_3)_2(1,2\text{-}I_2C_6H_4)\}_n]$	4	Polymeric	134
$[\{Ag_2(O_2CCCl_3)(HO_2CCCl_3)(1,2\text{-}I_2C_6H_4)\}_n]$	4	Polymeric	134

C.N. Coordination Number.

dppf = 1,1'-bis(diphenylphosphino)ferrocene, PPh_3 = triphenylphosphine, dppm = diphenylphosphinomethane, $C_{10}H_6(CO_2)_2$ = 1,8-naphthalenedicarboxylate, $C_{20}H_{42}N_2S_2$ = 3,3,7,7,11,11,15,15-octamethyl-1,9-dithia-5,13-diazacyclohexandecane, S-alkyne = 3,3,6,6-tetramethyl-1-thia-4-cycloheptyne.

Table 2.2 Examples of adducts of silver(I) carboxylates.

The polymeric structure is not invariably broken down. Thus, addition of pyridine to silver(I) benzoate produces a polymer $[Ag(C_6H_5CO_2)(C_5H_5N)_2]_n$ described as a modified Type D structure.[104]

There are several known structures of silver(I) carboxylate-phosphine complexes. The tetrameric structure (Fig. 2.9) of $[Ag(O_2CCH_3)(PPh_3)]_4$ is an example of such a complex.[127] The structure can be compared to a Type D structure. Each $(Ag\text{-}O\text{-}C\text{-}O)_2$ subunit can be described as having a 'boat' conformation with the silver atoms being trigonally or tetrahedrally coordinated.

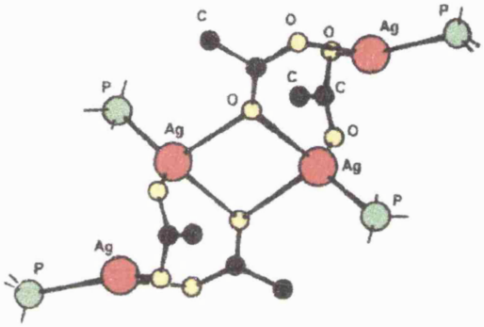

Figure 2.9 Structure of $[Ag(O_2CCH_3)(PPh_3)]_4$.[127]

Another example is the structure of $[(PPh_3Ag)_4(O_4C_{12}H_6)_2]\cdot 2C_6H_6$ ($O_4C_{12}H_6$ = naphthalene dicarboxylate) which consists of two discrete tetranuclear molecules.[131] The silver atoms are either bonded to one phosphorus atom from the triphenylphosphine ligand and to three oxygen atoms from the carboxylate groups or to only four oxygen atoms from the carboxylate groups producing tetrahedral arrangements. The carboxylate groups are both chelating and monodentate with respects to the silver centres.

The structures of $[Ag(O_2CCH_3)(PPh_3)_2]$,[1,129] $[Ag(O_2CCF_3)(PPh_3)_2]$,[124] $[Ag(O_2CC_3F_7)(PPh_3)_2]$[1] and $[Ag(O_2CH)(PPh_3)_2]$[128] are all monomers. The silver atom is bonded to two phosphorus atoms from triphenylphosphine ligands and to two oxygen atoms from a chelating carboxylato group (Fig. 2.10).

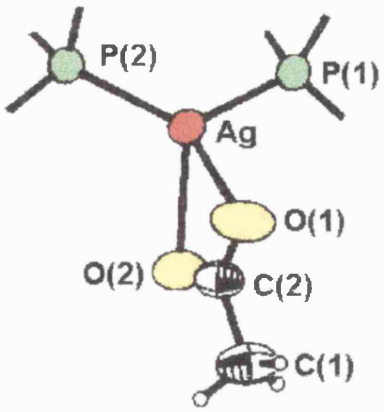

Figure 2.10 Structure of $[Ag(O_2CCH_3)(PPh_3)_2]$.[1,135]

A few examples of silver(I) carboxylate structures containing bis(phosphine) ligands are known.[125,126] Examples include $[Ag_2(O_2CCH_3)_2(dppm)]_2$, $[Ag(O_2CCH_3)(dppm)]_2$, $[Ag_2(O_2CH)_2(dppf)_3]\cdot 2CH_2Cl_2$, $[Ag_2(O_2CCH_3)_2(dppf)_2]$, $[Ag_2(O_2CC_6H_5)_2(dppf)]$ (dppm = bis(diphenylphosphino)methane, dppf = 1,1'-bis(diphenylphosphino)ferrocene).

The tetranuclear solid state structure of $[Ag_2(O_2CCH_3)_2(dppm)]_2$ is different from the dinuclear structure reported for the solution state.[126] The solid state structure consists of a central twelve-membered ring fused between two eight-membered rings. Each silver atom is bonded to one phosphorus atom from the phosphine ligand and two oxygen atoms from a chelating carboxylate group. One oxygen from each carboxyl group is also hydrogen bonded to a water molecule. The complex $[Ag_2(O_2CCH_3)_2(dppm)]_2$ reacts with two equivalents of dppm to give $[Ag(O_2CCH_3)(dppm)]_2$. The structure is described as dinuclear with the silver atoms doubly bridged by dppm ligands to form an eight-membered ring (Fig. 2.11). All silver atoms are coordinated by two phosphorus atoms from dppm ligands and to two oxygen atoms from a chelating carboxylate group.

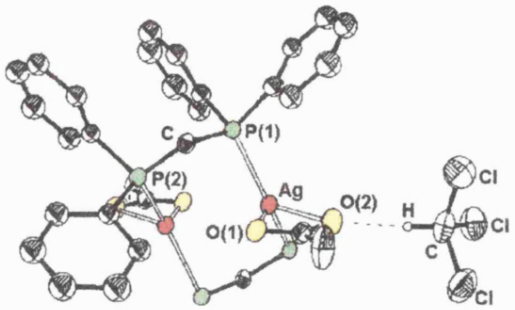

Figure 2.11 Structure of $[Ag(O_2CCH_3)(dppm)]_2$.[126]

The structure of $[Ag_2(O_2CCH_3)_2(dppf)]_2$ contains two $\{Ag_2(O_2CCH_3)_2(dppf)\}$moieties which are linked by two oxygen-silver bonds (Fig. 2.12).[125] The acetate groups are either bridging or triply bridging. All silver atoms are bonded to three oxygen atoms and to one phosphorus atom in a tetrahedral array.

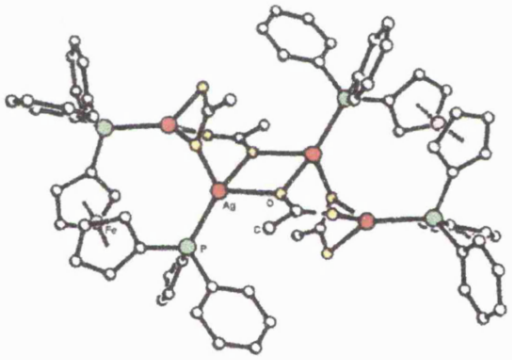

Figure 2.12 Structure of $[Ag_2(O_2CCH_3)_2(dppf)]_2$.[125]

Another example of a structure containing dppf ligands, is $[Ag_2(O_2CC_6H_5)_2(dppf)]$, which contains a distorted $Ag_2(carboxylate)_2$ group and a dppf ligand. The silver atoms adopt a trigonal arrangement.[125]

Examples of complexes with ligands other than phosphorus donors are also known. They include silver(I) acetate with a dithia-diaza macrocycle $[Ag(C_{20}H_{42}N_2S_2)(CH_3CO_2)]\cdot 2H_2O$ ($C_{20}H_{42}N_2S_2$ = 3,3,7,7,11,15,15-octamethyl-1,9-dithia-5,13-diazacyclohexadecane) and silver(I) carboxylates containing CH_2I_2 or an aryl iodide.[132,135,136]

The structure of $[Ag(C_{20}H_{42}N_2S_2)(CH_3CO_2)]\cdot 2H_2O$ is monomeric, with the silver atom bonded to one oxygen from a monodentate acetato ligand, and to two nitrogen and two sulfur atoms from the ligand giving a distorted trigonal bipyramidal arrangement.[132]

All silver(I) carboxylates containing CH_2I_2 or aryl iodides are described as polymers, containing carboxylate-bridged $Ag_2(carboxylate)_2$ dimers. The silver atoms adopt a tetrahedral or a trigonal geometry depending on the crystal structure.[135,136] The di-iodomethane or aryl iodides act as bridging ligand via iodine lone pairs.

Alkynes have also been used as ligands. The polymeric structure of $[Ag(CH_3CO_2)(S\text{-alkyne})]$ (S-alkyne = 3,3,6,6-tetramethyl-1-thia-cycloheptyne) contains $Ag_2(carboxylate)_2$ dimers.[133] One silver atom is bonded to two oxygen atoms from a chelating acetato group and one C≡C from the ligand giving a trigonal planar geometry, the other silver atom is bonded to two oxygens from an acetato group, one C≡C from the ligand and to one sulfur atom from another ligand giving a tetrahedral arrangement.

2.3 SYNTHETIC ROUTES.

Three different routes have been used to synthesise silver(I) carboxylates.

The first method involved reaction of silver(I) nitrate with the appropriate sodium carboxylate in water (eqn. 2.2).

$$RCO_2Na + AgNO_3 \longrightarrow RCO_2Ag + NaNO_3 \quad (2.2)$$

The second method involved reaction of silver(I) oxide with the carboxylic acid in water. The mixture is filtered to remove unreacted silver(I) oxide and the filtrate is evaporated to dryness to produce the silver salt (eqn. 2.3).

$$2\,RCO_2H + Ag_2O \longrightarrow 2\,RCO_2Ag + H_2O \quad (2.3)$$

This method requires the carboxylic acid to be soluble in water.

The third method involved solubilisation of the carboxylic acid by addition of a few drops of concentrated ammonia solution, gentle heating to remove excess ammonia followed by precipitation of the product by addition of silver(I) nitrate (eqn. 2.4).

$$RCO_2H + NH_4OH \longrightarrow RCO_2^-NH_4^+ \xrightarrow{AgNO_3} RCO_2Ag + NH_4NO_3 \quad (2.4)$$

In the previous section, 2.2, the structures of silver(I) carboxylates were described as polymeric. To break the polymeric structures, phosphine ligands have been added in the synthesis as ligands. The synthesis involves reaction of the silver(I) carboxylates with a toluene solution containing triphenylphosphine in a 1:2 ratio (eqn. 2.5).

$$RCO_2Ag + 2\,PPh_3 \xrightarrow{\text{toluene}} [Ag(O_2CR)(PPh_3)_2] \quad (2.5)$$

2.4 RESULTS AND DISCUSSION.

2.4.1 Synthesis.

A series of silver(I) carboxylates, $[Ag(O_2CR)]$ with different R groups [R = CH_2=CH, CH_2=CH(CH_2)$_2$, CH_3CH=C(CH_3), PhCH=CH], and their triphenylphosphine and 1,2-bis(phenylthio)ethane adducts have been successfully synthesised.

The syntheses of silver(I) carboxylates employed three different routes. Compound (**1**) $[Ag(O_2CCH_2CN)]$ resulted from the method summarised in equation 2.2 above, in a moderate yield (52%). Compounds (**3**) $[Ag(O_2CCH{=}CH_2)]$ and (**5**) $[Ag\{O_2C(CH_2)_2CH{=}CH_2\}]$ used the method of equation 2.3. A low yield was obtained for (**3**) (13%) but the method produced a good yield of (**5**) (72%). Compounds (**8**) $[Ag\{O_2C(CH_3)C{=}CHCH_3\}]$ and (**11**) $[Ag(O_2CCH{=}CHPh)]$ were prepared by the route shown in equation 2.4, with yields of 62% and 36%, respectively.

All triphenylphosphine adducts of silver(I) carboxylates synthesised $[Ag(O_2CR)(PPh_3)_2]$ (where R = CH_2=CH, CH_2=CH(CH_2)$_2$, CH_3CH=C(CH_3), PhCH=CH)

were obtained by reaction of one equivalent of silver(I) carboxylate and two equivalents of triphenylphosphine in toluene solvent, with yields varying from 52 to 84%.

Attempted syntheses of (*O*-cyanoacetato)*tris*(triphenylphosphine)silver(I) and (*O*-tiglato)*tris*(triphenylphosphine)silver(I) containing monodentate carboxylates but an additional phosphine ligand by using high PPh_3:Ag ratios were unsuccessful. Elemental analyses of the products showed the formation of only the bis(triphenylphosphine) compounds with chelating carboxylate groups.

The sulfur donor complexes (**7**) $[Ag\{O_2C(CH_2)_2CH{=}CH_2\}(PhSC_2H_4SPh)_2]$ and (**10**) $[Ag\{O_2C(CH_3)C{=}CHCH_3\}(PhSC_2H_4SPh)_2]$ ($PhSC_2H_4SPh$ = 1,2-bis(phenylthio) ethane) were synthesised using the same method. The appropriate silver(I) carboxylate (1 equivalent) was added to a stirred solution of 1,2-bis(phenylthio)ethane (2 equivalents) in ethanol. After 24 hours of stirring, the clear solution was filtered and the filtrate evaporated to dryness to produce a white solid in both cases. The same reaction was also attempted using a 1:1 ratio of reactants. In this case, the silver(I) carboxylate did not dissolve in the 1,2-bis(phenylthio)ethane solution even when left stirring for two days.

2.4.2 Infrared spectroscopy.

Infrared spectroscopy is a very useful technique for the study of metal carboxylates. Characteristic bands associated with the metal-oxygen stretching ν(M-O) and the carboxylate group can be detected. The ν(M-O) stretching bands are usually found at low frequencies; for example, ν(Ag-O) of silver(I) acetate was found at 284 cm^{-1}.[136] The infrared spectra of carboxylic acids display five characteristic bands in the regions 2700-2500 cm^{-1} [ν(OH)], 1700 cm^{-1} [ν(C=O)], 1400 cm^{-1} [ν(C-O)], 1300-1200 cm^{-1} [ν(C-O) and δ (OH)] and 900 cm^{-1} [δ (OH)]. However a coordinated carboxylate will obviously not show bands associated with -OH groups.[88]

This technique can be used to indicate the most likely coordination mode of the carboxylate group when coordinated to metals. There are four distinct modes of coordination, which possibly can be distinguished by infrared spectroscopy.[88] They are: ionic (I), unidentate (II), bidentate chelating (III) and bidentate bridging (IV), as shown in Figure 2.13.

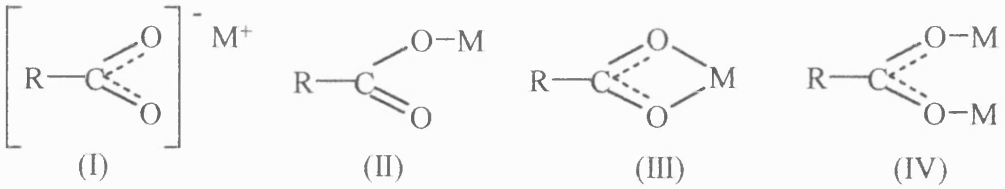

Figure 2.13 Coordination of carboxylate groups.[88]

The unidentate carboxylate mode (II) is substantially less symmetrical than the other three modes, which has consequences for its IR spectrum. Changes for the carboxylate group vibrational frequencies are compared to those of the ionic carboxylate (I), in which the carboxylate group is symmetrical.

Ionic carboxylates show no carbonyl group frequency at about 1700 cm^{-1} but show characteristic bands in the range 1650-1510 and 1400-1280 cm^{-1} due to the asymmetric stretch $\nu_a(CO_2^-)$ and symmetric stretch $\nu_s(CO_2^-)$, respectively.

It has been suggested that where the carboxylate is a unidentate ligand (II), a divergence of $\nu_a(CO_2^-)$ and $\nu_s(CO_2^-)$, symbolised as Δ_ν, compared with the free ion, is expected due to a difference in the bond order of the C-O bonds. For chelating and bridging modes (III) and (IV), a large separation $\nu_a(CO_2^-) - \nu_s(CO_2^-) = \Delta_\nu$, is not expected due the equivalence of the C-O bonds.

In general, bidentate chelating ligands exhibit a lower Δ_ν than bidentate bridging carboxylates therefore in summary:

$$\Delta_\nu \text{ (chelate)} < \Delta_\nu \text{ (bridging)} \approx \Delta_\nu \text{ (ionic)} << \Delta_\nu \text{ (unidentate)}.$$

Examples of each mode of coordination are given in Table 2.3.

Mode	Example	Δ_ν	Ref
Ionic	$[Na(O_2CMe)]$	164	137
Unidentate	$[Pd(phen)(MeCO_2)_2]$	244	138
Bidentate chelating	$[Zn(bpy)_2(MeCO_2)](ClO_4)\cdot H_2O$	130	139
Bidentate bridging	$[Cu(O_2CMe)_2(H_2O)]_2$	200	140

Phen = 1,10-phenanthroline, bpy = 2,2'-bipyridine

Table 2.3 Examples of Δ_ν values for each mode of coordination of the carboxylate group.

A study of structures of metal acetates has been carried out in order to determine the correlation between the bonding mode of the carboxylate and the value of Δ_v = $[\nu_a(CO_2^-) - \nu_s(CO_2^-)]$.[137] It has been concluded that a $\Delta_v > 200$ cm^{-1}, is indicative of a unidentate coordination. A Δ_v of < 150 cm^{-1} is indicative of bridging or chelating coordination. Finally, when $\Delta_v < 105$ cm^{-1}, a chelating coordination is proposed. These values were compared with $\Delta_v = 164$ cm^{-1} for the acetate group in $[Na(O_2CMe)]$, taken as the free ion.

The above rules can be useful in proposing the type of coordination mode of a complex containing a carboxylate group, when no crystal structure data are available. Infrared data are commonly used to differentiate between unidentate and all other coordination modes. The problems encountered using this technique are the practical difficulties in recording IR spectra and the assignment of the symmetric and asymmetric stretches. In addition, the presence of hydrogen bonding can affect the value of Δ_v. In summary, infrared data can give an indication of the carboxylate coordination mode in a complex, but must be used with caution and cannot be regarded as totally valid.

For the compounds synthesised in this work, asymmetric stretches $\nu_a(CO_2^-)$ were found within the range 1601-1498 cm^{-1} and the symmetric stretches $\nu_s(CO_2^-)$ were observed in the region 1477-1326 cm^{-1}. Table 2.4 summarises the frequencies of all $\nu_a(CO_2^-)$ and $\nu_s(CO_2^-)$ stretching vibrations for compounds (**1**) to (**12**). The observed separation is indicative of chelating or bridging modes of coordination.

All compounds also exhibit absorptions in the range 1653-1618 cm^{-1} due to the double bond ν(C=C) stretch from the unsaturated carboxylate group. These values are similar to those found for sodium acrylate (1640 cm^{-1})[141] and sodium tiglate (1662 cm^{-1}).

All triphenylphosphine adducts of silver(I) carboxylates exhibit an absorption band between 1437-1431 cm^{-1} due to P-C, which occurs at 1435 cm^{-1} in uncomplexed triphenylphosphine with a medium to strong intensity.

Compounds	$\nu_a(CO_2^-)$ (cm^{-1})	$\nu_s(CO_2^-)$ (cm^{-1})	Δ_ν[a]	Δ_ν Na salt
$[Ag(O_2CCH_2CN)]$ (**1**)	1601, 1568	1425, 1398	173	194
$[Ag(O_2CCH_2CN)(PPh_3)_2]$ (**2**)	1570	1404	166	194
$[Ag(O_2CCH{=}CH_2)]$ (**3**)	1541, 1510	1423	102	118[141]
$[Ag(O_2CCH{=}CH_2)(PPh_3)_2]$ (**4**)	1545	1417	128	118[141]
$[Ag\{O_2C(CH_2)_2CH{=}CH_2\}]$ (**5**)	1518	1404, 1354	139	140[141]
$[Ag\{O_2C(CH_2)_2CH{=}CH_2\}(PPh_3)_2]$ (**6**)	1585, 1574, 1556	1477, 1398	134	140[141]
$[Ag\{O_2C(CH_2)_2CH{=}CH_2\}(PhSC_2H_4SPh)_2]$ (**7**)	1579, 1558, 1537	1439, 1414, 1400	140	140[141]
$[Ag\{O_2C(CH_3)C{=}CHCH_3\}]$ (**8**)	1558, 1516, 1498	1383	141	142
$[Ag\{O_2C(CH_3)C{=}CHCH_3\}(PPh_3)_2]$ (**9**)	1523	1396	127	142
$[Ag\{O_2C(CH_3)C{=}CHCH_3\}(PhSC_2H_4SPh)_2]$ (**10**)	1516, 1500	1439, 1429	74	142
$[Ag(O_2CCH{=}CHC_6H_5)]$ (**11**)	1576, 1552	1448	116	133
$[Ag(O_2CCH{=}CHC_6H_5)(PPh_3)_2]$ (**12**)	1541	1437	104	133

a. $\Delta_\nu = \nu_a(CO_2^-) - \nu_s(CO_2^-)$

Table 2.4 Infrared bands of silver(I) carboxylates and their adducts.

2.4.3 NMR spectroscopy.

^1H, ^{13}C and ^{31}P NMR spectra were recorded for all compounds synthesised.

2.4.3.1 ^1H and ^{13}C NMR Spectroscopy.

In the ^1H NMR spectra, all expected proton signals were observed (see Experimental). The chemical shifts of the carboxylate protons of the adducts of the silver(I) carboxylates were not significantly different to those of the silver salts themselves.

The protons in compound (**3**) appeared as three doublets of doublets at 6.15, 5.98 and 5.53 ppm. The ^3J value observed between trans protons was 17.0 Hz and the ^3J value

between cis protons was 9.7 Hz. Similar ^{3}J values were observed for the triphenylphosphine adduct.

The ^{1}H NMR spectrum of compound (**5**) showed multiplets for the solvent peaks (d_6-DMSO) and the (CH_2) peaks of the silver salt in the same region causing assignment problems. Therefore a COSY ^{1}H-^{1}H spectrum was acquired. The spectrum showed a coupling of the (CH_2) protons to the protons attached to the terminal carbon. The J values (J_{trans} = 17.0 Hz and J_{cis} = 10.2 Hz) were similar to those found for compound (**3**).

In the ^{13}C NMR spectra (see Experimental for details), all resonances from the carboxylate CO_2 units were found between 166 ppm and 179 ppm. Theses values are lower than those of silver(I) carboxylates previously studied (174-185 ppm).[1] The CO_2 carbon chemical shift of compounds containing additional ligands shifted downfield by 3ppm when compared to the parent silver salt, except for (**2**), which shifted upfield by 3 ppm. Although there are other examples known where the CO_2 carbon signal of silver carboxylates shifted downfield by 2-3 ppm, on complexing with phosphines, such a minor shift might be due to the change of solvent used.

2.4.3.2 ^{31}P NMR spectroscopy.

The ^{31}P NMR spectra of compounds (**2**), (**4**), (**6**), (**9**) and (**12**) were recorded at room temperature and at low temperature. The ^{31}P data are summarised in Table 2.5.

At room temperature, the spectra showed a broad peak in the region 9.1 ppm to 10.9 ppm for each compound. The absence of ^{1}J(Ag-P) coupling indicates a rapid dissociation or exchange in solution.

The ^{31}P chemical shift difference between the complexes and free triphenylphosphine, known as the coordination shift and noted as $\Delta\delta$, is not sensitive to the nature of the carboxylate ligand, $\Delta\delta$ values only varying from 14.3 ppm to 16.1 ppm. Theses values are slightly higher to those of some triphenylphosphine adducts of silver(I) carboxylates already studied (10.8-13.2 ppm).[1]

Due to some solubility problems in $CDCl_3$ solvent, a $CDCl_3$-CH_2Cl_2 mixed solvent was used only for compound (**12**) and so -25°C was the lowest temperature at which the spectrum could be recorded.

The low temperature ^{31}P NMR spectrum for (**12**) showed once again a broad peak at +8 ppm.

Low temperature (-50°C) ^{31}P NMR spectra for (**2**), (**4**), (**6**) and (**9**) showed doublets arising from ^{107}Ag-^{31}P and ^{109}Ag-^{31}P spin-spin coupling. Both compounds (**4**) and (**6**) exhibit a doublet of doublets at +9.4 ppm and +9.6 ppm, respectively. However, the spectrum of compound (**2**) was found to be only partially resolved. The spectrum of compound (**9**) also consisted of only a partially resolved resonance at this temperature. The spectrum showed two peaks with partial doublets at +9.4 ppm.

The values found were shifted downfield when compared to the free ligand triphenylphosphine (-5.25 ppm). This confirms coordination via P atoms. The ^1J(Ag-P) values found are consistent with the values found for other silver(I) carboxylate bis(triphenylphosphine) complexes [^1J(Ag-P) ranges from 432 Hz in $[Ag(O_2CH)(PPh_3)_2]$[128] to 497 Hz in $[Ag(O_2CC_6H_2Me_3)(PPh_3)_2]$[1]. They can also be compared with the ^1J(Ag-P) of $[Ag(NO_3)(PR_3)_2]$ [R = Ph, t-Bu, p-MeC_6H_4, and CH_2CH_2CN] in which the nitrate group acts as a bidentate ligand [^1J(Ag-P) ranges from 470 Hz in $[Ag(NO_3)\{P(p\text{-}MeC_6H_4)_3\}_2]$[142] to 530 Hz in $[Ag(NO_3)\{P(CH_2CH_2CN)_3\}_2]$[143].

The ^{31}P NMR spectra are temperature dependent. The broad singlet observed at room temperature is likely to be the result of rapid dissociation of the Ag-P bond. At low temperature such a process is slowed down and therefore the expected two doublets are observed. The ^{31}P chemical shift values are not dependent on the nature of carboxylate groups. The difference in the chemical shift between that of compound (**2**) and the others is probably due to the electronegative CN of the cyanoacetate group, causing a downfield shift.

Compounds	^{31}P data at room temperature.		^{31}P data at low temperature.		
	δ(ppm)	Δδ	δ (ppm)	$^{1}J(^{107}Ag-P)$ (Hz)	$^{1}J(^{109}Ag-P)$ (Hz)
$[Ag(O_2CCH_2CN)(PPh_3)_2]$ (**2**)	+10.9	16.1	+10.9 (partial doublet)	451.8	488.7
$[Ag(O_2CCH{=}CH_2)(PPh_3)_2]$ (**4**)	+9.5	14.7	+9.6 (dd)	426.0	473.6
$[Ag\{O_2C(CH_2)_2CH{=}CH_2\}(PPh_3)_2]$ (**6**)	+9.4	14.6	+9.6 (dd)	426.1	469.9
$[Ag\{O_2C(CH_3)C{=}CHCH_3\}(PPh_3)_2]$ (**9**)	+9.1	14.3	+9.4 (partial doublet)	430.0	458.8
$[Ag(O_2CCH{=}CHC_6H_5)(PPh_3)_2]$ (**12**)	+9.2	14.4	+8.0 (s)	-	-

Table 2.5 ^{31}P NMR data of triphenylphosphine adducts of unsaturated silver(I) carboxylates.

2.4.4 Mass spectrometry.

The fragmentation patterns obtained from mass spectrometry are usually characteristic of types of compounds and can provide detailed information regarding molecular structure.

During this study, electrospray (ES) and the Fast Atom Bombardment (FAB) mass spectrometric techniques were used. Both are described as soft ionisation techniques.

Samples used for ES mass spectrometry were dissolved in water/methanol or acetonitrile solution then injected to the mass spectrometer.

Samples used for FAB mass spectrometry were dissolved in a 3-nitrobenzyl-alcohol (NOBA) matrix and then injected onto the surface of a probe. A beam of fast argon, xenon or caesium atoms then bombards the solution. In our case caesium was used. These fast caesium atoms are prepared by accelerating caesium ions to an energy of 25keV. The bombardment by a caesium beam produces charged species from the sample into the vapour phase, which are then analysed. The advantages of the FAB technique are production of high-mass cluster ions and the ability to obtain spectra at room temperature. A number of reviews in the literature explain the technique in detail.[144-146]

Compounds (**2**), (**5**), (**8**) and (**9**) were submitted for ES mass spectrometric analysis and the results are summarised in Table 2.6. The FAB mass spectra of compounds (**2**), (**7**), (**9**) and (**10**) have been obtained, the results being summarised in Table 2.7.

The fragments in the spectra are readily identified by the characteristic patterns imposed by the natural isotopic abundances, approximately 1:1 (^{107}Ag 51.82%; ^{109}Ag 48.18%) for the only two silver isotopes 107 and 109. For fragments containing a single silver atom, the pattern is seen as a doublet of approximately equal intensity at positions n, n+2. For those fragments containing two silver atoms, the pattern is a 1:2:1 ratio at positions n, n+2, n+4. For fragments containing three silver atoms, the pattern is a 1:3:3:1 ratio at positions n, n+2, n+4, n+6. Fragments containing more than three silver atoms are difficult to identify due to the low abundances of the high mass peaks.

All fragments were assigned from the fragmentation pathways described in the literature.[136,147,148]

Fragments have been grouped together on the basis of containing none, one or two silver atoms. The monomolecular ion was not detected for any of the compounds. The $[Ag(O_2CR)H]^+$ fragment at m/z 207, 209 was observed at 100% abundance for compound (**5**), whereas only a low abundance (16.3%) was observed for compound (**8**).

Fragments containing silver and methanol were observed at low abundance in the spectrum of compound (**5**) and at a higher abundance for compound (**8**). This is likely to be the result of the reaction of silver species reacting with the solvent (methanol) used for spraying.

The $[Ag_2(O_2CR)_2]^+$ fragment has been observed in low abundance (22.8%) in the spectrum of (**5**). This implies that the dimer survives in the vapour phase.

In the FAB mass spectra fragments such as $[Ag(PPh_3)_n]^+$ (where n = 1, 2) and $[Ag(PhSC_2H_4SPh)]^+$ have been identified as being present in high abundance, while $[AgO(PPh_3)_2]^+$ and $[Ag(PhSC_2H_4SPh)_2]^+$ were identified in low abundance. The presence of $[AgPPh_3]^+$ and $[Ag(PPh_3)_2]^+$ in high abundance suggests the tendency of silver(I) complexes to be linear, two coordinate species in gas phase.[149] The $[AgO(PPh_3)_2]^+$ fragment was also observed in the spectra of $[Ag(C_2Ph)(PPh_3)]$[150] and phosphine adducts of silver(I) carboxylates.[1]

The $[Ag(PhSC_2H_4SPh)_n]^+$ (where n = 1 or 2) fragments have also been observed previously in the spectra of $[Ag(cod)_2]^+ + PhSC_2H_4SPh$ (cod = 1,5-cyclooctadiene).[151] The structure of $[Ag(O_2CR)(PhSC_2H_4SPh)]^+$ might be similar to the structure of $[Ag(O_2CMe)(PhSC_2H_4SPh)]^+$ which can be linear or cyclic.

	(2)		(5)		(8)		(9)	
Fragments	m/z	%	m/z	%	m/z	%	m/z	%
Ag^+	-		-		107	4.2[a]	-	
$[Ag(L)]^+$	-		-		-		-	
$[Ag(L)_2]^+$	631	98.7[a]	-		-		631	45.8[a]
$[Ag(L)_3]^+$	893	5.7[a]	-		-		893	91.6[a]
$[Ag(R)(RH)]^+$	187	100[b]	-		-		-	
$[Ag(OMe)]^+$	-		139	22.9[a]	139	100[a]	-	
$[Ag(OMe)_2]^+$	-		171	7.8[a]	171	33.3[a]	-	
$[Ag(O_2CR)H]^+$	-		207	100[a]	207	16.6[a]	-	
$[Ag(O_2CR)(RCO_2H)]^+$	275	47.3[b]	307	48.5[a]	307	37.4[b]	305	100[b]
$[Ag(O_2CR)(OMe)]^+$	-		239	22.1[a]			-	
$[Ag_2(O_2CR)(L)_2]^+$	824	36.8[a]	-		-			
$[Ag_2(O_2CR)_2]^+$	-		415	22.8[a]	-		-	
Other silver	336	7.8[c]						
containing fragments.	483	5.2[c]						
(c. Ag, d. Ag_3)	661	17.1[d]						

m/z based on ^{107}Ag, $L = PPh_3$

a = ES^+, b = ES^-

Table 2.6 ES mass spectrometric fragments of silver(I) carboxylates and triphenylphosphine adducts of silver(I) carboxylates.

	(2)		(7)		(9)		(10)	
Fragments	m/z	%	m/z	%	m/z	%	m/z	%
$[(C_6H_4)_2P]^+$	183	29.6	-		183	21.6	-	
$[PPh_3]^+$	262	15.2	-		262	13.6	-	
Ag^+	-		107	42.0	-		107	37.5
$[Ag(L)]^+$	369	81.4	353	98.4	369	71.9	353	95.5
$[Ag(L)_2]^+$	631	100	599	49.3	631	100	599	14.6
$[AgO(L)_2]^+$	647	2.8	-		647	3.2	-	
$[Ag(SPh)]^+$	-		216	13.3	-		216	14.0
$[Ag(SPh)(CO_2)]^+$	-		260	15.4	-		260	7.0
$[Ag_2(O_2CR)(L)]^+$	-		561	9.5	-		599	9.5
$[Ag_2(O_2CR)(L)_2]^+$	822	1.5	-		-		-	
Other silver Containing fragments (c. Ag, d. Ag_3)	739 766	0.6[c] 0.95[d]	413	4.7[c]				

m/z based on ^{107}Ag, L = PPh_3 or $PhSC_2H_4SPh$.

Table 2.7 FAB mass spectrometric fragments of triphenylphosphine and 1,2-bis(phenylthio)ethane adducts of silver(I) carboxylates.

2.4.5 X-Ray Crystal Structure Determination of Silver(I) Tiglate.

The solid state structure of the molecule as determined by single crystal X-ray crystallography is depicted in Figures 2.14, 2.15.and 2.16. Crystals of silver(I) tiglate were grown slowly from a dimethylsulfoxide solution at room temperature. Relevant bond lengths and angles are summarised in Table 2.8 with further data provided in Appendix 2.

The structure of silver tiglate is a polymer based on a type B (see Figure 2.1) dimer with a syn-syn bis (carboxylato-O,O') arrangement for the carboxylate groups. The Ag-Ag separation [2.8532(10)Å] is shorter than that in metallic silver [2.89 Å], suggesting a direct metal-metal interaction across the eight-membered ring. However, a study suggested that short metal-metal distances do not necessarily imply metal-metal bonding.[109] The interaction between Ag(I) centres was studied using the EHMO approach. A repulsion, relative to two isolated Ag^+ centres, was observed when only 4d orbitals on silver were used in the calculation. However, by including silver 5s and 5p orbitals in the calculation the interaction becomes more attractive than two isolated Ag^+ centres.[96]

The structure can be compared to the polymeric structures of $[Zn(tiglate)_2]_n$ and $[Zn_2(tiglate)_3(crotonate)]_n$, in which each pair of zinc atoms are bridged by three syn-syn carboxylate groups and by one syn-anti carboxylate group.[152] In the latter mixed carboxylate structure, the crotonate takes up a syn-anti bridging conformation.

In the known dimeric structures of silver carboxylates, Ag-O distances range from 2.158(3) Å in silver(I) 4-fluorophenoxyacetate [105] to 2.387(3) Å in silver(I) maleate [95] and O-Ag-O angles from 155.8(1)° in silver(I) (2-carbamoylphenoxy)acetate [94] to 171.8(1)° in silver(I) 4-fluorophenoxyacetate [105]. In this particular structure the Ag-O distances [2.204(5), 2.207(5) Å] and O-Ag-O angle [158.0(2)°] confirm the dimeric structure. The linking Ag(1)-O(1)'' distance [2.490(4) Å] is a typical value for silver carboxylate dimers or polymers.

The silver atom is coordinated by three carboxylato oxygen atoms producing a T-shaped environment [O-Ag-O 103.33(14)°, 93.4(2)°]. If an additional bond is considered between Ag(1) and Ag(1)', then the silver atom can be considered to be four-coordinate.

The supramolecular structure of this complex is dominated by polymeric sheets of molecules, parallel to the ab plane and at the unit cell intervals along c, affording a distorted octahedral coordination sphere about the transition metal. Ag(1) (in the

asymmetric unit) bonds to O(1) of the same molecule and to both Ag(1) and O(2) of the lattice neighbour generated by the operator -x, 1-y, 1-z. An additional bond to silver arises by interaction with O(1) of the molecule generated via the 0.5+x, 1.5-y, z symmetry transformation. In the structure two long intermolecular interactions [Ag(1)-C(2) = 3.039(6) Å, Ag(1)-C(3) = 2.870(6) Å] are present between silver and the vinyl moiety of the residue generated by the transformation 1+x, y, z. These are too long to be considered as strong π-bonds when compared with π-bonds in silver trifluoroacetate·benzene [Ag-C = 2.42 Å] and in silver(I) maleate [Ag-C = 2.448(5), 2.529(4) Å]. However it is reasonable to propose that a weak π-bond is present particularly when compared with the silver-phenyl ring π-interactions found in silver(I) (2-carbamoylphenoxy)acetate [Ag-C = 3.094, 3.078(4) Å][94] and a phenyl-substituted cyclohexanecarboxylate structure [Ag-C = 2.76(3), 2.92(3) Å][120]. There is a possibility of another interaction between Ag(1) and O(2) [3.132(5) Å] generated by the operator -0.5-x, 0.5+y, -z. The overall geometry around the silver atom can be described as distorted octahedral.

It was also observed that the methyl of the tiglato group has changed position from trans to cis. The torsion angle of C(4)-C(3)-C(2)-C(5) of 1.4(10) ° is indicative of a cis position of the methyl of the tiglato group. This could be explained by the coordination of the silver atom, which pushes away the methyl therefore becoming a cis complex. Therefore strictly the compound is no longer the tiglate, rotation having generated an arrangement close to the alternative cis-2,3-dimethylacrylate anion.

Bond lengths (Å)	**Angles (°)**
Ag(1) - O(1) = 2.204(5)	O(1) - Ag(1) - O(2) #1 = 158.0(2)
Ag(1) - O(2)#1 = 2.207(5)	O(1) - Ag(1) - O(1) #2 = 103.33(14)
Ag(1) - O(1) #2 = 2.490(4)	O(2) #1 - Ag(1) - O(2) #2 = 93.4(2)
Ag(1) - Ag(1) #1 = 2.8532(10)	

#1: -x, -y+1, -z+1.

#2: x+1/2, -y+3/2, z.

Table 2.8 Relevant bond lengths and angles of complex (**8**).

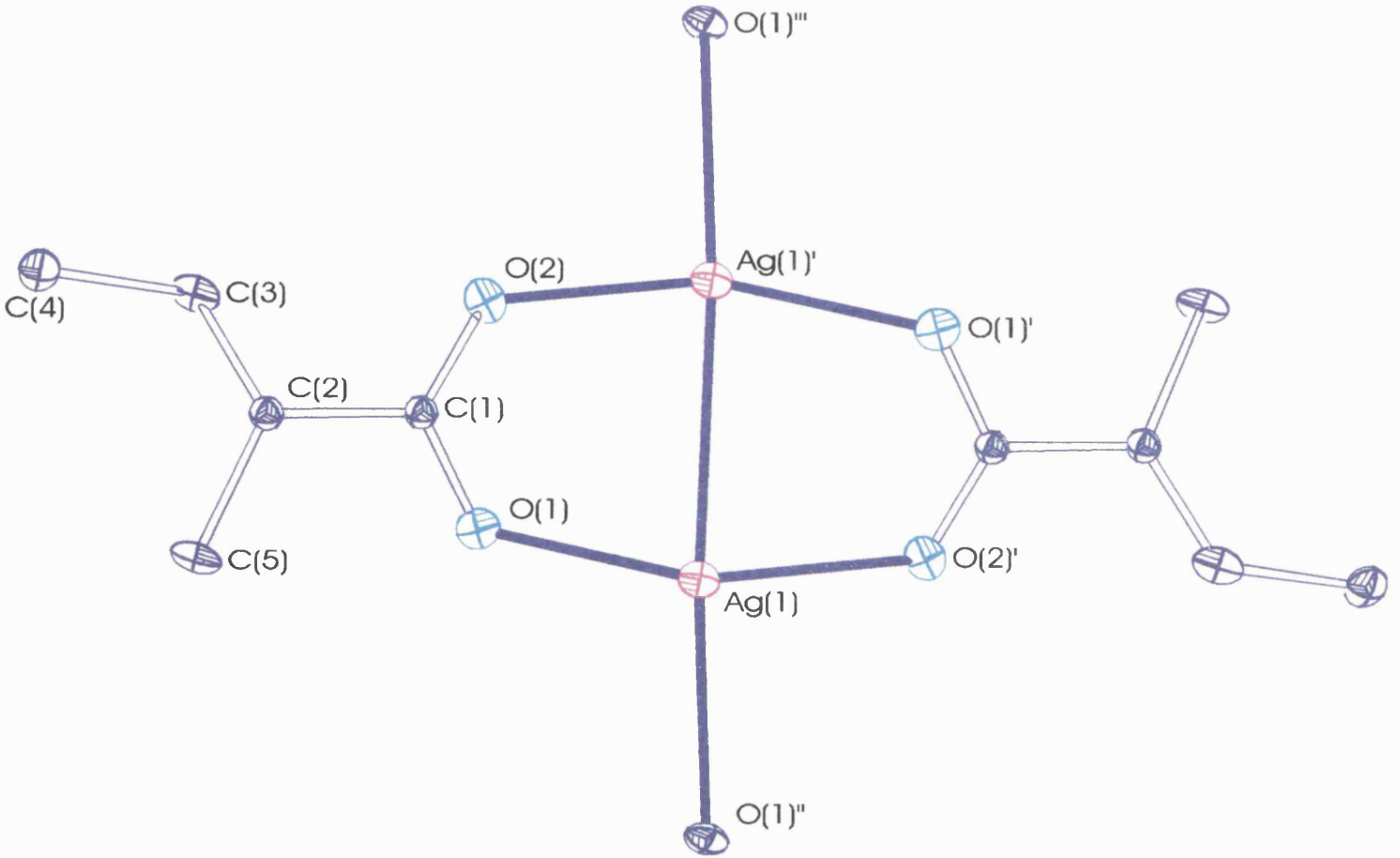

Asymmetric unit is denoted with unprimed labels.
Primed labels represent atoms generated by the transformation -x, 1-y, 1-z.
Doubly and triply primed labels pertain to atoms generated via the operations 0.5+x, 1.5-y, z and -0.5-x, -0.5+y, 1+z respectively.

Figure 2.14 Structure of Silver(I) Tiglate (**8**).

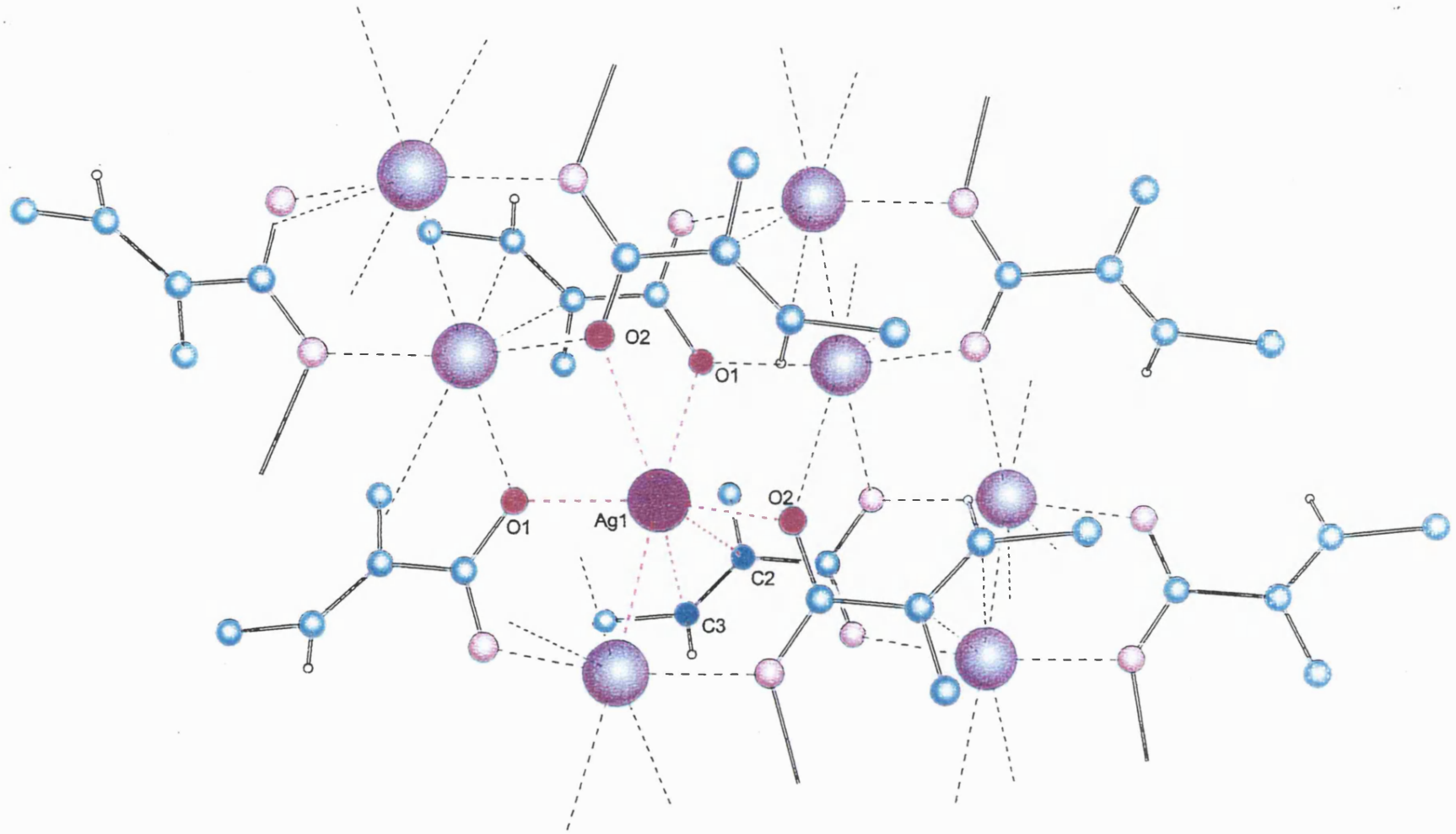

Figure 2.15 Polymeric structure of Silver(I) Tiglate (**8**).

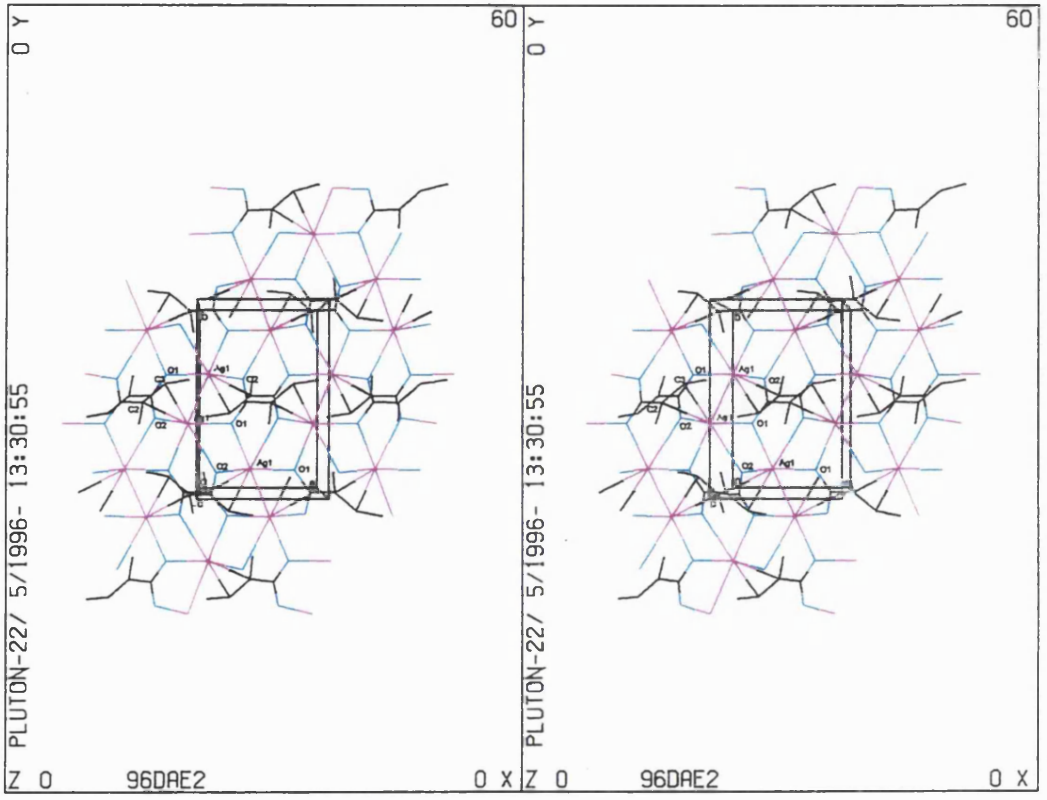

Figure 2.16 2-Dimentional polymeric arrangement of Silver(I) Tiglate (**8**).

2.4.6 X-ray Crystal Structure Determination of (*O,O'*Cyanoacetato) *bis*(triphenylphosphine)silver(I).

The structure of the molecule is presented in Figure 2.17 and Table 2.9 summarises relevant bond lengths and angles (See appendix 3 for further data). Crystals were grown slowly from an ethanol solution in a refrigerator.

The cyanoacetate can show many different modes of coordination. For example, in the structure of $\{[Nd(O_2CCH_2CN)_3(DMF)(H_2O)]\cdot H_2O\}_n$, the cyanoacetate ligands were found to be O-unidentate or O,O';O-bridging or chelating bidentate.[153] In $[Fe_3(\mu_3\text{-}O)(O_2CCH_2CN)_6(H_2O)_3]$[154], the cyanoacetate ligands were all O,O'-bridging bidentate and in $[Cd(O_2CCH_2CN)]_n$[155], the cyanoacetate ligands are O,O';O-bridging bidentate and O,O';N-bridging tridentate ligands. In $[Cu(O_2CCH_2CN)(PPh_3)_2]_2$ the copper atom is bonded via one oxygen from a unidentate cyanoacetate group and from the nitrogen of another cyanoacetate group.[156] Finally, in the structure of $[Cu(O_2CCH_2CN)_2H(PPh_3)_2]_2$, the copper atom is bonded to two nitrogens from the cyanoacetate group.[157]

The present complex is a monomer with a bidentate O,O'-cyanoacetate ligand and two triphenylphosphine ligands in which the silver has a highly distorted tetrahedral arrangement.

The cyanoacetate itself is polymeric with the bis(carboxylato-O,O') dimers containing an eight-membered central ring $[Ag(O\text{-}C\text{-}O)]_2$. The dimers are extended into a polymeric chain by a terminal linkage of N from a CN group to silver atoms of adjacent dimer units, with Ag-N distances of 2.370(6) Å.[96] Therefore this polymeric structure must be broken down on reaction with triphenylphosphine producing monomers in which the coordination mode of the cyanoacetate has changed from bridging to chelating. Unlike the parent cyanoacetate where the nitrogen of the CN group is used to generate the polymer, it is not coordinated to silver in the adduct.

The C≡N distance [1.103(6) Å] is shorter than in the parent silver(I) cyanoacetate [1.157(10) Å] [96] and in cadmium cyanoacetate [1.132(10) Å and 1.139(9) Å] [155] in which the CN group is bonded to a further metal atom.

The C-C≡N angle [178.9(8)°] is close to 180° and can be compared to those of silver(I) cyanoacetate [177.3(6) °] [96] and cadmium cyanoacetate [179.5(8)°].[155]

In this structure, the Ag-O distances [2.495(2), 2.427(2) Å] and the O-Ag-O angle [52.61(7)°] are similar to those of $[Ag(O_2CCH_3)(PPh_3)_2]$ [2.437(6) , 2.416(6) Å and 53.4 (2)°] [1] and $[Ag(O_2CC_2F_5)(PPh_3)_2]$ [2.495, 2.532 Å and 51.3(2)°].[1] However the Ag-O distances are considerably longer than in the parent silver(I) cyanoacetate [2.198(5), 2.187(4) Å] and the O-Ag-O angle [52.61(7)°] is much more acute than in the parent silver salt [162.6(2)°][96] as a result of the change in carboxylate coordination mode. As expected, the cyanoacetate group is planar. The slightly asymmetrical chelation of the cyanoacetate group, demonstrated by the Ag-O bond lengths and the Ag-O-C angles [89.0(2), 92.0(2)°], has also been noted in $[Cu(O_2CCH_3)(PPh_3)_2]$ [Cu-O-C angle 91.3(4) and 87.4(6)°].[158]

For silver carboxylate triphenylphosphine complexes, the Ag-P distances range from 2.426(2) Å in $[Ag(O_2CH)(PPh_3)_2]$ [128] to 2.452(4) Å in $[Ag(O_2CCH_3)(PPh_3)_2]$.[1] In the present structure, the Ag-P distances [2.4185(10), 2.4464(10) Å] are within this range. The P-Ag-P angle [127.93(3)°] is similar to those found in $[Ag(O_2CC_2F_5)(PPh_3)_2]$ [129.28(5)°][1] and $[Ag(O_2CCH_3)(PPh_3)_2]$ [129.7(2)°].[1]

Bond lengths (Å)	**Angles (°)**
Ag(1) – O(1) = 2.495(2)	O(1) – Ag(1) – O(2) = 52.61(7)
Ag(1) – O(2) = 2.427(2)	C(37) – O(1) – Ag(1) = 89.0(2)
Ag(1) – P(1) = 2.4185(10)	C(37) – O(2) – Ag(1) = 92.0(2)
Ag(1) – P(2) = 2.4464(10)	P(1) – Ag(1) – P(2) = 127.93(3)

Table 2.9 Relevant bond lengths and angles of complex (**2**).

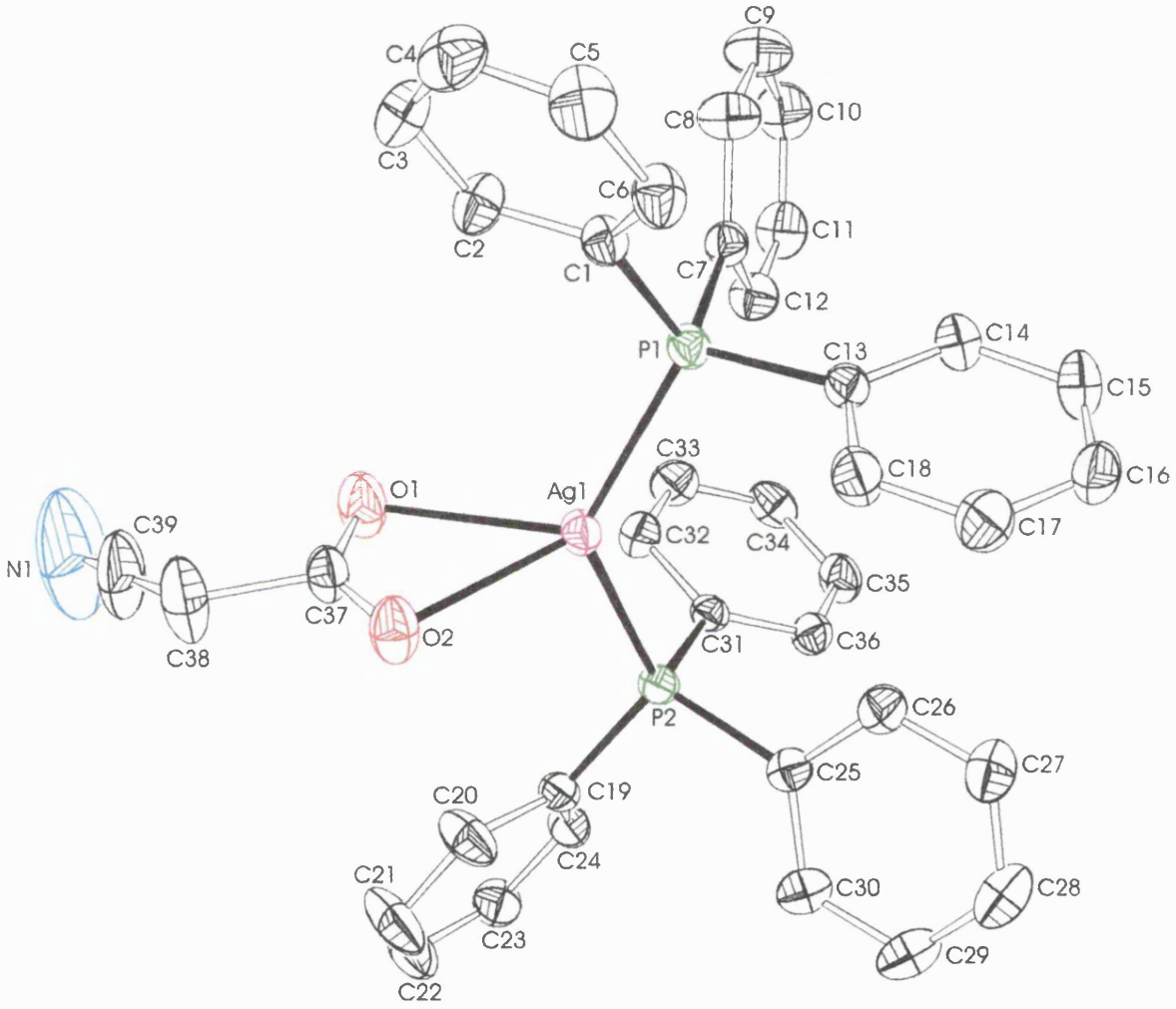

Figure 2.17 Structure of (*O,O'*-cyanoacetato)*bis*(triphenylphosphine)silver(I) (**2**).

2.4.7 X-Ray Crystal Structure Determination of (*O,O'*-Allylacetato) *bis*(triphenylphosphine)silver(I).

Crystals of (*O,O'*-allylacetato)*bis*(triphenylphosphine)silver(I) were grown slowly by recrystallisation from a toluene solution in a refrigerator. Selected bond lengths and angles are given in Table 2.10, with further data provided in Appendix 4.

A search of the literature has shown that no other structure of metal allylacetate compounds have been reported.

There are two independent molecules of (O,O'-allylacetato) *bis*(triphenylphosphine)silver(I) in the unit cell. A diagram of the molecule is shown in Figure 2.18. This complex is a monomer and the coordination geometry of silver is distorted tetrahedral. One chelating allylacetate ligand and two triphenylphosphine ligands coordinate the silver atom.

The bond distances and angles within the carboxylato ligand [Ag-O bond lengths: 2.401(3)Å and 2.464(4)Å and O-Ag-O angle 52.84(11)°] are similar to those of $[Ag(O_2CCH_3)(PPh_3)_2]$ [2.420(2)Å, 2.438(2)Å, 2.379(3)Å, 2.510(3)Å and 53.33(7)°,52.3(1)°],[129] $[Ag(O_2CC_2F_5)(PPh_3)_2]$ [2.495Å, 2.532(2)Å and 51.3(2)°][1] and $[Ag(O_2CH)(PPh_3)_2.HO_2CH]$ [2.550(7)Å 2.713(8)Å and 49.5(2)°].[128] The atoms Ag(1), O(1), O(2), C(37) and C(38) form a plane. The differing Ag-O bond lengths demonstrate the slightly asymmetric chelation of the allylacetate group and Ag-O-C angles of 93.5(2)° and 90.7(3)° are similar to those in $[Ag(O_2CCH_2CN)(PPh_3)_2]$ [89.0(2)° and 92.0(2)°] and $[Cu(O_2CCH_3)(PPh_3)_2]$ [91.3(4)° and 87.4(6)°] [158], being significantly less than the regular tetrahedral angle as a result of the small bite of chelating carboxylate groups.

The Ag-P distances in silver carboxylate triphenylphosphine complexes range from 2.404(1)Å in $[Ag(O_2CCH_3)(PPh_3)_2]\cdot 1.5H_2O$ [129] to 2.4608(8)Å in $[Ag(O_2CCH_3)(PPh_3)_2]$.[129] In this structure, the Ag-P distances [2.450(2)Å and 2.433(2)Å] are within this range. The P-Ag-P angle [126.23(4)°] is similar to those found in $[Ag(O_2CCH_2CN)(PPh_3)_2]$ [127.93(3)°] and $[Ag(O_2CCH_3)(PPh_3)_2]\cdot 1.5H_2O$ [128.53(5)°][129] being larger than the tetrahedral angle as a result of the bulky nature of the phosphine ligands and the presence of small-bite chelating carboxylate.

The C=C bond distance [1.12(3) Å] in this structure is shorter than the double bond in silver(I) tiglate [1.339(9) Å] and in (*O,O'*-tiglato)*bis*(triphenylphosphine)silver(I)

[1.318(4) Å]. In this structure, the distances between the silver atom and the C=C double bond of the alllylacetato group [Ag(1)-C(40) = 5.42(4) Å and Ag(1)-C(41) = 6.18(4) Å] are far too long to be considered as a weak π-bond when compared to the corresponding distances of silver(I) tiglate [Ag(1)-C(2) = 3.039(6) Å, Ag(1)-C(3) = 2.870(6) Å].

Bond lengths (Å)	**Angles (°)**
Ag(1) – O(1) = 2.401(3)	O(1) – Ag(1) – O(2) = 52.84(11)
Ag(1) – O(2) = 2.464(4)	C(37) – O(1) – Ag(1) = 93.5(2)
Ag(1) – P(1) = 2.450(2)	C(37) – O(2) – Ag(1) = 90.7(3)
Ag(1) – P(2) = 2.433(2)	P(1) – Ag(1) – P(2) = 126.23(4)

Table 2.10 Relevant bond lengths and angles of complex (**6**).

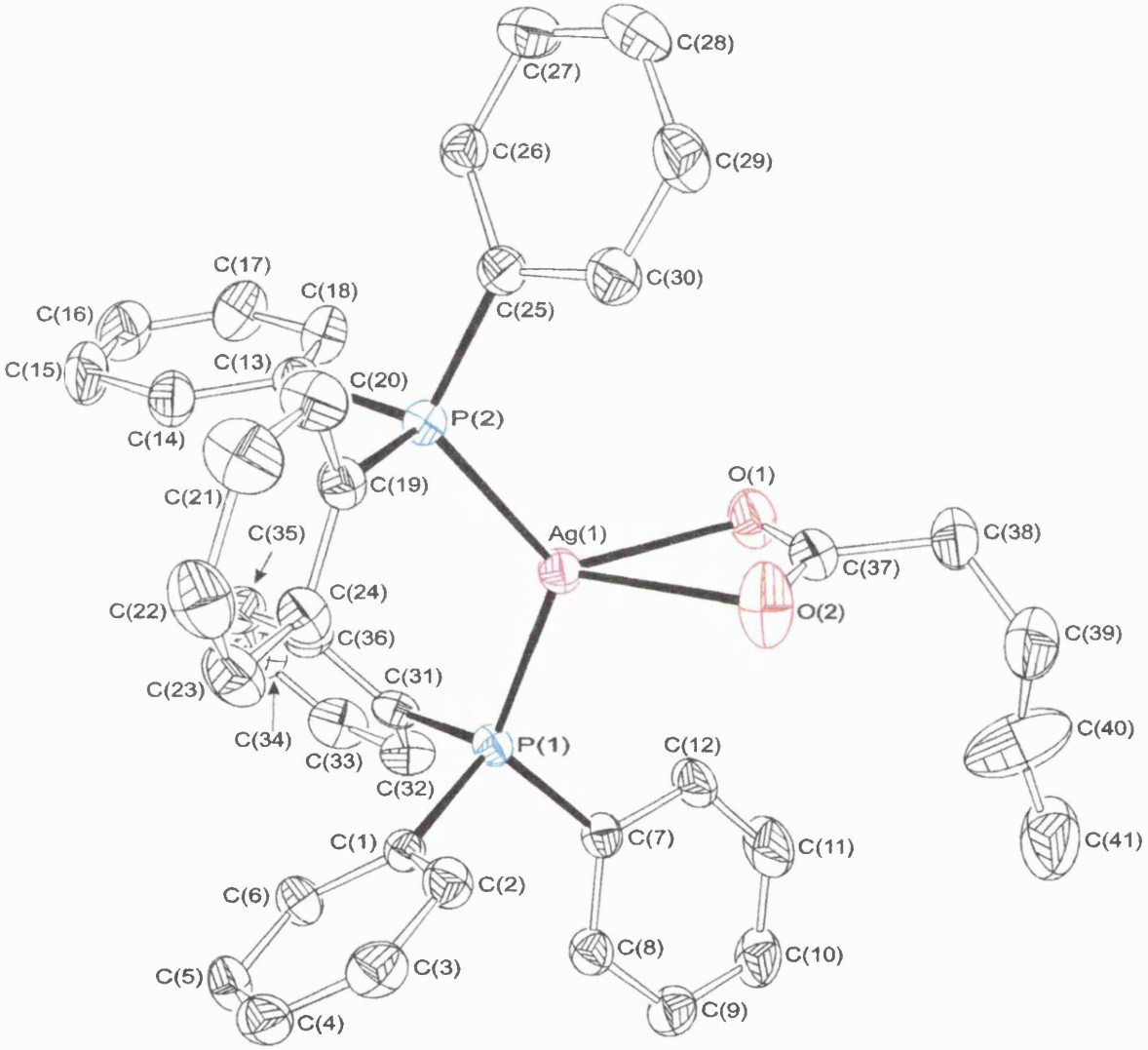

Figure 2.18 Structure of (*O,O'*-allylacetato)*bis*(triphenylphosphine)silver(I) (**6**).

2.4.8 X-Ray Crystal Structure Determination of (*O,O'*-Tiglato)*bis*(triphenylphosphine)silver(I).

Crystals of (*O,O'*-tiglato)*bis*(triphenylphosphine)silver(I) were grown by recrystallisation from a toluene solution in a refrigerator. Selected bond lengths and angles are given in Table 2.11 (See Appendix 5 for further data).

The structure can be compared to the structure of [Ru(BINAP) $\{O_2C(CH_3)C=CHCH_3\}_2$] (BINAP = 2,2'-bis(diphenylphosphino)-1,1'-binaphthyl) in which the tiglato is O,O'-chelating bidentate to the metal.[159] It was also found that there was no bonding interaction between the ruthenium atom and the C=C bond of the tiglato group.

The monomeric structure of the complex represented in Figure 2.19 is based on silver bonded to an O,O'-bidentate chelating tiglate ligand and two triphenylphosphine ligands giving the silver atom a distorted tetrahedral arrangement. The coordination mode of the tiglate has changed from bridging in the parent carboxylate to chelating in the complex. Unlike the parent tiglate where the double bond and a further oxygen from an adjacent tiglate ligand are used to generate the polymer, they are not coordinated to silver in the adduct.

The Ag-O bond distances in chelating carboxylato groups vary from 2.379(3) Å in $[Ag(O_2CCH_3)(PPh_3)_2]$[129] to 2.713(8) Å in $[Ag(O_2CH)(PPh_3)_2]$[128] and the O-Ag-O angle varies from 49.5(2)° in $[Ag(O_2CH)(PPh_3)_2.HCO_2H]$[128] to 53.7(1)° $[Ag(O_2CCH_3)(PPh_3)_2]\cdot 1.5H_2O$.[129] In this structure the Ag-O bonds [2.430(2)Å and 2.436(2)Å] are similar to those found in other silver (I) chelating carboxylato complexes but the O-Ag-O angle is slightly larger when compared to the values found in the literature. The tiglate group is planar. The Ag-O bond lengths [2.430(2)Å and 2.436(2)Å] and Ag-O-C angles [91.3(2)° and 91.7(2)°] indicate the presence of an essentially symmetric O,O'-chelation of the tiglate group.

The phosphorus ligands in the complex are unexceptional. Ag-P distances found in the complex [2.4099(7)Å and 2.4562(8)Å] are similar to those found in other silver(I) carboxylate bis(triphenylphosphine) complexes [2.404(1)Å to 2.4608(8)Å].[129] The P-Ag-P angle [131.11(2)°] is the second largest value recorded for silver carboxylate triphenylphosphine compounds. The C=C bond distance [1.318(4) Å] in this structure is

slightly shorter than the double bond in silver(I) tiglate [1.339(9) Å]. The distances between the silver atom and the C=C double bond of the tiglato group [Ag(1)-C(38) = 4.264(3) Å and Ag(1)-C(39) = 5.011(3) Å] are far too long to be considered as a weak π-bond when compared to the distances of silver(I) tiglate [Ag(1)-C(2) = 3.039(6) Å, Ag(1)-C(3) = 2.870(6) Å].

The methyl of the tiglato group has changed position from trans to cis as occurred in the parent tiglate structure. The torsion angle of C(41)-C(39)-C(38)-C(40) of 0.58(52)° is indicative of a cis position of the methyl of the tiglato group. This could be explained by the coordination of the silver atom, which pushes away the methyl therefore generating a cis complex. Therefore strictly the compound is no longer a tiglate but again rotation has produced a cis-2,3-dimethylacrylate rather than the trans-form.

Bond lengths (Å)	**Angles (°)**
Ag(1) – O(1) = 2.436(2)	O(1) – Ag(1) – O(2) = 53.86(6)
Ag(1) – O(2) = 2.430(2)	C(37) – O(1) – Ag(1) = 91.3(2)
Ag(1) – P(1) = 2.4099(7)	C(37) – O(2) – Ag(1) = 91.7(2)
Ag(1) – P(2) = 2.4562(8)	P(1) – Ag(1) – P(2) = 131.11(2)

Table 2.11 Relevant bond lengths and angles of complex (**9**).

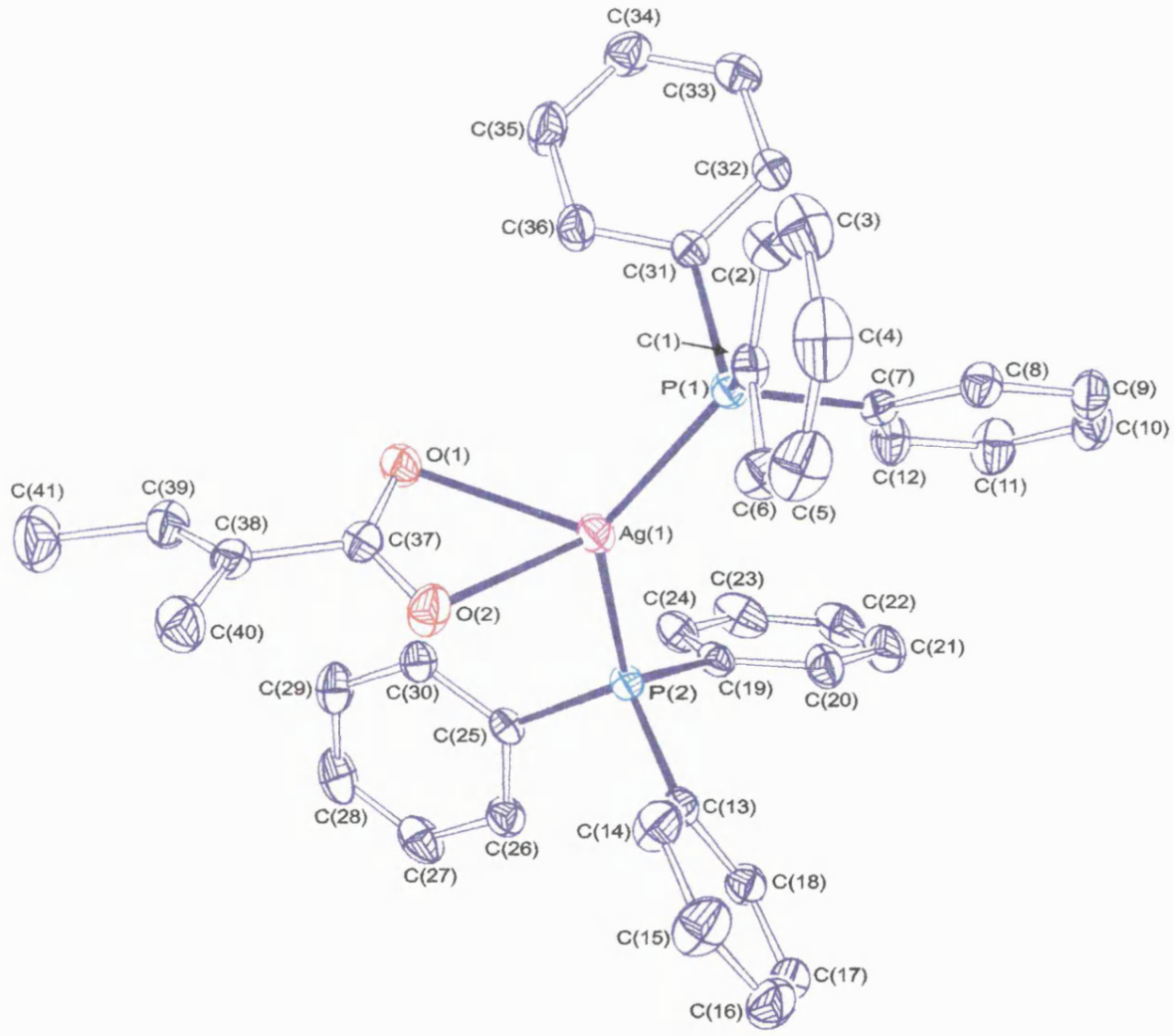

Figure 2.19 Structure of (*O,O'*-tiglato)*bis*(triphenylphosphine)silver(I) (**9**).

2.4.9 Thermogravimetric analysis (TGA).

TGA analyses were carried out on compounds (**2**), (**4**), (**6**), (**7**), (**9**), (**10**) and (**12**) under an inert helium atmosphere, in order to obtain information on their relative stabilities and to determine the temperature at which decomposition may start.

Compounds (**6**), (**7**), (**9**), (**10**) and (**12**) were found to decompose by a single thermal decomposition stage starting between 142°C and 198°C and finishing between 290°C and 325°C. The mass loss in this single stage correlates with the thermal decomposition of the whole molecule leaving a solid residue. No individual decomposition stages were evident.

The single stage decompositions of compounds (**6**), (**7**), (**9**), (**10**) and (**12**) are similar to the decomposition of mono(trimethylphosphine) adducts of silver(I) fluorocarboxylates,[160] silver(I) carboxylates[1] and bis(triphenylphosphine) adducts of silver(I) fluorocarboxylates.[1]

However, the thermal decomposition of compound (**4**) appears to be a two-stage process. The initial decomposition temperature of the first stage was at 116°C with a 2.6% mass loss (correlating to C_2H_2) and this was followed by a second stage between 197°C and 305°C.

The TGA of compound (**2**) showed a three-stage decomposition process. The first decomposition began at 142°C and resulted in a mass loss of 6%. This value may correspond with the loss of CO_2 (theoretical % = 6.1). The second stage started at 163°C with a mass loss of 7.3% by weight and the last stage covered the 192-302°C range with a loss of 68.3% by weight. The mass loss in the second stage correlates with the loss of $NCCH_2$ (theoretical % = 5.6) followed by the loss of triphenylphosphine (theoretical % = 73.2).

The final product after decomposition should be silver. The theoretical % weight residues for silver are given in Table 2.12. The experimental values found are much higher then the theoretical values except for compound (**2**). It is possible, therefore that the residue may also contain carbon and traces of silver(I) phosphate obtained by oxidation of

triphenylphosphine. Silver oxide would not be present in the residue due to its decomposition to the metal at 250°C. However, the weight of the residue remaining for compounds (**7**) and (**10**) suggests that it is most likely to be silver sulfide. But since in subsequent CVD testing, it was shown that some silver was formed in a N_2 atmosphere, it is possible that the residue is a mixture of silver and its sulfide.

Compounds	Decomposition temperature (°C)		Weight loss (%)	Detached group (% calc)	Residue remaining		
	$T_{initial}$	T_{final}			%found	$\%Ag_{calc}$	$\%Ag_2S_{calc}$
$[Ag(O_2CCH_2CN)(PPh_3)_2]$ (**2**)	142 163 192	163 192 302	6.1 7.3 68.3	CO_2 (6.1) $NCCH_2$ (5.6) 2 PPh_3 (73.2)	15.7	15.3	
$[Ag(O_2CCH{=}CH_2)(PPh_3)_2]$ (**4**)	116 197	146 305	2.6 76.5	C_2H_2 (3.7) 2 PPh_3 (74.6) 2 PPh_3 + HCO_2 (80.9)	17.4	15.1	
$[Ag\{O_2C(CH_2)_2CH{=}CH_2\}(PPh_3)_2]$ (**6**)	196	325	78.5	2 PPh_3 (71.7) 2 PPh_3 + RCO_2 (85.3) 2 PPh_3+ $CH_2{=}CHCH{=}CH_2$ (79.1)	17.9	14.7	
$[Ag\{O_2C(CH_2)_2CH{=}CH_2\}(PhSC_2H_4SPh)_2]$ (**7**)	142	290	85.3	2 $PhSC_2H_4SPh$ (70.4) 2 $PhSC_2H_4SPh$ + RCO_2 (84.6) 2 $PhSC_2H_4SPh$ + $CH_2{=}CHCH{=}CH_2$ (78.1)	17.3	15.4	17.7
$[Ag\{O_2C(CH_3)C{=}CHCH_3\}(PPh_3)_2]$ (**9**)	198	309	77.8	2 PPh_3 (71.7) 2 PPh_3 + RCO_2 (85.3) 2 PPh_3 + $CH_3C{\equiv}CCH_3$ (79.1)	19.2	14.7	
$[Ag\{O_2C(CH_3)C{=}CHCH_3\}(PhSC_2H_4SPh)_2]$ (**10**)	152	300	87.6	2 $PhSC_2H_4SPh$ (70.4) 2 $PhSC_2H_4SPh$ + RCO_2 (84.6) 2 $PhSC_2H_4SPh$ + $CH_3C{\equiv}CCH_3$ (78.1)	14.5	15.4	17.7
$[Ag(O_2CCH{=}CHC_6H_5)(PPh_3)_2]$ (**12**)	178	325	78.5	2 PPh_3 + RCO_2 (86.2) 2 PPh_3 + $(C_6H_5)C{\equiv}CH$ (80.4)	17.7	13.8	

Table 2.12 TGA analysis of triphenylphosphine and 1,2-bis(phenylthio)ethane adducts of silver(I) carboxylates.

2.4.10 CVD Testing of precursors.

Compounds (**2**), (**6**), (**7**), (**9**), (**10**) and (**12**) were tested as potential precursors for silver CVD, the results being summarised in Tables 2.15 and 2.16.

Films were grown on a glass substrate (SiCO) under a N_2 atmosphere at 1 bar pressure, using a horizontal cold wall reactor. The precursor was delivered in the gas phase as the aerosol of the compound dissolved in a solvent (THF, methanol or ethanol) and swept into the reactor using N_2 as the carrier gas.

SiCO is a glass coated on one surface, the composition of the coating being roughly equal parts of silicon, carbon and oxygen, hence the SiCO abbreviation. The purpose of the coating is (a) to generate a uniform nucleation surface, (b) to block Na^+ ions from diffusing from the glass into the coating, which would deteriorate both cosmetic and electrical properties and (c) to colour suppress the visible reflection.

The films grown were found to be 'soft' and could be scratched or damaged relatively easily by touching.

Morphologies of the deposited films were examined using various techniques e.g. visual inspection, Scanning Electron Microscopy (SEM), Energy Dispersive X-ray Spectrometry (EDXS) which was used to determine the purity of the films, sheet resistance and reflectance of the films.

A nucleation growth study was also carried out on compounds (**6**) and (**9**) and will be discussed later.

The quality and nature of the resulting films were found to be dependent on the precursor used.

Each precursor was tested at different concentrations, temperatures, N_2 gas flow rate and run time, and a summary of the data obtained is shown in Table 2.13.

Conditions	**(2)**	**(6)**	**(7)**	**(9)**	**(10)**	**(12)**
Concentration ($g.l^{-1}$)	12.5	12-18	12-25	21-46.6	15-23	45-47
Reactor temperature (°C)	300-546	300	250-300	300	200-348	200-398
N_2 gas flow rate ($l.min^{-1}$)	1.0-1.05	0.9-1.05	0.9-1.05	0.8-1.05	0.9-1.05	0.9-1.05
Run time (min)	22	32-92	35-75	20-69	34-76	29-70

Table 2.13 Conditions used in the CVD testing of adducts of silver(I) carboxylates.

Compound (**2**) did not produce any films at temperatures ranging from 300°C to 550°C.

Compound (**6**) was tested at 300°C, at different concentrations and N_2 gas flow rates. After a 32 minute run time, a thin yellow-brown film was observed. Therefore longer run times were attempted. After a 91 minute run time, a metallic thick grey film was obtained. With a decrease of run time to 66 minutes, a reflective transparent silver film was obtained.

Compound (**7**) produced a thin yellow-brown film on the glass substrate and an opaque grey-brown film on the top plate held at 300°C. With a decrease of temperature to 275°C and a run time of 35 minutes, a thinner yellow-brown film on the glass substrate and a brown silvery film on the top plate was observed. A silver mirror-like film was obtained on the top plate at 250°C after a 35 minute run time.

Compound (**9**) produced a transparent and reflective silver film after a 64 minute run time at 300°C with N_2 carrier gas flow rate of 1.0 $l.min^{-1}$.

Compound (**10**) was tested using two different solvents, ethanol and methanol. Films produced from ethanol solution were found to be yellow and very thin. By changing the solvent to methanol, and keeping the same concentration as in the previous tests, films were found to be thicker and varied from yellow to yellow-brown in colour. Once again, it was found that deposition also occurred on the top plate. A silver film was obtained on the top plate after a 34 minute run time at 250°C with a N_2 gas flow rate of 0.9-0.95 $l.min^{-1}$.

Although compound (**12**) was tested at different conditions, only thin yellow-brown films could be obtained.

Deposition on the top plate may be due to a thermophoretic effect.[161] Once the precursor is in the reactor, gas phase reaction occurs and then the precursor is adsorbed on to the glass substrate. However, due to thermal diffusion effects, the gas species in an initially homogeneous gas mixture will separate under the influence of a temperature gradient. In cold wall reactors, thermal diffusion is important because of the large temperature gradients present. Thermal diffusion causes large heavy gas molecules to concentrate in cold regions (e.g. top plate) of the reactor whereas small light molecules concentrate in the hotter parts of the reactors (e.g. glass substrate).

The estimated deposition rate was calculated from the ratio of the estimated thickness of the film over a run time period at a specified temperature. The estimated deposition rate for compounds (**6**), (**7**), (**9**) and (**10**) varied between 2.4 $nm.min^{-1}$ to 2.6 $nm.min^{-1}$. These values are much higher when compared to other phosphine adducts of silver(I) carboxylates already studied (0.4 to 1.4 $nm.min^{-1}$)

SEM studies of film morphologies showed a smooth texture for compounds (**6**) and (**9**) with grain sizes of 45-90 nm in diameter for compound (**6**) and 30-50 nm in diameter for compound (**9**) (Pictures 2.1 to 2.4). Films grown from compounds (**7**) and (**10**) appeared to be rough or uneven by comparison to compounds (**6**) and (**9**) (Pictures 2.5 and 2.6).

The compositions of these films were established by EDXS analysis. This technique did not provide quantitative analysis of impurities but did highlight the identities of impurities that are present. The analysis revealed that the films are composed mainly of silver with some C, O and Si impurities, the Si and O presumably arising from the glass substrate. Phosphorus was completely absent from all films grown (Spectrum 2.1). However, sulfur was detected in films grown from (**7**) and (**10**).

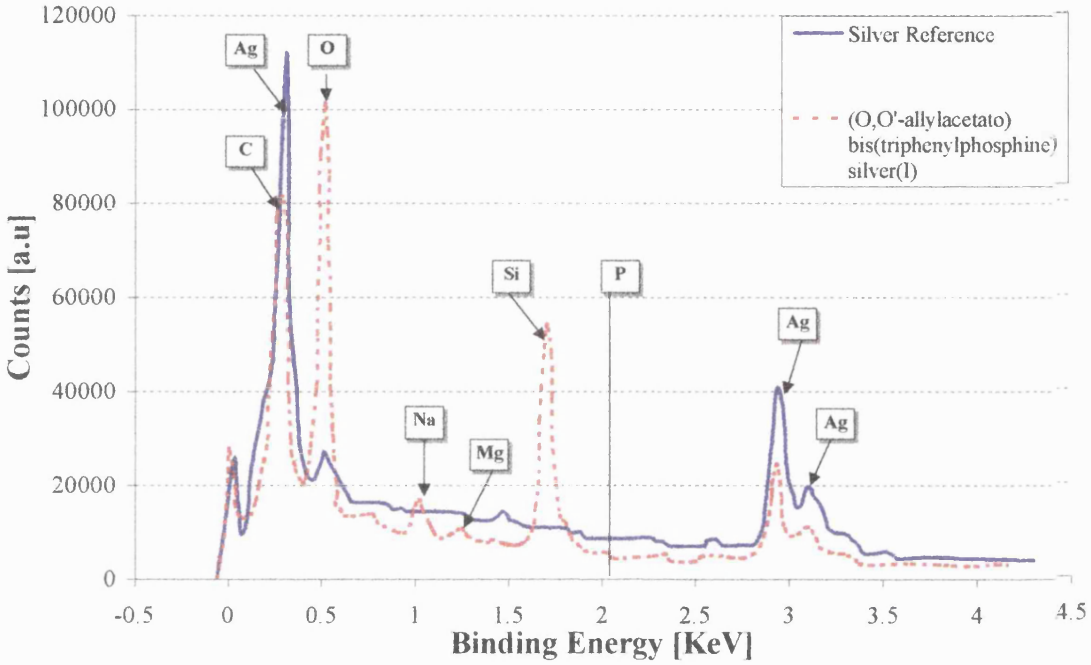

Spectrum 2.1 EDXS of (*O,O'*-allylacetato)*bis*(triphenylphosphine)silver(I) (**6**).

Table 2.14 summarises the energy at which electrons are ejected from different orbitals.

Atoms	Orbitals	Binding energy (keV)
C	1s	0.3
Ag	2p 3d	2.9 to 3.1 0.3
O	1s	0.5
Na	1s	1.0
Mg	1s	1.3
Si	1s	1.7

Table 2.14 Energy of electrons ejected from different orbitals.

Sheet resistance measurements were obtained for compounds (**6**) and (**9**). Sheet resistance per 25 mm^2 (depicted as □) were measured as 14 Ω/□ for (**6**) and 16 Ω/□ for (**9**). These values are considerably lower when compared to other phosphine adducts of silver(I) carboxylates already studied (168 to 17×10^6 Ω/□)[1], but higher when compared to triphenylphosphine adducts of silver(I) β-diketonates and β-ketoiminates (2.2. and 1.1 Ω/□)[1].

Reflectance measurements were carried out on films grown from compounds (**6**), (**7**), (**9**) and (**10**) and percentage reflectance reported at a wavelength of 0.55 μm, which corresponds to the sensitivity of the eye. A typical example is shown is Spectrum 2.1. Measurements were performed only on the coated surface for all films analysed. Films grown from precursors (**6**), (**7**) and (**9**) gave reflectance values at 0.55 μm ranging between 23% and 51%. These values are much higher when compared to other phosphine adducts of silver(I) carboxylates and flurocarboxylates already studied (0.5 to 49.7%)[1]. The reflectance of a film grown from compound (**6**), (51%) was found to be lower than that grown from [Ag(hfacNhex)(PPh_3)] (64.7 %)[1], reported as a good reflector. However, the maximum reflectance (66%) for a film grown from compound (**6**) was measured at a wavelength of 1.04 μm.

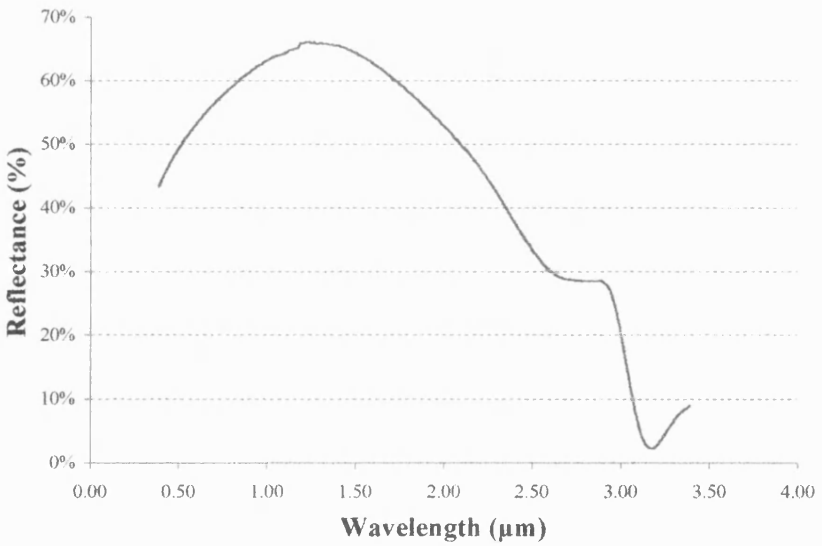

Spectrum 2.2 Reflectance measurements of a film grown from (*O,O'*-allylacetato)*bis* (triphenylphosphine)silver(I) (**6**).

Compounds	Visual appearance	SEM appearance	Detected impurities (EDXS)	Pictures
$[Ag(O_2CCH_2CN)(PPh_3)_2]$ (**2**)	No film produced.	-	-	
$[Ag\{O_2C(CH_2)_2CH{=}CH_2\}(PPh_3)_2]$ (**6**)	Transparent silver reflective film.	Smooth surface.	C, O	2.1 and 2.2
$[Ag\{O_2C(CH_2)_2CH{=}CH_2\}(PhSC_2H_4SPh)_2]$ (**7**)	Thin yellow film on glass and silver film on the top plate.	Rough or uneven surface.	C, S, O	2.5
$[Ag\{O_2C(CH_3)C{=}CHCH_3\}(PPh_3)_2]$ (**9**)	Transparent silver reflective film.	Smooth surface.	C, O	2.3 and 2.4
$[Ag\{O_2C(CH_3)C{=}CHCH_3\}(PhSC_2H_4SPh)_2]$ (**10**)	Thin yellow film on glass and silver film on the top plate.	Rough or uneven surface.	C, S, O	2.6
$[Ag(O_2CCH{=}CHC_6H_5)(PPh_3)_2]$ (**12**)	Transparent thin brown film.	-	C, O	-

Table 2.15 Appearance and properties of the films grown from adducts of silver(I) carboxylates.

Compounds	Run time (minutes)	Estimated thickness (nm) (± 20%)	Estimated deposition rate ($nm.min^{-1}$)	Sheet resistivity (Ω/□)	Reflectance (%) (measured at λ = 0.55 μm)
$[Ag(O_2CCH_2CN)(PPh_3)_2]$ (**2**)	24	-	-	-	-
$[Ag\{O_2C(CH_2)_2CH=CH_2\}(PPh_3)_2]$ (**6**)	66	170	2.5	14	51
$[Ag\{O_2C(CH_2)_2CH=CH_2\}(PhSC_2H_4SPh)_2]$ (**7**)	35	89	2.5	-	23
$[Ag\{O_2C(CH_3)C=CHCH_3\}(PPh_3)_2]$ (**9**)	64	168	2.6	16	49
$[Ag\{O_2C(CH_3)C=CHCH_3\}(PhSC_2H_4SPh)_2]$ (**10**)	34	84	2.4	-	15
$[Ag(O_2CCH=CHC_6H_5)(PPh_3)_2]$ (**12**)	66	-	-	-	-

Table 2.16 Properties of the films grown from adducts of silver(I) carboxylates.

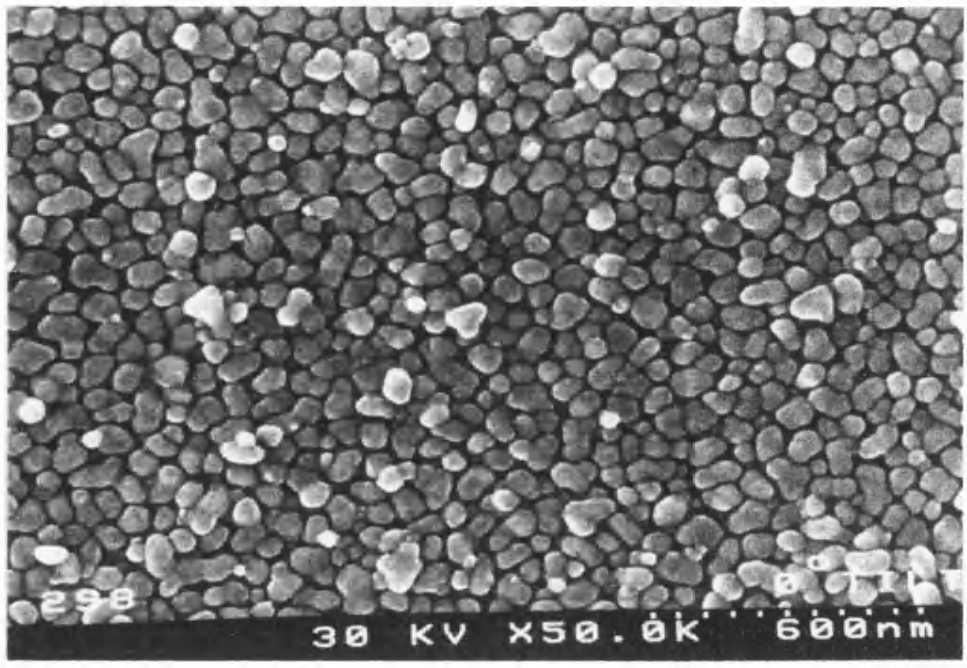

Picture 2.1 SEM image of a film grown from [Ag{$O_2C(CH_2)_2CH=CH_2$}(PPh_3)$_2$] (**6**).

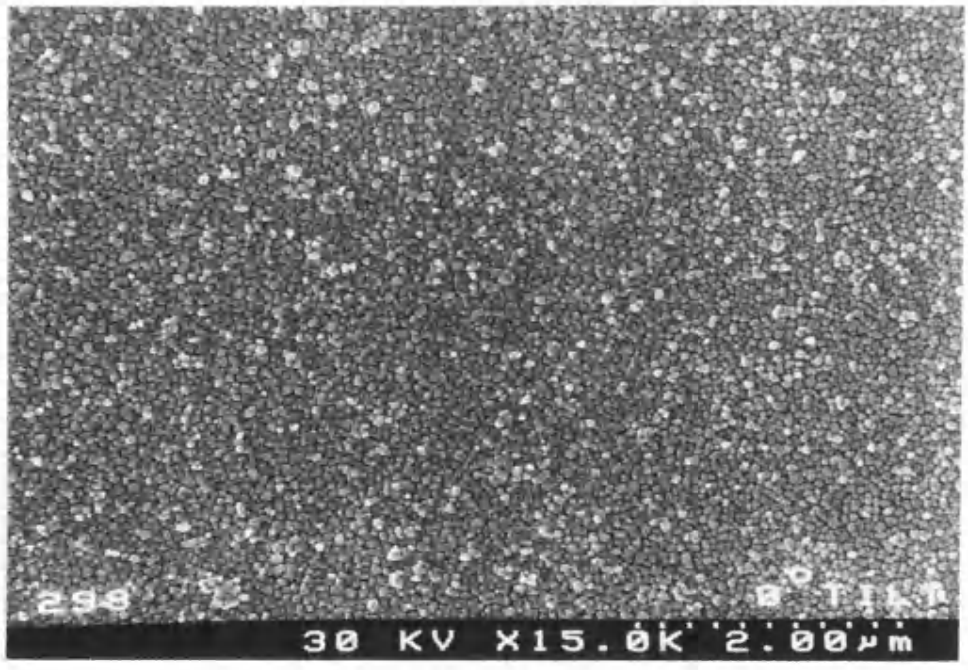

Picture 2.2 SEM image of a film grown from [Ag{$O_2C(CH_2)_2CH=CH_2$}(PPh_3)$_2$] (**6**).

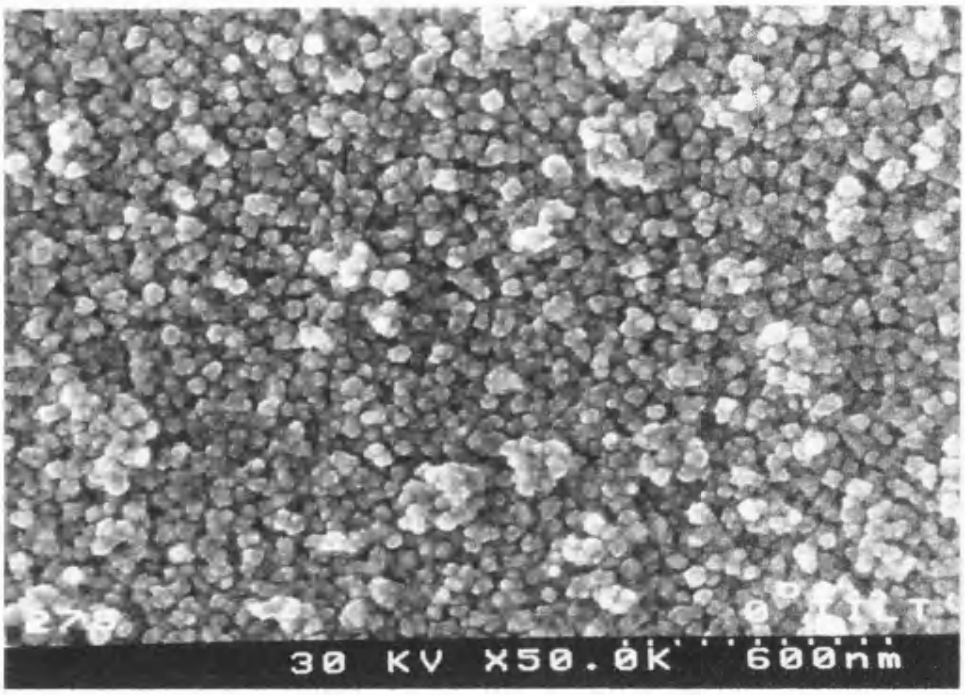

Picture 2.3 SEM image of a film grown from [Ag{$O_2C(CH_3)C{=}CHCH_3$}$(PPh_3)_2$] (**9**).

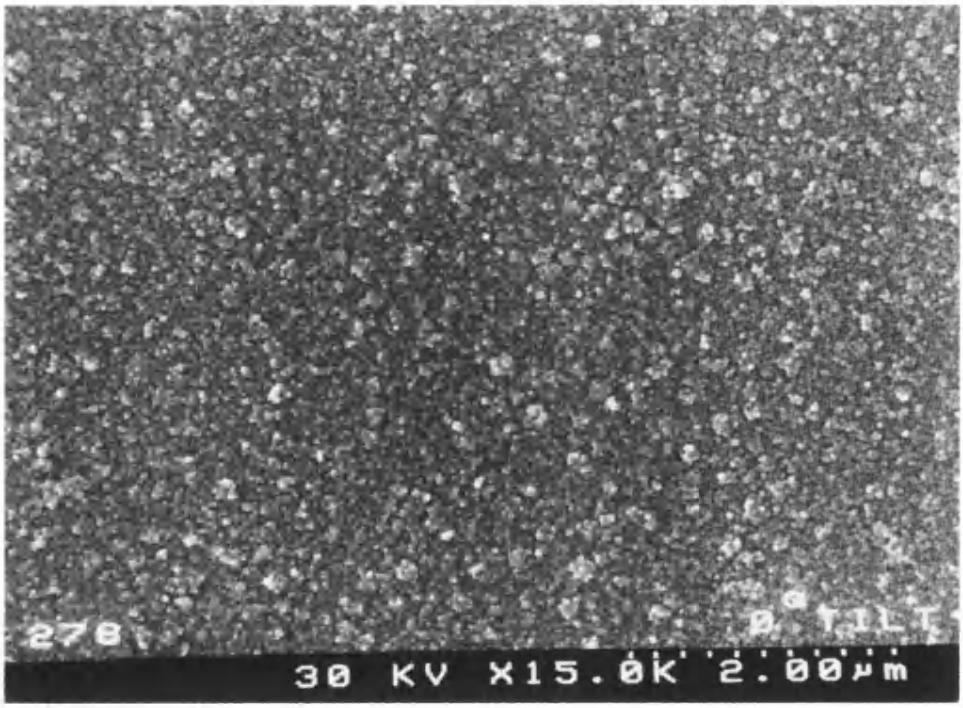

Picture 2.4 SEM image of a film grown from [Ag{$O_2C(CH_3)C{=}CHCH_3$}$(PPh_3)_2$] (**9**).

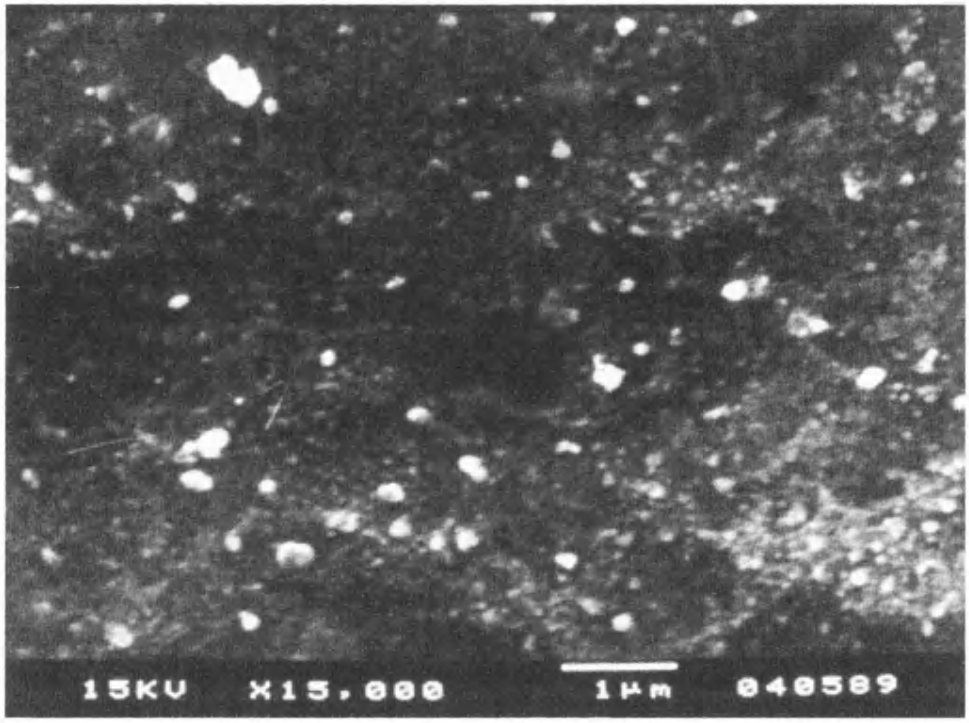

Picture 2.5 SEM image of a film grown from $[Ag\{O_2C(CH_2)_2CH=CH_2\}(PhSC_2H_4SPh)_2]$ (**7**).

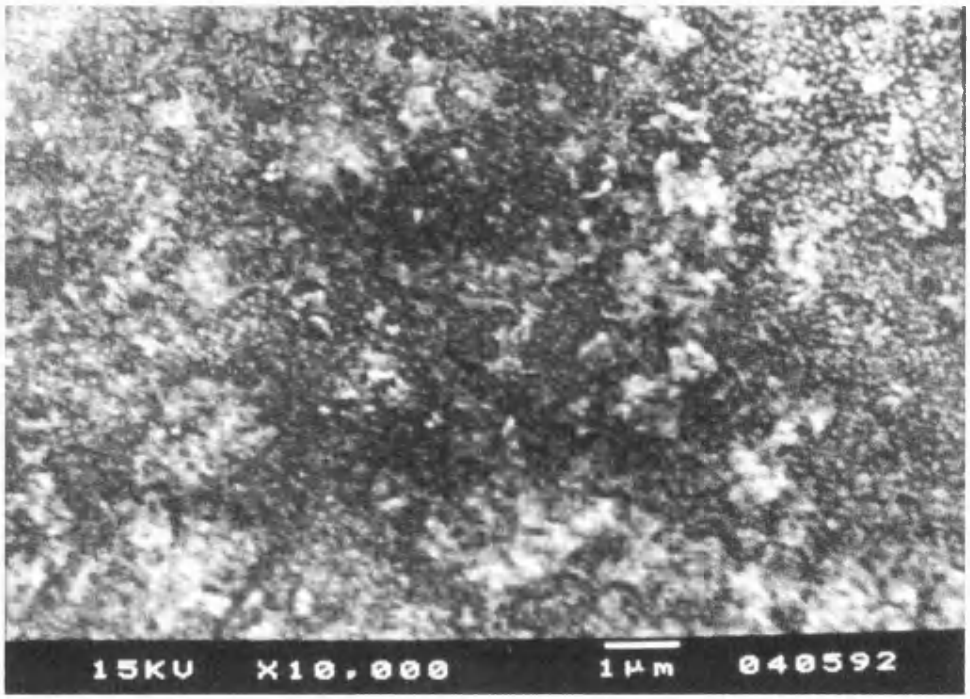

Picture 2.6 SEM image of a film grown from $[Ag\{O_2C(CH_3)C=CHCH_3\}(PhSC_2H_4SPh)_2]$ (**10**).

2.4.11 Nucleation growth study.

The growth of a metal-containing film on a surface should obey one of three classical modes: the layer or Francke–van der Merwe growth mode (A), the layer plus-island or Stranski-Krastanov growth mode (B) and the island or Volmer-Weber growth mode (C), illustrated in Figure 1.3 section 1.2.2.

Nucleation growth studies were carried out for compounds (**6**) and (**9**) in order to assess if the slow growth was a function of nucleation. This could manifest itself as either an inhibition rate or a growth rate i.e. proportional to island density. Silver films were grown on two different substrates, SiCO (4 mm thickness glass) and silica (3 mm thickness glass), under the fixed conditions shown below:

Temperature of the reactor: 250°C

N_2 gas flow rate: 1.4 $l.min^{-1}$

N_2 gas pressure: 1 bar

Run times: 20 min and 70 min.

Concentration of precursor: 7% w/w.

The precursor was delivered in the gas phase as an aerosol of the compound dissolved in methanol and swept into the reactor using N_2 as the carrier gas. Figure 2.20 shows a schematic representation of the CVD system used for this study. Table 2.17 summarises all the results obtained during this study.

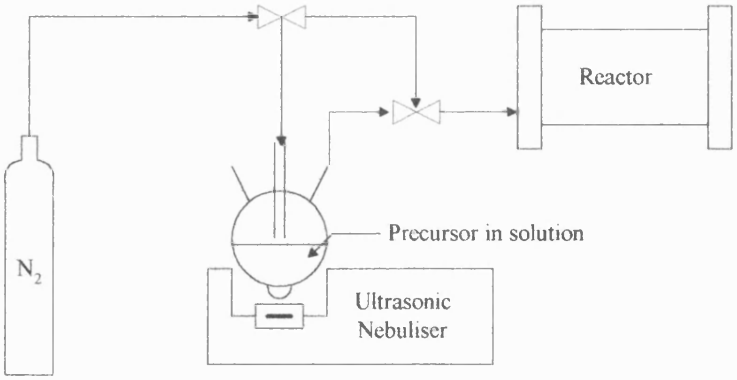

Figure 2.20 Schematic representation of the CVD system used in this study.

	T (min)	Subs	N	N/A	ϕ ($\times10^{-3}$) (μm)	ρ ($\times10^{-4}$) ($\mu m^2.\mu m^{-2}$)	P (nm)	G ($\mu m.$ min^{-1})	Visual appearance
Compound (6)									
Coating (A)	25	SiCO	780	288	27.5	5.9	30 - 55	1.4	Yellow coating.
Coating (B)	70	SiCO	528	195	39.9	12.5	40 - 65	0.6	Yellow coating.
Coating (C)	20	Silica	404	149	41.4	13	40 - 65	1.7	Yellow coating.
Coating (D)	70	Silica	259	96	91.1	65	55- 130	1.3	Yellow-brown, slightly metallic, coating.
Compound (9)									
Coating (E)	20	SiCO	136	50	26.5	5.5	20 - 75	1.3	Yellow coating.
Coating (F)	70	SiCO	294	108	29.5	6.8	55 - 75	0.4	Yellow-slightly brown coating.
Coating (G)	20	Silica	408	131	39.1	12	30 - 65	1.9	Yellow coating.
Coating (H)	70	Silica	320	131	58.8	27	45- 130	0.8	Yellow-brown, slightly metallic, coating.

T = Run time, Subs = Substrate, N = Number of particles found in 2.7 μm^2, N/A = Particle number/Area (Area = 2.7 μm^2), ϕ = Mean particle diameter, ρ = Density (Surface area of silver atoms/Surface area of glass), P = Particles size, G = Growth rate (ϕ/T).

Table 2.17 Characteristics of the coatings grown from compounds (**6**) and (**9**).

2.4.11.1 Nucleation growth study of the (O,O'-allylacetato)bis(triphenyl-phosphine)silver(I) precursor (6).

The growth of silver films from compound (**6**) on SiCO and silica glass substrates followed the island growth process (mode C) as shown by the photographs (2.7 to 2.14). Pictures 2.7 to 2.14 show the structure and surface density of the small clusters.

The mass coverage after a 25 minute run onto a SiCO glass substrate was found to be dense and uniform when compared with films grown from compound (**9**) (Pictures 2.7 and 2.8). The nucleation density was similar for both compounds (5.9×10^{-4} $\mu m^2.$ μm^{-2} and $5.5\times10^{-4}\mu m^2.$ μm^{-2}). The cluster size from coating (A) (30 to 55nm) did not vary as much

as clusters originating from coating (E) (20 to 75nm). After a 70 minute run onto a SiCO glass substrate, the size of the clusters increased (40 to 65nm) (Pictures 2.9 and 2.10). The nucleation density doubled when compared to the nucleation density after a 25 minute run.

On a silica glass substrate, the mass coverage did not change significantly. The grain sizes (40 to 65nm) and nucleation density after a 20 minute run were similar to those from a 70 minute run onto a SiCO glass substrate (Pictures 2.11 and 2.12). After a 70 minute run onto a silica glass substrate the mass coverage was found to be denser when compared with that from a 20 minute run. The cluster sizes (60 to 135nm) nearly doubled in this run (Pictures 2.13 and 2.14) and the nucleation density was five times higher than that found for the 20 minutes run.

2.4.11.2 Nucleation growth study of the (O,O'-tiglato)bis(triphenylphosphine) silver(I) precursor (9).

The growth of silver films from compound (**9**) on SiCO and silica glass substrates obeys the island growth mode as shown by the photographs (2.15 to 2.22).

The data of the pictures 2.15 to 2.22 reveal the structure and the surface density of the small clusters. The mass coverage of the metal film was found to be very low after a 20 minute run onto a SiCO glass substrate. The metal residing on the surface as small clusters or droplets have a diameter of roughly 20 to 75 nm. (Pictures 2.15 and 2.16). After a 70 minute run the mass coverage of the metal film and nucleation density have increased. The grain size of the clusters (55 to 75 nm) increased slightly. Pictures 2.17 and 2.18 show a larger number of big clusters having similar sizes when compared to the 20 minutes run (Picture 2.16).

On a silica glass substrate, the mass coverage after a 20 minute run was similar to those of a 70 minute run onto a SiCO glass substrate (Pictures 2.19 and 2.20). The nucleation density has increased by roughly one and a half times when compared to the nucleation density after a 70 minute run. The clusters are of smaller size (30 to 65 nm) than those formed on a SiCO glass substrate. After 70 minutes the mass coverage, the nucleation density and the size of the clusters have all increased (Pictures 2.21 and 2.22).

Table 2.17 shows that for compound (**6**) the number of particles in a defined surface area decreased with an increased run time. This could be explained as a coalescence of silver atoms to form continuous films. On both SiCO and silica glass

substrates the SEM pictures showed the coalescence. During this study, it was also observed that that the nucleation density and the size of the particles were dependent not only on the substrate used but also on the run time.

The nucleation growth characteristics can be divided into three types:[162]

Type 1. Inhibition period determined. During an initial inhibition period an increase in nucleation sites may or may not be observed. Then at a certain critical level of active species on the surface it will become energetically favourable for nucleation to commence and this will rapidly increase and then level off as new active species, energetically, favour growth rather than more nucleation.

Type 2. Active site limited. In this case, there are a limited number of energetically favoured nucleation sites and active species need to diffuse to these sites. After an extended period all attractive sites will have been consumed. The generated films will often exhibit an open structure or will have clearly definable crystals, with a rough surface. Film growth will be slow.

Type 3. Growth surface. Plenty of active sites are available for nucleation. Rapid growth of sites will follow causing the available surface to be filled and subsequent growth will occur as islands. Here growth and nucleation are dominated by either mass-transport, i.e. the speed that the active species reach the surface, or the kinetics of decomposition of the arrived precursor species into nucleation or growth species. Here nucleation site density will rapidly increase until coalescence occurs. There will be an approximately linear increase in nucleation site density, which will then quickly level off.

Each of these cases is of course an extreme situation and in reality more than one or all types of growth may be competing for dominance. In our case, Type 2 may be suspected because it seems that the growth occurs only where there is already a cluster. Pictures 2.12 and 2.14 shows that the cluster size has increased. There is also no sign of a growth on the empty substrate space available. However, we cannot rule out Type 1.

Films obtained during this study were very thin, their resulting colour being related to the thickness of the films. The first colour obtained in the growth of a silver film is

yellow which then changes to a mixture of yellow and brown to then become brown. The yellow coloration may be due to contamination, perhaps slight oxidation of the films when they are very thin. After the brown stage, a typical metallic silver film is formed. Unfortunately during this study using SiCO glass substrate, all the different colour changes were not observed. All the films were yellow or yellow- brown. However, there was a difference when using silica glass substrates. Films from 70 minute runs showed a slightly metallic aspect. The grain sizes of clusters are larger on silica glass substrates, therefore the nucleation is more advanced when compared with SiCO glass substrates.

Nucleation studies were carried out during a period of work at the Pilkington Technology Centre laboratory. During this study, no silver films were obtained which were of the quality of those obtained using our coater equipment at Bath. This is due to several factors.

- The volume above the glass to be coated was much larger in the Pilkington equipment (volume at Bath: 5×10^{-5} m^3, volume at Pilkington: 9×10^{-5} m^3).
- The velocity. At Bath University the velocity at which the mist is delivered was higher (0.21 $m.s^{-1}$) than at Pilkington (0.14 $m.s^{-1}$).
- The baffle in the coater is in a reversed position from that in use at Bath and as a result there was not direct contact with the glass substrate.
- A different reactor temperature was employed. The N_2 carrier gas flow was faster in the Bath equipment with the result that the temperature in the coater was reduced.

The selection of SiCO and silica as substrates, was based on the experience of researchers at Pilkington who were aware that these two surfaces frequently exhibit notable differences in the nucleation growth. This is certainly true of the growth of some metal oxide or nitride films. Pilkington experience,[169] and literature work,[163,10] showed, however, that for metals neither of these surfaces are good for nucleation. It is possible that a $SnCl_4$, or better still a $TiCl_4$, pretreatment of the surfaces could produce dramatic changes. The results obtained here support the above proposed outcome for SiCO and silica surfaces.

One of the biggest problems encountered during this study was the blockage of the delivery pipes and of the baffle. This was probably due to the temperature of the reactor

and to the speed at which the mist was delivered to the reactor. The N_2 gas flow rate was probably not high enough.

The nebuliser used in this nucleation study was the same as the one in use at Bath for the generation of films. However, it was found that the flask (250 cm^3) used to contain the precursor solution was too small. An increase of N_2 gas flow above to 1.5 $l.min^{-1}$ caused disruption of the mist, therefore deposition of the film was not total, some loss occurring.

The nebuliser in use at Pilkington was also tried during this study. Unlike the Bath nebuliser method, direct nebulisation is used. This means that the compound dissolved in a solvent is in direct contact with the piezoelectric transducer. As a result, the mist obtained was very thick but after a run of only several minutes the solution became warmer resulting in condensation of the mist in the pipes. The heat build up resulted in the loss of the solvent sheath around the precursor compound resulting in particulates being precipitated and these were carried in the gas stream into the coater.

In conclusion, the films produced from the adducts of unsaturated silver(I) carboxylates, were very encouraging. They show that it is possible to grow silver metallic films from carboxylate species containing phosphine ligands. Carbon was the main contaminant in theses films, although traces of sulfur were detected where 1,2-bis(phenylthio)ethane was used as an additional ligand. The R group from the carboxylate group (RCO_2) seems to play an important role in the film deposition. During this study, it was found that precursors containing phenyl rings e.g. compound (**12**), did not produce metallic silver films. It seems that the volatility is decreased by the presence of a phenyl ring. Compounds (**6**) and (**9**) are representative samples, which produced metallic silver films with reasonable properties.

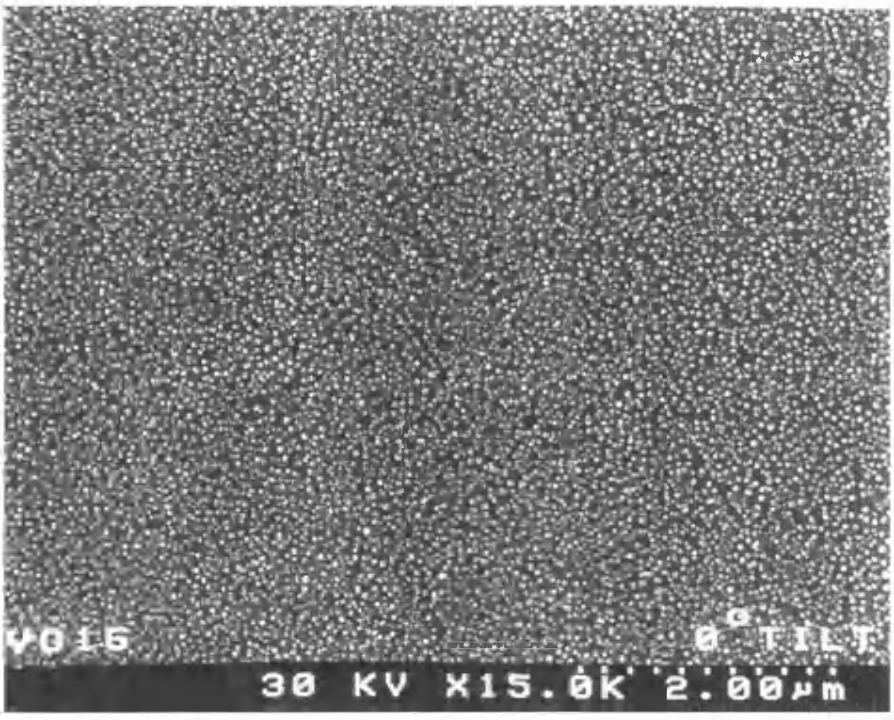

Picture 2.7 SEM image of a film grown from [Ag{$O_2C(CH_2)_2CH=CH_2$}$(PPh_3)_2$] (**6**) onto SiCO glass substrate after a 20 minute run.

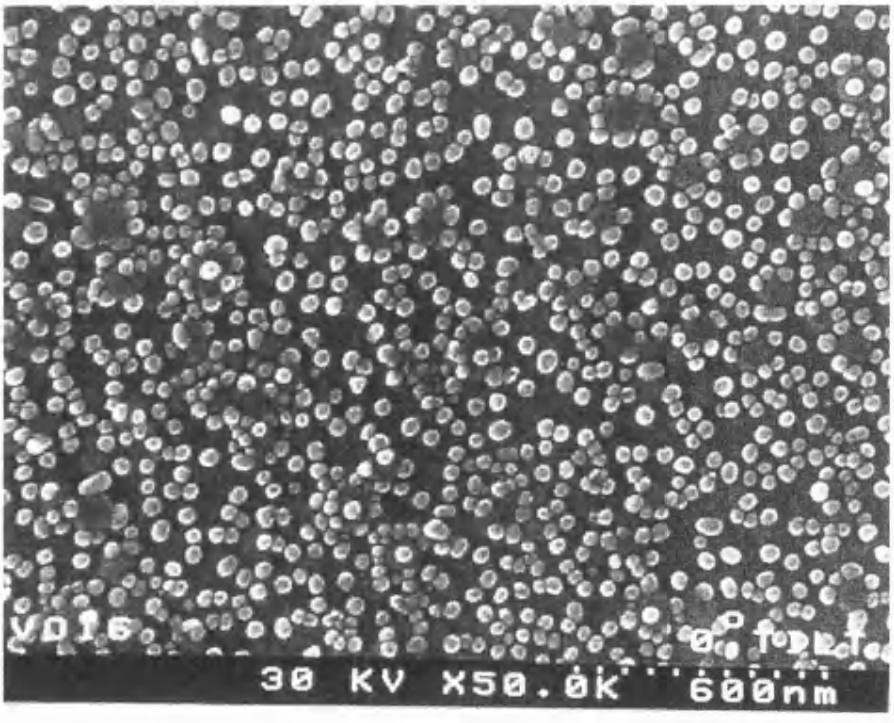

Picture 2.8 SEM image of a film grown from [Ag{$O_2C(CH_2)_2CH=CH_2$}$(PPh_3)_2$] (**6**) onto a SiCO glass substrate after 25 a minute run.

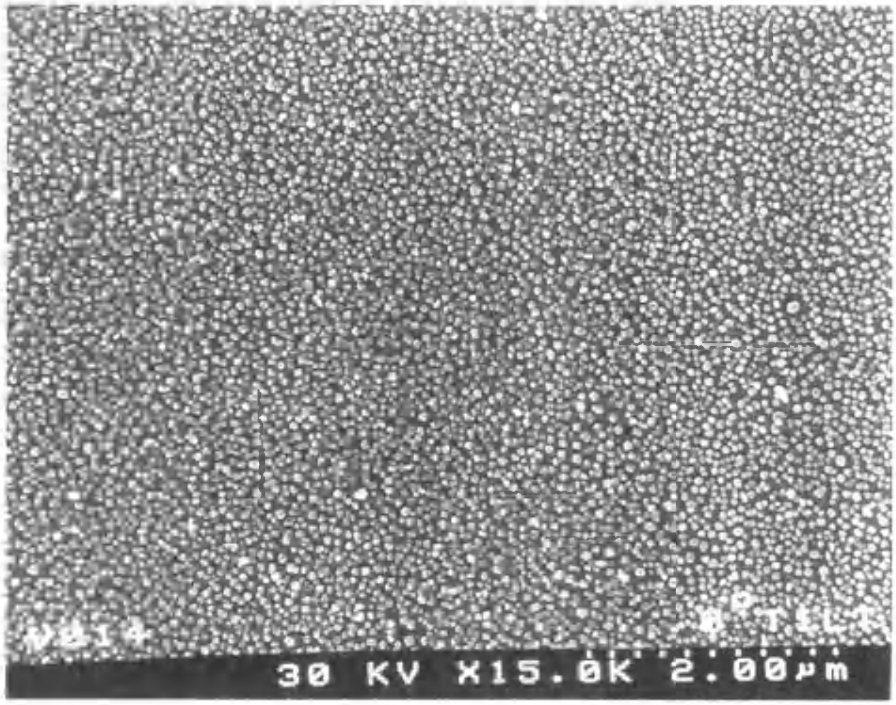

Picture 2.9 SEM image of a film grown from [Ag{$O_2C(CH_2)_2CH=CH_2$}(PPh_3)$_2$] (**6**) onto a SiCO glass substrate after 70 a minute run.

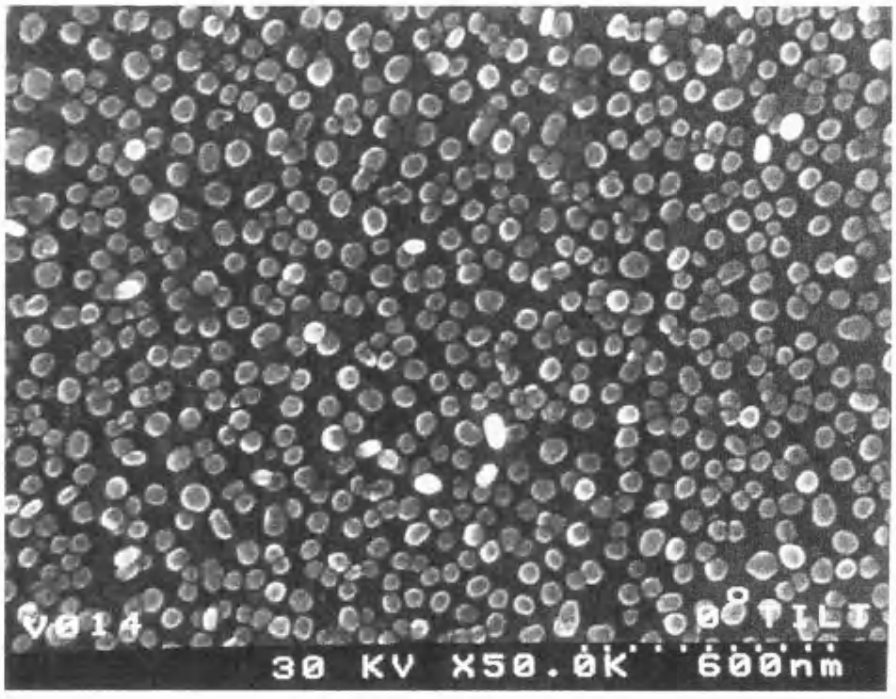

Picture 2.10 SEM image of a film grown from [Ag{$O_2C(CH_2)_2CH=CH_2$}(PPh_3)$_2$] (**6**) onto a SiCO glass substrate after a 70 minute run.

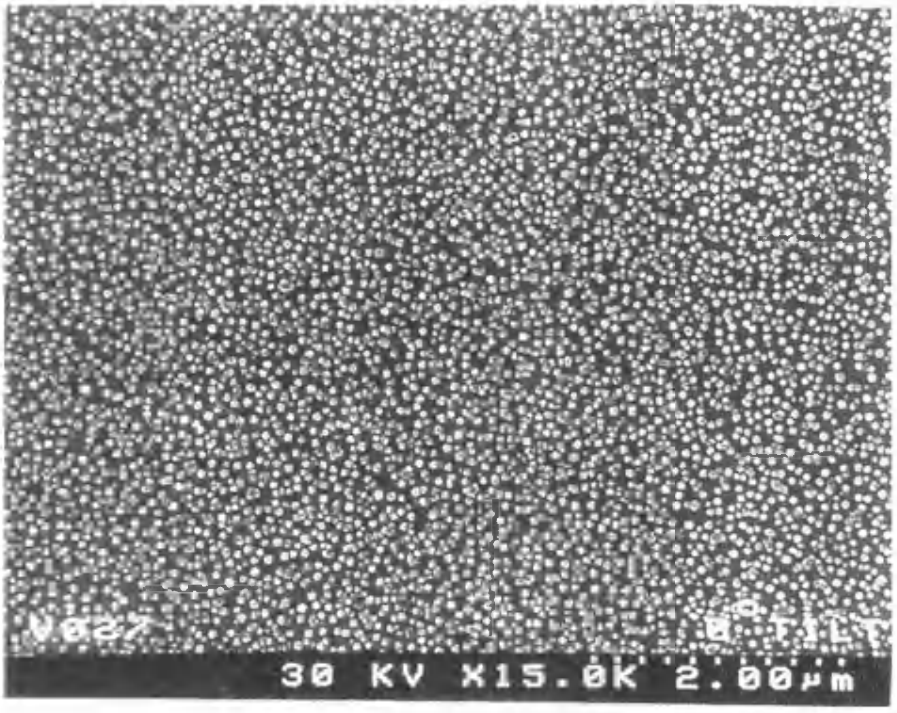

Picture 2.11 SEM image of a film grown from $[Ag(O_2C\{CH_2)_2CH{=}CH_2\}(PPh_3)_2]$ (**6**) onto a silica glass substrate after a 20 minute run.

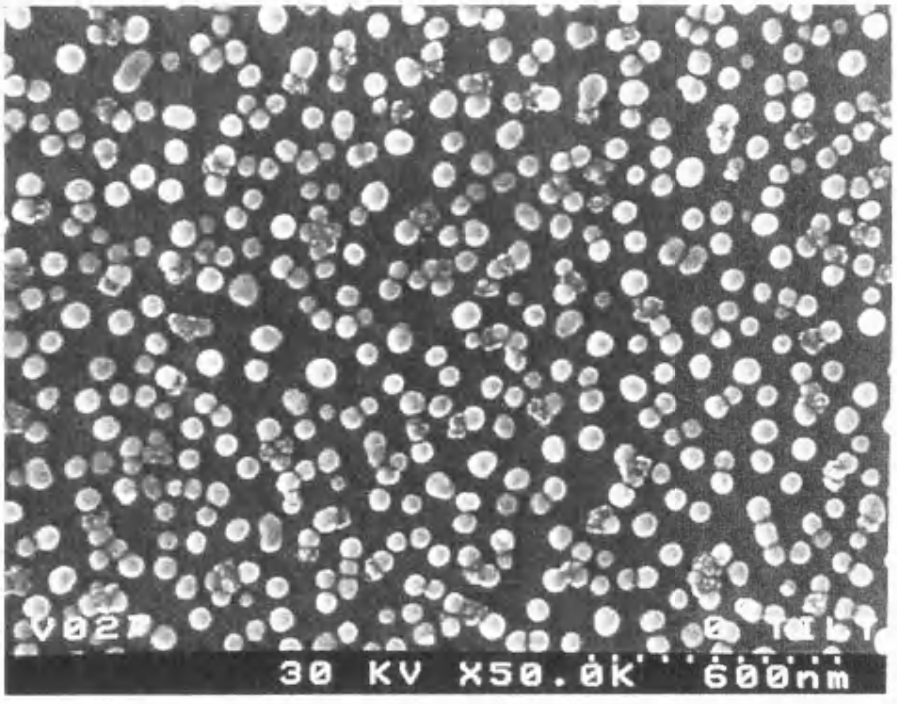

Picture 2.12 SEM image of a film grown from $[Ag\{O_2C(CH_2)_2CH{=}CH_2\}(PPh_3)_2]$ (**6**) onto a silica glass substrate after a 20 minute run.

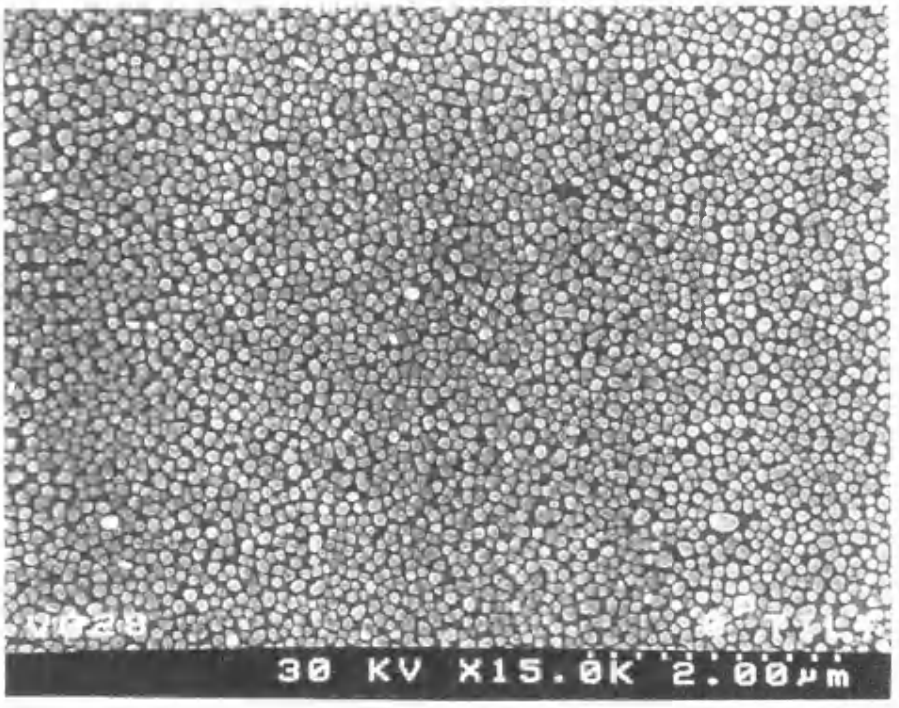

Picture 2.13 SEM image of a film grown from [Ag{$O_2C(CH_2)_2CH=CH_2$}(PPh_3)$_2$] (**6**) onto a silica glass substrate after a 70 minute run.

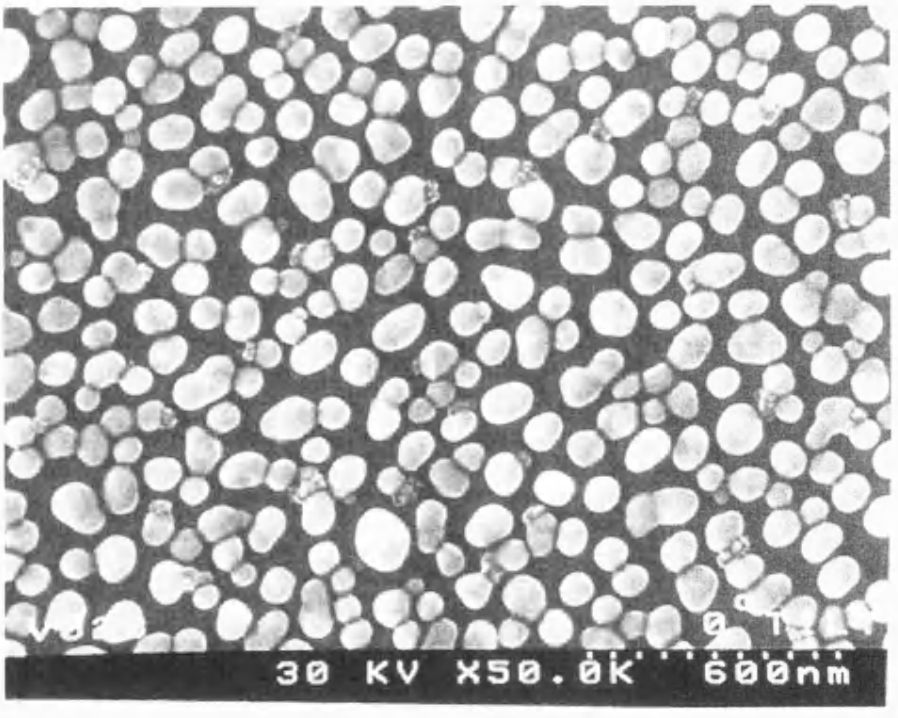

Picture 2.14 SEM image of a film grown from [Ag{$O_2C(CH_2)_2CH=CH_2$}(PPh_3)$_2$] (**6**) onto a silica glass substrate after a 70 minute run.

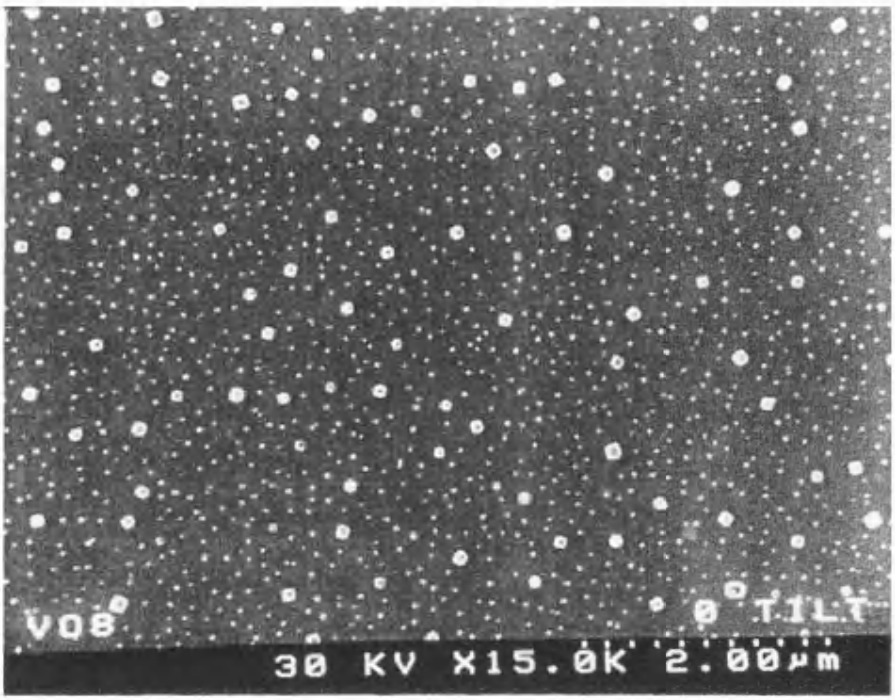

Picture 2.15 SEM image of a film grown from [Ag{$O_2CC(CH_3)$=$CHCH_3$}$(PPh_3)_2$] (**9**) onto a SiCO glass substrate after a 20 minute run.

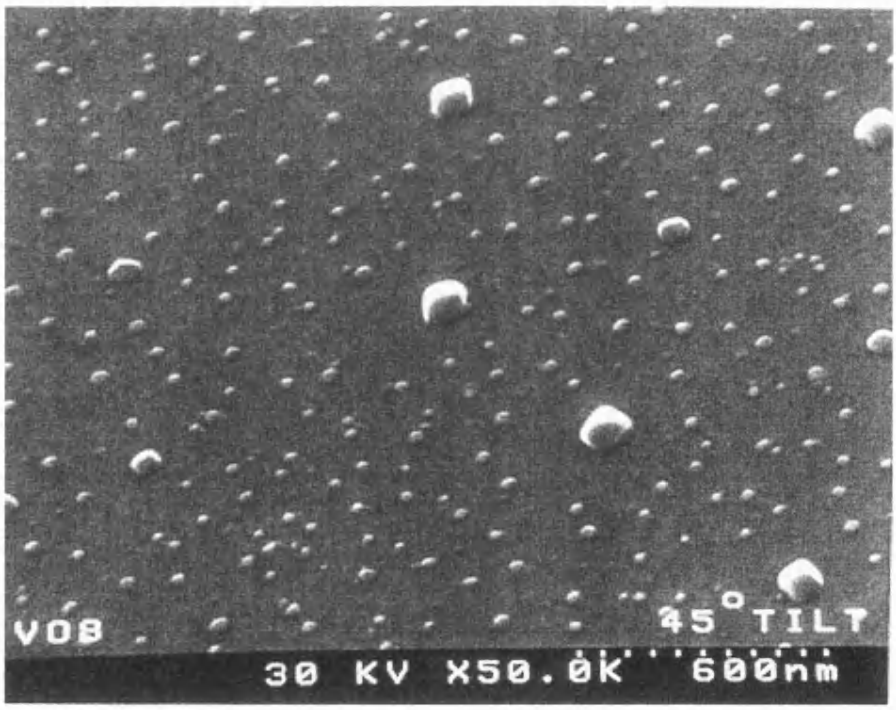

Picture 2.16 SEM image of a film grown from [Ag{$O_2C(CH_3)C$=$CHCH_3$}$(PPh_3)_2$] (**9**) onto a SiCO glass substrate after a 20 minute run.

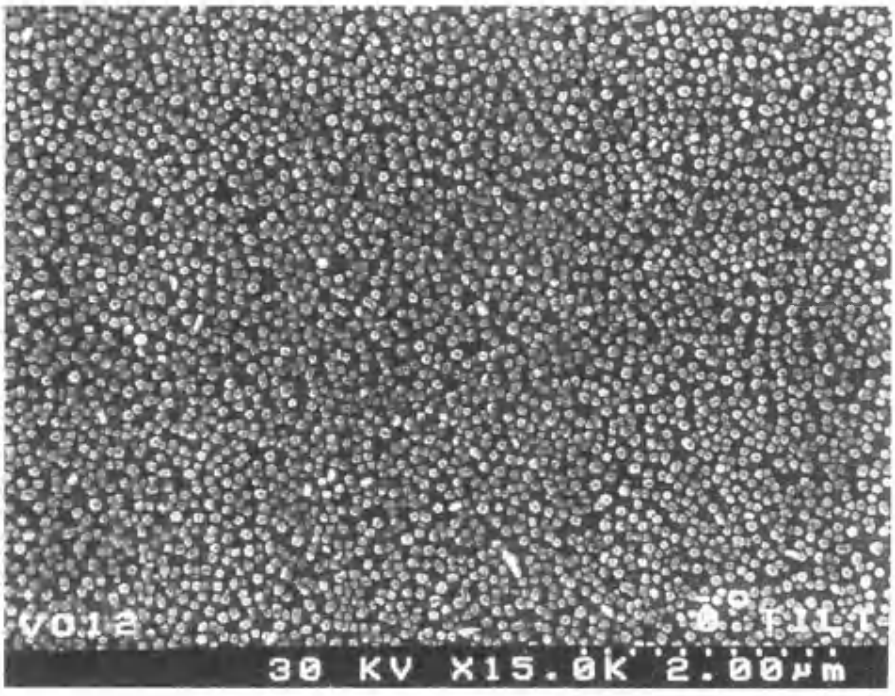

Picture 2.17 SEM image of a film grown from $[Ag\{O_2C(CH_3)C{=}CHCH_3\}(PPh_3)_2]$ (**9**) onto a SiCO glass substrate after a 70 minute run.

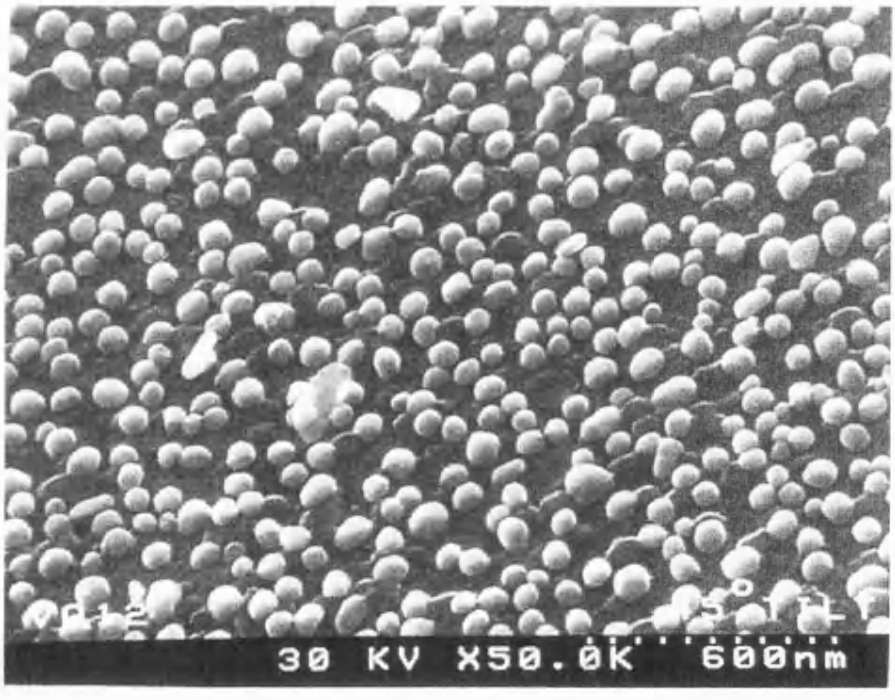

Picture 2.18 SEM image of a film grown from $[Ag\{O_2C(CH_3)C{=}CHCH_3\}(PPh_3)_2]$ (**9**) onto a SiCO glass substrate after a 70 minute run.

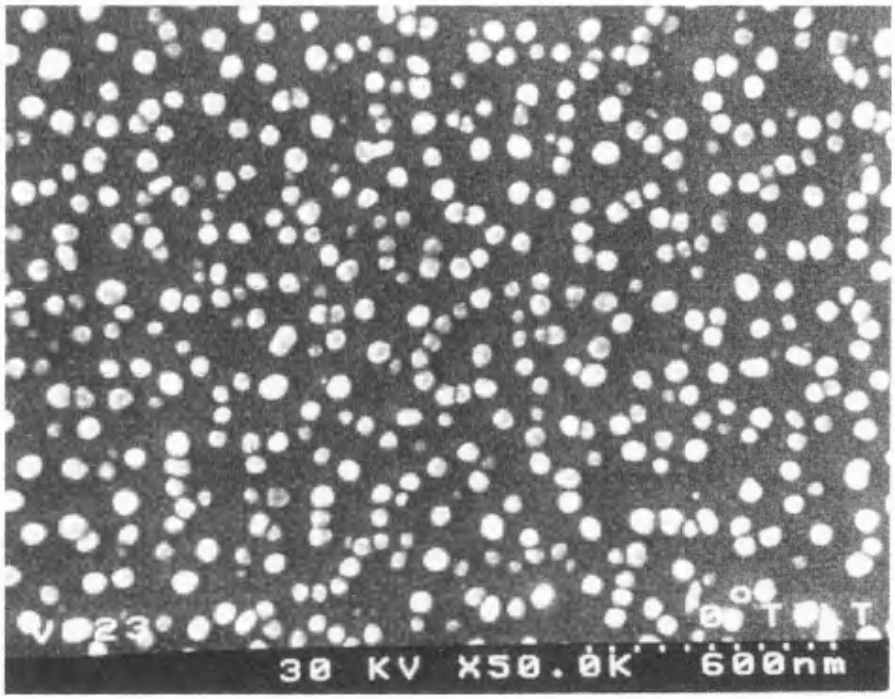

Picture 2.19 SEM image of a film grown from [Ag{$O_2C(CH_3)C{=}CHCH_3$}$(PPh_3)_2$] (**9**) onto a silica glass substrate after a 20 minute run.

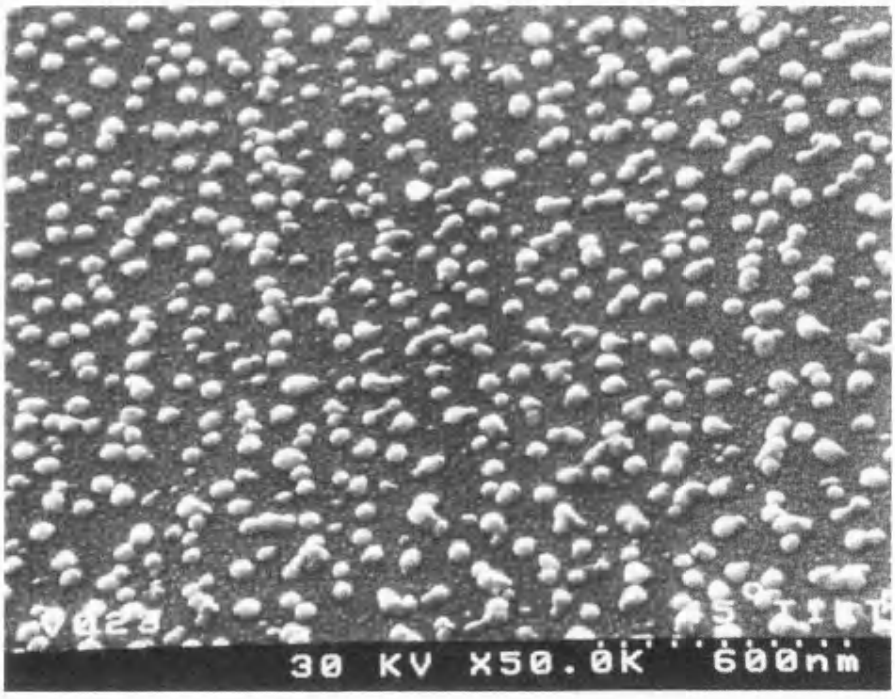

Picture 2.20 SEM image of a film grown from [Ag{$O_2C(CH_3)C{=}CHCH_3$}$(PPh_3)_2$] (**9**) onto a silica glass substrate after a 20 minute run.

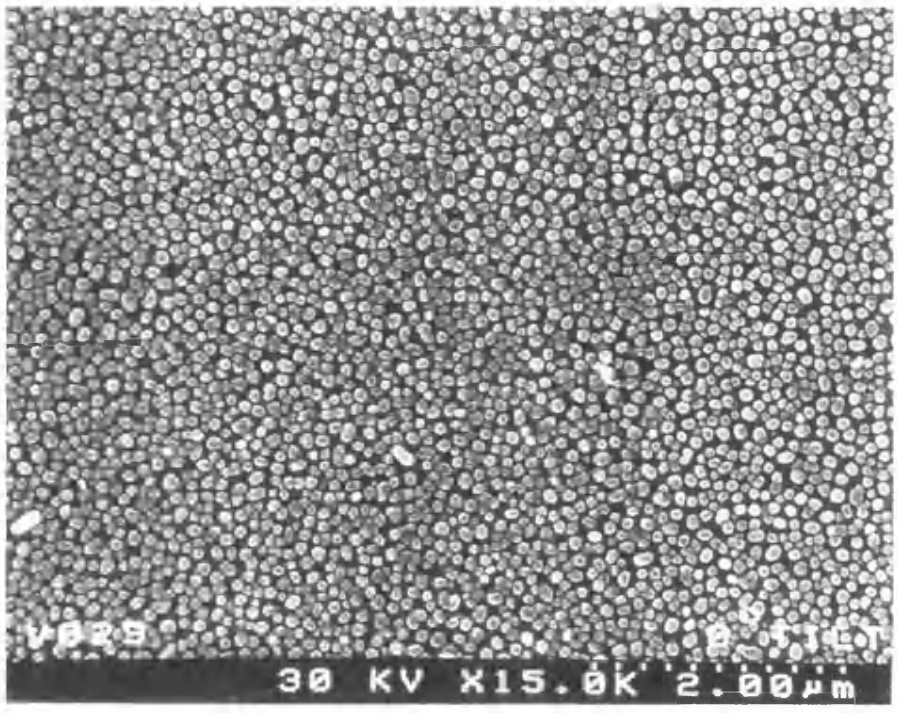

Picture 2.21 SEM image of a film grown from [Ag{$O_2C(CH_3)C{=}CHCH_3$}$(PPh_3)_2$] (**9**) onto a silica glass substrate after a 70 minute run.

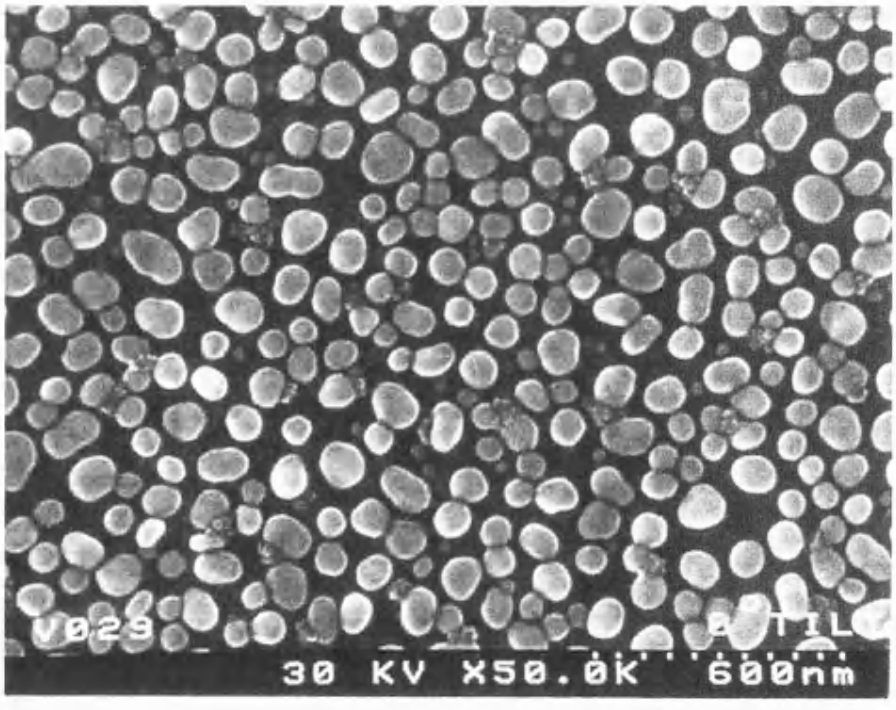

Picture 2.22 SEM image of a film grown from [Ag{$O_2C(CH_3)C{=}CHCH_3$}$(PPh_3)_2$] (**9**) onto a silica glass substrate after a 70 minute run.

2.5 EXPERIMENTAL.

All operations were carried out in subdued light with final storage of products in the dark.

Preparation of silver(I) cyanoacetate (1).

The compound was synthesised by the method given in reference 96.

A solution of silver nitrate (4.59 mmol) in water was added dropwise to a solution of cyanoacetic acid (4.59 mmol) and sodium hydroxide (4.59 mmol) in water. The resulting white precipitate was washed with water, ethanol, diethyl ether and dried *in vacuo*.

Yield: 69 %.

Analysis: Found (calculated for $C_3H_2AgNO_2$) C: 18.8 (18.8), H: 1.04 (1.05), N: 7.21 (7.3)%.

^{1}H NMR [δ(ppm), D_2O solution]: 3.47 (s, 2H, CH_2).

^{13}C NMR [δ(ppm), D_2O solution]: 169.2 (CO_2), 117.4 (CN), 26.1 (CH_2).

IR [(cm^{-1}) nujol mulls on NaCl]: 2268 s [ν(CN)], 1601 m [$\nu_{asym}(CO_2)$], 1568 w [$\nu_{asym}(CO_2)$], 1425 m [$\nu_{sym}(CO_2)$], 1398 w [$\nu_{sym}(CO_2)$].

Preparation of (*O,O'*-cyanoacetato)*bis*(triphenylphosphine)silver(I) (2).

Silver cyanoacetate (2.6 mmol) was added to a stirred solution of triphenylphosphine (5.2 mmol) in toluene (25 cm^3). After one to two hours the resulting beige precipitate was filtered, washed with toluene and dried *in vacuo* .

Yield: 52 %.

Analysis: Found (calculated for $C_{39}H_{32}AgO_2P_2$) C: 65.5 (65.4), H: 4.53 (4.50), N: 1.98 (1.95)%.

^{1}H NMR [δ(ppm), $CDCl_3$ solution]: 3.43 (s, 2H, CH_2), 7.69-7.53 (m, 30H, $P(C_6\underline{H}_5)_3$).

^{13}C NMR [δ(ppm), $CDCl_3$ solution]: 166.8 (CO_2), 133.7 (d, J 16.5 Hz, $P(\underline{C}_6H_5)_3$), 131.8 (d, J 28.7 Hz, $P(\underline{C}_6H_5)_3$), 130.1 (s, $P(\underline{C}_6H_5)_3$), 128.7 (d, J 10.0 Hz, $P(\underline{C}_6H_5)_3$), 117.1 (CN), 33.8 (CH_2).

^{31}P NMR [δ(ppm), $CDCl_3$ solution (+22°C)]: +10.9 (s).

^{31}P NMR [δ(ppm), $CDCl_3$ solution (-50°C)]: +10.9 [partial dd, ^{1}J (^{107}Ag-P) 451.8 Hz, ^{1}J (^{109}Ag-P) 488.7 Hz].

IR [(cm^{-1}) nujol mulls on NaCl]: 2253 m [ν(CN)], 1570 s [$\nu_{asym}(CO_2)$], 1433 s [ligand], 1404 w [$\nu_{sym}(CO_2)$].

Preparation of silver(I) acrylate (3).

Silver(I) oxide (4.31 mmol) was added to a stirred solution of acrylic acid (4.31 mmol) in water (40 cm^3). After one hour the mixture was filtered to remove the excess of silver oxide. The clear solution was evaporated to dryness to give a white solid.

Yield: 13 %.

Analysis: Found (calculated for $C_3H_3AgO_2$) C: 20.4 (20.1) , H: 1.71 (1.69) %.

^{1}H NMR [δ(ppm), d_6-DMSO solution]: $H_cH_bC{=}CH_aCO_2Ag$: 6.15 (dd, 1H, J_{ac} 17.0 Hz, J_{ab} 9.7 Hz, H_a), 5.98 (dd, 1H, J_{ac} 17.0 Hz, J_{bc} 2.9 Hz, H_c), 5.53 (dd, 1H, J_{ab} 9.7 Hz, J_{bc} 2.9 Hz, H_b).

^{13}C NMR [δ(ppm), d_6-DMSO solution]: 170.3 (CO_2), 135.2 (CH_2=), 125.0 (=CH).

IR [(cm^{-1}) nujol mulls on NaCl]: 1618 m [ν(C=C)], 1541 m [$\nu_{asym}(CO_2)$], 1510 s [$\nu_{asym}(CO_2)$], 1423 m [$\nu_{sym}(CO_2)$].

Preparation of (*O,O'*-acrylato)*bis*(triphenylphosphine)silver(I) (4).

Silver(I) acrylate (0.55 mmol) was added to a stirred solution of triphenylphosphine (1.1 mmol) in toluene (15 cm^3). After one to two hours the resulting white precipitate was filtered, washed with toluene and dried *in vacuo*.

Yield: 84 %.

Analysis: Found (calculated for $C_{39}H_{33}AgO_2P_2$) C: 67.0 (66.6), H: 4.88 (4.73)%.

^{1}H NMR [δ(ppm), $CDCl_3$ solution]: $H_cH_bC{=}CH_aCO_2Ag(P(C_6H_5)_3)_2$: 7.42-7.16 (m, 30H, $P(C_6\underline{H_5})_3$), 6.30 (dd, 1H, J_{ac} 17.0 Hz, J_{ab} 9.9 Hz, H_a), 6.10 (dd, 1H, J_{ac} 17.0 Hz, J_{bc} 2.7 Hz, H_c), 5.45 (dd, 1H, J_{ab} 9.9 Hz, J_{bc} 2.7 Hz, H_b).

^{13}C NMR [δ(ppm), $CDCl_3$ solution]: 173.4 (CO_2), 135.6 (CH_2=), 134.0 (d, J 17.6 Hz, P($\underline{C}_6H_5)_3$), 132.6 (d, J 26.5 Hz, P($\underline{C}_6H_5)_3$), 129.9 (s, P($\underline{C}_6H_5)_3$), 128.7 (d, J 10.0 Hz, P($\underline{C}_6H_5)_3$), 128.1 (=CH).

^{31}P NMR [δ(ppm), $CDCl_3$ solution (+22°C)]: +9.5 (s).

^{31}P NMR [δ(ppm), $CDCl_3$ solution (-50°C)]: +9.6 [dd, ^1J (^{107}Ag-P) 426.0 Hz, ^1J (^{109}Ag-P) 473.6 Hz].

IR [(cm^{-1}) nujol mulls on NaCl]: 1631 m [ν(C=C)], 1545 s [$\nu_{asym}(CO_2)$], 1435 m [ligand], 1417 m [$\nu_{sym}(CO_2)$].

Preparation of silver(I) allylacetate (5).

Silver(I) oxide (4.31 mmol) was added to a stirred solution of allylacetic acid (4.31 mmol) in water (40 cm^3). After one hour the mixture was filtered to remove the excess of silver oxide. The clear solution was evaporated to dryness to give a white solid.

Yield: 72 %.

Analysis: Found (calculated for $C_5H_7AgO_2$) C: 28.9 (29.0), H: 3.40 (3.41) %.

^1H NMR [δ(ppm), d_6-DMSO solution]: $H_cH_bC{=}CH_aCH_2CH_2CO_2Ag$: 5.90-5.80 (m, 1H, H_a), 4.96 (dd, 1H, J_{ac} 17.0 Hz, J_{bc} 7.8 Hz, H_c), 4.89 (dd, 1H, J_{ab} 10.2 Hz, J_{bc} 7.8 Hz, H_b), 2.23 (m, 4H, CH_2CH_2).

^{13}C NMR [δ(ppm), d_6-DMSO solution]: 176.4 (CO_2), 138.7 (=CH), 114.2 (CH_2=), 36.0 (CH_2), 30.6 (CH_2).

IR [(cm^{-1}) nujol mulls on NaCl]: 1641 w [ν(C=C)], 1518 s [$\nu_{asym}(CO_2)$], 1404 m [$\nu_{sym}(CO_2)$], 1354 w [$\nu_{sym}(CO_2)$].

Mass Spectrometry (m/z): 207 $(M+H)^+$ (100%).

Preparation of (*O,O'*-allylacetato)*bis*(triphenylphosphine)silver(I) (6).

Silver(I) allylacetate (5.8 mmol) was added to a stirred solution of triphenylphosphine (11.65 mmol) in toluene (40 cm^3). After one to hours the resulting beige precipitate was filtered, washed with toluene and dried *in vacuo*.

Yield: 82 %.

Analysis: Found (calculated for $C_{41}H_{37}AgO_2P_2$) C: 67.5 (67.3), H: 5.07 (5.10)%.

^{1}H NMR [δ(ppm), $CDCl_3$ solution]: $H_cH_bC{=}CH_aCH_2CH_2CO_2Ag(P(C_6H_5)_3)_2$: 7.43-7.23 (m, 30H, $P(C_6\underline{H}_5)_3$), 5.90-5.84 (m, 1H, H_a), 5.00 (d, 1H, J_{ac} 17.0 Hz, H_c), 4.85 (d, 1H, J_{ab} 9.2 Hz, H_b), 2.23 (m, 4H, CH_2CH_2).

^{13}C NMR [δ(ppm), $CDCl_3$ solution]: 179.5 (CO_2), 139.3 (=CH), 134.0 (d, J 16.5 Hz, $P(\underline{C}_6H_5)_3$), 132.7 (d, J 26.5 Hz, $P(\underline{C}_6H_5)_3$), 129.9 (s, $P(\underline{C}_6H_5)_3$), 128.7 (d, J 8.9 Hz, $P(\underline{C}_6H_5)_3$), 113.5 (CH_2=), 36.8 (CH_2), 31.2 (CH_2).

^{31}P NMR [δ(ppm), $CDCl_3$ solution (+22°C)]: +9.4 (s).

^{31}P NMR [δ(ppm), $CDCl_3$ solution (-50°)]: +9.6 [dd, ^{1}J (^{107}Ag-P) 426.1 Hz, ^{1}J (^{109}Ag-P) 469.9 Hz].

IR [(cm^{-1}) nujol mulls on NaCl]: 1639 w [ν(C=C)], 1585 w [$\nu_{asym}(CO_2)$], 1574 m [$\nu_{asym}(CO_2)$], 1556 s [$\nu_{asym}(CO_2)$], 1477 w [$\nu_{sym}(CO_2)$], 1431 s [ligand], 1398 w [$\nu_{sym}(CO_2)$].

Preparation of *bis*(1,2-bis(phenylthio)ethane)silver(I) allylacetate (7).

This reaction was performed under nitrogen.

Silver(I) allylacetate (14.2 mmol) was added to a stirred solution of 1,2-bis(phenylthio)ethane (28.4 mmol) in ethanol (150 cm^3). After 24 hours the clear solution was filtered and evaporated to dryness to give a white solid.

Yield: 86%.

Analysis: Found (calculated for $C_{33}H_{35}AgO_2S_4$) C: 56.6 (56.7), H: 5.07 (5.04)%.

^{1}H NMR [δ(ppm), $CDCl_3$ solution]: $H_cH_bC{=}CH_aCH_2CH_2CO_2Ag(C_6H_5SC_2H_4SC_6H_5)_2$: 7.40-7.37 (m, 10H, $C_6\underline{H}_5S$), 7.29-7.23 (m, 10H, $C_6\underline{H}_5S$), 5.97-5.87 (m, 1H, H_a), 5.05 (dd, 1H, J_{ac} 17.2 Hz, J_{bc} 1.5 Hz, H_c), 4.94 (dd, 1H, J_{ab} 12.0 Hz, J_{bc} 1.5 Hz, H_b), 3.05 (s, 8H, SC_2H_4S), 2.48-2.40 (m, 4H, CH_2CH_2).

^{13}C NMR [δ(ppm), $CDCl_3$ solution]: 179.6 (CO_2), 138.4(=CH), 133.2 ($\underline{C}_6H_5S$), 130.9($\underline{C}_6H_5S$), 129.1 ($\underline{C}_6H_5S$), 127.3 ($\underline{C}_6H_5S$), 113.2 (CH_2=), 35.7(CH_2), 34.0 (SC_2H_4S), 30.9 (CH_2).

IR [(cm^{-1}) nujol mulls on NaCl]: 1637 w [ν(C=C)], 1579 w [$\nu_{asym}(CO_2)$], 1558 w [$\nu_{asym}(CO_2)$], 1537 s [$\nu_{asym}(CO_2)$], 1439 w [$\nu_{sym}(CO_2)$], 1414 w [$\nu_{sym}(CO_2)$], 1400 w [$\nu_{sym}(CO_2)$].

Preparation of silver(I) tiglate (8).

Tiglic acid (i.e. trans-2,3-dimethylacrylic acid) (5.89 mmol) was suspended in 20 cm^3 of distilled water and stirred. The acid was solubilised by addition of concentrated ammonia solution until the solution was slightly ammoniacal. The solution was gently heated to remove excess ammonia and filtered to remove any unreacted acid. Silver(I) nitrate (5.89 mmol) in 5 cm^3 distilled water was added dropwise to the solution. The resulting white precipitate was filtered, washed with water, ethanol and diethyl ether and dried *in vacuo*.

Yield: 62 %.

Analysis: Found (calculated for $C_5H_7AgO_2$) C: 29.0 (29.0), H: 3.31 (3.41) %.

^{1}H NMR [δ(ppm), d_6-DMSO solution]: $H_3CCH{=}C(CH_3)CO_2Ag$: 6.58-6.55 (m, 1H, CH), 1.76 (d, 3H, J 1.1 Hz, $\underline{H_3}CCH{=}$), 1.67 (d, 3H, J 6.9 Hz, $=C(C\underline{H_3})$).

^{13}C NMR [δ(ppm), d_6-DMSO solution]: 172.1 (CO_2), 133.3, 131.0 ($H_3C\underline{C}H{=}\underline{C}(CH_3)CO_2$), 14.0, 13.9 ($H_3\underline{C}CH{=}C(\underline{C}H_3)CO_2$).

IR [(cm^{-1}) nujol mulls on NaCl]: 1645 m [ν(C=C)], 1558 w [$\nu_{asym}(CO_2)$], 1516 w [$\nu_{asym}(CO_2)$], 1498 m [$\nu_{asym}(CO_2)$], 1383 w [$\nu_{sym}(CO_2)$].

Mass spectrometry (m/z): 207 $(M+H)^+$ (16.6%).

Preparation of (*O,O'*-tiglato)*bis*(triphenylphosphine)silver(I) (9).

Silver(I) tiglate (10.1 mmol) was added to a stirred solution of triphenylphosphine (20.3 mmol) in toluene (70 cm^3). After one to two hours the resulting precipitate was filtered , washed with toluene and dried *in vacuo*.

Yield: 82 %.

Analysis: Found (calculated for $C_{41}H_{37}AgO_2P_2$) C: 67.5 (67.3), H: 5.17 (5.10)%.

^{1}H NMR [δ(ppm), $CDCl_3$ solution]: $H_3CCH{=}C(CH_3)CO_2Ag(P(C_6H_5)_3)_2$: 7.42-7.19 (m, 30H, $P(C_6\underline{H_5})_3$), 6.65-6.63 (m, 1H, CH), 1.91 (partial d, 3H, J 1.1 Hz, $\underline{H_3}CCH{=}$), 1.70 (d, 3H, J 6.9 Hz, $=C(C\underline{H_3})$).

^{13}C NMR [δ(ppm), $CDCl_3$ solution: 175.8 (CO_2), 134.4 ($H_3CCH{=}C(CH_3)CO_2$), 133.9 (d, J 16.5 Hz, $P(\underline{C_6}H_5)_3$), 132.6 (d, J 25.4 Hz, $P(\underline{C_6}H_5)_3$), 129.8 (s, $P(\underline{C_6}H_5)_3$), 129.1 ($H_3CCH{=}C(CH_3)CO_2$), 128.6 (d, J 8.8 Hz, $P(\underline{C_6}H_5)_3$), 13.9, 13.5 ($H_3\underline{C}CH{=}C(\underline{C}H_3)CO_2$).

^{31}P NMR [δ(ppm), $CDCl_3$ solution (+22°C)]: +9.1(s).

^{31}P NMR [δ(ppm), $CDCl_3$ solution (-50°)]: +9.4 [d, ^{1}J (^{107}Ag-P) 430.0 Hz, ^{1}J (^{109}Ag-P) 458.8 Hz].

IR [(cm^{-1}) nujol mulls on NaCl]: 1653 w [ν(C=C)], 1523 s [$\nu_{asym}(CO_2)$], 1435 s [ligand], 1396 w [$\nu_{sym}(CO_2)$].

Preparation of *bis*(1,2-bis(phenylthio)ethane)silver(I) tiglate (10).

This reaction was carried out under nitrogen.

Silver(I) tiglate (14.2 mmol) was added to a stirred solution of 1,2-bis(phenylthio)ethane (27.4 mmol) in ethanol (150 cm^3). After 24 hours the clear solution was filtered and evaporated to dryness to give a white solid.

Yield: 86%.

Analysis: Found (calculated for $C_{33}H_{35}AgO_2S_4$) C: 56.6 (56.7), H: 5.07 (5.04)%.

^{1}H NMR [δ(ppm), d_6-DMSO solution]: $H_3CCH{=}C(CH_3)CO_2Ag(C_6H_5SC_2H_4SC_6H_5)_2$: 7.34-7.22 (m, 20H, $C_6\underline{H}_5S$), 6.55-6.53 (m, 1H, CH), 3.15 (s, 8H, SC_2H_4S), 1.75 (d, 3H, $C\underline{H}_3CH{=}$), 1.67 (d, 3H, J 6.9 Hz, $=C(C\underline{H}_3)$).

^{13}C NMR [δ(ppm), $CDCl_3$ solution]: 134.2 ($\underline{C}_6H_5S$), 132.2 ($H_3CCH{=}C(CH_3)CO_2$), 130.5 ($\underline{C}_6H_5S$), 129.1 ($\underline{C}_6H_5S$), 126.9 ($\underline{C}_6H_5S$), 33.7 (SC_2H_4S), 14.2 ($H_3CCH{=}C(CH_3)CO_2$).

IR [(cm^{-1}) nujol mulls on NaCl]: 1647 w [ν(C=C)], 1516 w [$\nu_{asym}(CO_2)$], 1500 w [$\nu_{asym}(CO_2)$], 1439 w [$\nu_{sym}(CO_2)$], 1429 w [$\nu_{sym}(CO_2)$].

Preparation of silver(I) *trans*-cinnamate (11).

Trans-cinnamic acid (5.89 mmol) was suspended in 20 cm^3 of distilled water and stirred. The acid was solubilised by addition of concentrated ammonia solution until the solution was slightly ammoniacal. The solution was gently heated to remove any excess of ammonia and filtered to remove any unreacted acid. Silver nitrate (5.89 mmol) in 5 cm^3 water was added dropwise to the solution. The resulting white precipitate was filtered and washed with water, ethanol and diethyl ether and dried *in vacuo*.

Yield: 36 %.

Analysis: found (calculated for $C_9H_7AgO_2$) C: 42.5 (42.4), H: 2.71 (2.77) %.

IR [(cm^{-1}) nujol mulls on NaCl]: 1633 s [ν(C=C)], 1576 m [$\nu_{asym}(CO_2)$], 1552 m [$\nu_{asym}(CO_2)$], 1448 w [$\nu_{sym}(CO_2)$].

Preparation of (*O,O'-trans*-cinnamato)*bis*(triphenylphosphine)silver(I) (12).

Silver(I) *trans*-cinnamate (1.96 mmol) was added to a stirred solution of triphenylphosphine (3.92 mmol) in toluene (25 cm^3). After two hours no precipitate appeared. The solution was filtered and evaporated to dryness to give a white solid.

Yield: 60 %.

Analysis: Found (calculated for $C_{45}H_{37}AgO_2P_2$) C: 71.15 (69.3), H: 5.10 (4.78) %.

^{1}H-NMR [δ(ppm), $CDCl_3$ solution]: $(C_6H_5)CH_a{=}CH_bCO_2Ag(P(C_6H_5)_3)_2$: 7.51-7.15 (m, 35H, $P(C_6\underline{H}_5)_3$, $C_6\underline{H}_5$), 6.72 (d, 2H, J_{ab} 15.9, H_a, H_b).

^{13}C NMR [δ(ppm), $CDCl_3$ solution]: 173.6 (CO_2), 138.3 ($C_6H_5CH{=}CHCO_2$), 136.8 ($C_6H_5CH{=}CHCO_2$), 134.0 (d, J 16.5 Hz, $P(\underline{C}_6H_5)_3$), 132.7 (d, J 26.5 Hz, $P(\underline{C}_6H_5)_3$), 129.9 (s, $P(\underline{C}_6H_5)_3$), 128.9 ($C_6H_5CH{=}CHCO_2$), 128.7 (d, J 10.0 Hz, $P(\underline{C}_6H_5)_3$), 128.3 (d, J 17.6 Hz, $C_6H_5CH{=}CHCO_2$), 128.1 ($C_6H_5CH{=}CHCO_2$), 127.3 ($C_6H_5CH{=}CHCO_2$), 126.3 ($C_6H_5CH{=}CHCO_2$), 125.2 ($C_6H_5CH{=}CHCO_2$).

^{31}P NMR [δ(ppm), $CDCl_3$ solution (+22°C)]: +9.2 (s).

^{31}P NMR [δ(ppm), $CDCl_3$ -CH_2Cl_2 solution (-25°C)]: + 8.0 (s).

IR [(cm^{-1}) nujol mulls on NaCl]: 1633 m [ν(C=C)], 1541 s [$\nu_{asym}(CO_2)$], 1437 w [$\nu_{sym}(CO_2)$].

Chapter Three

Silver(I) alkoxides and aryloxides and their triphenylphosphine adducts

3.1 INTRODUCTION.

Metal alkoxides are a very important class of compounds. The applications of metal alkoxides depend on their chemical reactivity, their volatility and their solubility in common organic solvents.

Depending on their chemical reactivity, metal alkoxides have found use as catalysts in organic synthesis. For example, aluminium alkoxides are used as catalysts in the Meerwein-Ponndorf-Verley reaction and titanium and vanadium alkoxides, known as Ziegler-Natta catalysts, in olefin polymerisation.[164] Metal alkoxides have also found use as accelerators for the drying of paints and inks. Due to their solubility in organic solvents and their volatility, metal alkoxides have been used as precursors for sol-gel and MOCVD techniques.

Metal alkoxides are more commonly used in the sol-gel technique because they tend to hydrolyse rapidly to produce metal oxides. In CVD, they also tend to produce metal oxide films instead of thin metallic films. Examples of precursors leading to oxides include $Zr(OR)_4$[165] and $R_3Sn(OR)$.[166] $[Cu(O^tBu)]_4$[167,168] and its adduct $[Cu(O^tBu)(PMe_3)]$[169] are examples where thin copper metal films have been deposited by CVD.

As stated earlier, volatility is an important property for CVD precursors. Early studies on alkoxides demonstrated that the steric effect of the alkyl group controlled volatility.[165] It was found that alkoxides containing less bulky alkyl groups tend to be oligomers. Oligomerisation results from the oxygen of the alkoxy group, bonding to 1, 2 or 3 metals as follows:

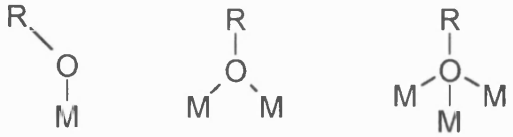

Terminal Bridging (μ_2) Bridging (μ_3)

Mass spectrometric studies on some metal alkoxides showed that oligomers are retained even in the vapour phase.[164,165,170] This means that more energy is required to vaporise a dimer or trimer than a monomer. During a study it was also discovered that the

covalent radius of the metal affected volatility. It was found that volatility decreased with increase of covalent radius.

For more general details on the field of alkoxide chemistry, several books[164] and reviews[165,170-172] have been published in recent years.

Although the chemistry of most metal alkoxides is well established, very little is known about silver alkoxides or aryloxides as a result of their instability.[173]

The main reason for choosing this class of compound for study is that although such compounds have been little explored, analogous copper(I) alkoxides have been used as precursors for CVD of copper. So even given the probable instability, we speculated that silver alkoxides might also be viable for this application.

The advantage of silver(I) alkoxides or aryloxides as precursors for silver CVD is that they should have a good level of volatility. This may counterbalance the likely sensitivity of silver(I) alkoxides or aryloxides to moisture and light, which could cause some handling problems.

This chapter will briefly describe the structural chemistry and synthetic routes known for this class of compounds. The introduction will be followed by details of the synthesis, characterisation and CVD testing of silver(I) alkoxides or aryloxides, prepared in this work.

3.2 STRUCTURAL CHEMISTRY.

The known structural chemistry of silver(I) alkoxides or aryloxides is very limited, only a few silver(I) aryloxides complexes having established structures.

An example of a complex containing an Ag-O-aryl bond system is [Ag($OC_6H_2Cl_3$-2,4,5)].[174] The complex has a polymeric structure. The silver atom is bonded to three oxygens from three different aryloxide ligands and to one carbon from another aryl ring which uses its oxygen to bond to another silver. This gives an overall trigonal pyramidal geometry (Fig. 3.1). In the structure, a further weak interaction is also observed between the silver atom and a chlorine atom, giving the silver atom a trigonal bipyramid geometry. The oxygen of an aryloxide group is bridging, producing the polymeric structure.

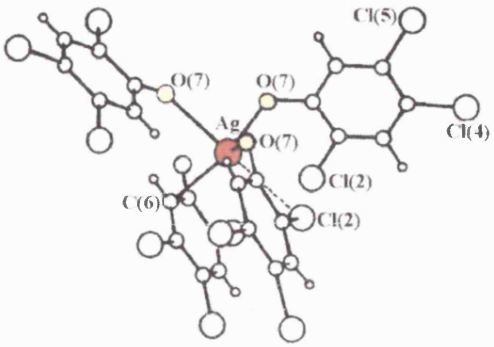

Figure 3.1 Partial structure of $[Ag(OC_6H_2Cl_3\text{-}2,4,5)]$.[174]

A further crystal structure of a silver(I) aryloxide with triphenylphosphine ligands has been determined. Thus monomeric $[Ag(OC_6H_2Cl_3\text{-}2,4,6)(PPh_3)_2]$ has a phenolate ligand and two triphenylphosphine ligands, the silver atom taking up a trigonal planar arrangement (Fig. 3.2).[175] As before, a further weak Ag...Cl interaction is present. The parent silver(I) 2,4,6-trichlorophenolate must have a polymeric structure similar to $[Ag(OC_6H_2Cl_3\text{-}2,4,5)]$, the polymeric structure being broken down on reaction with triphenylphosphine producing monomers.

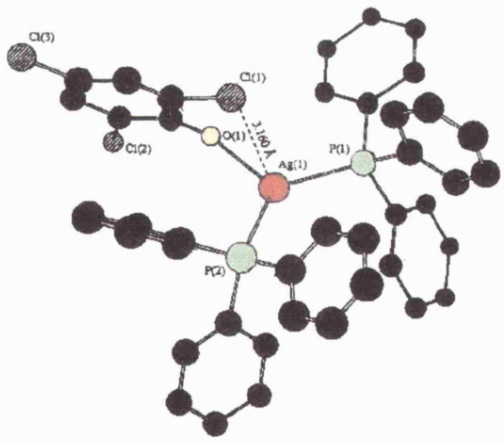

Figure 3.2 Structure of $[Ag(OC_6H_2Cl_3\text{-}2,4,6)(PPh_3)_2]$.[175]

An example of a silver(I) aryloxide containing a macrocyclic polythiaether ligand is given by $[Ag_2(18S6)(pic)_2]$ (18S6 = 1,4,7,10,13,16-hexathiacyclotetradecane, pic = picrate) (Fig. 3.3: (a)).[176] One silver atom is bonded to four sulfur atoms from the ligand giving a distorted tetrahedral arrangement. The second silver atom is bonded to one oxygen

(O1A) from the picrate (Fig. 3.3: (b)) and to four sulfurs from the ligand giving a distorted trigonal bipyramid geometry.

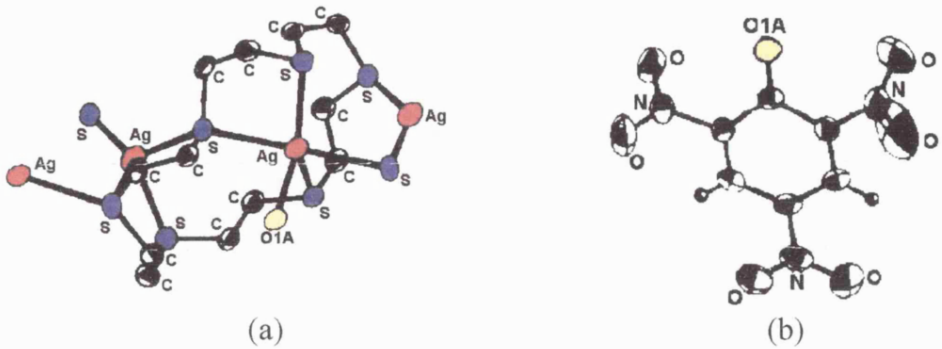

Figure 3.3 (a) Partial structure of $[Ag_2(18S6)(pic)_2]$. (b) Structure of the picrate anion.[176]

Another example of an Ag-phenoxy system is a complex containing quinolinol ligands.[177] The structure of $[Ag_2(C_9H_6NOH)_2(C_9H_6NO)_2(PPh_3)_2]^+(CH_3CO_2)^-\cdot H_2O$ contains two $[Ag(PPh_3)(C_9H_6NOH)(C_9H_6NO)]^+$ complex cations (Fig. 3.4). The dimeric cation is generated by hydrogen bonding employing the hydroxyl proton of the neutral quinolinol ligand. Each silver atom is bonded to one P from triphenylphosphine, one N from a neutral quinolinol ligand and to both N and O atoms from an anionic quinolinolate ligand. The geometry around each silver atom is distorted tetrahedral.

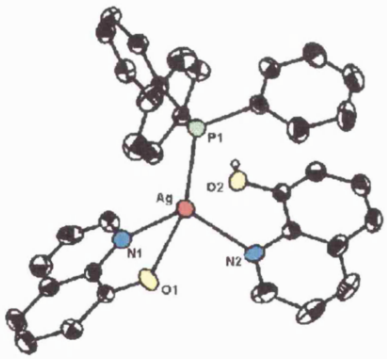

Figure 3.4 Structure of an individual $[Ag(PPh_3)(C_9H_6NOH)(C_9H_6NO)]^+$ cation.[177]

3.3 SYNTHETIC ROUTES.

The majority of silver(I) alkoxides or aryloxides have been prepared by reaction of silver salts with the appropriate sodium or lithium alkoxide in presence of the parent alcohol or THF as solvent as follows:

$$RO\text{-}Li + AgY \longrightarrow RO\text{-}Ag + LiY \quad \textbf{(3.1)}$$

A study of silver(I) alkoxides revealed that the reaction between silver ions and alkoxide ions is rapid at room or low temperature and is independent of counterions, oxygen or light. It was found that the reaction produced a grey-black or grey-brown precipitate in all cases studied. Reaction of silver(I) perchlorate with lithium methoxide or lithium ethoxide gave pure silver. Reaction with lithium tert-butoxide or lithium iso-propoxide produced precipitates, which appeared to be a mixture of pure silver, silver(I) alkoxide and other substances containing silver, carbon and hydrogen. It was concluded that silver(I) alkoxides are unstable when compared to silver(I) aryloxides.[173]

A second method involved the reaction of silver(I) oxide with a phenol in presence of aqueous acetone.[178]

$$Ag_2O + \text{excess ROH} \xrightarrow{\text{acetone:}H_2O(9:1)} RO\text{-}Ag + H_2O \quad \textbf{(3.2)}$$

Silver(I) picrate has been prepared by this method.

In the previous section 3.2, the structures of silver(I) aryloxides were described as polymeric. To break the polymeric structures, phosphine ligands have been added in the syntheses as co-ligands.[175] Two methods have been employed to synthesise these phosphine-containing compounds. The first method involves reaction of silver(I) aryloxide with two moles of triphenylphosphine in diethyl ether solution (eqn. 3.3). The second method involves reaction of a mixture of one mole of silver(I) oxide, 2 moles of an aryl alcohol and 4 moles of triphenylphosphine, in refluxing toluene (eqn. 3.4).

$$RO\text{-}Ag + 2\,PPh_3 \xrightarrow{\text{diethyl ether}} [Ag(OR)(PPh_3)_2] \quad \textbf{(3.3)}$$

$$Ag_2O + 2\,ROH + 4\,PPh_3 \xrightarrow{\text{toluene}} 2\,[Ag(OR)(PPh_3)_2] + H_2O \quad \textbf{(3.4)}$$

3.4 RESULTS AND DISCUSSION.

3.4.1 Synthesis.

The first part of this study, was focused on the synthesis of silver(I) alkoxides or aryloxides using the same methods as employed by others for the preparation of copper(I) alkoxides or aryloxides.

Attempts were made to prepare silver(I) tert-butoxide using the same method as used for copper(I) tert-butoxide[179] with silver(I) chloride replacing copper(I) chloride. A mixture of silver(I) chloride and lithium tert-butoxide in anhydrous THF solution, was stirred for 5 hours and filtered. Evaporation of the filtrate gave a white product, which decomposed on contact with air.

Attempts were made to synthesise silver(I) 3-ethyl-3-pentanolate by the method of the analogous copper(I) alkoxide with silver(I) tetrafluoroborate replacing copper(I) chloride.[180] A mixture of sodium hydride and tert-butyl alcohol in anhydrous THF solution was stirred until H_2 evolution ceased and filtered to remove excess sodium hydride. Using a syringe, a solution of silver(I) tetrafluoroborate in anhydrous THF was added to the sodium tert-butoxide solution, stirred for 24 hours and filtered. The mixture produced a brown solid, the carbon and hydrogen analysis of which did not correspond to the expected product.

Attempts to synthesise silver(I) 2,6-dimethylphenolate following the method of reference 181, produced a green solid, which was more stable than the above silver(I) alkoxides. A solution of 2,6-dimethylphenol in dichloromethane was added to a suspension of sodium hydride in dichloromethane. When the evolution of H_2 ceased, the mixture was filtered to remove excess sodium hydride. Silver(I) chloride was added and the mixture was stirred for 21 hours. The mixture was filtered and the resulting product was dried *in vacuo*. The carbon analysis of the product was encouraging, however the hydrogen value was much too high (Analysis: Found (calculated for C_8H_9AgO) C: 44.5 (41.95), H: 7.53 (3.96)%).

Attempts to prepare silver(I) 2,4,6-tris(dimethylaminomethyl)phenolate using the same method as for the gallium(III) analogue[182], produced a pale brown solid. A solution of lithium 2,4,6-tris(dimethylaminomethyl)phenolate in anhydrous toluene was added slowly to a solution of silver(I) chloride in anhydrous toluene cooled to -78°C. The reaction mixture was allowed to warm to room temperature and stirred overnight. The mixture was filtered and the filtrate was evaporated to dryness to produce a pale brown solid, which was found to be stable for several weeks at room temperature. The nitrogen of the dimethylaminomethyl group may be acting as a donor thus stabilising the product for an extended period. The C, H and N analysis did not correspond to the expected product (Analysis: Found (calculated for $C_{15}H_{26}AgN_3O$)) C: 66.0 (48.4), H: 9.62 (7.04), N: 14.7 (11.3)%).

All the results obtained suggested that uncomplexed silver(I) alkoxides or aryloxides are unstable. These results confirmed the instability of silver(I) alkoxides and aryloxides reported by Macomber et al.[173] Therefore the focus of the work shifted to two alternative approaches, which could assist in stabilising these compounds. The first was using a bulky alkoxide or an aryloxide containing additional donor atoms and the second was using additional ligands such as phosphines to trap the unstable alkoxides or aryloxides.

This work largely focused on the isolation of aryloxides because they seemed to be slightly more stable than alkoxides, although some further work was carried out on silver(I) alkoxides as described below.

A series of triphenylphosphine adducts of silver(I) alkoxides or aryloxides have been successfully synthesised. The majority of the compounds synthesised were obtained by reaction in toluene of one equivalent of silver(I) oxide, two equivalents of a phenol and 4 equivalents of triphenylphosphine, with yields varying from 36 to 82%.

The synthesis of compound (**13**) $[Ag(OC_6H_2Cl_3\text{-}2,4,6)(PPh_3)_2]$ was carried out by a method reported in the literature.[175] The yield obtained was high (81%).

Compound (**14**) $[Ag(OC_6H_5)(PPh_3)_3]\cdot C_6H_5OH$ was prepared in the same manner as $[(PhO)Cu(PPh_3)_2]$.[183] A mixture of silver(I) oxide (1 equivalent), phenol (2 equivalents)

and triphenylphosphine (4 equivalents) in anhydrous toluene, was heated to 75°C for 10 hours and the reaction mixture then filtered. Some silver oxide remained unreacted. The product was obtained as a beige solid by precipitation from the filtrate. A moderate yield was obtained (36%).

Compounds (**15**) $[Ag\{OC_6H_2(CH_2NMe_2)_3\text{-}2,4,6\}(PPh_3)_2]$, (**16**) $[Ag(OC_6H_4Me\text{-}2)(PPh_3)_2]$ and (**17**) $[Ag(OC_6H_4Me\text{-}2)(PPh_3)_3]\cdot(HOC_6H_4Me\text{-}2)$ were synthesised using the same method. A mixture of silver(I) oxide (1 equivalent), the appropriate phenol (2 equivalents) and triphenylphosphine (4 equivalents) in anhydrous toluene was stirred overnight at room temperature. Although reactions were carried out in the dark, the products precipitated as grey solids in all cases. Attempted recrystallisations of compounds (**14**), (**15**) and (**16**) in anhydrous toluene always produced silver films on the side of the flask when left in air. In the absence of air, a brown solid was produced. It was also observed that these triphenylphosphine adducts of silver(I) aryloxides tend to decompose when heated above 80°C. They also tended to react with chlorinated solvents to form $[AgCl(PPh_3)_n]$ (where n = 2 or 3). Compound (**17**) could be recrystallised from a warm anhydrous toluene solution. Colourless crystals could be grown from the solution and one crystal was selected for a crystal structure determination. The crystal structure will be discussed later.

Attempts were also made to prepare triphenylphosphine adducts of silver alkoxides, without isolation of the alkoxides themselves.

The first experiment attempted was a reaction between equimolar amounts of lithium tert-butoxide and $[AgCl(PPh_3)_3]$ in anhydrous THF, at room temperature. After 90 minutes, the mixture was filtered and the filtrate evaporated to dryness to give a white solid compound (**18**) $[Ag(OCMe_3)(PPh_3)_3]$. This compound was stable in air and not significantly light sensitive. Unfortunately, attempts to repeat this synthesis were unsuccessful. Therefore, several alternative routes were explored to synthesise compound (**18**).

The $[AgCl(PPh_3)_3]$ complex was found to be very stable possessing a strong Ag-Cl bond, which was difficult to break. It is known that Ag-F and Ag-O bond strengths are lower than Ag-Cl, so cleavage of these bonds should be easier allowing a fluorine or oxide-

alkoxide exchange to occur. Thus, the first alternative method attempted was a reaction of $[Ag(BF_4)(PPh_3)_3]$ or $[Ag(NO_3)(PPh_3)_3]$ (1 equivalent) with lithium tert-butoxide (1 equivalent) in anhydrous THF. The mixture was stirred overnight at room temperature in the dark. The mixture was filtered and the resulting white solid was dried *in vacuo* for a few hours. ^1H NMR spectra of the products did not show a peak at about 1.3 ppm expected if the tert-butoxy group had been incorporated in the products.

A second approach was to replace lithium tert-butoxide by tert-butoxytrimethylsilane $[Me_3SiOCMe_3]$ in the hope that Me_3Si would prove to be a better leaving group. An equimolar mixture of $[Ag(BF_4)(PPh_3)_3]$ and $[Me_3SiOCMe_3]$ in anhydrous THF, was stirred overnight at room temperature. The mixture was filtered and the white solid produced was investigated using ^1H NMR spectroscopy. Once again the product obtained did not contain a tert-butoxy group.

The third attempt consisted of producing the silver(I) alkoxide then allowing it to react it with triphenylphosphine. A solution of silver(I) tetrafluoroborate in anhydrous dichloromethane was cooled to -20°C. Using a syringe, tert-butoxytrimethylsilane in anhydrous dichloromethane was added slowly to the flask containing the silver(I) tetrafluoroborate solution. The clear solution was stirred at -20°C for 7 hours. A solution of triphenylphosphine in anhydrous dichloromethane was then added slowly to the flask and the mixture was left to stir overnight at room temperature. The only product obtained was $[Ag(BF_4)(PPh_3)_3]$.

In the fourth attempt 15-crown-5 was used to break the polymeric structure of lithium tert-butoxide. A solution of lithium tert-butoxide in anhydrous THF was cooled to 0°C, then 15-crown-5 was added slowly to the solution using a syringe. After 20 minutes, a solution of $[AgCl(PPh_3)_3]$ in anhydrous THF was added dropwise. The mixture was left to stir overnight at room temperature. The resulting yellow solution was filtered giving a yellow solid, which became brown and sticky on contact with air. The filtrate was evaporated to dryness producing a white solid. Once again the ^1H NMR spectrum did not show a resonance at 1.25 ppm indicative of a tert-butoxy group.

The final method attempted consisted of producing the silver(I) alkoxide by reacting silver(I) trifluorosulfonate [CF_3SO_3Ag] with lithium tert-butoxide then adding triphenylphosphine in the reaction to hopefully produce the desired compound. A solution of lithium tert-butoxide in anhydrous toluene was cooled to -20°C. Addition of a solution of silver(I) trifluorosulfonate in anhydrous toluene produced a yellow-orange and finally a brown mixture, which was stirred at -20°C for 4 hours. A solution of triphenylphosphine in anhydrous toluene was then added slowly to the brown mixture, the colour changing to light brown. The mixture was stirred overnight then filtered giving a brown solid. Once again the solid was not the desired product.

3.4.2 Infrared spectroscopy.

Infrared spectroscopy is of less importance for the study of metal alkoxides or aryloxides when compared to metal carboxylates. This technique can be used to show characteristic bands relating to metal-oxygen ν(M-O) and carbon-oxygen ν(C-O) vibrations. The ν(M-O) bands are usually found at low frequencies (400-450 cm^{-1})[184] and the C-O stretching bands normally appear in the 1000-1200 cm^{-1} region depending on the nature of the alcohol. For example, the C-O stretch of a tertiary alcohol usually appears at about 1150 cm^{-1}, while the C-O stretch of phenol appears at about 1230 cm^{-1}.[185]

During this study, only C-O stretches were characterised. Table 3.1 summarises the frequencies of all C-O stretching vibrations for compounds (**13**) to (**18**).

Compounds	ν (C-O) (cm^{-1})
$[Ag(OC_6H_2Cl_3\text{-}2,4,6)(PPh_3)_2]$ (**13**)	1244 (m)
$[Ag(OC_6H_5)(PPh_3)_3{\cdot}C_6H_5OH]$ (**14**)	1248 (w)
$[Ag\{OC_6H_2(CH_2NMe_2)_3\text{-}2,4,6\}(PPh_3)_2]$ (**15**)	1229 (w)
$[Ag(OC_6H_4Me\text{-}2)(PPh_3)_2]$ (**16**)	1278 (m)
$[Ag(OC_6H_4Me\text{-}2)(PPh_3)_3{\cdot}2\text{-}MeC_6H_4OH]$ (**17**)	1244 (m)
$[Ag(OCMe_3)(PPh_3)_3]$ (**18**)	1157 (m)

Table 3.1 Infrared spectroscopy of triphenylphosphine adducts of silver(I) alkoxides and aryloxides.

The C-O stretch of the aryloxides were found in the range 1229-1278 cm^{-1}. These values are in good agreement to those found in gold(I) aryloxide complexes[186] and copper(I) aryloxides complexes[183] [ν (C-O) ~ 1270 – 1150 cm^{-1}]. The C-O stretch of the alkoxide was found at 1157 cm^{-1}, which is similar to the C-O stretch of the parent tertiary alcohol.

The infrared spectrum of compound (**17**) recorded as a nujol mull, did not show characteristic hydrogen bonding bands in the region between 3200-2500 cm^{-1}.[187] These bands might be hidden by nujol peaks because in a hexachlorobutadiene mull, weak peaks appeared in the region 3051 to 2920 cm^{-1}, suggesting some intramolecular hydrogen bonding. Compound (**14**) also showed a weak peak at 3184 cm^{-1}, which is indicative of intramolecular hydrogen bonding.

3.4.3 NMR spectroscopy.

^{1}H, ^{13}C and ^{31}P NMR spectra were recorded for all compounds synthesised.

3.4.3.1 ^{1}H and ^{13}C NMR Spectroscopy.

The ^{1}H NMR spectrum of compound (**13**) showed peaks due to PPh_3 protons at 7.38-7.24ppm and the chlorophenolate protons at 6.97ppm. The peak area ratio between the PPh_3 and the chlorophenolate protons agreed well with the assigned formula for the compound.

The ^{1}H NMR spectrum of compound (**14**) showed overlapping multiplets for PPh_3, PhOH and PhO protons at 7.31-6.71 ppm. A small broad peak at 6.40 ppm was assigned to the hydrogen of the hydroxyl group in phenol.

In the ^{1}H NMR spectrum of compound (**15**), the ortho and the para NMe_2 groups appeared as singlets at 2.28 ppm and 2.21 ppm with a 2:1 ratio. The methylene protons of the CH_2NMe_2 groups in ortho and para positions appeared as singlets at 3.52 ppm and 3.29ppm respectively with a 2:1 ratio. The methylene protons of the CH_2NMe_2 groups behaved differently to those of $[(Me_2NCH_2)_3C_6H_2OGaCl_2]_2$[182] where a single CH_2 proton resonance indicates equivalent ortho and para CH_2NMe_2 methylene groups. In the silver compound, it seems that the CH_2NMe_2 methylene groups in ortho and para positions are magnetically inequivalent. However, the spectrum correlates with that of the free substituted phenol where the ortho and para methylene groups are detected as singlets at 2.27 ppm and 2.20 ppm, respectively.

The ^{1}H NMR spectrum of compound (**16**) showed a multiplet at 7.40-7.24 ppm from the protons of PPh_3 and o-cresolate groups. A singlet assigned to the methyl group of the o-cresolate ligand appeared at 2.21 ppm shifted slightly downfield when compared to the free o-cresol (2.18 ppm).

The ^{1}H NMR spectrum of compound (**17**) showed once again a multiplet at 7.35-7.25 ppm from hydrogens of the PPh_3, o-cresolate, o-cresol and toluene moieties. A singlet assigned to the methyl protons of toluene appeared at 2.35 ppm. The methyl from both the o-cresolate and o-cresol groups appeared at 2.24 ppm, shifted downfield when compared to the free o-cresol (2.18 ppm).

The ^{1}H NMR spectrum of compound (**18**) showed a multiplet at 7.36-7.19 ppm from the PPh_3 protons and a singlet at 1.25 ppm from the tert-butoxy group.

In the ^{13}C NMR spectra, all resonances from the aryloxide C-O units were found between 154 and 160 ppm. These values are similar to those of the free phenols. The carbon of the alkoxy group in the tert-butoxide was found at 32 ppm.

The ^{13}C NMR spectrum of compound (**17**) was difficult to assign. Carbon resonances associated with the PPh_3, o-cresol and toluene carbons present in the compound were assigned by comparison with the related resonances of free PPh_3, o-cresol and toluene. Carbons from the o-cresolate were deduced after consideration of the free o-cresol carbon resonances. The assignments should be viewed with some caution, as other alternative assignments may be reasonable.

3.4.3.2 ^{31}P NMR spectroscopy.

The ^{31}P NMR spectra of compounds (**13**) to (**17**) were recorded at room temperature and at low temperature.

At room temperature all spectra showed a broad peak in the region 5.5 to 9.5 ppm for each compound. The absence of $^{1}J(Ag-P)$ coupling indicates a rapid dissociation or exchange in solution. The ^{31}P NMR data are summarised in Table 3.2.

The ^{31}P chemical shift difference between the complexes and free triphenylphosphine, known as the coordination shift and noted as $\Delta\delta$, is not sensitive to the nature of the aryloxide ligand. $\Delta\delta$ values range from 9.9 to 14.7 ppm. This is consistent with earlier results obtained as mentioned in chapter 2.

Due to some solubility problems in $CDCl_3$ solvent, a mixture of $CDCl_3$-CH_2Cl_2 was used and so -25°C was the lowest temperature at which the spectra could be recorded.

Low temperature ^{31}P-NMR spectra showed once again a broad peak in the region 4.5-9.4 ppm for each compound except for compound (**13**), which consisted of a broad doublet at 9.38 ppm resulting from Ag-P spin-spin coupling. The value of $^{1}J(Ag-P)$ in compound (**13**) (345 Hz), is smaller than those found for triphenylphosphine adducts of silver(I) carboxylates but can be compared to the range of $^{1}J(Ag-P)$ coupling constants found for trigonal or linear bis(phosphine)silver(I) complexes (278 Hz to 503 Hz).[85]

Compounds	^{31}P-data at room temperature (δ ppm)	Δδ	^{31}P-data at low temperature (δ ppm)
$[Ag(OC_6H_2Cl_3\text{-}2,4,6)(PPh_3)_2]$ (**13**)	+9.47	14.71	+9.38 (d) ^{1}J(Ag-P) 345 Hz
$[Ag(OC_6H_5)(PPh_3)_3{\cdot}C_6H_5OH]$ (**14**)	+5.58	10.82	+5.08 (s)
$[Ag\{OC_6H_2(CH_2NMe_2)_3\text{-}2,4,6\}(PPh_3)_2]$ (**15**)	+8.00	13.24	+7.32 (s)
$[Ag(OC_6H_4Me\text{-}2)(PPh_3)_2]$ (**16**)	+7.97	13.21	+6.77 (s)
$[Ag(OC_6H_4Me\text{-}2)(PPh_3)_3{\cdot}2\text{-}MeC_6H_4OH]$ (**17**)	+4.75	9.99	+4.51 (s)

Table 3.2 ^{31}P NMR data of triphenylphosphine adducts of silver(I) aryloxides.

3.4.4 Mass spectrometry.

The FAB (Fast Atom Bombardment) mass spectra of compounds (**13**), (**14**), (**15**) and (**17**) have been obtained, the results being summarised in Table 3.3.

The metal-containing fragments in the spectra are readily identified by the characteristic patterns imposed by the natural isotopic abundances, approximately 1:1 for silver isotopes 107 and 109.

Fragments have been grouped together on the basis of containing none, one or two silver atoms. The molecular ion was not detected for any of the compounds except (**17**), where a low abundance cluster centred at m/z 1109 was observed.

Fragments such as $[Ag(PPh_3)_n]^+$ (where n= 1, 2) have been identified as being present in high abundance, while $[AgO(PPh_3)_2]^+$ and $[Ag(PPh_3)_3\text{-}H]^+$ were identified in low abundance. The presence of $[Ag(PPh_3)]^+$ and $[Ag(PPh_3)_2]^+$ in high abundance suggests the tendency of silver(I) complexes to be linear, two coordinate, species in gas phase.[149]

The $[AgO(PPh_3)_2]^+$ fragment has been observed in low abundance previously in the spectra of $[Ag(C_2Ph)(PPh_3)]$[150] and triphenylphosphine adducts of silver(I) β- diketonates.[1] The $[Ag(PPh_3)_3\text{-}H]$ fragment was also observed in triphenylphosphine adducts of silver(I) β- diketonates in low abundance.[1]

No fragments containing aryloxide groups were observed for any of the compounds. It is suggested that the compounds decompose at an early stage, in the spectrometer.

	(**13**)		(**14**)		(**15**)		(**17**)	
Fragments	m/z	%	m/z	%	m/z	%	m/z	%
$[(C_6H_4)_2P]^+$	183	41.6	-		183	22.1	183	47.4
$[PPh_3]^+$	262	24.8	262	24.5	262	21.9	262	27.3
$[Ag(PPh_3)]^+$	369	77.3	369	82.1	369	100	369	81.4
$[Ag(PPh_3)_2]^+$	631	100	631	100	631	56	631	100
$[AgO(PPh_3)_2]^+$	647	63	647	2.2	647	2.7	647	4.5
$[Ag(PPh_3)_3\text{-}H]^+$	892	1.5	892	1.45	892	0.6	892	4.01
$[M]^+$	-		-		-		1109	0.15
$[M+O]^+$	-		-		-		1125	0.56
$[Ag_2(CO)(PPh_3)_2]^+$	-		-		766	3.7	766	3.23
$[Ag_2(OH)(PPh_3)_3]^+$	-		-		-		1017	0.37
Other silver	775	13.6	382	21.6	133	42.2	663	1.4
containing	937	7.6	775	2.5	221	61.4	739	1.67
fragments			833	0.8	589	7.0	757	1.9
					742	4.9	775	3.27
					1004	0.9		

Table 3.3 Mass spectrometry fragments of triphenylphosphine adducts of silver(I) aryloxides.

3.4.5 X-Ray Crystal Structure Determination of (o-Cresolato-*O*)*tris*(triphenylphosphine)silver(I).o-cresol.toluene solvate.

Crystals were grown slowly from toluene solution in a refrigerator. The structure is illustrated in Figure 3.5. Relevant bond lengths and angles are summarised in Table 3.4 (See Appendix 6 for further data).

The asymmetric unit in this crystal structure contains one molecule of (o-cresolato-*O*)*tris*(triphenylphosphine)silver(I), one molecule of o-cresol and one disordered toluene solvent molecule of recrystallisation. The silver atom is bonded to the oxygen of the o-cresolato ligand and to three phosphorus atoms from the triphenylphosphine ligands, giving a distorted tetrahedral arrangement.

The Ag-O bond length [2.386(5) Å] is within the range observed for silver(I) aryloxides, for example the Ag-O distance in $[Ag(OC_6H_2Cl_3)(PPh_3)_2]$ is 2.255 Å[175] and the Ag-O distances in $[Ag(OC_6H_2Cl_3)]$ range from 2.317(3) to 2.543(3) Å.[174] In the quinolinol complex $[Ag(PPh_3)(C_9H_6NOH)(C_9H_6NO)]^+$, the Ag-O bonds are slightly longer [2.529(4) and 2.546(4) Å].[177]

The P-Ag-O angles range from 98.36(14)° to 107.8(2)° in the crystal structure. These angles are smaller than the P-Ag-O angles of $[Ag(OC_6H_2Cl_3)(PPh_3)_2]$ [115.4(1) and 113.4(1) °][175] and $[Ag(PPh_3)(C_9H_6NOH)(C_9H_6NO)]^+$ [122.17(9) and 119.96(9)°].[177]

The Ag-P distances of 2.539(2) Å, 2.540(2) Å and 2.577(2) Å are longer than those found in $[Ag(OC_6H_2Cl_3)(PPh_3)_2]$ [2.444(1) and 2.451(1) Å][175] and $[Ag(PPh_3)(C_9H_6NOH)(C_9H_6NO)]^+$ [2.3802(13) and 2.3765(13) Å].[177] However, they are similar to those found in four-coordinate tris(triphenylphosphine)silver(I) halides, $AgXL_3$, and derivatives e.g. 2.506(3) Å in $[Ag(BF_4)(PPh_3)_3]$[188] to 2.780(3) Å in $[AgI(PPh_3)_3]$ [189].

Although the P-Ag-P angles in the crystal structure [116.41(7), 111.08(7) and 115.73(6)°] are less than the P-Ag-P angle in $[Ag(OC_6H_2Cl_3)(PPh_3)_2]$ [131.1(1)°][175], they are similar to those found in $AgX(PPh_3)_3$ complexes i.e. 107.00(7)° in $[AgI(PPh_3)_3]$[189] to 119.3(1)°in $[Ag(BF_4)(PPh_3)_3]$.[188]

In the crystal structure, hydrogen bonding was noted between the o-cresolate oxygen O(1) and the phenolic proton H(2A) of the o-cresol molecule, which is not directly coordinated to the silver. The hydrogen H(2A) was found in the solution of the structure and was refined at a distance of 0.98 Å from O(2). The O(1)-O(2) [2.565(9) Å] and H(2A)-O(1) [1.59(4) Å] bond distances are similar to those of $[(PMe_3)_3Rh(OC_6H_4Me\text{-}4)(HOC_6H_4Me\text{-}4)]$ [O(1)-O(2): 2.62 Å, O(1)-H: 1.4 ± 0.1Å].[190] The O(2)-H(2A)-O(1) angle [170(10)°] was found to be nearly linear. This is comparable to other H-bonded structures.[191]

The toluene solvent disorder was extreme and difficult to model. After several attempts, the most satisfactory refinement was achieved by assuming the solvent electron density as two rigid phenyl groups in the occupancy ratio of 52:48 for partial carbons C(69)-C(74) and C(75)-C(80), respectively. Unfortunately, it was impossible to locate and refine the associated partial methyl carbon of the toluene.

Bond lengths (Å)	**Angles (°)**
Ag(1)-O(1) = 2.386(5)	O(1)-Ag(1)-P(1) = 98.36(14)
Ag(1)-P(1) = 2.577(2)	O(1)-Ag(1)-P(2) = 105.2(2)
Ag(1)-P(2) = 2.539(2)	O(1)-Ag(1)-P(3) = 107.8(2)
Ag(1)-P(3) =2.540(2)	P(2)-Ag(1)-P(3) = 116.41(7)
O(1)-O(2) = 2.565(9)	P(2)-Ag(1)-P(1) = 111.08 (7)
H(2A)-O(1) = 1.59(4)	P(3)-Ag(1)-P(1) = 115.73(6)
	O(2)-H(2A)-O(1) = 170(10)

Table 3.4 Relevant bond lengths and angles of complex (**17**).

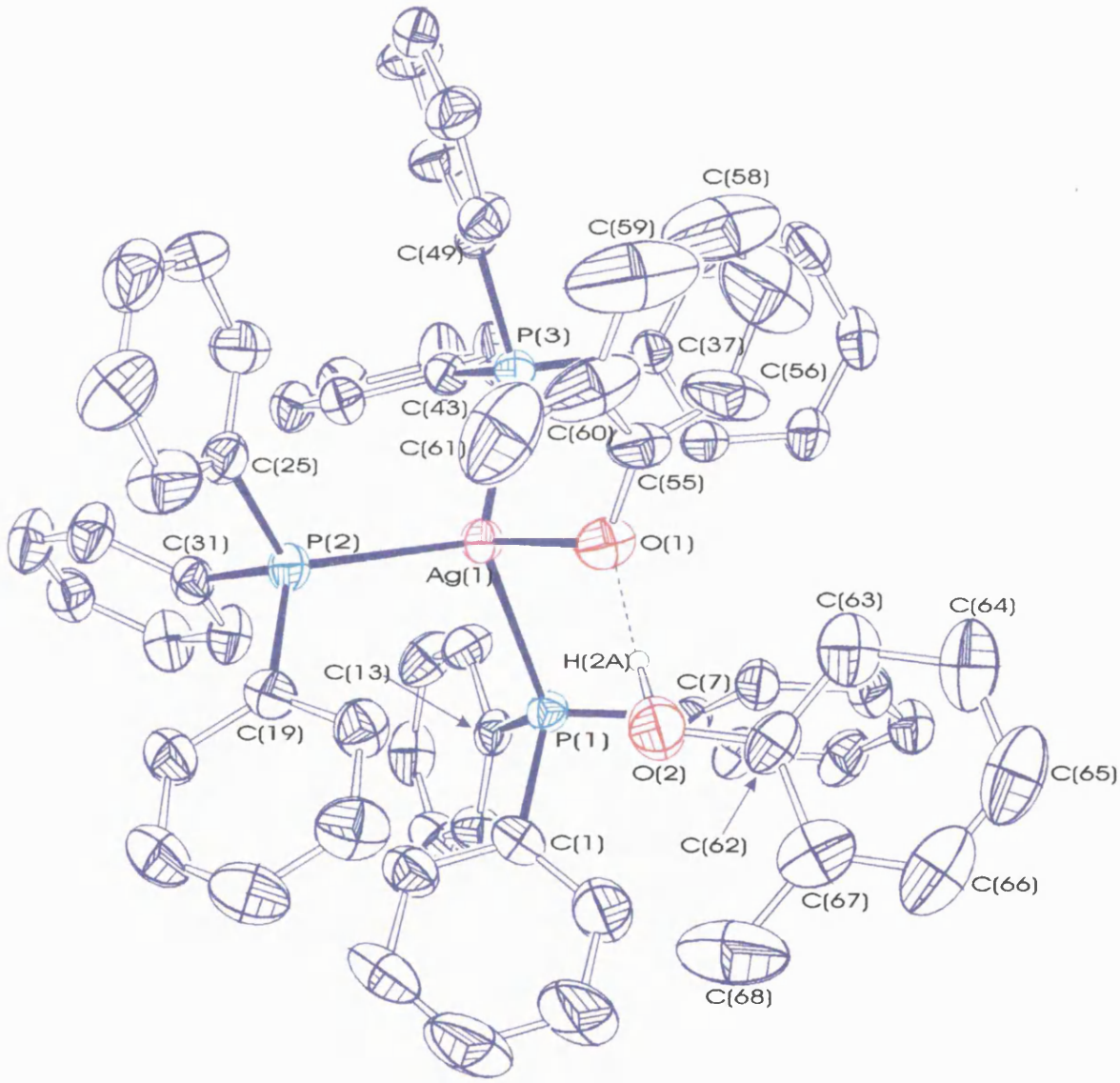

Figure 3.5 Structure of (o-cresolato-*O*)*tris*(triphenylphosphine)silver(I).o-cresol.toluene solvate (**17**).

3.4.6 Thermogravimetric analysis (TGA).

TGA analyses were carried out on compounds (**13**), (**14**), (**15**), (**16**) and (**17**) under an inert helium atmosphere in order to obtain information on their relative stabilities and to determine the temperature at which decomposition may start.

All compounds except (**16**) were found to decompose by a two-stage process, however the temperature ranges varied widely from one compound to another. Thus, the first step starts between 55-195°C and finishes between 140-320°C. The second step starts between 90-330°C and finishes between 290-380°C.

The TGA of compound (**16**) revealed a single thermal decomposition stage starting at 130°C and finishing at 310°C with a mass loss of 75.1%. The weight loss in this single step relates to the complete thermal decomposition of the whole molecule leaving silver as the residue.

Compound (**13**) started decomposing at a higher temperature when compared to the other compounds. The first step covered the temperature range 195-320°C with a 62.4% mass loss, which may correspond to a loss of two triphenylphosphine ligands (% theoretical: 63.3). The second step started at 330°C with a mass loss of 17.5%, which may correspond to a loss of $Cl_2C_6H_3O$ (% theoretical: 19.4) (see Figure 3.6).

The first decomposition step of compound (**14**) began at 110°C and resulted in a weight loss of 17.2%. This value may correspond to the loss of the free phenol and phenolate groups (% theoretical: 17.3). The second step started at 180°C with a mass loss of 68.1%. This correlates reasonably well to the loss of three triphenylphosphine ligands (% theoretical: 72.7).

Compound (**15**) started decomposing at 55°C with a mass loss of 63.1% for the first stage. The second step occurred between 290-315°C with an 11.1% weight loss. The mass loss of the first step correlates with loss of two triphenylphosphine ligands (% theoretical: 58.5) and this may be followed by loss of two CH_2NMe_2 groups.

Decomposition of compound (**17**) began at 110°C with a weight loss of 7.1% for the first stage. This corresponds to a loss of o-cresol (% theoretical: 9.7). This was followed by thermal decomposition of (o-cresolato-*O*)*tris*(triphenylphosphine)silver(I).

The final product after decomposition of each compound should be silver metal. The theoretical % weight residues for silver metal are given in Table 3.5. The experimental values found are much higher than the theoretical value except for compound (**14**). The

residue of compound (**13**) may be AgCl (% theoretical: 17.3). It is possible therefore that the residue may also contain traces of carbon and traces of silver(I) phosphate obtained by oxidation of triphenylphosphine. Silver oxide would not be present in the residue due to its decomposition to the metal at about 200°C.

Compounds	Decomposition temperature (°C) $T_{initial}$	T_{final}	Weight loss (%)	Detached group (%calculated)		Residue remaining %found	$\%Ag_{calc}$
$[Ag(OC_6H_2Cl_3\text{-}2,4,6)(PPh_3)_2]$ (**13**)	195	320	62.4	$2PPh_3$	(63.3)	19.6	13.0
	330	380	17.5	$Cl_2C_6H_3O$	(19.4)	(% AgCl: 17.3)	
$[Ag(OC_6H_5)(PPh_3)_3{\cdot}C_6H_5OH]$ (**14**)	110	180	17.2	PhOH + PhO	(17.3)	11.4	10.0
	180	290	68.2	2 PPh_3	(72.7)		
$[Ag\{OC_6H_2(CH_2NMe_2)_3\}(PPh_3)_2]$ (**15**)	55	270	63.1	2 PPh_3	(58.5)	20.9	12.0
				2 PPh_3 + 1 CH_2NMe_2	(65.0)		
	290	315	11.1	2 CH_2NMe_2	(12.9)		
$[Ag(OC_6H_4Me\text{-}2)(PPh_3)_2]$ (**16**)	130	310	75.1	2 PPh_3	(63.3)	19.9	14.6
				2 PPh_3 + 1 PhO	(85.4)		
$[Ag(OC_6H_4Me\text{-}2)(PPh_3)_3{\cdot}2\text{-}MeC_6H_4OH]$ (**17**)	110	140	7.1	$2\text{-}MeC_6H_4OH$	(9.7)	15.3	9.7
	150	300	74.4	3 PPh_3	(70.9)		
				3 PPh_3 + $2\text{-}MeC_6H_4O$	(80.5)		

Table 3.5 TGA analysis of triphenylphosphine adducts of silver(I) aryloxides.

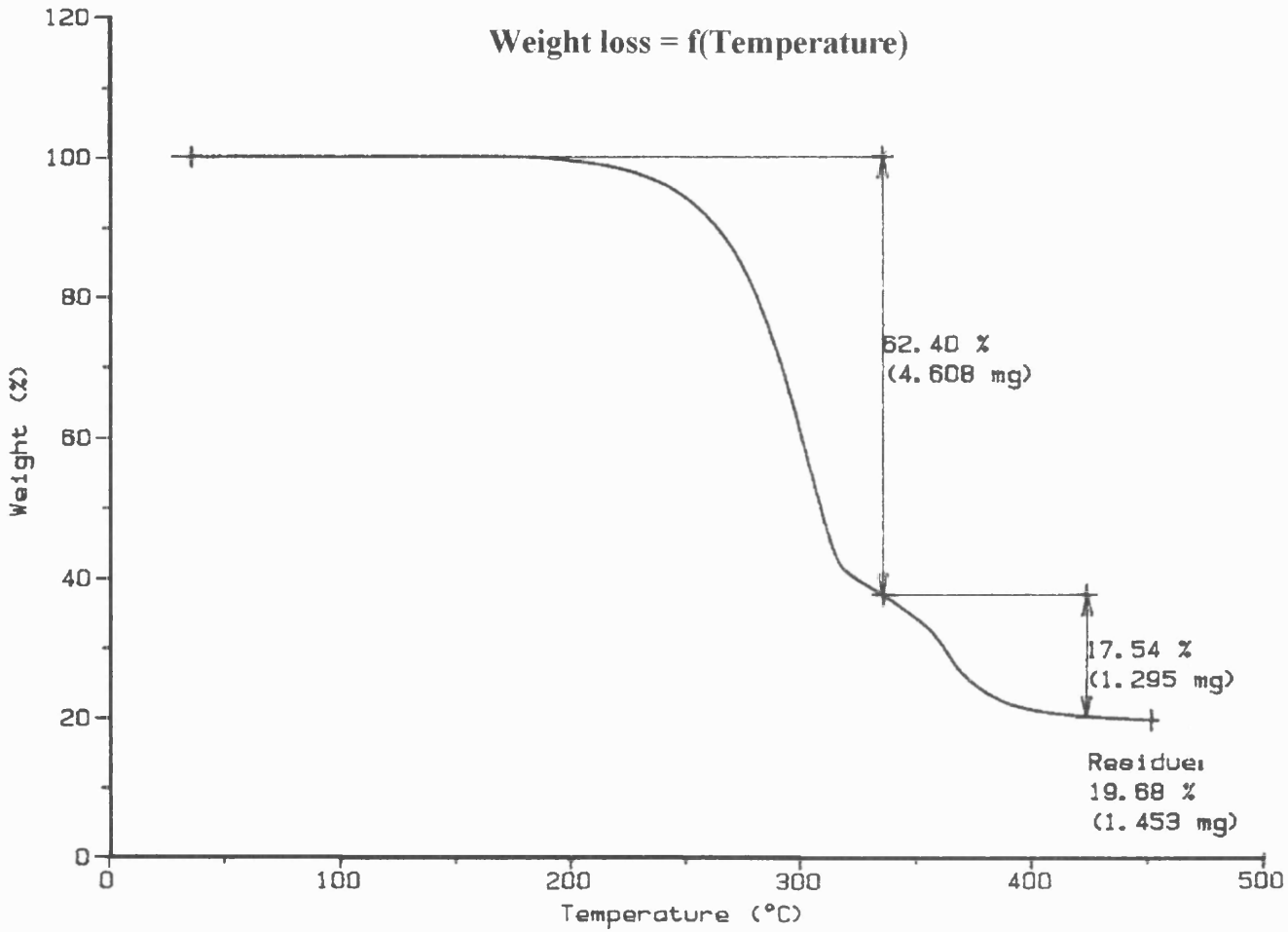

Figure 3.6 TG curve of compound (**13**).

3.4.7 CVD Testing of precursors.

Films were grown from precursor compounds (**13**), (**15**) and (**17**) using a horizontal cold wall reactor. Films were grown over a period of 17 to 104 minutes on glass substrates under different temperature conditions and a N_2 atmosphere of one bar pressure (Table 3.6). The precursor was delivered to the gas phase as an aerosol of the compound dissolved in anhydrous THF and swept into the reactor using N_2 as carrier gas. The solvent used had to be anhydrous otherwise the compound decomposed in the solution.

The films grown were found to be thin, soft and could be easily scratched or damaged relatively easily by touching.

Conditions	(**13**) $[Ag(OC_6H_2Cl_3)(PPh_3)_2]$	(**15**) $[Ag\{OC_6H_2(CH_2NMe_2)_3\}(PPh_3)_2]$	(**17**) $[Ag(OC_6H_4Me\text{-}2)(PPh_3)_3 \cdot 2\text{-}MeC_6H_4OH]$
Concentration ($g.l^{-1}$)	50-120	63-65	13-36
Temperature of the reactor (°C)	300-596	300	250-398
N_2 gas flow rate ($l.min^{-1}$)	0.8-1.05	0.95-1	0.5-1
Run time (min)	17-88	41-106	20-104

Table 3.6 Conditions of CVD testing of triphenylphosphine adducts of silver(I) aryloxides.

The quality of the films was dependent on the precursor used. Each precursor was tested at different concentrations, temperature, N_2 carrier gas flow rate and run time. None of the precursors of this series produced good quality silver mirrors.

Compound (**13**) did not produce a silver film at 300°C, 400°C and 596°C with a N_2 flow rate of 1-1.05 $l.min^{-1}$. Even with an increase of concentration, a decrease of N_2 flow rate and increase of run time, there was no sign of even a thin yellow silver film. In every case a thin grey film was obtained.

Compound (**15**) was tested at 300°C, with a constant concentration and almost constant N_2 flow rate (see Table 3.6). After 41 minutes run time, a thin yellow film was observed. Therefore a longer run was attempted. After 106 minutes run time, a thick yellow-brown film was obtained.

Compound (**17**) at low concentration, did not produce a film at 200°C, with a N_2 flow rate of 0.5 $l.min^{-1}$. With an increase of temperature, and N_2 flow rate, a very thin yellow film was observed. Even with an increase of concentration, temperature and run time, the best film obtained was a thin yellow-brown film.

Films were examined using Energy Dispersive X-ray spectroscopy (EDXS). Due to poor quality of the films SEM, sheet resistivity and reflectivity measurements have not been carried out. Table 3.7 summarises the conditions used and characterisation of the films obtained.

The compositions of these films were established by Energy Dispersive X-ray analysis. This technique did not provide quantitative analysis of impurities but did highlight impurities that are present. Due to poor conductivity of the films, the analysis did not give conclusive results, but the analysis revealed that the films contain silver with some carbon, oxygen and silicon impurities. The silicon and oxygen may arise from the glass substrate.

In conclusion, the films obtained from the triphenylphosphine adducts of the aryloxides were of poor quality. This might be explained by the presence of the aryloxide, which might reduce the volatility of the compounds. This was also observed in the compounds reported in the previous chapter. To verify this proposal, it would be interesting to test a triphenylphosphine adduct of an alkoxide to see if there was a difference. Should better quality films not be produced, it would be reasonable to conclude that silver(I) alkoxides and aryloxides are volatile but generally not suitable for deposition of silver films. This conclusion would agree with previous literature reports on the use of metal alkoxides or aryloxides. In CVD, metal alkoxides tend to produce metal oxide films rather than metallic films.

Compounds	Concentration ($g.l^{-1}$)	Temperature of the reactor (°C)	N_2 gas flow rate ($l.min^{-1}$)	Run time (min)	Visual appearance	Detected impurities (EDXS)
$[Ag(OC_6H_2Cl_3\text{-}2,4,6)(PPh_3)_2]$ (**13**)	120	300	0.8-0.85	88	Thick pale grey film	C
$[Ag\{OC_6H_2(CH_2NMe_2)_3\}(PPh_3)_2]$ (**15**)	65	300	1.0	106	Thick yellow brown film	C
$[Ag(OC_6H_4Me\text{-}2)(PPh_3)_3 \cdot 2\text{-}MeC_6H_4OH]$ (**17**)	33	300	1.0	75	Thin yellow brown film	C

Table 3.7 Conditions of formation, visual appearance and analysis of silver films grown from triphenylphosphine adducts of aryloxides.

3.5 EXPERIMENTAL.

All operations were carried out under nitrogen and in subdued light with final storage of products in the dark.

Preparation of (2,4,6-trichlorophenolato-*O,Cl*)*bis*(triphenylphosphine)silver(I) (13).

The compound was synthesised by the method of reference 175.

A mixture of silver(I) oxide (1 mmol), 2,4,6-trichlorophenol (2.2 mmol) and triphenylphosphine (4.4 mmol) was heated in refluxing toluene (75 cm^3) for two hours. The hot mixture was filtered and petroleum ether (60-80° boiling range) was added to the clear solution until a solid precipitated. The white precipitate was filtered, washed with toluene and dried *in vacuo*.

Yield: 81%

Analysis: Found (calculated) for $C_{42}H_{32}AgCl_3OP_2$. C: 60.9 (60.9), H: 3.87 (3.89)%.

^1H NMR [δ(ppm), $CDCl_3$ solution]: 7.38-7.24 (m, 30H, $P(C_6\underline{H}_5)_3$), 6.97 (s, 2H, 2,4,6-$Cl_3C_6\underline{H}_2O$).

^{13}C NMR [δ(ppm), $CDCl_3$ solution]: 160.0 (CO), 133.9 (d, J 16.5 Hz, $P(\underline{C}_6H_5)_3$), 132.6 (2,4,6-$Cl_3\underline{C}_6H_2O$), 132.1 (d, J 27.0 Hz, $P(\underline{C}_6H_5)_3$), 130.1 (s, $P(\underline{C}_6H_5)_3$), 128.8 (d, J 10.0 Hz, $P(\underline{C}_6H_5)_3$), 127.1 (2,4,6-$Cl_3\underline{C}_6H_2O$), 123.7 (2,4,6-$Cl_3\underline{C}_6H_2O$), 112.7 (2,4,6-$Cl_3\underline{C}_6H_2O$).

^{31}P NMR [δ(ppm), $CDCl_3$ solution, (+22°C)]: +9.47 (s)

^{31}P NMR [δ(ppm), $CDCl_3$-CH_2Cl_2 solution, (- 25°C)]: +9.38 [d unresolved, ^1J (Ag-P) 345 Hz].

IR [(cm^{-1}) nujol mulls on NaCl]: 1583 w, 1558 w, 1516 w, 1435 s, 1244 m [ν(C-O)].

Preparation of (phenolato-*O*)*tris*(triphenylphosphine)silver(I).phenol (14).

This compound was prepared in the same way as $[(PhO)Cu(PPh_3)_2]$[183] with silver(I) oxide replacing copper(I) oxide.

A mixture of silver(I) oxide (10 mmol), phenol (20 mmol) and triphenylphosphine (40 mmol) in toluene (80 cm^3) was heated to 75°C for 10 hours. The pale brown solution was filtered while still hot and then allowed to cool to room temperature. After allowing

the filtrate to stand overnight in the dark, the product precipitated as beige solid. This solid was filtered, washed with dry toluene and dried *in vacuo*.

Yield: 36 %.

Analysis: Found (calculated) for $C_{66}H_{56}AgO_2P_3$. C: 73.0 (73.2), H: 5.45 (5.18)%.

^{1}H NMR [δ(ppm), $CDCl_3$ solution]: 7.31-6.71 (m, 55H, $P(C_6\underline{H}_5)_3$, $C_6\underline{H}_5OH$, $C_6\underline{H}_5O$), 6.40 (s, 1H, $C_6H_5O\underline{H}$).

^{13}C NMR [δ(ppm), $CDCl_3$ solution]: 160.5(CO), 133.7 (d, J 15.4 Hz, $P(\underline{C}_6H_5)_3$), 132.4 (d, J 17.6 Hz, $P(\underline{C}_6H_5)_3$), 130.1(s, $P(\underline{C}_6H_5)_3$), 128.9 (d, J 8.8 Hz, $P(\underline{C}_6H_5)_3$), 128.1 ($\underline{C}_6H_5O$), 116.8 ($\underline{C}_6H_5O$), 116.6 ($\underline{C}_6H_5O$).

^{31}P NMR [δ(ppm), $CDCl_3$ solution, (+22°C)]: +5.58 (s).

^{31}P NMR [δ(ppm), $CDCl_3$-CH_2Cl_2 solution, (- 25°C)]: +5.08 (s).

IR [(cm^{-1}) nujol mulls on NaCl]: 3368 w (br), 3184 w [ν(O-H)], 1622 m, 1606 w, 1585 w, 1435 s, 1248 w (br) [ν(C-O)].

Preparation of [2,4,6-tris(dimethylaminomethyl)phenolato-*O*]*bis*(triphenylphosphine) silver(I) (15).

A mixture of silver(I) oxide (4.3 mmol), 2,4,6-tris(dimethylaminomethyl)phenol (8.6 mmol) and triphenylphosphine (17 mmol) in toluene (40 cm^3) was stirred overnight under nitrogen at room temperature. The resulting dark mixture was filtered and the filtrate was allowed to stand at room temperature. The product precipitated as a grey solid. This product was filtered, washed with dry toluene and dried *in vacuo*.

Yield: 66%

Analysis: Found (calculated) for $C_{51}H_{56}AgN_3OP_2$. C: 67.6 (68.3), H: 6.19 (6.29), N: 4.45 (4.69)%.

^{1}H NMR [δ(ppm), $CDCl_3$ solution]: 7.43-7.23 (m, 30H, $P(C_6\underline{H}_5)_3$), 6.94 (s, 2H, 2,4,6-$(Me_2NCH_2)_3C_6\underline{H}_2O$), 3.52 (s, 4H, $C\underline{H}_2N$), 3.29 (s, 2H, $C\underline{H}_2N$), 2.28 (s, 12H, $(C\underline{H}_3)_2N$), 2.21 (s, 6H, $(C\underline{H}_3)_2N$).

^{13}C NMR [δ(ppm), $CDCl_3$ solution]: 155.5 (s, CO), 134.0 (d, J 16.5 Hz, $P(\underline{C}_6H_5)_3$), 132.5 (d, J 26.4 Hz, $P(\underline{C}_6H_5)_3$), 130.0 (s, $P(\underline{C}_6H_5)_3$), 128.7 (d, J 8.9 Hz, $P(\underline{C}_6H_5)_3$), 128.3 (2,4,6-$(Me_2NCH_2)_3\underline{C}_6H_2O$), 123.0 (2,4,6-$(Me_2NCH_2)_3\underline{C}_6H_2O$), 63.8 ($CH_2N$), 60.3 ($CH_2N$), 45.1 ($N(CH_3)_2$), 44.8 ($N(CH_3)_2$).

^{31}P NMR [δ(ppm), $CDCl_3$ solution, (+22°C)]: +8.00 (s).

^{31}P NMR [δ(ppm), $CDCl_3$-CH_2Cl_2 solution, (- 25°C)]: +7.32 (s).

IR [(cm^{-1}) nujol mulls on NaCl]: 1604 m, 1435 w, 1358 w, 1311 s, 1229 w [ν(C-O)], 1170 w [ν(C-N)], 1142 w [ν(C-N)].

Preparation of (o-cresolato-*O*)*bis*(triphenylphosphine)silver(I) (16).

A mixture of silver(I) oxide (4.3 mmol), o-cresol (8.6 mmol) and triphenylphosphine (17 mmol) in toluene (40 cm^3) was stirred overnight at room temperature. The resulting grey mixture was filtered and the grey solid was washed with dry toluene and dried *in vacuo*.

Yield: 75%.

Analysis: Found (calculated) for $C_{43}H_{37}AgOP_2$. C: 69.3 (69.8), H: 5.06 (5.04)%.

^{1}H NMR [δ(ppm), $CDCl_3$ solution]: 7.40-7.24 (m, 34H, $P(C_6\underline{H}_5)_3$, 2-$MeC_6\underline{H}_4O$), 2.21 (3H, s, CH_3).

^{13}C NMR [δ(ppm), $CDCl_3$ solution]: 154.1 (CO), 134.0 (d, J 16.5 Hz, $P(\underline{C}_6H_5)_3$), 132.5 (d, J 25.4 Hz, $P(\underline{C}_6H_5)_3$), 130.8 (2-$Me\underline{C}_6H_4O$), 129.9 (s, $P(\underline{C}_6H_5)_3$), 128.8 (d, J 10.0 Hz, $P(\underline{C}_6H_5)_3$), 126.9 (2-$Me\underline{C}_6H_4O$), 123.8 (2-$Me\underline{C}_6H_4O$), 120.2 (2-$Me\underline{C}_6H_4O$), 114.9 (2-$Me\underline{C}_6H_4O$), 15.7 (2-$\underline{C}H_3C_6H_4O$).

^{31}P NMR [δ(ppm), $CDCl_3$ solution, (+22°C)]: +7.97(s).

^{31}P NMR [δ(ppm), $CDCl_3$-CH_2Cl_2 solution, (-25°C)]: +6.77 (s).

IR [(cm^{-1}) nujol mulls on NaCl]: 1622 w, 1583 m, 1435 m, 1294 w, 1278 m [ν(C-O)].

Preparation of (o-cresolato-*O*)*tris*(triphenylphosphine)silver(I).o-cresol. toluene solvate (17).

A mixture of silver oxide (13 mmol), o-cresol (26 mmol) and triphenylphosphine (51 mmol) in toluene (100 cm^3) was stirred overnight at room temperature. The resulting grey mixture was filtered and the grey solid was dried *in vacuo*.

Yield: 82%.

Analysis: Found (calculated) for $C_{75}H_{68}AgO_2P_3$. C: 74.9 (74.9), H: 5.65 (5.70)%.

^{1}H NMR [δ(ppm), $CDCl_3$ solution]: 7.35-7.25 (m, 58H, $P(C_6\underline{H}_5)_3$, 2-$MeC_6\underline{H}_4O$, 2-$MeC_6\underline{H}_4OH$, $C_6\underline{H}_5CH_3$), 2.35 (s, 3H, $C_6H_5C\underline{H}_3$), 2.24 (s, 6H, 2-$C\underline{H}_3C_6H_4O$, 2-$C\underline{H}_3C_6H_4OH$).
^{13}C NMR [δ(ppm), $CDCl_3$ solution]: 156.3 (CO), 136.4 ($\underline{C}_6H_5CH_3$), 133.9 (d, J 16.5 Hz, $P(\underline{C}_6H_5)_3$), 133.3 (d, J 17.6 Hz, $P(\underline{C}_6H_5)_3$), 132.6 (2-$Me\underline{C}_6H_4O$), 132.1 (2-$Me\underline{C}_6H_4O$), 132.0 (2-$Me\underline{C}_6H_4O$), 130.4 (2-$Me\underline{C}_6H_4OH$), 129.7 (s, $P(\underline{C}_6H_5)_3$), 129.0 ($\underline{C}_6H_5CH_3$), 128.7 (d, J 8.8 Hz, $P(\underline{C}_6H_5)_3$), 128.4 ($\underline{C}_6H_5CH_3$), 128.2 (2-$Me\underline{C}_6H_4O$), 126.7 (2-$Me\underline{C}_6H_4OH$), 125.2 (2-$Me\underline{C}_6H_4O$, $\underline{C}_6H_5CH_3$), 124.3 (2-$Me\underline{C}_6H_4OH$), 118.6 (2-$Me\underline{C}_6H_4OH$), 115.5 (2-$Me\underline{C}_6H_4OH$), 21.4 ($C_6H_5\underline{C}H_3$), 16.2 (2- $\underline{C}H_3C_6H_4O$).
^{31}P-NMR [δ(ppm), $CDCl_3$ solution, (+22°C)]: +4.75 (s).
^{31}P-NMR [δ(ppm), $CDCl_3$-CH_2Cl_2 solution, (-25°C)]: +4.51 (s).
IR [(cm^{-1}) nujol mulls on NaCl]: 1581 w, 1435 m, 1244 m [ν(C-O)].
Mass spectrometry (m/z): 1109 (M^+) (0.15%).

Preparation of (tert-butoxy)*tris*(triphenylphosphine)silver(I) (18).

Solid $[AgCl(PPh_3)_3]$ (0.1 mmol) was dissolved in hot anhydrous THF (3 cm^3) and this solution was added dropwise using a syringe to a THF solution (5 cm^3) containing lithium tert-butoxide (0.1 mmol). After 90 minutes, the cloudy solution was filtered and evaporated to dryness to give a white solid.
Analysis: Found (calculated) for $C_{58}H_{54}AgOP_3$. C: 71.6 (71.6), H: 6.09 (5.96)%.
^{1}H NMR [δ(ppm), $CDCl_3$ solution]: 7.36-7.19 (m, 45H, $P(C_6\underline{H}_5)_3$), 1.25 (s, 9H, $(C\underline{H}_3)_3CO$).
^{13}C NMR [δ(ppm), $CDCl_3$ solution]: 134.0 (d, J 16.5 Hz, $P(\underline{C}_6H_5)_3$), 133.6 (d, J 17.6 Hz, $P(\underline{C}_6H_5)_3$), 129.6 (s, $P(\underline{C}_6H_5)_3$), 128.7 (d, J 8.8 Hz, $P(\underline{C}_6H_5)_3$), 32.0 $(CH_3)_3\underline{C}O$), 29.6 $(\underline{C}H_3)_3CO$).
IR [(cm^{-1}) nujol mulls on NaCl]: 1653 w, 1437 w, 1157 m [ν(C-O)].

A number of alternative syntheses were carried out with the aim of preparing (**18**), but none were successful. These are briefly mentioned below.

(**a**) The method described above was repeated using $[Ag(BF_4)(PPh_3)_3]$ or $[Ag(NO_3)(PPh_3)_3]$ in anhydrous THF solution.

(**b**) The method previously successful in synthesising (**13**) was attempted. Silver(I) oxide (4.3 mmol), 2-methyl-propane-2-ol (8.6 mmol) and triphenylphosphine (17 mmol) were reacted. The resulting white product was not the required product.

(**c**) $[Ag(BF_4)(PPh_3)_3]$ (1mmol), tert-butoxytrimethylsilane $[Me_3SiOCMe_3]$ (1 mmol) and anhydrous THF (30 cm^3) were stirred for 24 hours at room temperature. The mixture was filtered and the white solid obtained was dried *in vacuo*, but was not the required product.

(**d**) A solution of tert-butoxytrimethylsilane (2.5 mmol) in CH_2Cl_2 (5 cm^3) was added slowly using a syringe to a cold solution of silver(I) tetrafluoroborate (2.5 mmol) in anhydrous CH_2Cl_2 (10 cm^3). The clear solution was stirred for 7 hours at -20°C. A solution of triphenylphosphine (7.55 mmol) in anhydrous CH_2Cl_2 (15 cm^3) was added to the clear solution using a syringe. The solution was stirred overnight at room temperature and evaporated to dryness to give a white solid. This was not the required product.

(**e**) Using a syringe 15-crown-5 (1 mmol) was added to a solution of lithium tert-butoxide (1mmol) in anhydrous THF (20 cm^3) previously cooled to 0°C. After 20 minutes a solution of $[AgCl(PPh_3)_3]$ (1 mmol) in anhydrous THF (70 cm^3) was added slowly to the mixture using a syringe. The yellow solution was stirred overnight, filtered and evaporated to dryness to give a white product. Again this was not the required product.

(**f**) Using a syringe, a solution of silver(I) trifluorosulfonate $[CF_3SO_3Ag]$ (1.9 mmol) in anhydrous THF (10 cm^3) was added slowly to a solution of lithium tert-butoxide (1.9 mmol) in anhydrous THF (20 cm^3) cooled to -20°C. The mixture became yellow-orange and finally brown. The brown mixture was left to stir at -20°C for 4 hours. A solution of triphenylphosphine (57.8 mmol) in anhydrous THF (18 cm^3) was added dropwise to the brown mixture to give a beige colour. The mixture was stirred overnight at room temperature and filtered to give a beige solid, but this again was not the required product.

Chapter Four

Silver(I) complexes containing sulfur ligands

4.1 INTRODUCTION.

Metal complexes with sulfur-containing ligands have found applications in areas such as medicine, material science and organic synthesis. For example, gold(I) thiolates have been studied in relation to chemotherapy for arthritis.[192] Metal complexes with sulfur-containing ligands have been used as models for the study of the active sites in metalloproteins and the therapeutical activity of some metal derivatives.[193]

Copper(I) thiolates have been found to behave as semiconductors.[192] Metal thiocarbamates and monothiocarboxylates have been used as precursors for the formation of metal sulfide thin films. Examples of precursors include gallium or indium thiocarboxylates[194,37] and thiocarbamates,[195] cadmium and zinc thiocarboxylates[38] and calcium, strontium and barium thiocarboxylates.[196] Thin films of In_2S_3 or Ga_2S_3 have found use in optoelectronic devices. Thin films of CdS and ZnS have been used as optical coatings in solar cell technology and are also used in display applications because of their excellent host lattices for luminescent materials.

Copper(I) arenethiolates have found use as catalysts with Grignard reagents in organic syntheses.[192]

Dithiocarboxylate complexes have also been used in analytical chemistry. They also have been used as fungicides, pesticides, vulcanisation accelerators, flotation agents and high pressure lubricants.[197] Silver(I) N,N-diethyldithiocarbamate has been used in the analytical determination of arsenic.[198]

Metal complexes with sulfur-containing ligands have been chosen as potential precursors for silver CVD because it was thought that they should be more thermally stable than alkoxide and aryloxide complexes. Monothiocarboxylate ligands are interesting because they contain both a hard oxygen donor and a soft sulfur donor, which can lead to aggregation of soft and hard metal centres. However, there are a few problems such as formation of polymeric structures, which may reduce solubility in most organic solvents and the decomposition of these products which may lead to the generation of a metal sulfide.

This chapter will describe the structural chemistry and various synthetic routes known for this class of compounds. The introduction will be followed by details of the synthesis, characterisation and CVD testing of new silver(I) monothiocarboxylate complexes produced in this work.

4.2 STRUCTURAL CHEMISTRY.

4.2.1 Silver(I) thiolate complexes.

Until recently, the known structural chemistry of silver(I) thiolates was very limited. Based on molecular weight measurements, it was suggested that for $[AgSR]_n$ where R was a tertiary alkyl group n = 8, but where R was a secondary alkyl group n = 12. Primary alkanethiolates, which were usually insoluble, gave unreliable high molecular weights, indicative of highly polymeric structures.[56]

The crystal structure of several silver(I) thiolates have now been reported in the literature. Thiolate ligands have a tendency for bridging metal atoms producing polymeric structures.

Silver(I) thiolates have a wide range of different structures, where the sulfur atom is bonded to two or more silver atoms. Examples of molecular complexes are given in Table 4.1, the complexes being subdivided according to the number of silver atoms contained in the structure. For each group the main features of the structural geometry will be discussed.

Compounds	Core of the structure	Ref
$[AgSC(SiMe_2Ph)_3]_3$	Ag_3S_3	199
$[AgSC(SiMe_3)_3]_4$	Ag_4S_4	199
$[Ag(SC_6H_4\text{-}o\text{-}SiMe_3)]_8$	Ag_4S_4	200
$[AgSSi(O^tBu)_3]_4$	Ag_4S_4	201
$[AgSCH(SiMe_3)_2]_8$	Ag_4S_4	199
$[Ag_4\{SCH_2(SiMe_3)\}_3]_n\text{-}(OCH_3)_n$	Ag_4S_4	199
$[Ag_4(SPh)_4(PPh_3)_4]$	Ag_4S_4	202

Compounds	Core of structure	Ref
$\{Ag_{13}(\mu\text{-}SC_5H_9NHMe)_{16}]^{13+}\}_n$ 13 ClO_4^-	Ag_4S_4 and Ag_6S_6	203
$[Ag_5(S^tBu)_6]^-$ Et_4N^+	Ag_5S_6	204
$[Ag_5(SPh)_7]^{2-}$ 2 Me_4N^+	Ag_5S_7	205
$[Ag_6(SC_5H_3N\text{-}3\text{-}SiMe_2Ph)_6]$	Ag_6S_6	206
$[Ag_6(SC_6H_4Cl)_6(PPh_3)_5]$	Ag_6S_6	207
$[Ag_6(SPh)_8]^{2-}$ 2 Me_4N^+	Ag_6S_8	208
$[Ag(SCMeEt_2)]_8$	Ag_8S_8	204
$[Ag_8(SCMeEt_2)_8(PPh_3)_2]$	Ag_8S_8	209, 210
$[Ag_8(SC_5H_3N\text{-}3\text{-}SiMe_2Ph)_6]^{2+}$ 2 $[Ag(NO_3)_2]^-$	Ag_8S_6	206
$[Ag_{12}(SC_6H_{11})_{12}]$	$Ag_{12}S_{12}$	211
$[Ag_{14}(S^tBu)_{14}(PPh_3)_4]$	$Ag_{14}S_{14}$	209, 210

Table 4.1 Examples of silver(I) thiolate complexes.

There are no monomeric structures known for silver(I) thiolates that have a formula [Ag(SR)]. Known monomeric species are usually of the type $[Ag(SR)L_n]$ where L is a ligand. The structure of $[Ag(SCN_4Ph)(PPh_3)_2]\cdot CH_2Cl_2$, represented in Figure 4.1, is a monomer, where the silver atom is bonded to two phosphorus atoms and to one sulfur atom from the tetrazole thiolate ligand, giving a trigonal geometry.[212]

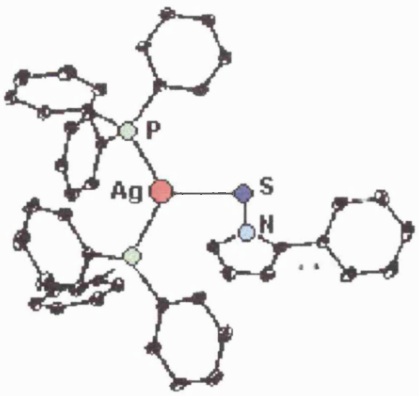

Figure 4.1 Structure of $[Ag(SCN_4Ph)(PPh_3)_2]\cdot CH_2Cl_2$.[212]

4.2.1.a Trimeric complex.

The structure of $[AgSC(SiMe_2Ph)_3]_3$ represented in Figure 4.2 consists of a puckered six-membered ring of alternating Ag and S atoms, Ag_3S_3.[199] The irregular geometry of the Ag_3S_3 ring is the consequence of constraints imposed by ring closure. All sulfur atoms are bridging to two silver atoms, which have a non-linear geometry.

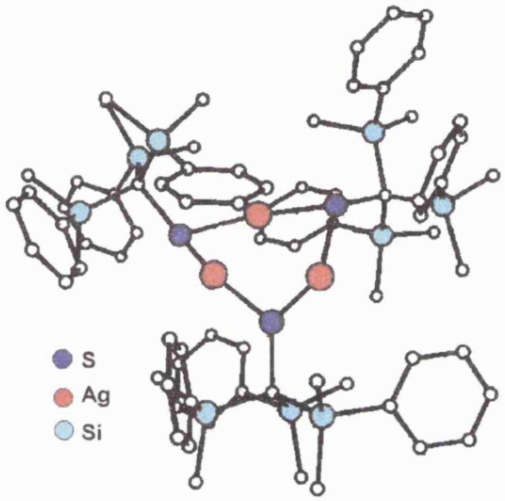

Figure 4.2 Structure of $[AgSC(SiMe_2Ph)]_3$.[199]

4.2.1.b Tetrameric complexes.

Tetrameric silver(I) thiolates are more common than trimeric complexes. They often form eight-membered Ag_4S_4 rings of alternating Ag and S atoms. Depending on the type of the ring, silver atoms are found to be two-coordinate or a mixture of two- and three-coordinate. Table 4.2 summarises different examples of Ag_4S_4 rings.

Ag_4S_4 Core. Ag S Si P	**Structure description**	**Silver geometry and sulfur coordination**	**Ref**
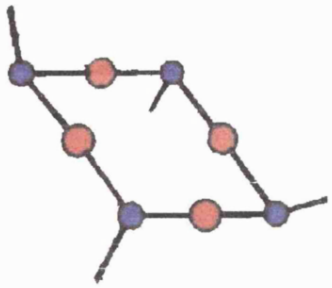 $[AgSC(SiMe_3)_3]_4$	Shallow crown	All silver atoms have a nearly linear geometry. All sulfur atoms are bridging.	199
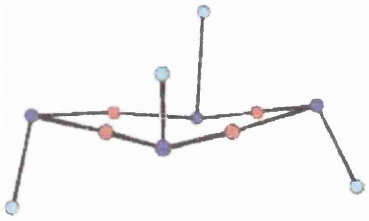 $[AgSSi(O^tBu)_3]_4$	Nearly planar	All silver atoms have a nearly linear geometry. All sulfur atoms are bridging.	201
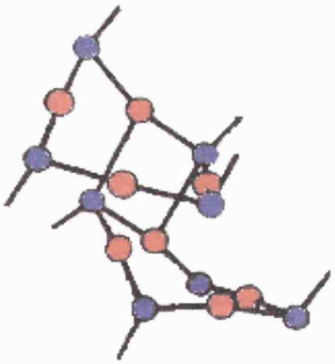 $[AgSCH(SiMe_3)_2]_8$	Bis-cyclic structural form, which is connected by a weak secondary Ag…S interactions.	Three silver atoms have a linear geometry, while the fourth silver has a T-shaped geometry. All sulfur atoms are bridging.	199
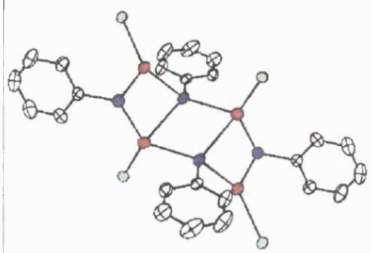 $[Ag_4(SPh)_4(PPh_3)_4]$	Highly distorted chair conformation.	Two silver atoms adopt a trigonal geometry, while the other two have a distorted tetrahedral geometry. Two sulfur atoms are bridging, while the other two are bonded to three silver atoms.	202

Table 4.2 Examples of Ag_4S_4 core rings.

4.2.1.c Pentameric complexes.

Pentameric silver(I) thiolates are less common. The structure of $\{Ag_5[\mu_2\text{-}S(CH_2)_3NHMe_2]_3[\mu_2\text{-}S(CH_2)_3NMe_2]_3\}(ClO_4)_2$ consists of a Ag_5S_6 core cage, which can be described as a trigonal bipyramid of metal atoms enclosed within a regular trigonal prism of doubly bridging thiolate ligands (Fig. 4.3).[213] In this example, the silver atoms adopt either a nearly linear geometry or a trigonal geometry.

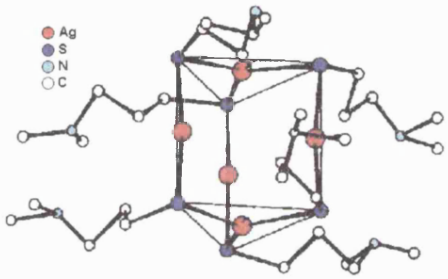

Figure 4.3 Structure of $[Ag_5[\mu_2\text{-}S(CH_2)_3NHMe_2]_3[\mu_2\text{-}S(CH_2)_3NMe_2]_3\}(ClO_4)_2$.[213]

Another example of a complex containing a Ag_5S_6 core cage, is $[Ag_5(S^tBu)_6]^-$.[204] The six sulfur atoms are doubly bridging. Two silver atoms have a trigonal planar geometry and three silver atoms have a nearly linear geometry. The Ag_5 polyhedron is best described as a trigonal bipyramid, whereas the S_6 polyhedron is best described as a distorted prism.

The structure of $[Ag_5(SPh)_7]^{2-}$ contains an irregular Ag_5S_7 cage, represented in Figure 4.4.b.[205] All the sulfur atoms are doubly bridging. Four silver atoms have a trigonal planar geometry while the fifth one has a nearly linear geometry. The cage can be visualised as an expansion of an Ag_4S_6 cage (Fig. 4.4.a) by opening of two of the trigonal coordination planes of the S_6 octahedron and replacing the S atom, which linked them by a linear S-Ag-S group.

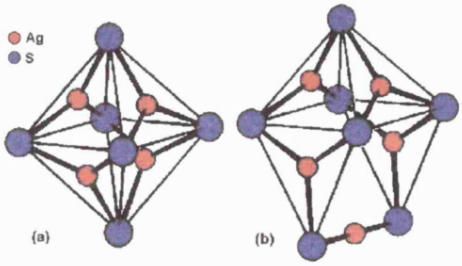

Figure 4.4 (a) Ag_4S_6 core. (b) Ag_5S_7 core.[205]

4.2.1.d Hexameric complexes.

Examples of hexameric complexes include $[Ag_6(SC_6H_4Cl)_6(PPh_3)_5]$, $[Ag(SC_5H_3N\text{-}3\text{-}SiMe_2Ph)]_6$ and $[Ag_6(SPh)_8](NMe_4)_2$. Their core structures are represented in Table 4.3.

Core structure. Ag S N P	Structure description.	Ref.
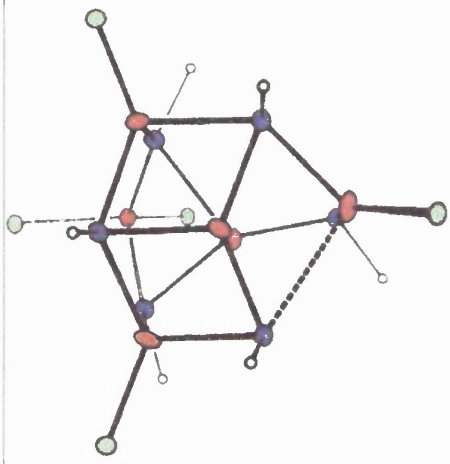	The structure of $[Ag_6(SC_6H_4Cl)_6(PPh_3)_5]$ contains an Ag_5S_6 central cage with PPh_3 ligands terminal at three of the silver atoms and an $Ag(PPh_3)_2$ appendage inserted between two bridging thiolates. The Ag_5S_6 cage contains a basal unit, which consists of an irregular hexagon of alternating Ag and S atoms centred by a silver atom with a trigonal geometry. Five of the sulfur atoms are triply bridging while the sixth is doubly bridging and the silver atoms have a trigonal or tetrahedral geometry.	207
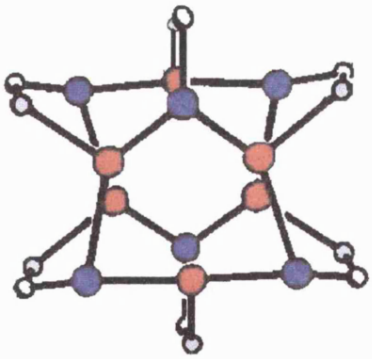	The structure of $[Ag_6(SC_5H_3N\text{-}3\text{-}SiMe_2Ph)_6]$ is described as a 'paddlewheel'. The Ag_6S_6 unit is composed of two adjacent Ag_3S_3 rings. All sulfur atoms are doubly bridging and the silver atoms have distorted trigonal planar geometry.	206
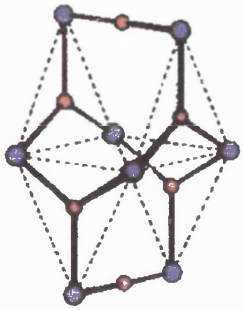	The structure of $[Me_4N]_2[Ag_6(SPh)_8]$ in which the anion contains an irregular Ag_6S_8 ring, where two silver atoms have linear geometry and four silver atoms have trigonal planar geometry.	208

Table 4.3 Examples of core structures of hexameric complexes.

4.2.1.e Octameric complexes.

There are few examples of complexes containing eight silver atoms. They include $[Ag_8(SCMeEt_2)_8]$,[204] $[Ag_8(SCMeEt_2)_8(PPh_3)_2]$[209,210] and $[Ag_8(SC_5H_3N\text{-}3\text{-}SiMe_2Ph)_6]^{2+}$ $[Ag(NO_3)_2]_2^-$.[206]

The structure of $[Ag_8(SCMeEt_2)_8]$ is described as a cyclic zigzag structure (Fig. 4.5). All silver atoms have nearly linear geometry and all sulfur atoms are bridging.

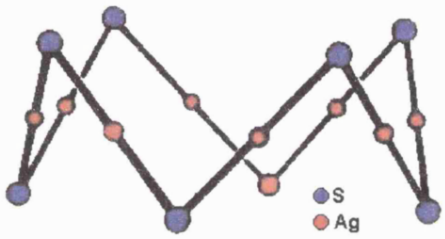

Figure 4.5 Partial structure of $[Ag_8(SCMeEt_2)_8]$.[204]

The structure of $[Ag_8(SCMeEt_2)_8(PPh_3)_2]$ contains two Ag_4S_4 rings, of the types $Ag_4(\mu\text{-}SR)_4$ and $(Ph_3PAg)_2Ag_2(\mu\text{-}SR)_4$.[209,210] They face each other and are connected by 4 weak secondary Ag...S interactions. The silver atoms have a nearly linear geometry but expanded to trigonal geometry when coordinated to PPh_3 ligands.

The structure of the cation of $[Ag_8(SC_5H_3N\text{-}3\text{-}SiMe_2Ph)_6]^{2+}[Ag(NO_3)_2]_2^-$ contains a Ag_8S_6 core (Fig. 4.6).[206] The Ag_8 polyhedron exhibits hexagonal bipyramidal geometry with two silver atoms from $[Ag(NO_3)_2]^-$ units associated as two weakly interacting arms. The silver atoms adopt linear, trigonal planar or tetrahedral geometry, depending on their position in the overall structure.

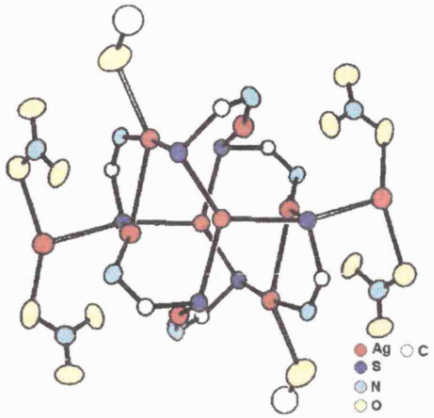

Figure 4.6 Partial structure of $[Ag_8(SC_5H_3N\text{-}3\text{-}SiMe_2Ph)_6]^{2+}[Ag(NO_3)_2]_2^-$.[206]

4.2.1.f Higher complexes.

Examples of complexes containing more than eight silver atoms in their structure include $[Ag_{12}(SC_6H_{11})_{12}]$[211] and $[Ag_{14}(S^tBu)_{14}(PPh_3)_4]$.[209,210]

The structure of $[Ag_{12}(SC_6H_{11})_{12}]$ was first described as being a 1-D polymer with an infinite chain composed of Ag and S atoms, surrounded by the cyclohexyl groups.[214] Later, the structure was described as being composed of cyclic molecules. The ring contains two weak secondary bonds and is described as possessing an elongated 'chaise longue' conformation (Fig. 4.7). The geometry around the silver atoms is near linear or trigonal.

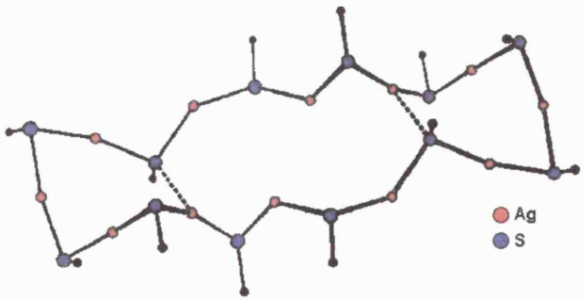

Figure 4.7 Structure of $[Ag_{12}(SC_6H_{11})_{12}]$.[211]

$[Ag_{14}(S^tBu)_{14}(PPh_3)_4]$ is the highest complex which does not have a polymeric structure.[209,210] The structure contains a single 28-membered $Ag_{14}S_{14}$ heterocycle with only four triphenylphosphine ligands. The ring is folded such that its digonal and trigonal

segments lie approximately in the shape of a box. There are four types of segments (see Figure 4.8). (a) Eight opposed zigzag linear segments in opposite faces of the box, (b) four linear crossover segments on another pair of faces, (c) four trigonal segments which contains the bonded phosphorus atoms and which connect to (d) two linear end segments, one in each end of the box. Ten silver atoms have linear geometry and four silver atoms have trigonal geometry. There are no secondary Ag…S interactions in this structure.

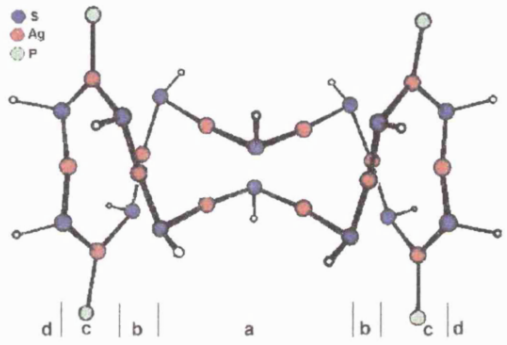

Figure 4.8 Structure of $[Ag_{14}(S^tBu)_{14}(PPh_3)_4]$ = see the above text for explanation of a – d.[209]

4.2.1.g Polymeric structures.

There are few examples of polymeric structures. Examples include $[Ag(SCMeEt_2)]_\infty$,[215] $\{[AgSC_6H_2{}^iPr_3\text{-}2,4,6]_4\cdot CHCl_3\}_n$,[216] $[Ag_{13}(\mu\text{-}SC_5H_9NHMe)_{16}]_n^{13+}$,[203] and $[Ag_4\{SCH_2(SiMe_3)\}_3]_n\text{-}(OCH_3)_n$.[199] All these complexes have 1-D polymeric structures.

The structure of $\{[AgSC_6H_2{}^iPr_3\text{-}2,4,6]_4\cdot CHCl_3\}_n$ consists of a double stranded belt polymer (Fig. 4.9), alternating Ag and S atoms forming the strands.[216] All sulfur atoms are doubly bridging. The strands are connected by weak Ag-Ag links.

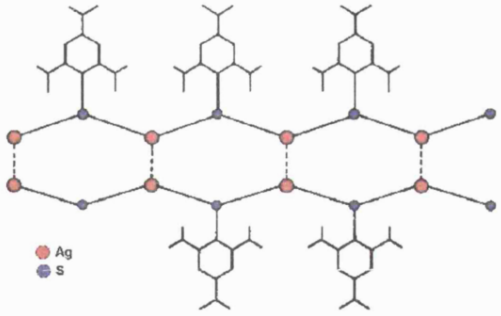

Figure 4.9 Structure of $[\{[AgSC_6H_2{}^iPr_3\text{-}2,4,6]_4{\cdot}CHCl_3\}_n]$.[216]

The structure of $[Ag(SCMeEt_2)]_\infty$ is another example of a chain structure.

The polymeric structure of $[Ag_{13}(\mu\text{-}SC_5H_9NHMe)_{16}]^{13+}$ contains $Ag_{10}S_{16}$ units linked by three silver atoms.[203] Each unit consists of a central $Ag_6(\mu\text{-}SR)_6$ core and two $Ag_4(\mu\text{-}SR)_4$ rings. The silver atoms have linear, trigonal or tetrahedral geometry. The sulfur atoms are doubly or triply bridging.

The structure of $[Ag_4\{SCH_2(SiMe_3)_3\}_4]_n\text{-}(OCH_3)_n$ is described as composed of 1-D kinked chains of fused Ag_4S_4 rings and cross-linked through other Ag_4S_4 rings.[199] The structure contains four different type of rings and are described as non-planar, distinct butterfly and two nearly planar (Fig. 4.10). All the silver atoms exhibit nearly linear geometry except two, which have a trigonal planar geometry.

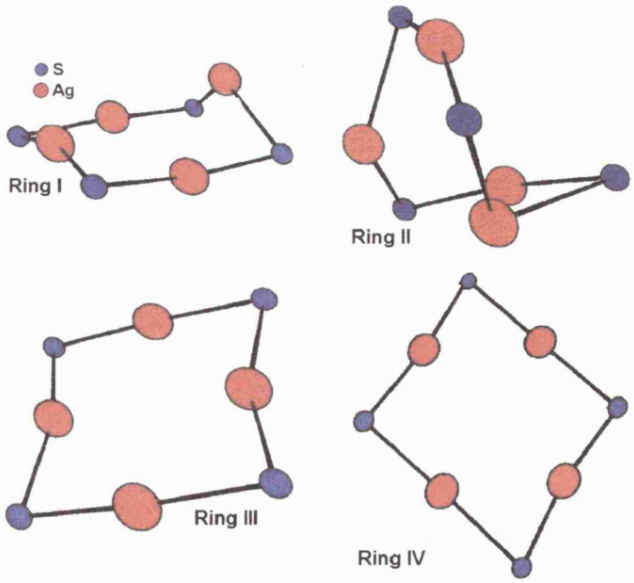

Figure 4.10 Schematic representation of the four rings.[199]

The structures of $[AgS(CH_2)_3CH_3]$[217] and $[Ag_2\{S(CH_2)_5S\}]$[218] exhibit infinite sheets described as non-molecular layered structures.

The structures of $[AgSAr]_\infty$ (Ar = SC_6H_4X-4, X = H or Cl) are examples of 2-D structures, which contain layers of silver and sulfur atoms. Each silver atom has a trigonal planar geometry.[219]

Recently, the structure of $[\{Ag_8(\mu_4\text{-}SC_2H_4\text{-}NH_3)_6Cl_6\}Cl_2]_n$ has been reported as a 1-D chain structure with all the sulfur atoms bonded to four silver atoms, which have tetrahedral geometry.[220]

4.2.2 Silver(I) monothiocarboxylates.

The known structural chemistry of silver(I) monothiocarboxylates is very limited.

An example of a complex containing a COS group is $[(C_3H_7)_2NCOSAg]_6$.[221] The complex contains discrete hexameric molecules, the silver atoms forming almost a regular octahedron in the molecule. Each oxygen atom is linked to one silver atom, while the sulfur atoms are linked to two silver atoms (Fig. 4.11). The silver atoms have a coordination number of three.

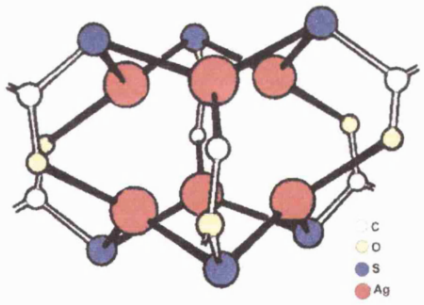

Figure 4.11 Illustration of the central part of the hexameric molecule of $[(C_3H_7)_2NCOSAg]_6$.[221]

The structure of the μ-dithio-oxalate complex $[(PPh_3)_2Ag(SOC_2SO)Ag(PPh_3)_2]$, represented in Figure 4.12, is another example of complex containing a COS group.[222] Each silver atom is bonded to two phosphorus atoms from PPh_3 ligands, one sulfur atom and one oxygen atom from the 1,2-dithiooxalate group, in a trans-arrangement.

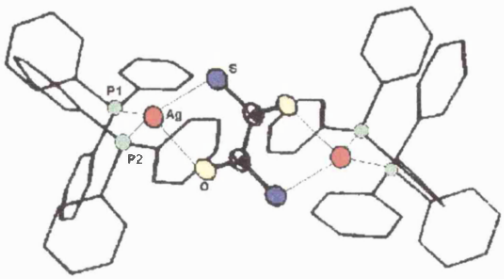

Figure 4.12 Structure of $[(PPh_3)_2Ag(SOC_2SO)Ag(PPh_3)_2]$.[222]

Another example of complex containing a COS group is the trithiooxalate $[\{PPh_3)_2Ag\}_2(SOC_2S_2)]$.[223] Each silver atom is bonded to two sulfur atoms and to two phosphorus atoms, forming a distorted tetrahedron (Fig. 4.13). The coordination around each silver atom is different as a result of one sulfur of the trithiooxalate ligand being bonded to both metals, whereas the other two sulfurs bond to only one metal. The oxygen atom is not involved in any coordination.

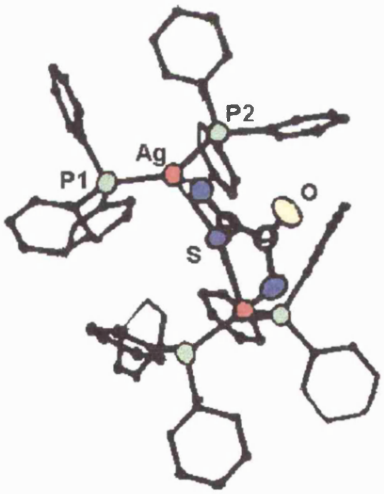

Figure 4.13 Structure of $[\{PPh_3)_2Ag\}_2(SOC_2S_2)]$.[223]

4.2.3 Silver(I) dithiocarboxylates and dithiocarbamates.

4.2.3.a Silver(I) dithiocarboxylates.

Dithiocarboxylate complexes have been little studied because of the instability of the RCS_2^- anion.

Those silver(I) dithiocarboxylates that have been studied are found to have polymeric chain structures e.g. $[Ag_4(S_2C\text{-}o\text{-}C_6H_4CH_3)_4]_n$[193] or clusters e.g. $[Ag_4(2,4,6\text{-}(CH_3)_3C_6H_2CS_2)_4(py)_3]\cdot 0.5py$, $[Ag_4(o\text{-}CH_3C_6H_4CS_2)_4(py)_4]$ and $[(C_3H_7)_4N]_2[Ag_4\{2,4,6\text{-}(CH_3)_3C_6H_2CS_2\}_6]\cdot 0.5DMF\cdot H_2O$.[224] The 1,1-dithiolate anion $[S_2C{=}C(CN)_2]^{2-}$, although not strictly a dithiocarboxylate, also forms analogous complexes such as $[Ag_8\{S_2C{=}C(CN)_2\}_6]^{4-}$ and $[Ag_6\{S_2C{=}C(CN)_2\}_6]^{6-}$.[225,226]

In the polymeric structure of $[Ag_4(S_2C\text{-}o\text{-}C_6H_4CH_3)_4]_n$ (Fig. 4.14), each dithio-o-toluato group acts as a tridentate ligand. One sulfur atom is coordinated to only one silver atom whereas the other sulfur atom bridges to two silver atoms. Each silver atom has a distorted square pyramidal geometry.

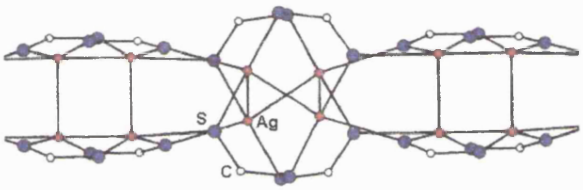

Figure 4.14 Structure of $[Ag_4(S_2C\text{-}o\text{-}C_6H_4CH_3)_4]_n$.[193]

Examples of clusters include, $[Ag_4(o\text{-}CH_3C_6H_4CS_2)_4(py)_4]$, $[Ag_4\{2,4,6\text{-}(CH_3)_3C_6H_2CS_2\}_4(py)_3]\cdot 0.5py$ and $[(C_3H_7)_4N]_2[Ag_4\{2,4,6\text{-}(CH_3)_3C_6H_2CS_2\}_6]\cdot 0.5DMF\cdot H_2O$.[224] They form tetrahedral, distorted tetrahedral and planar clusters, respectively. In the structure of $[Ag_4\{2,4,6\text{-}(CH_3)_3C_6H_2CS_2\}_4(py)_3]\cdot 0.5py$, three silver atoms have a tetrahedral arrangement, while the fourth has a trigonal arrangement. The structure of $[Ag_4(o\text{-}CH_3C_6H_4CS_2)_4(py)_4]$ is represented in Figure 4.15.[224] Each silver atom is bonded to three sulfur atoms and to one nitrogen atom from a pyridine ligand in a distorted tetrahedral manner.

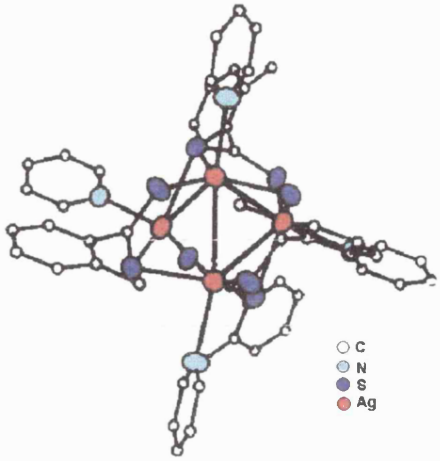

Figure 4.15 Structure of $[Ag_4(o\text{-}CH_3C_6H_4CS_2)_4(py)_4]$.[224]

The reaction of $[Ag(S_2C\text{-}p\text{-}C_6H_4CH_3)]_n$ with PPh_3 produced a dimeric complex (Fig. 4.16) in which the dithio-p-toluato groups bridge two silver atoms. One sulfur atom of the dithio p-toluato atom is bonded to both silver atoms to form a planar four-membered ring. The other is bonded to only one silver atom. Thus the dithio-p-toluato group is tridentate and acts both as a bridging and a chelating ligand. Both silver atoms have a distorted tetrahedral arrangement.

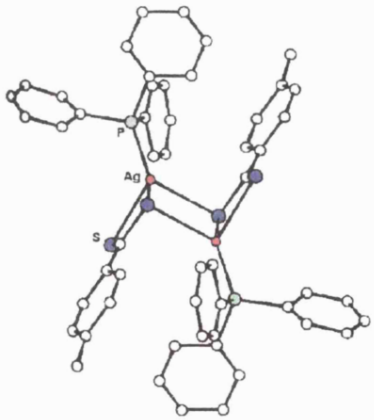

Figure 4.16 Structure of $[Ag(S_2C\text{-}p\text{-}C_6H_4CH_3)(PPh_3)]_2$.[227]

4.2.3.b Silver(I) dithiocarbamates.

The dithiocarbamates $[AgS_2CN(n\text{-}C_3H_7)_2]_6$,[228] $[AgS_2CN(i\text{-}C_3H_7)_2]_6$[197] and $[Ag(S_2CNEt_2]_6$[197] are discrete hexameric molecules. In the structure of $[AgS_2CN(i\text{-}C_3H_7)_2]_6$, one sulfur is bonded to a single silver atom while the second sulfur atom is bonded to two silver atoms (Fig 4.17).[228]

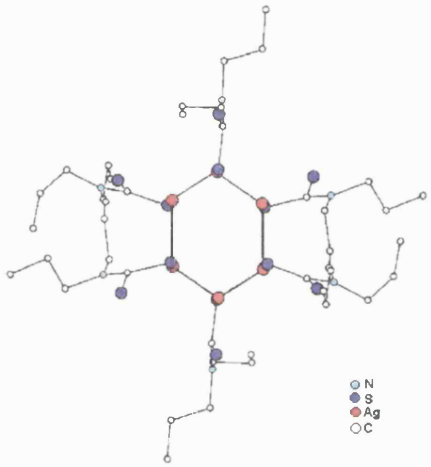

Figure 4.17 Structure of $[AgS_2CN(n\text{-}C_3H_7)_2]_6$.[228]

Recently the structure of $[Ag\{Fc(S_2CNEt)_2\}]_n(ClO_4)_n$ (Fc = $Fe(\eta^5\text{-}C_5H_4)_2$] has been reported. The molecule consists of 1,1'-bis(diethyldithiocarbamato)ferrocene units bridging silver atoms.[229] The silver atoms are bonded to sulfur atoms of different ferrocene moieties, producing a linear S-Ag-S segment. The silver atom is also weakly bonded to two carbons, one from each cyclopentadienyl ring giving a tetrahedral arrangement.

The dithiocarbamate ligands of silver(I) dithiocarbamate complexes containing triphenylphosphine ligands are chelating. An example is $[Ag(S_2CNC_5H_8)(PPh_3)_2]$, which has a similar structure to many bis(triphenylphosphine)silver(I) carboxylates.[230] The complex is a monomer with a bidentate pyrrolidine carbodithioato ligand and two triphenylphosphine ligands in which the silver atom has a distorted tetrahedral arrangement (Fig. 4.18).

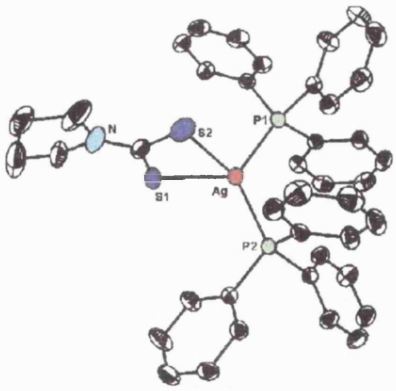

Figure 4.18 Structure of $[Ag(S_2CNC_5H_8)(PPh_3)_2]$.[230]

4.3 SYNTHETIC ROUTES.

4.3.1 Synthesis of silver(I) thiolates.

Silver(I) thiolates have been prepared by deprotonation of thiols. The reaction is carried out in acetonitrile solvent in a presence of a base (eqn. 4.1).[199]

$$RSH + AgNO_3 \longrightarrow RSAg + HNO_3 \quad (\mathbf{4.1})$$

Where R = Alkyl, aryl.

A second method involves reaction of a thiol in acetone with addition of a solution of silver(I) nitrate.[218]

Syntheses of triphenylphosphine adducts of silver(I) thiolates have been carried out by direct reaction of silver(I) thiolate and triphenylphosphine in toluene or chloroform solvents, at room temperature followed by gentle warming for between 15 and 45 minutes. Filtration followed by addition of propanol to the filtrate produces the required complex.[207,209]

4.3.2 Synthesis of silver(I) monothiocarboxylates.

No synthetic routes have been reported for silver(I) monothiocarboxylates. The only relevant synthesis reported is that of a dithiooxalate complex.

The compound $[(PPh_3)_2Ag(SOC_2SO)Ag(PPh_3)_2]$ was synthesised by reaction of a solution of potassium 1,2-dithiooxalate in pyridine with a solution of $[AgCl(PPh_3)_3]$ in pyridine. Stirring, followed by slow addition of water produces a brown solution and the product precipitated from the filtrate on addition of more water.[222]

4.3.3 Synthesis of silver(I) dithiocarboxylates.

Silver(I) dithiocarboxylates complexes can be prepared by two different methods.

The first method involves reaction of the ammonium salt of the dithiocarboxylic acid with silver(I) nitrate in dimethylformamide (DMF) (eqn. 4.2).[223]

$$RCS_2^-NH_4^+ + AgNO_3 \xrightarrow{DMF} RCS_2Ag + NH_4NO_3 \quad \textbf{(4.2)}$$

The main problem with this method is the prior synthesis of the dithiocarboxylic acid or the sodium salt. Dithiocarboxylic acids decompose very rapidly to the corresponding disulfides, however the sodium salt is slightly more stable when kept in ether solution.

The second method involves reaction of silver(I) bromide with LiR (R = aryl) in ether solution at 0°C. After one hour, the solution is cooled to -20°C and CS_2 is slowly added to the solution to effect insertion of CS_2 into the Ag-C σ-bond giving the required dithiocarboxylate. The solution is then evaporated to dryness.[193]

The synthesis of triphenylphosphine adducts of silver(I) dithiocarboxylates has also been reported. The method involves reaction of an organolithium compound and $[AgCl(PPh_3)]_4$ in excess CS_2 (eqn. 4.3).[231]

$$RLi + [AgCl(PPh_3)]_4 \xrightarrow{CS_2} RCS_2Ag(PPh_3)_2 \quad \textbf{(4.3)}$$

The σ-pentamethylcyclopentadienyldithiocarboxylate compound $[(C_5Me_5CS_2)Ag(PPh_3)_2]$ has been prepared by this method.[231]

4.3.4 Synthesis of silver(I) dithiocarbamates.

The synthesis of silver(I) dithiocarbamates usually involves reaction of silver(I) nitrate with the sodium or potassium salt of the dithiocarbamate in an alcohol.

Their triphenylphosphine adducts can be synthesised as colourless crystals by reaction of the bis[acetato(triphenylphosphine)silver(I)] with the ammonium salt of the dithiocarbamate in absolute ethanol.[230]

4.4 RESULTS AND DISCUSSION.

4.4.1 Synthesis.

A series of silver(I) complexes with sulfur-containing ligands have been synthesised. Three different groups of sulfur-containing ligands have been used. They are thiolates, monothiocarboxylates and dithiocarbamates. Silver(I) thiolates as well as silver(I) monothiocarboxylates and their triphenylphosphine adducts were synthesised in relatively high yields (81-95%) whereas the triphenylphosphine adduct of silver(I) diethyldithiocarbamate was synthesised in a moderate yield (37%).

Silver(I) thiolates were prepared by reaction of silver nitrate and the corresponding thiol in acetone. Silver(I) 1-propanethiolate (**19**) [$Ag(SCH_2CH_2CH_3)$] was found to be more stable in air and light than silver(I) dodecanethiolate (**20**) [$Ag\{S(CH_2)_{11}CH_3\}$], which changed colour (pale yellow to salmon) after several weeks, when exposed to light.

Attempts to prepare a triphenylphosphine adduct of silver(I) 1-propanethiolate were unsuccessful.

The first method attempted was the reaction of silver(I) 1-propanethiolate and PPh_3 in toluene in 1:3 ratio. The silver compound did not dissolve in the toluene solution of PPh_3 at room temperature.

The second consisted of using a large excess of PPh_3. A mixture of PPh_3 and silver(I) 1-propanethiolate (ratio 11:1) were heated to produce a melt in which no silver(I) 1-propanethiolate remained unreacted. Using a syringe, anhydrous toluene was added to

the melted mixture and the solvent was refluxed for 6 hours. The mixture was filtered while still hot giving a grey silvery solid. Petroleum ether (60-80° boiling range) was added to the filtrate until a solid precipitated from the solution. The grey solid obtained was not soluble in any common solvent and was not the expected product.

The final method attempted consisted of using a solvent with a higher boiling point. The reaction of silver(I) 1-propanethiolate and PPh_3 (ratio 1:11) was carried out in refluxing o-xylene. The colour of the mixture changed from brown-orange to green after 4 hours reflux. After 21 hours reflux, the solution was still green and no silver(I) 1-propanethiolate remained undissolved. The solution was filtered while still hot and the filtrate was placed in an ice bath. A dark grey product precipitated from the filtrate. Once again the product obtained was not soluble in common organic solvent and the elemental analysis suggested the presence of the original silver(I) 1-propanethiolate.

Silver(I) monothiocarboxylates were prepared using different methods. Silver(I) monothiobenzoate (**24**) [Ag(SOCPh)] was prepared the same way as the silver(I) thiolates by reaction of monothiobenzoic acid with silver(I) nitrate in acetone solution. The product was obtained in a high yield (88%).

Attempts to prepare silver(I) monothioacetate [$Ag(SOCCH_3)$] using the same method as the thiolates was not successful. The reaction of monothioacetic acid with silver(I) oxide produced a brown solid, which was not the desired product. Reaction of the sodium salt of monothioacetic acid with silver(I) nitrate produced also a brown solid, which once again was not the expected product.

Triphenylphosphine adducts of silver(I) monothiocarboxylates were prepared by three different routes.

The first method used was similar to the preparation of $[\{PPh_3)_2Ag\}_2(O_2C_2S_2)]$[162] with potassium monothioacetate replacing the dithiooxalate. A solution of $[AgCl(PPh_3)_3]$ in dichloromethane was stirred vigorously with a solution of potassium monothioacetate in water. The solvent layers were separated. Hexane was added to the dichloromethane layer and the solution was left to stand for few days. The crystals obtained were not the expected bis(triphenylphosphine) adduct but rather the mono(triphenylphosphine) adduct. Details of the X-ray crystal structure will be discussed later in this chapter.

The second method used was similar to that used to prepare triphenylphosphine adducts of silver(I) carboxylates. Silver(I) monothiobenzoate was added to a solution of

PPh_3 in toluene. The clear solution was stirred, filtered and evaporated to dryness to produce a pale grey solid. The elemental analysis suggested that the product was the bis(triphenylphosphine) adduct.

The last method carried out was the exchange reaction of a bis(triphenylphosphine)silver(I) carboxylate with the sodium salt of a monothiocarboxylic acid. A solution of (acetato)*bis*(triphenylphosphine)silver(I) in ethanol was added slowly to a solution of monothiobenzoic acid or monothioacetic acid and sodium hydroxide in ethanol. The product precipitated as a grey solid. The yields obtained were slightly higher (89-91%) when compared to the previous method (84%).

Preparation of (diethyldithiocarbamato)*bis*(triphenylphosphine)silver(I) (**26**) $[Ag(S_2CNEt_2)(PPh_3)_2]$ was similar to the method described above except that the monothiocarboxylic acid and sodium hydroxide were replaced by sodium diethyldithiocarbamate. A moderate yield was obtained (37%).

Attempts were also made to prepare the dithiocarboxylate complexes $[Ag(S_2CMe)(PPh_3)_2]$ and $[Ag(S_2CPh)(PPh_3)_2]$. Syntheses of $[MeCS_2Na]$ and $[PhCS_2Na]$ were carried using literature methods.[232,233] This involved reactions of an excess of CS_2 with a solution of methyl or phenyl magnesium bromide Grignards in ether cooled to 0°C. The mixtures were left to stand for 24 hours in a refrigerator. Water was added to the resulting dark red mixtures, then dilute HCl was added until the ether phases became dark red. The layers were separated. A solution of sodium hydroxide was added in order to obtain the sodium salt of the appropriate dithioacid.

The reactions of $[RCS_2Na]$ (R = Me or Ph) with silver(I) nitrate or silver(I) acetate produced dark brown or red-brown solids, which were not the expected products. The reaction of $[RCS_2Na]$ with (acetato)*bis*(triphenylphosphine)silver(I) in ethanol produced a brown-red solid. Recrystallisation of this product led to decomposition.

4.4.2 Infrared spectroscopy.

All important infrared bands are summarised in Table 4.4.

The infrared spectra of silver(I) thiolates display one particularly characteristic band at 1220-1240 cm^{-1} due to a (S-CH_2) wag. The band at 2600-2550 cm^{-1}, characteristic of S-H stretching was absent, therefore the reaction was assumed to be complete.

The IR spectra of silver(I) monothiocarboxylates and their triphenylphosphine adducts showed three different characteristic bands at 1630-1570 cm^{-1}, 1201 cm^{-1} and 947-918 cm^{-1} due to ν(C=O), ν(Ph-C), and ν(C-S), respectively.[234]

The ν(C=O) band in compound (**22**) $[Ag(SOCCH_3)(PPh_3)]_4$ was easy to assign whereas in compounds (**23**) $[Ag(SOCCH_3)(PPh_3)_2]$, (**24**) [Ag(SOCPh)] and (**25**) $[Ag(SOCPh)(PPh_3)_2]$, it was more difficult to differentiate carboxylate and phenyl bands. The ν(C=O) found in the region 1651-1626 cm^{-1} for compounds (**22**) and (**23**), are slightly higher in frequency when compared to the corresponding bands of $[Zn(SOCBu^t)_2(TMEDA)]$ and $[Cd(SOCBu^t)_2(TMEDA)]$ (TMEDA = N,N,N',N'-tetramethylethylenediamine) (1612-1578 cm^{-1}).[39]

The ν(C-S) strectches were found at 947 cm^{-1} for compounds (**22**) and (**23**). For compounds (**24**) and (**25**), the ν(C-S) were found in the region 933-918 cm^{-1}, typical of a single bond between C and S.

The ν(Ph-C) band in compounds (**24**) and (**25**) was found at 1201 cm^{-1}, which is similar to those found in [n-BuSn(SOCPh)$_3$] or $[In(SOCPh)_4]^-[Et_3NH]^+$ (1213 cm^{-1} to 1204 cm^{-1}).[234] These relatively low frequencies suggest that the ligand is monodentate, this band being found at higher frequencies for bidentate coordination e.g. 1230 cm^{-1} in $[Cl_2Sn(SOCPh)_2]$.[234]

The IR spectrum of compound (**26**) showed medium intensity bands in the region 1261-1210 cm^{-1}, which may be attributed to ν(CS_2^-) vibrations.

Compounds	**S-CH_2wag**	**ν(C=O)**	**ν(Ph-C)**	**ν(C-S)**	**ν(CS_2^-)**
[Ag($SCH_2CH_2CH_3$)] (**19**)	1224				
[Ag{$S(CH_2)_{11}CH_3$}] (**20**)	1240				
[Ag(SOCMe)(PPh_3)]$_4$ (**22**)		1630		947	
[Ag(SOCMe)(PPh_3)$_2$] (**23**)		1651,1626		947	
[Ag(SOCPh)] (**24**)		1603,1589 1574	1201	918,931	
[Ag(SOCPh)(PPh_3)$_2$] (**25**)		1585,1543	1201	933	
[Ag(S_2CNEt_2)(PPh_3)$_2$] (**26**)					1261,1209

Table 4.4 Infrared bands of silver(I) complexes with sulfur-containing ligands.

4.4.3 NMR spectroscopy.

^1H, ^{13}C and ^{31}P NMR spectra were recorded for all compounds synthesised.

4.4.3.1 ^1H and ^{13}C NMR spectroscopy.

^1H and ^{13}C NMR studies gave the expected results. Table 4.5 summarises the ^{13}C NMR chemical shifts of all compounds analysed.

As expected, the ^1H NMR spectra of compounds (**22**) and (**23**) do not show a signal around 4.7 ppm relating to the proton from –SH. This is indicative of the absence of free thiol. The methyl group protons show a signal shifted slightly upfield (2.23 ppm in both compounds) when compared to free monothioacetic acid (2.40 ppm).

The ^1H NMR spectrum of compound (**25**) showed a multiplet at 7.42-7.24 ppm due to protons of both triphenylphosphine and monothiobenzoate ligands.

In the ^{13}C NMR spectra, all resonances from the monothiocarboxylate COS unit and dithiocarbamate CS_2 unit were found between 204 and 210 ppm. Literature values for the COS chemical shift in compounds containing the monothiocarboxylate group vary from 201 ppm in $[Ga(SOCMe)_2Me(dmpy)]$[37] to 250 ppm in $[Cd(SOCMe)_2(TMEDA)]$.[38] The chemical shifts found in compounds (**22**), (**23**) and (**25**) are within this range. The carbon COS chemical shifts of compounds (**22**) and (**23**) are downfield of the corresponding free monothioacetic acid (195.5 ppm) resonance.[235]

The CS_2 carbon chemical shift in compound (**26**) can be compared to the $\underline{C}S_2$ chemical shifts of $[Me_2In(S_2CNEt_2)]$ and $[Et_2In(S_2CNEt_2)]$ (201-203ppm).[195]

Compounds	COS δ(ppm)	CS_2 δ(ppm)
$[Ag(SOCMe)(PPh_3)]_4$ (**22**)	207.9	
$[Ag(SOCMe)(PPh_3)_2]$ (**23**)	209.3	
$[Ag(SOCPh)(PPh_3)_2]$ (**25**)	204.3	
$[Ag(S_2CNEt_2)(PPh_3)_2]$ (**26**)		209.1

Table 4.5 ^{13}C NMR data for triphenylphosphine adducts of silver(I) monothiocarboxylates and dithiocarbamate.

4.4.3.2 ^{31}P NMR spectroscopy.

Compounds (**22**), (**23**), (**25**) and (**26**) were also investigated using ^{31}P NMR spectroscopy. The results are summarised in Table 4.6.

At room temperature, all spectra consisted of only a broad peak in the region +6 to +9ppm. The absence of $^{1}J(Ag\text{-}P)$ coupling indicates a rapid dissociation or exchange in the solution.

The ^{31}P chemical shift difference between the complexes and free triphenylphosphine, known as the coordination shift and noted as $\Delta\delta$, is not very sensitive to the nature of the monothiocarboxylate or dithiocarbamate ligands. $\Delta\delta$ values range from

11.2 to 14.0 ppm. This is consistent with earlier results obtained as mentioned in Chapters 2 and 3.

The phosphorus chemical shifts at room temperature were found to be within the same range as those of the triphenylphosphine adducts of silver(I) aryloxides (4.7 to 9.5 ppm) but at a lower field when compared to those of the triphenylphosphine adducts of silver(I) carboxylates (9.1-10.8 ppm). The chemical shift of the phosphorus changed slightly on increasing the number of triphenylphosphine ligands from one to two.

Compounds	**^{31}P NMR data at room temperature δ(ppm)**	**Δδ**
$[Ag(SOCMe)(PPh_3)]_4$ (**22**)	+ 8.8	14.0
$[Ag(SOCMe)(PPh_3)_2]$ (**23**)	+ 6.6	11.8
$[Ag(SOCPh)(PPh_3)_2]$ (**25**)	+ 7.0	12.2
$[Ag(S_2CNEt_2)(PPh_3)_2]$ (**26**)	+ 6.0	11.2

Table 4.6 ^{31}P NMR data at room temperature for triphenylphosphine adducts of silver(I) monothiocarboxylates and dithiocarbamates.

4.4.4 Mass spectrometry.

Compounds (**23**) and (**25**) were submitted for FAB (Fast Atom Bombardment) mass spectrometric analysis. The results are summarised in Table 4.7.

The fragments in the spectra are readily identified by the characteristic patterns imposed by the natural isotopic abundances, approximately 1:1 for silver isotopes 107 and 109. See Chapter 2 section 2.4.4.

Fragments have been grouped together on the basis of containing none, one or two silver atoms. The molecular ion was not found in any of the spectra.

Fragments such as $[Ag(PPh_3)_n]$ (where n= 1, 2) have been identified as being present in high abundance, while $[AgS(PPh_3)]$ and $[AgS(PPh_3)_2]$ were identified in low abundance. The presence of $[Ag(PPh_3)]$ and $[Ag(PPh_3)_2]$ in high abundance suggests the tendency of silver(I) complexes to be linear, two-coordinate species in the gas phase.[149]

Fragments containing Ag_2 units were identified in both compounds, at low abundance for $[Ag_2(SOCR)(PPh_3)H]$ and at a higher abundance for $[Ag_2(SOCR)(PPh_3)_2H]$.

	(**23**) $[Ag(SOCMe)(PPh_3)_2]$		(**25**) $[Ag(SOCPh)(PPh_3)_2]$	
Fragments	m/z	%	m/z	%
$[(C_6H_4)_2P]^+$	183	31.5	183	37.2
$[PPh_3]^+$	262	17.2	262	28.0
$[Ag(PPh_3)]^+$	369	100	369	100
$[Ag(PPh_3)_2]^+$	631	91.5	631	79.8
$[AgS(PPh_3)]^+$	401	7.0	401	7.6
$[AgS(PPh_3)_2]^+$	663	4.4	663	3.8
$[Ag_2(SOCR)(PPh_3)H]^+$	553	5.7	615	10.8
$[Ag_2(SOCR)(PPh_3)_2H]^+$	815	22.9	877	26.7
Other silver containing fragments			1123	3.8

Table 4.7 Mass spectrometry of triphenylphosphine adducts of silver(I) monothiocarboxylates.

4.4.5 X-Ray Crystal Structure Determination of [(Monothioacetato)(triphenylphosphine)silver(I)]tetramer.bis(dichloromethane) solvate.

Crystals of the above complex were grown slowly from a solution of dichloromethane and hexane at room temperature. The structure is illustrated in Figure 4.19. Relevant bond lengths and angles are summarised in Table 4.8 (See Appendix 7 for further data).

The asymmetric unit in this structure consists of one half of a tetramer and one molecule of dichloromethane. The remainder of the metal complex is generated via the symmetry operation 1-x, -y, -z.

The structure of [(monothioacetato)(triphenylphosphine)silver(I)]tetramer. bis(dichloromethane) solvate consists of a discrete eight-membered ring of alternating Ag and S atoms, Ag_4S_4, arranged as a chair or a step structure, usually known for halide bridged analogues with bulky phosphine ligands.

Known Ag_4S_4 rings take up nearly planar[201] or non-planar octagonal,[236] butterfly or shallow crown[199] geometries. The present example shows a new structural type, a chair or step structure which for thio-containing species was previously only known for $[Cu_4(SPh)_4(PPh_3)_4]$,[237] although in this case it is distorted. However, since this work was completed a published structure of $[Ag_4(SPh)_4(PPh_3)_4]$[202] shows the same ring geometry.

The sulfur atoms act as bridging ligands. The silver atoms are bonded to two sulfurs from monothioacetate groups and to one phosphorus atom from a triphenylphosphine ligand giving a distorted trigonal geometry.

This structure can be compared to the structure of $[Ag_4(O_2CCH_3)_4(PPh_3)_4]$ in which the carboxylate groups also act as bridging ligands and two silver atoms adopt a trigonal geometry.[127]

The Ag-S bonds in Ag_4S_4 rings vary from 2.360(8) Å in $[AgSC(SiMe_3)_3]_4$ [199] to 2.64(2) Å in $[Ag_4\{SCH_2(SiMe_3)\}_3]_n(OCH_3)_n]$[199]. In the present structure, the Ag-S bonds [2.532(3), 2.564(3), 2.505(3), and 2.506(3) Å] are within the range and are similar to those found in $[(PPh_3)_2Ag(SOC_2SO)Ag(PPh_3)_2]$ [2.513(2) Å].[222]

The Ag(2)-S(1)' bond [3.001(3) Å] along the 'hinge' of the chair is similar to the Ag-S bond in $[Ag_4(SPh)_4(PPh_3)_4]$ [3.0006(8) Å].[202]

The Ag(1)-Ag(2)' distance [3.481(1) Å] is very long when compared to the Ag-Ag distance in $[Ag_4(SPh)_4(PPh_3)_4]$ [3.1300(3) Å],[202] and therefore can be considered as non-bonding.

The structures of $[Cu_4(SPh)_4(PPh_3)_4]$ and $[Ag_4(SPh)_4(PPh_3)_4]$ show a bending of the terminal Cu_2S_2 and Ag_2S_2 rings along the Cu-Cu or Ag-Ag axes, respectively, while in the parent structure the terminal Ag_2S_2 are nearly planar. The central Ag_2S_2 ring is planar [Ag-S = 2.506(3), 3.001(3) Å, Ag-S-Ag angle = 98.214(3)°] and can be compared to the Cu_2S_2 ring in $[Cu_4(SPh)_4(PPh_3)_4]$ [Cu-S = 2.418(2), 2.482(2) Å, Cu-S-Cu angle = 88.0(1)°][237] and to the Ag_2O_2 in $[Ag_4(O_2CCH_3)_4(PPh_3)_4]$ [Ag-O = 2.320(7), 2.475(7) Å, Ag-O-Ag angle = 101.1(3)°].

The Ag-P bond lengths [2.425(3) and 2.422(3) Å] are similar to those found in the triphenylphosphine adducts of silver thiolates [2.405(4) Å in $[Ag_6(SC_6H_4Cl)_6(PPh_3)_5]$[207] to 2.459(8) Å in $[Ag_{14}(S^tBu)_{14}(PPh_3)_4]$[209]] and to the triphenylphosphine adducts of silver(I) carboxylates.[1]

The oxygen from the monothioacetate group is not involved in coordination to silver (see Figure 4.19). The C-O bond distances [1.187(14) and 1.189(14) Å] are slightly shorter than those found in other monothiocarboxylate complexes [1.213(5) to 1.262(3) Å] and indicative of much double bond character.

The C-S bond distance in monothiocarboxylate complexes vary from 1.719(5) Å in $[Cd(SOCBu^t)_2(Lut)_2]$[238]to 1.759(4) Å in [n-BuSn(SOCPh)$_3$][234] and in silver(I) thiolates between 1.76(1) Å in $[Ag_6(SC_6H_4Cl)_6(PPh_3)_5]$[207] to 1.96(7) Å in $[Ag(SCMeEt_2)]_\infty$[215] . In the present structure, the C-S bond distances [1.785(13) and 1.772(12) Å] are within those ranges and are similar to the C-S bonds in $[Cu_4(SPh)_4(PPh_3)_4]$ [1.772(3) and 1.780(3) Å].[237]

The OCS angles [121.3(10) and 120.9(10)°] are similar to those found in [n-BuSn(SOCPh)$_3$] [119.8(3)°] and $[In(SOCPh)_4]^-[Et_3NH]^+$ [121.14(4)°].[234]

Bond distances (Å)	**Bond angles (°)**
Ag(1)-S(1) = 2.564(3)	P(1)-Ag(1)-S(2) = 133.06(11)
Ag(1)-S(2) = 2.532(3)	P(1)-Ag(1)-S(1) = 122.88(11)
Ag(2)-S(2)#1 = 2.505(3)	P(2)-Ag(2)-S(2)#1 = 128.50(11)
Ag(2)-S(1) = 2.506(3)	P(2)-Ag(2)-S(1) = 119.14(11)
Ag(1)-P(1) = 2.425(3)	S(2)-Ag(1)-S(1) = 102.66(10)
Ag(2)-P(2) = 2.422(3)	S(2)#1-Ag(2)-S(1) = 111.93(11)
S(1)-C(39) = 1.785(13)	O(1)-C(37)-S(2) = 121.3(10)
S(2)-C(37) = 1.772(12)	O(2)-C(39)-S(1) = 120.9(10)

Table 4.8 Relevant bond distances and bond angles of compound (**22**).

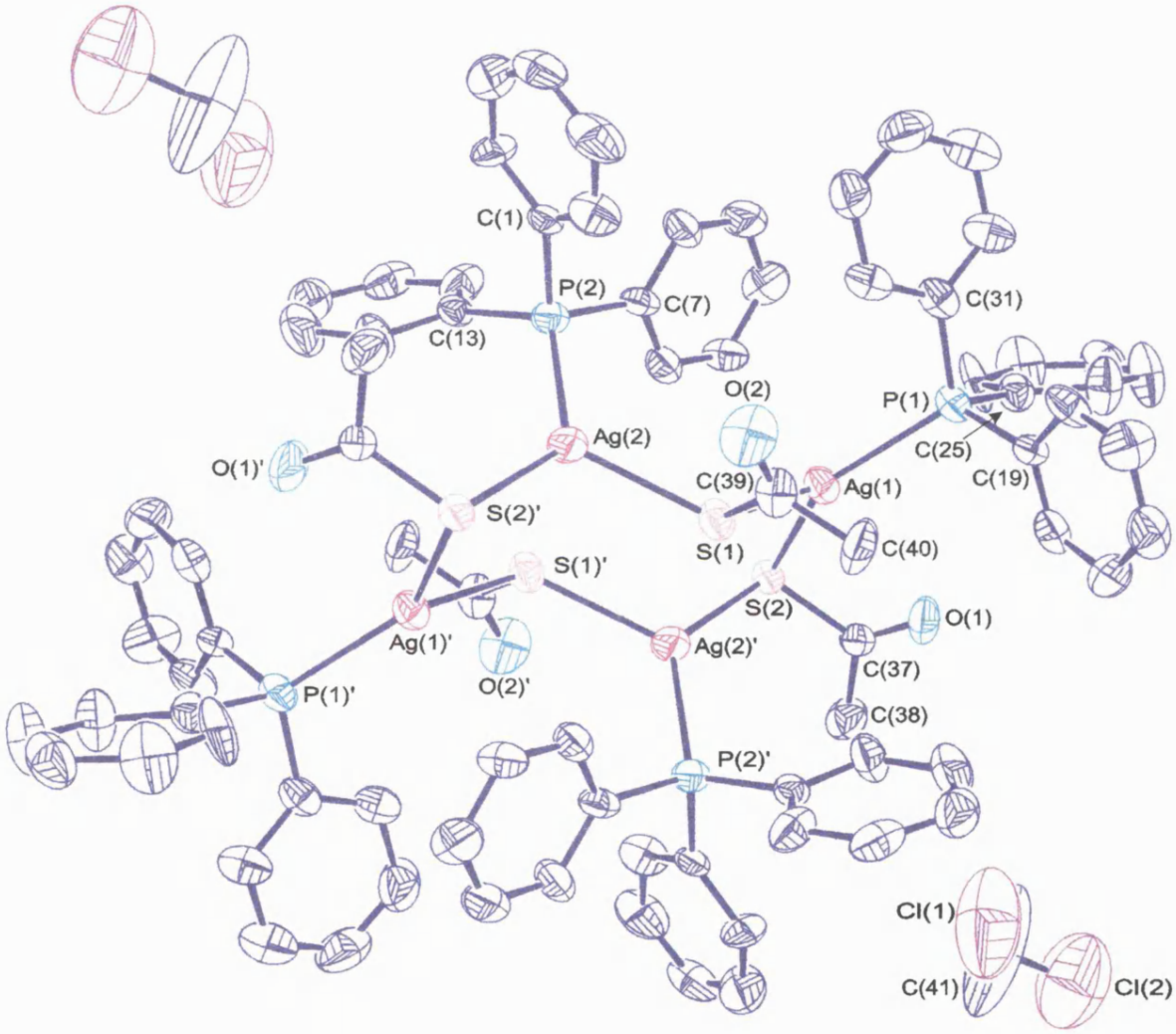

Figure 4.19 Structure of [(monothioacetato)(triphenylphosphine)silver(I)] tetramer.bis(dichloromethane)solvate (**22**).

4.4.6 Thermogravimetric analysis (TGA).

TGA analyses were carried out on compounds (**23**) and (**25**) under an inert helium atmosphere in order to obtain information on their relative stabilities and to determine the temperature at which decomposition may start.

Both compounds were found to decompose in a single-stage process. Compound (**23**) started decomposing at 138°C, the process being complete by 285°C with a mass loss of 83.4%. Compound (**25**) started decomposing at 157°C, was complete by 328°C and involved a mass loss of 84.1%. The weight losses in this single-stage process relate to thermal decomposition of the whole molecule leaving a solid residue. From the weight of residue remaining, this is most likely to be silver sulfide (Ag_2S). But since in subsequent CVD testing it was shown that some silver was formed in a N_2 atmosphere, it is also possible that the residue contains silver.

The single stage decompositions of compounds (**23**) and (**25**) are similar to the decompositions of $[Zn(SOCMe)_2(Lut)_2]$, $[Cd(SOCMe)_2(Lut)_2]$, $[Zn(SOCBu^t)_2(Lut)_2]$ and $[Cd(SOCBu^t)_2(Lut)_2]$ (Lut = Lutidine), where the final products are zinc sulfide or cadmium sulfide.[238] However, the decomposition mode is different to those of $[Ga(SOCMe)_2Me(dmpy)]$ (dmpy = 3,5-dimethylpyridine)[37] and $[In(SOCMe)_4]^-[Hdmpy]^+$,[194] which decompose in two-stage processes. The first stage decomposition of $[Ga(SOCMe)_2Me(dmpy)]$ corresponds to the loss of dmpy and thioacetic anhydride. The second step corresponds to the loss of acetone, the final product being Ga_2S_3. $[In(SOCMe)_4]^-[Hdmpy]^+$ decomposed via loss of thioacetic acid followed by a fundamental loss leaving In_2S_3.[194]

For compounds (**23**) and (**25**), the final product after decomposition should be silver metal or silver sulfide. However, the weights of the residues left are greater than the calculated values. It is possible, therefore, that the residue may contain traces of carbon and traces of silver(I) phosphate obtained by oxidation of triphenylphosphine. Silver(I) oxide would not be present in the residue due to its decomposition to the metal at 200°C. Complexes containing monothiocarboxylate ligands are known to decompose to produce metal sulfides, therefore the remaining residue in both compounds analysed could be Ag_2S.

Silver sulfide is known to melt at 825°C and decomposes at about 1000°C, therefore it is reasonable to suggest that silver sulfide would exist under these experimental conditions. The theoretical percentages of 17.5 and 16.1% respectively for the weight of the residue remaining agree well with the formation of silver sulfide. If it is silver sulfide, the organic species eliminated will be thioacetic anhydride or thiobenzoic anhydride.

Compounds	Decomposition temperature (°C) T_i	T_f	Weight loss (%)	Detached group (%calculated)	Residue remaining % (a) found (b) Ag_{calc} (c) Ag_2S_{calc}		
$[Ag(SOCMe)(PPh_3)_2]$ (**23**)	138	285	83.4	$2PPh_3$ + ½ MeCOOSCMe (82.6)	18.7[a]	15.2[b]	17.5[c]
$[Ag(SOCPh)(PPh_3)_2]$ (**25**)	157	328	84.1	2 PPh_3 + ½ PhCOOSCPh (84.0)	18.4[a]	14.0[b]	16.1[c]

Table 4.9 Table of TGA analysis for compounds (**23**) and (**25**).

4.4.7 CVD testing of precursors.

Films were grown from precursors (**23**) and (**25**) on glass substrates (SiCO) under a N_2 atmosphere at 1 bar pressure, using a horizontal cold wall reactor. The precursor was delivered to the gas phase as an aerosol of the compound dissolved in toluene and swept into the reactor using N_2 as carrier gas.

The films grown were found to be soft and could be easily scratched or damaged relatively easily by touching.

The deposited films were analysed by scanning electron microscopy (SEM) to examine the film morphologies and by Energy Dispersive X-ray Spectrometry (EDXS) to determine the purity of the films.

The quality and nature of the films were dependent on the precursor used. Both precursors were tested at constant concentration, but at different temperatures, carrier gas N_2 flow rates and run times (Table 4.10). Neither of the precursors produced good quality silver mirrors.

By varying the conditions, deposition only occurred at the back-end of the top plate of the reactor. Characteristics of the films varied as a function of the conditions. The films were found to be not uniform, a gradation of thickness being observed. Films were found to be thicker towards the exit port of the reactor.

Compound (**23**) did not produce a film after a 30 minute run at 200°C with a carrier gas flow of 1 $l.min^{-1}$. Deposition occurred after a 47 minute run at 250°C with a carrier gas flow of 0.8 $l.min^{-1}$. A thin pale grey film was deposited on the top plate. By increasing the run time, films were darker. An increase of reactor temperature to 398°C produced a thin pale grey film. At 300°C, thin films were obtained. At a higher carrier gas flow (1 $l.min^{-1}$) and 30 minutes run time, films were pale grey. At a lower gas flow rate (0.8 $l.min^{-1}$) and longer run time films were dark grey.

Compound (**25**) did not produce a film after a 22 minute run between 200-300°C with a carrier gas flow of 1 $l.min^{-1}$. Deposition of a thin pale grey film on the top plate occurred at 400°C. An increase of temperature to 497°C, produced a grey film slightly darker then the one produced at 400°C. By reducing the temperature to 348°C and the carrier gas flow to 0.8 $l.min^{-1}$, thin grey films were obtained on the top plate. The colour of the film was dependent once again on the run time. For short runs, films were pale grey, and for long runs films were dark grey.

Deposition on the top plate may be due to a thermophoretic effect.[161] Once the precursor is in the reactor, gas phase reaction occurs and then the precursor is adsorbed on to the glass substrate. However, due to thermal diffusion effects, the gas species in an initially homogeneous gas mixture will separate under the influence of a temperature gradient. In cold wall reactors, thermal diffusion is important because of the large temperature gradients present. Thermal diffusion causes large heavy gas molecules to concentrate in cold regions (e.g. top plate) of the reactor whereas small light molecules concentrate in the hotter parts of the reactors (e.g. glass substrate).

Conditions	(**23**) [Ag(SOCMe)(PPh_3)$_2$]	(**25**) [Ag(SOCPh)(PPh_3)$_2$]
Concentration ($g.l^{-1}$)	25	16
Temperature of the reactor (°C)	200-398	200-497
N_2 gas flow rate ($l.min^{-1}$)	0.8-1.0	0.8-1.05
Run time (min)	30-75	22-49

Table 4.10 Conditions of CVD testing for triphenylphosphine adducts of silver(I) monothiocarboxylates.

The SEM studies of the film morphologies showed an uneven surface for both compounds when compared to compounds (**6**) and (**9**). See pictures 4.1 and 4.2.

The compositions of these films were established by EDXS analysis. This technique did not provide quantitative analysis of impurities but did highlight the identities of impurities that are present. The analysis revealed that the films are silver with some C, S, O and Si impurities, the Si and O presumably originating from the glass substrate. Phosphorus was completely absent from all films grown. However, sulfur was detected in all cases except in the lighter part of the film grown from (**23**) (Table 4.11).

In conclusion, the films obtained from triphenylphosphine adducts of the monothiocarboxylates were of poor quality. This might be explained by the decomposition modes of the compounds, which lead to formation of silver sulfide, already observed in the TGA analysis. The EDXS analysis also detected the presence of sulfur in the films. Therefore, it can be conclude that films obtained from triphenylphosphine adducts of the silver(I) monothiocarboxylates contain at least some silver sulfide instead of pure silver.

Compounds	Temperature of the reactor (°C)	N_2 gas flow rate ($l.min^{-1}$)	Run time (min)	Visual appearance	SEM analysis	Detected impurities (EDXS)
$[Ag(SOCMe)(PPh_3)_2]$ (**23**)	249	0.8-0.85	75	Dark grey film on the top plate	Rough and uneven structure.	C, O, S
	299	0.9	47	Pale grey film becoming darker on the top plate.		C, O, S (lighter part of the film). C, O (darker part of the film).
$[Ag(SOCPh)(PPh_3)_2]$ (**25**)	348	0.8	49	Pale grey film becoming darker on the top plate.	Rough and uneven structure.	C, O, S

Table 4.11 Conditions of formation, visual appearance and analysis of silver films grown from triphenylphosphine adducts of silver(I) monothiocarboxylates.

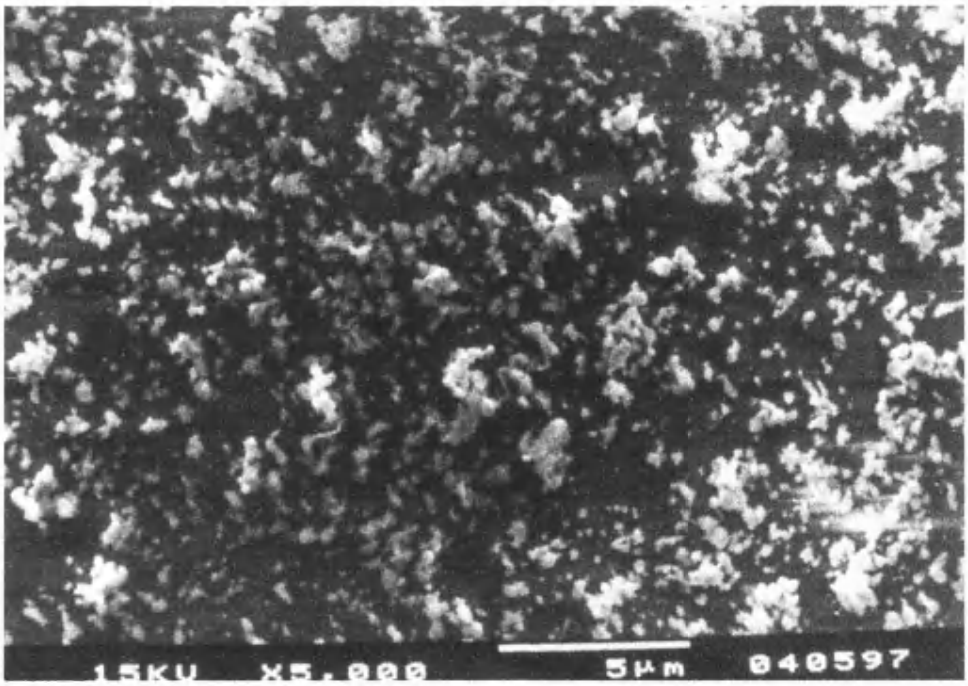

Picture 4.1 SEM image of a film produced from $[Ag(SOCCH_3)(PPh_3)_2]$ (**23**).

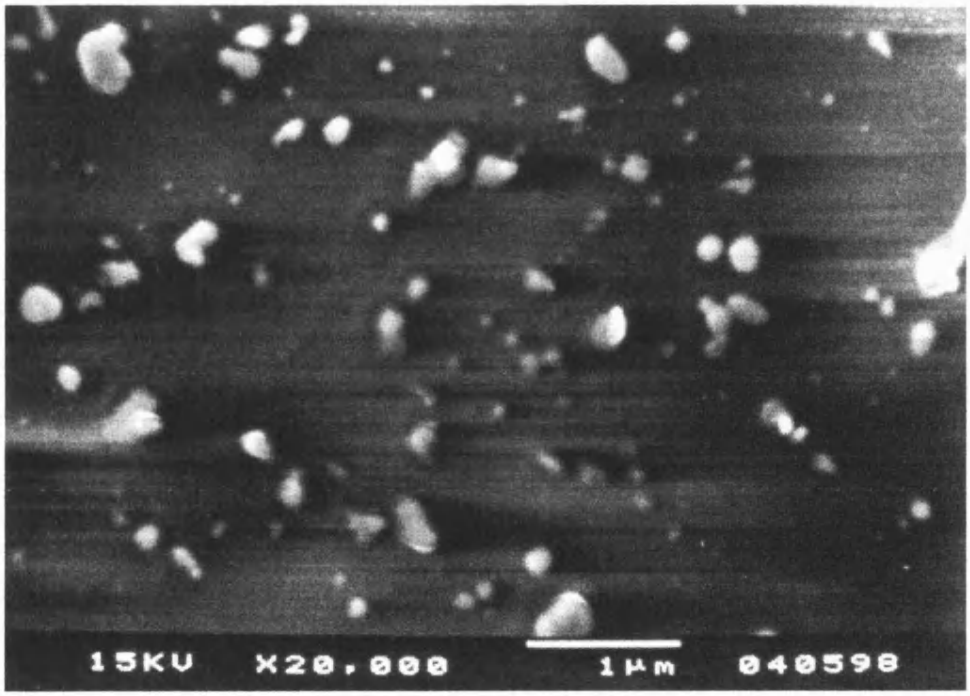

Picture 4.2 SEM image of a film produced from $[Ag(OSCPh)(PPh_3)_2]$ (**25**).

4.5 EXPERIMENTAL.

All operations were carried out under nitrogen and in subdued light with final storage of products in the dark.

Preparation of silver(I) 1-propanethiolate (19).

A solution of silver nitrate (5.9 mmol) in distilled water (5 cm^3) was added slowly to a stirred solution of 1-propanethiol (5.9 mmol) in acetone (10 cm^3). The mixture was filtered and the resulting pale yellow solid was washed with acetone, water and dried *in vacuo.*

Yield: 95%.

Analysis: Found (calculated) for C_3H_7AgS. C: 19.8 (19.7), H: 3.85 (3.88)%.

IR [(cm^{-1}) nujol mulls on NaCl]: 1224 s (S-CH_2 wag).

Preparation of silver(I) 1-dodecanethiolate (20).

A solution of silver nitrate (5.9 mmol) in distilled water (5 cm^3) was added slowly to a solution of 1-dodecanethiol (5.9 mmol) in acetone (10 cm^3). The mixture was filtered and the pale yellow solid was washed with acetone, water and dried *in vacuo.*

Yield: 81%.

Analysis: Found (calculated) for $C_{12}H_{25}AgS$. C: 46.9 (46.6), H: 8.15 (8.15)%.

IR [(cm^{-1}) nujol mulls on NaCl]: 1240 w (S-CH_2 wag).

Attempted preparation of (1-propanethiolato)*tris*(triphenylphosphine)silver(I) (21).

Method A.

Silver(I) 1-propanethiolate (2.7 mmol) and a large excess of triphenylphosphine (29.5 mmol) were heated to above the melting point of triphenylphosphine to produce a melt. Anhydrous toluene (20 cm^3) was added using a syringe to the dark green melt and the resulting mixture was heated to reflux for 6 hours. The green mixture was filtered while still hot giving a silvery grey solid. Petroleum ether (60-80° boiling range) was added to

the filtrate until a further grey solid precipitated from the solution. The mixture was filtered and the second grey solid was dried *in vacuo*, and analysed.

Analysis: Found (calculated) for $C_{57}H_{52}AgP_3S$. C: 35.0 (70.6), H: 4.14 (5.40)%.

IR [(cm^{-1}) nujol mulls on NaCl]: 1224 s (S-CH_2 wag).

Method B.

A mixture of silver(I) 1-propanethiolate (1.6 mmol) and triphenylphosphine (11.5 mmol) in o-xylene (25 cm^3) was heated to reflux. The colour of the mixture changed from brown-orange to green after 4 hours reflux. After 21 hours reflux the solution was still green. The green solution was filtered while still hot and then the filtrate was placed in an ice bath for 25 minutes. Filtration gave a dark grey silvery solid, which was washed with o-xylene and dried *in vacuo*.

Analysis: Found (calculated) for $C_{57}H_{52}AgP_3S$. C: 20.1 (70.6), H: 3.82 (5.40)%.

IR [(cm^{-1}) nujol mulls on NaCl]: 1224 s (S-CH_2 wag).

Preparation of [(monothioacetato)(triphenylphosphine)silver(I)]tetramer.bis(dichloromethane)solvate (22).

A solution of potassium monothioacetate (0.2 mmol) in distilled water (3 cm^3) was added dropwise to a stirred solution of [$AgCl(PPh_3)_3$] (0.2 mmol) in dichloromethane (10 cm^3). The solution was stirred vigorously for 30 minutes and then the solvent layers separated. Hexane was added to the dichloromethane layer and the solution was left to stand for few days. Colourless crystals came out of the solution after few days.

Analysis: Found (calculated) for $C_{82}H_{76}Ag_4Cl_4O_4P_4S_4$. C: 53.65 (50.5), H: 4.07 (3.92)%.

^{1}H NMR [δ(ppm), $CDCl_3$ solution]: 7.44-7.26 (m, 15H, $P(C_6\underline{H}_5)_3$), 5.29 (s, 1H, 0.5 CH_2Cl_2), 2.23 (s, 3H, CH_3).

^{13}C NMR [δ(ppm), $CDCl_3$ solution]: 207.9 (COS), 134.0 (d, J 16.5 Hz, $P(\underline{C}_6H_5)_3$), 133.4 (d, J 25.8 Hz, $P(\underline{C}_6H_5)_3$), 130.0 (s, $P(\underline{C}_6H_5)_3$), 128.7 (d, J 9.1 Hz, $P(\underline{C}_6H_5)_3$), 36.3 ($\underline{C}H_3COS$), 32.4 (CH_2Cl_2).

^{31}P NMR [δ(ppm), $CDCl_3$ solution, (+22°C)]: +8.8(s).

IR [(cm^{-1}) nujol mulls on NaCl]: 1630 s [ν(C=O)], 1435 w, 947 m [ν(C-S)].

Preparation of (thioacetato)*bis*(triphenylphosphine)silver(I) (23).

A solution of (acetato)*bis*(triphenylphosphine)silver(I) (14.4 mmol) in ethanol (100 cm^3) was added slowly to a solution of monothioacetic acid (14.4 mmol) and sodium hydroxide (14.4 mmol) in acetone (15 cm^3) and distilled water (5 cm^3). The mixture was filtered and the resulting pale grey solid was washed with ethanol and dried *in vacuo*.

Yield: 89%.

Analysis: Found (calculated) for $C_{38}H_{33}AgOP_2S$. C: 64.3 (64.5), H: 4.69 (4.70)%.

^1H NMR [δ(ppm), $CDCl_3$ solution]: 7.37-7.20 (m, 30H, $P(C_6\underline{H}_5)_3$), 2.23 (s, 3H, CH_3).

^{13}C NMR [δ(ppm), $CDCl_3$ solution]: 209.3 (COS), 133.9 (d, J 16.5 Hz, $P(\underline{C}_6H_5)_3$), 133.4 (d, J 18.7 Hz, $P(\underline{C}_6H_5)_3$), 129.7 (s, PPh_3), 128.7 (d, J 8.8 Hz, $P(\underline{C}_6H_5)_3$), 36.6 ($\underline{C}H_3COS$).

^{31}P NMR [δ(ppm), $CDCl_3$ solution, (+22°C)]: +6.6 (s).

IR [(cm^{-1}) nujol mulls on NaCl]: 1651 w, 1626 w [ν(C=O)], 1601 w, 1435 m, 947 w [ν(C-S)].

Preparation of silver(I) monothiobenzoate (24).

A solution of silver nitrate (2.9 mmol) dissolved in distilled water (5 cm^3) was added dropwise to a solution of monothiobenzoic acid (2.9 mmol) in acetone (15 cm^3). The mixture was filtered and the greenish solid was washed with acetone, water and dried in a desiccator.

Yield: 88%.

Analysis: Found (calculated) for C_7H_5AgOS. C: 34.6 (34.3), H: 2.01 (2.05)%.

IR [(cm^{-1}) nujol mulls on NaCl]: 1603 s, 1589 w, 1574 s [ν(C=O)], [phenyl]], 918 s [ν(C-S)].

Preparation of (monothiobenzoato)*bis*(triphenylphosphine)silver(I) (25).

Method A.

Silver(I) monothiobenzoate (0.8 mmol) was added to a solution of triphenylphosphine (1.6 mmol) in toluene (20 cm^3). The clear solution was stirred for 30 minutes, filtered and evaporated to dryness to give a pale yellow solid.

Yield: 84%.

Analysis: Found (calculated) for $C_{43}H_{35}AgOP_2S$. C: 67.8 (67.1), H: 4.66 (4.58)%.

Method B.

A solution of (acetato)*bis*(triphenylphosphine)silver(I) (14.4 mmol) in ethanol (100 cm^3) was added slowly to a solution of monothiobenzoic acid (14.4 mmol) and sodium hydroxide (14.4 mmol) in acetone (15 cm^3) and distilled water (5 cm^3). The mixture was filtered and the resulting pale grey solid was washed with ethanol and dried *in vacuo*.

Yield: 91%.

Analysis: Found (calculated) for $C_{43}H_{35}AgOP_2S$. C: 66.9 (67.1), H: 4.51 (4.58)%.

^{1}H NMR [δ(ppm), $CDCl_3$ solution]: 7.37-7.14 (m, $P(C_6\underline{H}_5)_3$, $C_6\underline{H}_5COS$)

^{13}C NMR [δ(ppm), $CDCl_3$ solution]: 204.6 (COS), 142.7 ($\underline{C}_6H_5COS$), 133.9 (d, J 16.5 Hz, $P(\underline{C}_6H_5)_3$), 133.3 (d, J 19.8 Hz, $P(\underline{C}_6H_5)_3$), 130.6 ($\underline{C}_6H_5COS$), 129.6 (s, $P(\underline{C}_6H_5)_3$), 128.6 (d, J 8.8 Hz, $P(\underline{C}_6H_5)_3$), 128.4 ($\underline{C}_6H_5COS$), 127.1 ($\underline{C}_6H_5COS$).

^{31}P NMR [δ(ppm), $CDCl_3$ solution, (+22°C)]: +7.0 (s).

IR [(cm^{-1}) nujol mulls on NaCl]: 1585 w [ν(C=O)], 1543 m, 1433 w, 933 s [ν(C-S)].

Preparation of (diethyldithiocarbamato)*bis*(triphenylphosphine)silver(I) (26).

A solution of (acetato)*bis*(triphenylphosphine)silver(I) (0.3 mmol) in ethanol (10 cm^3) was added slowly to a solution of sodium diethyldithiocarbamate (0.3 mmol) in ethanol (10 cm^3). The resulting white solid was filtered and recrystallised from hot ethanol.

Yield: 37 %.

Analysis: Found (calculated) for $C_{41}H_{40}AgNP_2S_2$. C: 63.0 (63.1), H: 5.06 (5.16), N: 1.76 (1.79)%.

^{1}H NMR [δ(ppm), $CDCl_3$ solution]: 7.42-7.24 (m, 30H, $P(C_6H_5)_3$), 4.01 (q, 4H, J 7.0 Hz, CH_2), 1.29 (t, 6H, J 7.0 Hz, CH_3).

^{13}C NMR [δ(ppm), $CDCl_3$ solution]: 209.1 (NCS_2), 134.5 (d, J 18.4 Hz, $P(\underline{C}_6H_5)_3$), 134.2 (d, J 18.4 Hz, $P(\underline{C}_6H_5)_3$), 129.7 (s, $P(\underline{C}_6H_5)_3$), 128.6 (d, J 9.2 Hz, $P(\underline{C}_6H_5)_3$), 49.0 (CH_2), 12.6 (CH_3).

^{31}P NMR [δ(ppm), $CDCl_3$ solution, (+22°C)]: +6.0 (s).

IR [(cm^{-1}) nujol mulls on NaCl]: 1558 w, 1437 w (sh), 1261 m, 1209 m [$\nu(CS_2^-)$].

Conclusions and Further work

CONCLUSIONS

Three different classes of compounds have been investigated as potential precursors for silver CVD. The compounds synthesised have been fully characterised and have been tested as precursors using Aerosol Assisted Chemical Vapour Deposition (AACVD) methodology. These conclusions aim to compare the compounds synthesised in Chapters 2 to 4 and to assess their suitability as precursors for AACVD of silver. Selected results from CVD testing are summarised in Table 5.1.

In terms of the ease of preparation and handling, silver(I) carboxylates containing unsaturated carboxylate anions and their triphenylphosphine and 1,2-bis(phenylthio)ethane adducts were extremely easy to prepare and usually produced in moderately high yields. They are air stable and easy to handle. The starting materials were readily available and at low cost except for the ligand 1,2-bis(phenylthio)ethane which was synthesised in a low yield.

The silver(I) alkoxides and aryloxides caused some synthetic problems. The parent compounds were found to be unstable so attempts were made to stabilise them using additional triphenylphosphine ligands. The triphenylphosphine adducts of the silver(I) aryloxides were synthesised in moderate yields and were found to be air stable. However they were found to be sensitive to moisture. In addition, their stability was reduced at higher temperature or in solution, which created some handling difficulties.

The silver(I) complexes containing sulfur ligands were generally easy to synthesise. Unfortunately all silver(I) thiolates synthesised were insoluble in most common organic solvents and therefore could not be tested as precursors for silver CVD. Attempts to react the silver(I) thiolates with triphenylphosphine in order to break the polymeric structure of the silver(I) thiolate were unsuccessful. However related complexes containing monothiocarboxylate or dithiocarbamate groups were easy to synthesise in reasonable yields. They were stable in air and easy to handle.

In terms of CVD testing, the films produced from the adducts of silver(I) carboxylates were very encouraging. They show that it is possible to grow transparent silver metallic films with reasonable reflectivity. Carbon was the main contaminant in these films, although traces of sulfur were detected where 1,2-bis(phenylthio)ethane was

used as an additional ligand. The R group from the carboxylate group (RCO_2) seems to play an important role in the film deposition. It was found that precursors containing phenyl rings e.g. compound (**12**), $[Ag(O_2CCH{=}CHPh)(PPh_3)_2]$, did not produce a metallic film. It seems that the volatility is decreased by the presence of a phenyl ring.

In contrast to the adducts of silver(I) carboxylates, the films obtained from triphenylphosphine adducts of aryloxides were of poor quality. This might be explained by the presence of the phenyl ring, which might reduce the volatility of the compounds as observed for the carboxylates. To verify this proposal it would be interesting to examine the volatility of a triphenylphosphine adduct of an alkoxide as a comparison. Literature on the production of films from other metal alkoxides or aryloxides indicates that metal alkoxides and aryloxides are volatile but they are generally not suitable for deposition of metals.

The films obtained from triphenylphosphine adducts of the monothiocarboxylates were of poor quality. This might be explained by the decomposition modes of the compounds, leading to the formation of silver sulfide rather than the pure metal, as observed in the TGA analysis. The EDXS analysis also detected the presence of sulfur in the films. Therefore it can be concluded that films obtained from triphenylphosphine adducts of the silver(I) monothiocarboxylates contain at least some silver sulfide instead of pure silver.

In terms of the quality of the films produced, a large variation was found in the three classes of precursors investigated. Table 5.1 shows selected results from the films analysed in order to highlight direct comparisons.

Overall, the carboxylates were the best group of precursors and compounds (**6**) $[Ag\{O_2C(CH_2)_2CH{=}CH_2\}(PPh_3)_2]$ and (**9**) $[Ag\{O_2C(CH_3)C{=}CHCH_3\}(PPh_3)_2]$ are representative samples which produced metallic silver films with reasonable properties.

Compounds	Reactor Temperature (°C)	Run Time (minutes)	Surface Morphology	Detected impurities (EDXS)	Reflectance (%) at 0.55 μm	Sheet Resistance (Ω/□)
[Ag $\{O_2C(CH_2)_2CH=CH_2\}(PPh_3)_2$] (**6**)	300	66	Transparent silver reflective film. Smooth surface.	C, O	51	19
[Ag$\{O_2C(CH_2)_2CH=CH_2\}(PhSC_2H_4SPh)_2$] (**7**)	250	35	Yellow film on glass and a transparent silver film on the top plate. Rough or uneven surface.	C, S, O	23	-
[Ag$\{O_2C(CH_3)C=CHCH_3\}(PPh_3)_2$] (**9**)	300	64	Transparent silver reflective film. Smooth surface.	C, O	49	14
[Ag$\{O_2C(CH_3)C=CHCH_3\}(PhSC_2H_4SPh)_2$] (**10**)	250	34	Yellow film on glass and silver film on the top plate. Rough or uneven surface.	C, S, O	15	-
[Ag$(O_2CCH=CHC_6H_5)(PPh_3)_2$] (**12**)	300	66	Transparent brown film.	C, O	-	-
[Ag$(OC_6H_2Cl_3$-2,4,6$)(PPh_3)_2$] (**13**)	300	88	Pale grey film.	C	-	-
[Ag$\{OC_6H_2(CH_2NMe_2)_3$-2,4,6$\}(PPh_3)_2$] (**15**)	300	106	Yellow brown film.	C	-	-
[Ag$(OC_6H_4Me$-2$)(PPh_3)_3 \cdot 2$-MeC_6H_4OH] (**17**)	300	75	Yellow brown film.	C	-	-
[Ag(SOCMe)$(PPh_3)_2$] (**23**)	300	47	Dark grey film on the top plate. Rough and uneven structure.	C, O, S	-	-
[Ag(SOCPh)$(PPh_3)_2$] (**25**)	348	49	Pale grey film becoming darker on the top plate. Rough and uneven structure.	C, O, S	-	-

Table 5.1 Selected data for the comparison of films grown from silver(I) complexes precursor.

FURTHER WORK

During this study, the CVD testing performed was simply for screening purposes and significant improvements could be made by changing the conditions in order to optimise the deposition. Initial work was carried out on a nucleation growth study on compounds (**6**) and (**9**). This work could be extended to include pre-treatment of the glass substrate with $SnCl_4$ or $TiCl_4$ and incorporation of O_2 gas or a H_2/N_2 gas mixture could improve the film growth.

The ligand used during this study was mainly triphenylphosphine because it is cheap and easy to handle. However it would be interesting to change the ligand to trimethylphosphine, for example, in the hope of producing more volatile compounds. Another possibility for increasing volatility would be to use fluorinated compounds (e.g. fluorinated unsaturated carboxylic acids, fluorinated phenols or alkoxides).

It is known that silver complexes containing β-diketonate or β-ketoiminate groups are volatile and produce good quality films.[1] Therefore it would be interesting to synthesise silver complexes containing both a carboxylate group and an alkoxide group or a carboxylate group and a β-diketonate or β-ketoiminate group.

Appendices

APPENDIX ONE

Starting materials.

Preparation of tris(triphenylphosphine)silver(I) chloride.

This compound was synthesised by the method given in reference 189.

Silver(I) chloride (3 mmol) was refluxed overnight in a solution of triphenylphosphine (9 mmol) in acetonitrile (100 cm^3). The solution was filtered while still hot and then allowed to cool to room temperature. After allowing the filtrate to stand overnight in the dark, the product precipitated as colourless crystals. These crystals were filtered, washed with acetonitrile and dried *in vacuo*.
Yield: 71 %

Preparation of tris(triphenylphosphine)silver(I) tetrafluoroborate.

This compound was synthesised by the method given in reference 188.

Using a syringe a solution of triphenylphosphine (15 mmol) in dichloromethane (60 cm^3) was added slowly to a solution of silver(I) tetrafluoroborate (5 mmol) in dichloromethane (30 cm^3), at room temperature in the dark. The clear solution was left to stir for an hour and petroleum ether (60-80° boiling range) was added slowly to the solution until a solid precipitated. The white solid was filtered, washed with dichloromethane and dried *in vacuo*.
Yield: 62 %

Preparation of tris(triphenylphosphine)silver(I) nitrate.

This compound was prepared by the method given in reference 142.

A hot solution of silver(I) nitrate (2.5 mmol) in acetonitrile (2 cm^3) was added to a warm solution of triphenylphosphine (75 mmol) in ethanol (80 cm^3). The resulting clear solution

was stirred for another few minutes then allowed to cool to room temperature. After allowing the solution to stand overnight in the dark, the product precipitated as a white crystalline solid. This solid was filtered, washed with ethanol and dried in a desiccator.
Yield: 62 %

Preparation of (acetato)*bis*(triphenylphosphine)silver(I).

This compound was prepared by the method given in reference 1.

Silver(I) acetate (34.8 mmol) was added to a stirred solution of triphenylphosphine (89.6 mmol) in toluene (50 cm^3). After 18 hours the resulting beige precipitate was filtered, washed with toluene and dried *in vacuo*.
Yield: 83 %

Preparation of 1,2-bis(phenylthio)ethane.

This compound was synthesised by the method given in reference 239.

Using a syringe 1,2-dibromoethane (65 mmol) was added to a solution of sodium thiophenolate (130 mmol) in absolute ethanol (250 cm^3). The mixture was stirred at room temperature for 15 minutes then heated to reflux for two hours. The resulting white mixture was filtered while still hot and the white solid was recrystallised from absolute ethanol. The filtrate was allowed to cool to room temperature. A white solid precipitated from the filtrate. This solid was filtered and recrystallised from absolute ethanol. Both batches were the desired product.
Yield: 36%

Reagents and solvents.

All carboxylic acids, phenols, thiols, sodium diethyldithiocarbamate, monothiocarboxylic acids, triphenylphosphine, silver(I) nitrate, silver(I) tetrafluoroborate, silver(I) trifluorosulfonate, tert-butoxytrimethylsilane, magnesium turnings, and sodium hydride were purchased from Aldrich, Lancaster or M&G Chemicals and were used

without further purification. Silver(I) oxide was purchased from M&G Chemicals and was washed several times with large amounts of distilled water and dried *in vacuo*, before use.

Tetrahydrofuran and toluene were distilled over sodium/benzophenone and dichloromethane was distilled over sodium hydride prior to use. Ethanol, diethyl ether, acetonitrile, acetone, o-xylene and petroleum ether (60-80° boiling range) were stored over molecular sieves for several days before use.

APPENDIX TWO

Crystallographic data for silver(I) tiglate (8).

A crystal of approximate dimensions 0.4 x 0.3 x 0.3 mm was used for data collection.

Crystal data: $C_5H_7AgO_2$, M = 206.98, Monoclinic, a = 5.9650(10), b = 8.956(2), c = 10.292(2) Å, β = 91.51(2)°, U = 549.6(2) Å^3, space group $P2_1/a$, Z = 4, D_c = 2.501 g.cm^{-3}, (μMo-K_α) = 3.556 mm^{-1}, F(000) = 400. Crystallographic measurements were made at 170(2)°K on a CAD4 automatic four-circle diffractometer in the range 3.01<θ<21.97°. Data (676 reflections) were corrected for Lorentz and polarization and also for absorption.[240] (Max. and Min absorption corrections; 1.000, 0.228 respectively)

In the final least squares cycles C(1) and C(2) were isotropically refined, while remaining atoms were treated anisotropically. Hydrogen atoms were included at calculated positions where relevant except for H(3) which was located in the penultimate difference Fourier map, and refined at a distance of 0.98Å from C(3).

The supramolecular structure of this complex is dominated by polymeric sheets of molecules, (parallel to the *ab* plane and at unit cell intervals along c), affording a distorted octahedral coordination sphere about the transition metal. Typically, Ag(1) (in the asymmetric unit as presented) bonds to O(1) of the same molecule, and to both Ag(1) and O(2) of the lattice neighbour generated by the operator *-x, 1-y, 1-z.* An additional bond to silver arises by interaction with O(1) of the molecule generated via the *0.5+x,1.5-y, z* symmetry transformation. These four bonds are loosely planar (largest deviation from least squares plane of all 5 atoms; 0.14 Å). The octahedral arrangement about silver is completed two substantially weaker interactions, one to the vinyl moiety of the residue generated by the transformation *1+x, y, z,* and another to O(2), as a consequence of the operator *-0.5-x, 0.5+y, -z.* [Ag(1)-C(2), 3.039(6), Ag(1)-C(3), 2.870(6), Ag(1)-O(2), 3.132(5) Å]

The solution of the structure (SHELX86)[82] and refinement (SHELX93)[83] converged to a conventional [i.e. based on 613 reflections with $Fo>4\sigma(Fo)$] $R1$ = 0.0357 and $wR2$ = 0.0947. Goodness of fit = 1.154. The max. and min. residual densities were 0.812 and -0.788 eÅ^{-3} respectively. The asymmetric unit (shown in Fig. 2.14), along with the labelling scheme used was produced using ORTEX.[241] Final fractional atomic co-

ordinates and isotropic thermal parameters, bond distances and angles are given in Tables A2.2 and A2.3 respectively. Anisotropic temperature factors are given in Table A2.4 and hydrogen coordinates and isotropic temperature factor in Table A2.5.

Table A2.1 Crystal data and structure refinement for (**8**).

Identification code	96DAE2
Empirical formula	$C_5 H_7 Ag O_2$
Formula weight	206.98
Temperature	170(2) K
Wavelength	0.70930 Å
Crystal system	Monoclinic
Space group	$P2_1/a$
Unit cell dimensions	a = 5.9650(10)Å
	b = 8.956(2)Å β= 91.51(2)°
	c = 10.292(2)Å
Volume	549.6(2) $Å^3$
Z	4
Density (calculated)	2.501 Mg/m^3
Absorption coefficient	3.556 mm^{-1}
F(000)	400
Crystal size	0.4 x 0.3 x 0.3 mm
Theta range for data collection	3.01 to 21.97°
Index ranges	-6<=h<=6; 0<=k<=9; 0<=l<=10
Reflections collected	676
Independent reflections	676 [R(int) = 0.0000]
Refinement method	Full-matrix least-squares on F^2
Data / restraints / parameters	674 / 1 / 69
Goodness-of-fit on F^2	1.154
Final R indices [$I>2\sigma(I)$]	R1 = 0.0357 wR2 = 0.0947
R indices (all data)	R1 = 0.0400 wR2 = 0.1024
Largest diff. peak and hole	0.812 and -0.788 $eÅ^{-3}$
Weighting scheme	calc $w=1/[\sigma^2(Fo^2)+(0.0721P)^2+1.0654P]$ where $P=(Fo^2+2Fc^2)/3$
Extinction coefficient	0.0047(20)
Extinction expression	$Fc^*=kFc[1+0.001xFc^2\lambda^3/\sin(2\theta)]^{-1/4}$

Table A2.2 Atomic coordinates (x 10^4) and equivalent isotropic displacement parameters ($Å^2$ x 10^3) for (**8**). U(eq) is defined as one third of the trace of the orthogonalized Uij tensor.

Atom	x	y	z	U(eq)
Ag(1)	813(1)	6324(1)	4402(1)	23(1)
O(1)	-2630(8)	6291(4)	3571(4)	17(1)
O(2)	-3542(8)	3961(5)	4129(5)	18(1)
C(1)	-3882(9)	5135(6)	3505(6)	14(1)
C(2)	-5748(9)	5191(6)	2508(6)	14(1)
C(3)	-7433(11)	4211(7)	2596(6)	17(1)
C(4)	-9362(11)	3998(8)	1654(7)	20(2)
C(5)	-5548(12)	6296(6)	1421(7)	18(2)

Table A2.3 Bond lengths [Å] and angles [°] for (**8**).

Ag(1)-O(1)	2.204(5)	O(2)#1-Ag(1)-O(1)#2	93.4(2)
Ag(1)-O(2)#1	2.207(5)	O(1)-Ag(1)-Ag(1)#1	80.35(11)
Ag(1)-O(1)#2	2.490(4)	O(2)#1-Ag(1)-Ag(1)#1	82.03(13)
Ag(1)-Ag(1)#1	2.8532(10)	O(1)#2-Ag(1)-Ag(1)#1	174.44(11)
O(1)-C(1)	1.277(7)	C(1)-O(1)-Ag(1)	124.7(4)
O(1)-Ag(1)#3	2.490(4)	C(1)-O(1)-Ag(1)#3	119.4(4)
O(2)-C(1)	1.246(8)	Ag(1)-O(1)-Ag(1)#3	102.0(2)
O(2)-Ag(1)#1	2.207(5)	C(1)-O(2)-Ag(1)#1	123.9(4)
C(1)-C(2)	1.495(9)	O(2)-C(1)-O(1)	124.7(6)
C(2)-C(3)	1.339(9)	O(2)-C(1)-C(2)	119.4(5)
C(2)-C(5)	1.501(9)	O(1)-C(1)-C(2)	115.7(5)
C(3)-C(4)	1.497(10)	C(3)-C(2)-C(1)	118.6(6)
		C(3)-C(2)-C(5)	123.9(6)
O(1)-Ag(1)-O(2)#1	158.0(2)	C(1)-C(2)-C(5)	117.5(5)
O(1)-Ag(1)-O(1)#2	103.33(14)	C(2)-C(3)-C(4)	127.3(6)

Symmetry transformations used to generate equivalent atoms:

#1 -x,-y+1,-z+1

#2 x+1/2,-y+3/2,z

#3 x-1/2,-y+3/2,z

Table A2.4 Anisotropic displacement parameters ($Å^2$ x 10^3) for (**8**). The anisotropic displacement factor exponent takes the form: $-2\pi^2$ [h^2 a* 2 U11 + ... + 2 h k a* b* U12]

Atom	U11	U22	U33	U23	U13	U12
Ag(1)	23(1)	24(1)	23(1)	7(1)	-1(1)	-4(1)
O(1)	19(3)	19(3)	13(3)	-3(2)	4(2)	3(2)
O(2)	17(2)	25(2)	11(2)	-2(2)	7(2)	5(2)
C(3)	28(4)	14(3)	9(4)	2(3)	12(3)	6(3)
C(4)	17(3)	23(3)	19(4)	0(3)	6(3)	-2(3)
C(5)	21(4)	21(4)	13(4)	-1(2)	9(3)	0(2)

Table A2.5 Hydrogen coordinates (x 10^4) and isotropic displacement parameters ($Å^2$ x 10^3) for (**8**).

Atom	x	y	z	U(eq)
H(3)	-7622(130)	3577(61)	3247(52)	20
H(4A)	-10649(21)	3661(43)	2112(8)	29
H(4B)	-8971(26)	3267(33)	1017(23)	29
H(4C)	-9703(44)	4928(12)	1230(29)	29
H(5A)	-4193(34)	6108(27)	965(23)	27
H(5B)	-5508(64)	7290(6)	1771(8)	27
H(5C)	-6814(34)	6198(29)	832(21)	27

APPENDIX THREE

Crystallographic data for (*O,O'*-cyanoacetato) *bis*(triphenylphosphine)silver(I) (2).

A crystal of approximate dimensions 0.3 x 0.3 x 0.3 mm was used for data collection.

Crystal data: C_{39} H_{32} Ag N O_2 P_2, M = 716.47, Triclinic , a = 12.689(3), b = 12.850(2), c = 13.351(3) Å , α = 65.160(10), β = 61.89(2), γ = 72.21(2)°, U = 1726.7(6) $Å^3$, space group $P\bar{1}$ (No. 2), Z = 2, D_c = 1.378 $g.cm^{-3}$, (μMo-K_α) = 0.710 mm^{-1}, F(000) = 732. Crystallographic measurements were made at 293(2)°K on a CAD4 automatic four-circle diffractometer in the range $2.01<\theta<23.93°$. Data (5692 reflections) were corrected for Lorentz and polarization but not for absorption.

In the final least squares cycles all atoms were allowed to vibrate anisotropically. Hydrogen atoms were included at calculated positions where relevant.

The solution of the structure (SHELX86)[82] and refinement (SHELX93)[83] converged to a conventional [i.e. based on 4589 reflections with $Fo>4\sigma(Fo)$] $R1$ = 0.0249 and $wR2$ = 0.0639. Goodness of fit = 0.920. The max. and min. residual densities were 0.405 and -0.222 $eÅ^{-3}$ respectively. The asymmetric unit (shown in Fig. 2.17), along with the labelling scheme used was produced using ORTEX.[241] Final fractional atomic co-ordinates and isotropic thermal parameters, bond distances and angles are given in Tables A3.2 and A3.3, respectively. Anisotropic temperature factors are given in Table A3.4 and hydrogen coordinates and isotropic temperature factor in Table A3.5.

Table A3.1 Crystal data and structure refinement for (**2**).

Identification code	96DAE1
Empirical formula	$C_{39}H_{32}AgNO_2P_2$
Formula weight	716.47
Temperature	293(2)° K
Wavelength	0.70930 Å
Crystal system	Triclinic
Space group	$P\bar{1}$
Unit cell dimensions	a = 12.689(3)Å α= 65.160(10)°
	b = 12.850(2)Å β= 61.89(2)°
	c = 13.351(3)Å γ= 72.21(2)°
Volume	1726.7(6) $Å^3$
Z	2
Density (calculated)	1.378 Mg/m^3
Absorption coefficient	0.710 mm^{-1}
F(000)	732
Crystal size	0.3 x 0.3 x 0.3 mm
Theta range for data collection	2.01 to 23.93°
Index ranges	0<=h<=14; -13<=k<=14; -13<=l<=15
Reflections collected	5692
Independent reflections	5418 [R(int) = 0.0097]
Refinement method	Full-matrix least-squares on F^2
Data / restraints / parameters	5415 / 0 / 407
Goodness-of-fit on F2	0.920
Final R indices [I>2σ(I)]	R1 = 0.0249 wR2 = 0.0639
R indices (all data)	R1 = 0.0365 wR2 = 0.0724
Largest diff. peak and hole	0.405 and -0.222 $eÅ^{-3}$
Weighting scheme	calc $w=1/[\sigma^2(Fo^2)+(0.0447P)^2+1.1845P]$ where $P=(Fo^2+2Fc^2)/3$
Extinction coefficient	0.0075(5)
Extinction expression	$Fc^*=kFc[1+0.001xFc^2\lambda^3/\sin(2\theta)]^{-1/4}$

Table A3.2 Atomic coordinates (x 10^4) and equivalent isotropic displacement parameters ($Å^2$ x 10^3) for (**2**). U(eq) is defined as one third of the trace of the orthogonalized Uij tensor.

Atom	x	y	z	U(eq)
Ag(1)	1082(1)	2228(1)	2262(1)	47(1)
P(1)	-841(1)	2555(1)	3842(1)	43(1)
P(2)	2811(1)	3286(1)	1267(1)	41(1)
N(1)	1743(9)	696(6)	-1605(7)	262(5)
O(1)	1000(3)	1712(2)	697(3)	94(1)
O(2)	1899(2)	415(2)	1843(2)	71(1)
C(1)	-1875(2)	1499(2)	4510(2)	46(1)
C(2)	-2133(3)	1263(3)	3739(3)	61(1)
C(3)	-2947(3)	505(3)	4179(3)	72(1)
C(4)	-3468(3)	-46(3)	5387(4)	78(1)
C(5)	-3153(3)	120(3)	6153(3)	80(1)
C(6)	-2362(3)	895(3)	5724(3)	62(1)
C(7)	-1728(2)	3946(2)	3402(2)	47(1)
C(8)	-2971(3)	4103(3)	3856(3)	69(1)
C(9)	-3594(3)	5183(3)	3501(4)	85(1)

C(10)	-2985(4)	6118(3)	2696(3)	79(1)
C(11)	-1750(3)	5972(3)	2242(3)	70(1)
C(12)	-1125(3)	4901(2)	2583(3)	58(1)
C(13)	-624(2)	2596(2)	5076(2)	46(1)
C(14)	-1025(3)	3560(3)	5441(3)	60(1)
C(15)	-735(4)	3579(3)	6311(3)	77(1)
C(16)	-73(3)	2654(3)	6830(3)	75(1)
C(17)	323(3)	1696(3)	6486(3)	78(1)
C(18)	61(3)	1663(3)	5603(3)	65(1)
C(19)	4094(2)	2975(2)	-31(2)	46(1)
C(20)	4403(3)	1861(3)	-48(3)	77(1)
C(21)	5393(4)	1602(3)	-1011(4)	104(2)
C(22)	6043(3)	2436(3)	-1947(3)	85(1)
C(23)	5719(3)	3545(3)	-1958(3)	64(1)
C(24)	4745(2)	3816(2)	-999(2)	53(1)
C(25)	3453(2)	3199(2)	2272(2)	46(1)
C(26)	2667(3)	3260(3)	3408(3)	59(1)
C(27)	3099(3)	3213(3)	4205(3)	73(1)
C(28)	4314(4)	3082(3)	3885(3)	78(1)
C(29)	5100(3)	3014(3)	2772(3)	76(1)
C(30)	4679(3)	3074(3)	1962(3)	60(1)
C(31)	2340(2)	4820(2)	658(2)	40(1)
C(32)	1652(3)	5152(3)	-15(3)	55(1)
C(33)	1235(3)	6296(3)	-463(3)	64(1)
C(34)	1491(3)	7132(3)	-255(3)	64(1)
C(35)	2179(3)	6821(2)	387(3)	63(1)
C(36)	2601(2)	5671(2)	848(3)	51(1)
C(37)	1536(3)	759(3)	1038(3)	60(1)
C(38)	1803(5)	-111(3)	411(4)	109(2)
C(39)	1778(6)	342(4)	-710(5)	124(2)

Table A3.3 Bond lengths [Å] and angles [°] for (**2**).

Ag(1)-P(1)	2.4185(10)	C(1)-P(1)-Ag(1)	116.65(9)
Ag(1)-O(2)	2.427(2)	C(31)-P(2)-C(25)	104.44(11)
Ag(1)-P(2)	2.4464(10)	C(31)-P(2)-C(19)	102.78(11)
Ag(1)-O(1)	2.495(2)	C(25)-P(2)-C(19)	105.49(12)
P(1)-C(13)	1.816(3)	C(31)-P(2)-Ag(1)	109.60(8)
P(1)-C(7)	1.821(3)	C(25)-P(2)-Ag(1)	114.13(9)
P(1)-C(1)	1.824(3)	C(19)-P(2)-Ag(1)	118.92(8)
P(2)-C(31)	1.815(2)	C(37)-O(1)-Ag(1)	89.0(2)
P(2)-C(25)	1.825(3)	C(37)-O(2)-Ag(1)	92.0(2)
P(2)-C(19)	1.827(3)	C(2)-C(1)-C(6)	118.8(3)
N(1)-C(39)	1.103(6)	C(2)-C(1)-P(1)	117.3(2)
O(1)-C(37)	1.219(4)	C(6)-C(1)-P(1)	123.8(2)
O(2)-C(37)	1.226(4)	C(1)-C(2)-C(3)	120.8(3)
C(1)-C(2)	1.380(4)	C(4)-C(3)-C(2)	119.8(3)
C(1)-C(6)	1.380(4)	C(3)-C(4)-C(5)	119.8(3)
C(2)-C(3)	1.386(4)	C(4)-C(5)-C(6)	120.7(3)
C(3)-C(4)	1.364(5)	C(5)-C(6)-C(1)	119.9(3)
C(4)-C(5)	1.370(5)	C(8)-C(7)-C(12)	118.4(3)
C(5)-C(6)	1.384(5)	C(8)-C(7)-P(1)	123.0(2)
C(7)-C(8)	1.379(4)	C(12)-C(7)-P(1)	118.6(2)
C(7)-C(12)	1.394(4)	C(9)-C(8)-C(7)	120.3(3)
C(8)-C(9)	1.381(5)	C(8)-C(9)-C(10)	120.5(3)
C(9)-C(10)	1.377(5)	C(11)-C(10)-C(9)	119.6(3)
C(10)-C(11)	1.370(5)	C(10)-C(11)-C(12)	120.2(3)

C(11)-C(12)	1.370(4)	C(11)-C(12)-C(7)	120.9(3)
C(13)-C(14)	1.385(4)	C(14)-C(13)-C(18)	118.6(3)
C(13)-C(18)	1.385(4)	C(14)-C(13)-P(1)	122.7(2)
C(14)-C(15)	1.384(4)	C(18)-C(13)-P(1)	118.5(2)
C(15)-C(16)	1.358(5)	C(15)-C(14)-C(13)	120.0(3)
C(16)-C(17)	1.362(5)	C(16)-C(15)-C(14)	120.9(3)
C(17)-C(18)	1.386(4)	C(17)-C(16)-C(15)	119.9(3)
C(19)-C(24)	1.374(4)	C(16)-C(17)-C(18)	120.4(3)
C(19)-C(20)	1.371(4)	C(13)-C(18)-C(17)	120.3(3)
C(20)-C(21)	1.387(5)	C(24)-C(19)-C(20)	118.7(3)
C(21)-C(22)	1.354(5)	C(24)-C(19)-P(2)	122.7(2)
C(22)-C(23)	1.354(5)	C(20)-C(19)-P(2)	118.6(2)
C(23)-C(24)	1.381(4)	C(19)-C(20)-C(21)	119.4(3)
C(25)-C(30)	1.382(4)	C(22)-C(21)-C(20)	121.1(3)
C(25)-C(26)	1.388(4)	C(23)-C(22)-C(21)	119.9(3)
C(26)-C(27)	1.381(4)	C(22)-C(23)-C(24)	119.7(3)
C(27)-C(28)	1.368(5)	C(19)-C(24)-C(23)	121.0(3)
C(28)-C(29)	1.367(5)	C(30)-C(25)-C(26)	118.5(3)
C(29)-C(30)	1.383(4)	C(30)-C(25)-P(2)	123.4(2)
C(31)-C(36)	1.379(4)	C(26)-C(25)-P(2)	118.1(2)
C(31)-C(32)	1.394(4)	C(27)-C(26)-C(25)	120.8(3)
C(32)-C(33)	1.372(4)	C(28)-C(27)-C(26)	119.9(3)
C(33)-C(34)	1.373(5)	C(29)-C(28)-C(27)	119.9(3)
C(34)-C(35)	1.365(4)	C(28)-C(29)-C(30)	120.7(3)
C(35)-C(36)	1.383(4)	C(25)-C(30)-C(29)	120.1(3)
C(37)-C(38)	1.535(4)	C(36)-C(31)-C(32)	118.3(2)
C(38)-C(39)	1.372(6)	C(36)-C(31)-P(2)	123.7(2)
		C(32)-C(31)-P(2)	118.0(2)
P(1)-Ag(1)-O(2)	124.33(6)	C(33)-C(32)-C(31)	120.6(3)
P(1)-Ag(1)-P(2)	127.93(3)	C(32)-C(33)-C(34)	120.5(3)
O(2)-Ag(1)-P(2)	104.89(7)	C(35)-C(34)-C(33)	119.5(3)
P(1)-Ag(1)-O(1)	115.66(7)	C(34)-C(35)-C(36)	120.6(3)
O(2)-Ag(1)-O(1)	52.61(7)	C(31)-C(36)-C(35)	120.5(3)
P(2)-Ag(1)-O(1)	106.75(8)	O(1)-C(37)-O(2)	126.4(3)
C(13)-P(1)-C(7)	103.63(12)	O(1)-C(37)-C(38)	118.1(3)
C(13)-P(1)-C(1)	106.12(12)	O(2)-C(37)-C(38)	115.5(3)
C(7)-P(1)-C(1)	104.42(12)	C(39)-C(38)-C(37)	116.4(4)
C(13)-P(1)-Ag(1)	110.55(9)	N(1)-C(39)-C(38)	178.9(8)
C(7)-P(1)-Ag(1)	114.34(9)		

Table A3.4 Anisotropic displacement parameters ($Å^2$ x 10^3) for (**2**). The anisotropic displacement factor exponent takes the form: $-2\pi^2[h^2 a^* 2 U11 + ... + 2 h k a^* b^* U12]$

Atom	U11	U22	U33	U23	U13	U12
Ag(1)	46(1)	47(1)	47(1)	-21(1)	-11(1)	-11(1)
P(1)	43(1)	46(1)	40(1)	-17(1)	-11(1)	-11(1)
P(2)	38(1)	38(1)	47(1)	-16(1)	-13(1)	-7(1)
N(1)	483(14)	209(7)	212(7)	-117(6)	-256(9)	68(8)
O(1)	125(2)	73(2)	127(2)	-60(2)	-91(2)	38(2)
O(2)	107(2)	52(1)	65(1)	-20(1)	-49(1)	-1(1)
C(1)	50(1)	44(1)	41(1)	-13(1)	-13(1)	-10(1)
C(2)	77(2)	64(2)	51(2)	-11(1)	-29(2)	-26(2)
C(3)	87(2)	68(2)	85(2)	-21(2)	-47(2)	-23(2)
C(4)	78(2)	62(2)	94(3)	-13(2)	-31(2)	-31(2)
C(5)	94(3)	70(2)	59(2)	-9(2)	-13(2)	-37(2)
C(6)	76(2)	60(2)	49(2)	-17(1)	-18(2)	-21(2)

C(7)	48(2)	51(2)	43(1)	-17(1)	-17(1)	-9(1)
C(8)	51(2)	69(2)	74(2)	-15(2)	-22(2)	-10(2)
C(9)	58(2)	83(3)	99(3)	-24(2)	-34(2)	6(2)
C(10)	88(3)	63(2)	85(2)	-22(2)	-48(2)	10(2)
C(11)	86(2)	53(2)	71(2)	-13(2)	-34(2)	-13(2)
C(12)	57(2)	52(2)	60(2)	-15(1)	-21(1)	-11(1)
C(13)	41(1)	54(2)	42(1)	-20(1)	-10(1)	-11(1)
C(14)	67(2)	60(2)	57(2)	-28(1)	-23(2)	-6(1)
C(15)	99(3)	79(2)	73(2)	-44(2)	-35(2)	-11(2)
C(16)	75(2)	106(3)	60(2)	-38(2)	-27(2)	-19(2)
C(17)	81(2)	93(3)	69(2)	-32(2)	-44(2)	6(2)
C(18)	74(2)	63(2)	65(2)	-31(2)	-35(2)	7(2)
C(19)	39(1)	44(1)	57(2)	-23(1)	-15(1)	-5(1)
C(20)	69(2)	46(2)	86(2)	-30(2)	-3(2)	-7(2)
C(21)	95(3)	63(2)	120(3)	-57(2)	4(3)	-4(2)
C(22)	66(2)	90(3)	84(2)	-55(2)	3(2)	-10(2)
C(23)	56(2)	77(2)	55(2)	-26(2)	-10(1)	-17(2)
C(24)	49(2)	51(2)	56(2)	-23(1)	-12(1)	-9(1)
C(25)	47(1)	37(1)	53(2)	-10(1)	-22(1)	-8(1)
C(26)	55(2)	66(2)	62(2)	-24(2)	-22(2)	-12(1)
C(27)	87(2)	81(2)	62(2)	-22(2)	-31(2)	-24(2)
C(28)	96(3)	82(2)	76(2)	-8(2)	-53(2)	-30(2)
C(29)	62(2)	84(2)	85(3)	-9(2)	-42(2)	-21(2)
C(30)	52(2)	62(2)	62(2)	-11(1)	-25(1)	-12(1)
C(31)	35(1)	42(1)	39(1)	-16(1)	-10(1)	-5(1)
C(32)	62(2)	57(2)	55(2)	-20(1)	-29(1)	-9(1)
C(33)	69(2)	64(2)	59(2)	-13(2)	-37(2)	1(2)
C(34)	71(2)	47(2)	57(2)	-13(1)	-24(2)	6(1)
C(35)	77(2)	42(2)	75(2)	-27(2)	-32(2)	0(1)
C(36)	54(2)	44(2)	63(2)	-22(1)	-28(1)	-3(1)
C(37)	78(2)	48(2)	66(2)	-28(2)	-34(2)	-1(2)
C(38)	181(5)	74(2)	103(3)	-51(2)	-80(3)	13(3)
C(39)	208(6)	105(3)	120(4)	-63(3)	-110(4)	15(3)

Table A3.5 Hydrogen coordinates (x 10^4) and isotropic displacement parameters (Å^2 x 10^3) for (**2**).

Atom	x	y	z	U(eq)
H(2)	-1757(3)	1616(3)	2913(3)	74
H(3)	-3137(3)	373(3)	3653(3)	87
H(4)	-4037(3)	-534(3)	5689(4)	94
H(5)	-3473(3)	-291(3)	6971(3)	95
H(6)	-2159(3)	1008(3)	6252(3)	75
H(8)	-3391(3)	3478(3)	4404(3)	83
H(9)	-4432(3)	5280(3)	3808(4)	102
H(10)	-3408(4)	6845(3)	2461(3)	95
H(11)	-1335(3)	6602(3)	1701(3)	84
H(12)	-287(3)	4809(2)	2263(3)	69
H(14)	-1490(3)	4194(3)	5102(3)	71
H(15)	-996(4)	4233(3)	6542(3)	92
H(16)	110(3)	2674(3)	7418(3)	89
H(17)	771(3)	1061(3)	6846(3)	93
H(18)	346(3)	1012(3)	5364(3)	78
H(20)	3953(3)	1283(3)	581(3)	92
H(21)	5615(4)	843(3)	-1013(4)	125
H(22)	6710(3)	2247(3)	-2582(3)	102
H(23)	6152(3)	4123(3)	-2609(3)	77

H(24)	4527(2)	4579(2)	-1009(2)	64
H(26)	1841(3)	3333(3)	3636(3)	71
H(27)	2563(3)	3269(3)	4957(3)	88
H(28)	4606(4)	3040(3)	4425(3)	94
H(29)	5925(3)	2927(3)	2558(3)	91
H(30)	5221(3)	3029(3)	1206(3)	72
H(32)	1473(3)	4594(3)	-163(3)	66
H(33)	777(3)	6507(3)	-911(3)	77
H(34)	1196(3)	7906(3)	-550(3)	77
H(35)	2367(3)	7387(2)	515(3)	75
H(36)	3064(2)	5469(2)	1289(3)	61
H(38A)	2594(5)	-544(3)	343(4)	131
H(38B)	1222(5)	-656(3)	924(4)	131

APPENDIX FOUR

Crystallographic data for (*O,O'*-allylacetato) *bis*(triphenylphosphine)silver(I) (6).

A crystal of approximate dimensions 0.3 x 0.3 x 0.3 mm was used for data collection.

Crystal data: C_{41} H_{37} Ag O_2 P_2, M = 731.52, Triclinic, a = 12.806(5), b = 12.996(4), c = 13.056(6) Å, α = 66.26(3), β = 62.40(3), γ = 72.79(3)°, U = 1746.6(12) Å^3, space group $P\bar{1}$ (No.2), Z = 2, D_c = 1.391 g.cm^{-3}, μ(Mo-K_α) = 0.703 mm^{-1}, F(000) = 752. Crystallographic measurements were made at 293(2)°K on a CAD4 automatic four-circle diffractometer in the range $2.01<\theta<23.93°$. Data (5758 reflections) were corrected for Lorentz and polarization, and linear decay (7%) of the crystal in the X-ray beam. An absorption correction was not applied.

In the final least squares cycles all atoms were allowed to vibrate anisotropically. Hydrogen atoms were included at calculated positions where relevant. The olefinic carbons [C(40), C(41)] were disordered in the ratio 55:45 with positions C(40A) and C(41A). (These partial carbon positions were treated isotropically in the first instance, to establish their associated site occupancy factors, which were subsequently fixed before proceeding to anisotropic refinement.)

The solution of the structure (SHELX86)[82] and refinement (SHELX93)[83] converged to a conventional [i.e. based on 4705 reflections with $Fo>4\sigma(Fo)$] $R1$ = 0.0324 and $wR2$ = 0.0991. Goodness of fit = 1.061. The max. and min. residual densities were 0.441 and -0.332 eÅ^{-3} respectively. The asymmetric unit (shown in Fig. 2.18), along with the labelling scheme used was produced using ORTEX.[241] Final fractional atomic co-ordinates and isotropic thermal parameters, bond distances and angles are given in Tables A4.2 and A4.3, respectively. Anisotropic temperature factors are given in Table A4.4 and hydrogen coordinates and isotropic temperature factor in Table A4.5.

Table A4.1 Crystal data and structure refinement for (**6**).

Identification code	97vol/dae
Empirical formula	$C_{41}\ H_{37}\ Ag\ O_2\ P_2$
Formula weight	731.52
Temperature	293(2)°K
Wavelength	0.70930 Å
Crystal system	Triclinic
Space group	$P\bar{1}$ (No.2)
Unit cell dimensions	a = 12.806(5)Å α = 66.26(3)°
	b = 12.996(4)Å β = 62.40(3)°
	c = 13.056(6)Å γ = 72.79(3)°
Volume	1746.6(12) $Å^3$
Z	2
Density (calculated)	1.391 Mg/m^3
Absorption coefficient	0.703 mm^{-1}
F(000)	752
Crystal size	0.3 x 0.3 x 0.3 mm
Theta range for data collection	2.01 to 23.93 °.
Index ranges	-14<=h<=0; -14<=k<=14; -14<=l<=13
Reflections collected	5758
Independent reflections	5477 [R(int) = 0.0174]
Refinement method	Full-matrix least-squares on F^2
Data / restraints / parameters	5466 / 2 / 435
Goodness-of-fit on F^2	1.061
Final R indices [$I>2\sigma(I)$]	R1 = 0.0324 wR2 = 0.0991
R indices (all data)	R1 = 0.0441 wR2 = 0.1109
Largest diff. peak and hole	0.441 and -0.332 $eÅ^{-3}$
Weighting scheme	calc $w=1/[\sigma^2(Fo^2)+(0.0693P)^2+0.8933P]$ where $P=(Fo^2+2Fc^2)/3$
Extinction coefficient	0.0023(7)
Extinction expression	$Fc^*=kFc[1+0.001xFc^2\lambda^3/\sin(2\theta)]^{-1/4}$

Table A4.2 Atomic coordinates (x 10^4) and equivalent isotropic displacement parameters ($Å^2$ x 10^3) for (**2**). U(eq) is defined as one third of the trace of the orthogonalized Uij tensor.

Atom	x	y	z	U(eq)
Ag(1)	1168(1)	7222(1)	7173(1)	42(1)
P(1)	2847(1)	8295(1)	6213(1)	37(1)
P(2)	-705(1)	7510(1)	8840(1)	38(1)
O(1)	1900(3)	5461(2)	6724(3)	64(1)
O(2)	911(4)	6715(3)	5685(4)	85(1)
C(1)	2370(3)	9808(3)	5644(3)	36(1)
C(2)	1629(4)	10131(3)	5029(4)	49(1)
C(3)	1207(4)	11266(4)	4609(4)	58(1)
C(4)	1516(4)	12075(4)	4795(4)	57(1)
C(5)	2268(4)	11767(3)	5389(4)	56(1)
C(6)	2689(3)	10632(3)	5816(4)	46(1)
C(7)	4130(3)	8001(3)	4899(3)	41(1)
C(8)	4743(3)	8837(3)	3922(4)	49(1)
C(9)	5729(4)	8556(4)	2960(4)	61(1)
C(10)	6092(4)	7461(5)	2976(5)	72(1)

C(11)	5489(5)	6639(5)	3936(6)	86(2)
C(12)	4487(4)	6890(4)	4897(5)	65(1)
C(13)	-508(3)	7589(3)	10104(3)	42(1)
C(14)	-921(4)	8542(4)	10475(4)	55(1)
C(15)	-659(5)	8591(5)	11373(5)	74(1)
C(16)	13(5)	7697(5)	11900(4)	72(1)
C(17)	410(4)	6742(5)	11544(4)	67(1)
C(18)	168(4)	6696(4)	10641(4)	56(1)
C(19)	-1642(3)	8842(3)	8433(3)	44(1)
C(20)	-2873(4)	8939(4)	8901(5)	61(1)
C(21)	-3527(4)	9965(4)	8549(6)	76(1)
C(22)	-2980(5)	10909(4)	7737(5)	71(1)
C(23)	-1770(5)	10824(4)	7277(5)	64(1)
C(24)	-1100(4)	9793(3)	7611(4)	52(1)
C(25)	-1688(3)	6443(3)	9510(3)	42(1)
C(26)	-2118(3)	5806(3)	10723(3)	45(1)
C(27)	-2889(4)	5027(4)	11146(4)	59(1)
C(28)	-3244(4)	4900(4)	10360(5)	67(1)
C(29)	-2805(5)	5512(4)	9145(5)	66(1)
C(30)	-2025(4)	6265(4)	8720(4)	58(1)
C(31)	3477(3)	8198(3)	7252(3)	43(1)
C(32)	4691(4)	8037(4)	6963(4)	58(1)
C(33)	5103(5)	7970(5)	7810(5)	73(1)
C(34)	4329(5)	8086(5)	8912(5)	74(1)
C(35)	3129(5)	8251(4)	9212(4)	69(1)
C(36)	2700(4)	8298(4)	8394(4)	55(1)
C(37)	1456(4)	5763(3)	5968(4)	49(1)
C(38)	1596(6)	4917(4)	5364(5)	75(1)
C(39)	1799(7)	5411(6)	4062(6)	94(2)
C(40)	3149(20)	5615(30)	3364(19)	144(11)
C(41)	3746(22)	6001(25)	2400(22)	138(10)
C(40A)	2853(18)	5998(15)	3098(24)	105(8)
C(41A)	3806(53)	5575(79)	2886(80)	322(53)

Table A4.3 Bond lengths [Å] and angles [°] for (**6**).

Ag(1)-O(1)	2.401(3)	C(7)-P(1)-Ag(1)	118.74(13)
Ag(1)-P(2)	2.433(2)	C(25)-P(2)-C(13)	105.8(2)
Ag(1)-P(1)	2.450(2)	C(25)-P(2)-C(19)	103.6(2)
Ag(1)-O(2)	2.464(4)	C(13)-P(2)-C(19)	103.1(2)
P(1)-C(31)	1.823(4)	C(25)-P(2)-Ag(1)	115.83(13)
P(1)-C(1)	1.824(4)	C(13)-P(2)-Ag(1)	113.01(12)
P(1)-C(7)	1.826(4)	C(19)-P(2)-Ag(1)	114.26(14)
P(2)-C(25)	1.819(4)	C(37)-O(1)-Ag(1)	93.5(2)
P(2)-C(13)	1.827(4)	C(37)-O(2)-Ag(1)	90.7(3)
P(2)-C(19)	1.827(4)	C(6)-C(1)-C(2)	119.0(3)
O(1)-C(37)	1.235(5)	C(6)-C(1)-P(1)	123.5(3)
O(2)-C(37)	1.230(5)	C(2)-C(1)-P(1)	117.5(3)
C(1)-C(6)	1.379(5)	C(3)-C(2)-C(1)	120.1(4)
C(1)-C(2)	1.387(5)	C(4)-C(3)-C(2)	120.5(4)
C(2)-C(3)	1.385(6)	C(3)-C(4)-C(5)	120.0(4)
C(3)-C(4)	1.365(7)	C(4)-C(5)-C(6)	119.8(4)
C(4)-C(5)	1.379(7)	C(1)-C(6)-C(5)	120.6(4)
C(5)-C(6)	1.387(6)	C(8)-C(7)-C(12)	119.3(4)
C(7)-C(8)	1.373(6)	C(8)-C(7)-P(1)	122.7(3)
C(7)-C(12)	1.380(6)	C(12)-C(7)-P(1)	118.1(3)
C(8)-C(9)	1.390(6)	C(7)-C(8)-C(9)	119.9(4)

C(9)-C(10)	1.354(7)	C(10)-C(9)-C(8)	120.6(4)
C(10)-C(11)	1.350(8)	C(11)-C(10)-C(9)	119.5(4)
C(11)-C(12)	1.384(7)	C(10)-C(11)-C(12)	121.5(5)
C(13)-C(18)	1.379(6)	C(7)-C(12)-C(11)	119.1(4)
C(13)-C(14)	1.381(6)	C(18)-C(13)-C(14)	118.6(4)
C(14)-C(15)	1.389(7)	C(18)-C(13)-P(2)	118.4(3)
C(15)-C(16)	1.370(8)	C(14)-C(13)-P(2)	122.8(3)
C(16)-C(17)	1.374(7)	C(13)-C(14)-C(15)	120.3(4)
C(17)-C(18)	1.375(6)	C(16)-C(15)-C(14)	120.5(4)
C(19)-C(24)	1.382(6)	C(15)-C(16)-C(17)	119.2(4)
C(19)-C(20)	1.387(6)	C(16)-C(17)-C(18)	120.5(4)
C(20)-C(21)	1.377(7)	C(17)-C(18)-C(13)	120.9(4)
C(21)-C(22)	1.375(8)	C(24)-C(19)-C(20)	118.5(4)
C(22)-C(23)	1.365(7)	C(24)-C(19)-P(2)	118.6(3)
C(23)-C(24)	1.385(6)	C(20)-C(19)-P(2)	122.9(3)
C(25)-C(26)	1.379(5)	C(21)-C(20)-C(19)	120.1(4)
C(25)-C(30)	1.403(6)	C(22)-C(21)-C(20)	121.0(5)
C(26)-C(27)	1.393(6)	C(23)-C(22)-C(21)	119.4(4)
C(27)-C(28)	1.378(7)	C(22)-C(23)-C(24)	120.2(4)
C(28)-C(29)	1.374(7)	C(23)-C(24)-C(19)	120.8(4)
C(29)-C(30)	1.376(7)	C(26)-C(25)-C(30)	118.3(4)
C(31)-C(36)	1.391(6)	C(26)-C(25)-P(2)	125.0(3)
C(31)-C(32)	1.390(6)	C(30)-C(25)-P(2)	116.7(3)
C(32)-C(33)	1.394(7)	C(25)-C(26)-C(27)	120.3(4)
C(33)-C(34)	1.356(8)	C(28)-C(27)-C(26)	120.3(4)
C(34)-C(35)	1.370(8)	C(29)-C(28)-C(27)	120.2(4)
C(35)-C(36)	1.384(6)	C(30)-C(29)-C(28)	119.7(4)
C(37)-C(38)	1.520(6)	C(29)-C(30)-C(25)	121.2(4)
C(38)-C(39)	1.478(8)	C(36)-C(31)-C(32)	118.1(4)
C(39)-C(40A)	1.50(2)	C(36)-C(31)-P(1)	118.3(3)
C(39)-C(40)	1.58(2)	C(32)-C(31)-P(1)	123.6(3)
C(40)-C(41)	1.12(3)	C(31)-C(32)-C(33)	120.2(5)
C(40A)-C(41A)	1.13(7)	C(34)-C(33)-C(32)	120.6(5)
		C(33)-C(34)-C(35)	120.1(5)
O(1)-Ag(1)-P(2)	122.60(10)	C(34)-C(35)-C(36)	120.2(5)
O(1)-Ag(1)-P(1)	107.96(10)	C(35)-C(36)-C(31)	120.7(4)
P(2)-Ag(1)-P(1)	126.23(4)	O(2)-C(37)-O(1)	122.9(4)
O(1)-Ag(1)-O(2)	52.84(11)	O(2)-C(37)-C(38)	119.0(4)
P(2)-Ag(1)-O(2)	112.49(11)	O(1)-C(37)-C(38)	118.2(4)
P(1)-Ag(1)-O(2)	111.89(12)	C(39)-C(38)-C(37)	114.9(5)
C(31)-P(1)-C(1)	104.0(2)	C(38)-C(39)-C(40A)	123.8(13)
C(31)-P(1)-C(7)	104.6(2)	C(38)-C(39)-C(40)	105.6(9)
C(1)-P(1)-C(7)	103.5(2)	C(41)-C(40)-C(39)	136(2)
C(31)-P(1)-Ag(1)	114.04(12)	C(41A)-C(40A)-C(39)	124(5)
C(1)-P(1)-Ag(1)	110.47(12)		

Table A4.4 Anisotropic displacement parameters ($Å^2$ x 10^3) for (**6**). The anisotropic displacement factor exponent takes the form: $-2\pi^2[h^2 a^* 2 U11 + ... + 2 h k a^* b^* U12]$

Atom	U11	U22	U33	U23	U13	U12
Ag(1)	41(1)	41(1)	45(1)	-17(1)	-14(1)	-6(1)
P(1)	35(1)	33(1)	43(1)	-13(1)	-15(1)	-4(1)
P(2)	40(1)	38(1)	36(1)	-13(1)	-13(1)	-6(1)
O(1)	95(2)	47(2)	67(2)	-16(1)	-51(2)	-3(2)
O(2)	103(3)	74(2)	114(3)	-53(2)	-79(3)	32(2)
C(1)	32(2)	35(2)	39(2)	-14(1)	-11(1)	-2(1)

C(2)	56(2)	48(2)	51(2)	-14(2)	-27(2)	-9(2)
C(3)	63(3)	60(3)	51(2)	-9(2)	-34(2)	1(2)
C(4)	58(2)	40(2)	54(2)	-9(2)	-18(2)	4(2)
C(5)	64(3)	39(2)	65(3)	-24(2)	-23(2)	-2(2)
C(6)	45(2)	40(2)	57(2)	-15(2)	-25(2)	-2(2)
C(7)	37(2)	42(2)	47(2)	-19(2)	-16(2)	-1(2)
C(8)	44(2)	47(2)	52(2)	-21(2)	-13(2)	-4(2)
C(9)	49(2)	70(3)	55(3)	-26(2)	-7(2)	-12(2)
C(10)	53(3)	83(4)	78(3)	-51(3)	-7(2)	-3(2)
C(11)	79(4)	58(3)	103(4)	-51(3)	-9(3)	4(3)
C(12)	67(3)	41(2)	71(3)	-29(2)	-6(2)	-7(2)
C(13)	37(2)	48(2)	38(2)	-14(2)	-10(2)	-11(2)
C(14)	66(3)	48(2)	51(2)	-22(2)	-24(2)	0(2)
C(15)	105(4)	70(3)	61(3)	-37(3)	-31(3)	-13(3)
C(16)	80(3)	97(4)	58(3)	-31(3)	-33(3)	-17(3)
C(17)	64(3)	83(3)	59(3)	-26(2)	-34(2)	3(2)
C(18)	56(2)	64(3)	55(2)	-29(2)	-26(2)	6(2)
C(19)	48(2)	40(2)	47(2)	-15(2)	-21(2)	-3(2)
C(20)	50(2)	54(2)	72(3)	-13(2)	-24(2)	-5(2)
C(21)	50(3)	64(3)	105(4)	-22(3)	-35(3)	6(2)
C(22)	80(3)	48(3)	95(4)	-25(3)	-53(3)	12(2)
C(23)	83(3)	40(2)	76(3)	-11(2)	-43(3)	-7(2)
C(24)	57(2)	45(2)	58(2)	-16(2)	-28(2)	-6(2)
C(25)	43(2)	38(2)	43(2)	-12(2)	-18(2)	-3(2)
C(26)	48(2)	41(2)	46(2)	-17(2)	-18(2)	-1(2)
C(27)	56(2)	49(2)	60(3)	-6(2)	-17(2)	-15(2)
C(28)	60(3)	46(2)	92(4)	-12(2)	-27(3)	-19(2)
C(29)	79(3)	62(3)	78(3)	-24(2)	-43(3)	-17(2)
C(30)	76(3)	56(2)	50(2)	-11(2)	-31(2)	-19(2)
C(31)	44(2)	33(2)	46(2)	-3(2)	-21(2)	-7(2)
C(32)	46(2)	63(3)	59(3)	-9(2)	-24(2)	-11(2)
C(33)	68(3)	76(3)	83(4)	-7(3)	-48(3)	-15(2)
C(34)	89(4)	83(3)	64(3)	-5(3)	-44(3)	-33(3)
C(35)	88(4)	75(3)	51(3)	-14(2)	-30(2)	-26(3)
C(36)	52(2)	63(3)	50(2)	-14(2)	-19(2)	-16(2)
C(37)	52(2)	44(2)	56(2)	-18(2)	-23(2)	-5(2)
C(38)	107(4)	63(3)	69(3)	-30(2)	-35(3)	-18(3)
C(39)	129(6)	97(4)	81(4)	-38(3)	-49(4)	-24(4)
C(40)	129(23)	174(26)	71(10)	18(13)	-53(13)	0(17)
C(41)	115(17)	194(20)	120(13)	-109(15)	24(12)	-72(15)
C(40A)	100(14)	55(9)	105(18)	-5(9)	-29(14)	15(8)
C(41A)	150(46)	436(111)	439(112)	-194(89)	-156(60)	30(54)

Table A4.5 Hydrogen coordinates (x 10^4) and isotropic displacement parameters (Å^2 x 10^3) for (**6**).

Atom	x	y	z	U(eq)
H(2)	1414(4)	9585(3)	4898(4)	59
H(3)	710(4)	11478(4)	4197(4)	70
H(4)	1219(4)	12834(4)	4522(4)	68
H(5)	2492(4)	12318(3)	5502(4)	67
H(6)	3190(3)	10425(3)	6223(4)	55
H(8)	4498(3)	9591(3)	3904(4)	58
H(9)	6142(4)	9124(4)	2300(4)	73
H(10)	6752(4)	7278(5)	2330(5)	86
H(11)	5753(5)	5886(5)	3952(6)	103
H(12)	4060(4)	6317(4)	5533(5)	78

H(14)	-1377(4)	9154(4)	10123(4)	65
H(15)	-941(5)	9235(5)	11619(5)	88
H(16)	198(5)	7735(5)	12492(4)	87
H(17)	845(4)	6122(5)	11915(4)	80
H(18)	465(4)	6054(4)	10391(4)	67
H(20)	-3256(4)	8309(4)	9453(5)	74
H(21)	-4352(4)	10022(4)	8864(6)	91
H(22)	-3431(5)	11598(4)	7504(5)	85
H(23)	-1395(5)	11461(4)	6736(5)	77
H(24)	-275(4)	9741(3)	7279(4)	62
H(26)	-1892(3)	5896(3)	11260(3)	54
H(27)	-3166(4)	4591(4)	11962(4)	71
H(28)	-3782(4)	4400(4)	10653(5)	81
H(29)	-3035(5)	5417(4)	8612(5)	79
H(30)	-1714(4)	6663(4)	7893(4)	69
H(32)	5230(4)	7973(4)	6204(4)	69
H(33)	5917(5)	7845(5)	7617(5)	87
H(34)	4613(5)	8053(5)	9464(5)	88
H(35)	2600(5)	8331(4)	9967(4)	82
H(36)	1884(4)	8397(4)	8610(4)	66
H(38A)	2259(6)	4338(4)	5448(5)	89
H(38B)	885(6)	4549(4)	5798(5)	89
H(39A)	1281(7)	6121(6)	3917(6)	112
H(39B)	1649(7)	4893(6)	3794(6)	112
H(40)	3543(20)	5344(30)	3886(19)	173
H(41A)	3452(22)	6302(25)	1792(22)	166
H(41B)	4537(22)	6023(25)	2206(22)	166
H(40A)	2716(18)	6752(15)	2649(24)	126
H(41C)	3969(53)	4822(79)	3321(80)	387
H(41D)	4426(53)	5980(79)	2278(80)	387

APPENDIX FIVE

Crystallographic data for (*O,O'*-Tiglato) *bis*(triphenylphosphine)silver(I) (9).

A crystal of approximate dimensions 0.3 x 0.3 x 0.25 mm was used for data collection.

Crystal data: C_{41} H_{37} Ag O_2 P_2, M = 731.52, Monoclinic, a = 10.616(2), b = 18.141(3), c = 18.628(3) Å, β = 103.23(2)°, U = 3492.3(10) Å^3, space group $P2_1/c$, Z = 4, D_c = 1.391 g.cm^{-3}, μ(Mo-K_α) = 0.703 mm^{-1}, F(000) = 1504. Crystallographic measurements were made at 293(2)°K on a CAD4 automatic four-circle diffractometer in the range $2.24<\theta<23.92°$. Data (5789 reflections) were corrected for Lorentz and polarization but not for absorption.

In the final least squares cycles all atoms were allowed to vibrate anisotropically. Hydrogen atoms were included at calculated positions where relevant except in the case of the proton attached to the olefinic carbon C(39), which was located and refined at a distance of 0.9 Å from the parent atom.

The solution of the structure (SHELX86)[82] and refinement (SHELX93)[83] converged to a conventional [i.e. based on 4272 reflections with $Fo>4\sigma(Fo)$] $R1$ = 0.0239 and $wR2$ = 0.0546. Goodness of fit = 1.047. The max. and min. residual densities were .337 and -.381eÅ^{-3} respectively. The asymmetric unit (shown in Fig. 2.19), along with the labelling scheme used was produced using ORTEX.[241] Final fractional atomic co-ordinates and isotropic thermal parameters, bond distances and angles are given in Tables A5.2 and A5.3, respectively. Anisotropic temperature factors are given in Table A5.4 and hydrogen coordinates and isotropic temperature factor in Table A5.5.

Table A5.1 Crystal data and structure refinement for (**9**).

Identification code	96dae7
Empirical formula	$C_{41} H_{37} Ag O_2 P_2$
Formula weight	731.52
Temperature	293(2)°K
Wavelength	0.70930 Å
Crystal system	Monoclinic
Space group	$P2_1/c$
Unit cell dimensions	a = 10.616(2)Å b = 18.141(3)Å β= 103.23(2)° c = 18.628(3)Å
Volume	3492.3(10) $Å^3$
Z	4
Density (calculated)	1.391 Mg/m^3
Absorption coefficient	0.703 mm^{-1}
F(000)	1504
Crystal size	0.3 x 0.3 x 0.25 mm
Theta range for data collection	2.24 to 23.92°
Index ranges	0<=h<=12; 0<=k<=20; -21<=l<=20
Reflections collected	5789
Independent reflections	5462 [R(int) = 0.0247]
Refinement method	Full-matrix least-squares on F^2
Data / restraints / parameters	5459 / 1 / 421
Goodness-of-fit on F^2	1.047
Final R indices [I>2σ(I)]	R1 = 0.0239 wR2 = 0.0546
R indices (all data)	R1 = 0.0460 wR2 = 0.0647
Largest diff. peak and hole	.337 and -.381 $eÅ^{-3}$
Weighting scheme	calc $w=1/[\sigma^2(Fo^2)+(0.0283P)^2+2.2795P]$ where $P=(Fo^2+2Fc^2)/3$
Extinction coefficient	0.0032(2)
Extinction expression	$Fc^*=kFc[1+0.001xFc^2\lambda^3/\sin(2\theta)]^{-1/4}$

Table A5.2 Atomic coordinates (x 10^4) and equivalent isotropic displacement parameters ($Å^2$ x 10^3) for (**9**). U(eq) is defined as one third of the trace of the orthogonalized Uij tensor.

Atom	x	y	z	U(eq)
Ag(1)	1380(1)	1982(1)	1210(1)	38(1)
P(1)	749(1)	3203(1)	757(1)	31(1)
P(2)	3521(1)	1452(1)	1738(1)	31(1)
O(1)	-153(2)	1047(1)	614(1)	44(1)
O(2)	10(2)	1233(1)	1800(1)	52(1)
C(1)	-432(2)	3697(1)	1147(1)	34(1)
C(2)	-1387(3)	4143(2)	729(2)	42(1)
C(3)	-2151(3)	4578(2)	1073(2)	57(1)
C(4)	-1963(3)	4574(2)	1825(2)	66(1)
C(5)	-1035(3)	4126(2)	2239(2)	65(1)
C(6)	-282(3)	3684(2)	1905(2)	50(1)
C(7)	2056(2)	3879(1)	860(1)	32(1)
C(8)	1929(3)	4606(1)	1057(2)	40(1)
C(9)	2938(3)	5099(2)	1088(2)	48(1)
C(10)	4072(3)	4876(2)	925(2)	53(1)
C(11)	4214(3)	4150(2)	737(2)	59(1)

C(12)	3218(3)	3654(2)	711(2)	47(1)
C(13)	3978(2)	1684(1)	2716(1)	35(1)
C(14)	2986(3)	1818(2)	3067(2)	55(1)
C(15)	3249(4)	2020(2)	3802(2)	71(1)
C(16)	4502(4)	2091(2)	4193(2)	64(1)
C(17)	5504(3)	1950(2)	3859(2)	51(1)
C(18)	5253(3)	1747(2)	3128(2)	43(1)
C(19)	4911(2)	1731(1)	1377(1)	36(1)
C(20)	5527(3)	2400(2)	1573(2)	49(1)
C(21)	6571(3)	2610(2)	1293(2)	64(1)
C(22)	6998(3)	2167(2)	813(2)	67(1)
C(23)	6391(3)	1516(2)	591(2)	66(1)
C(24)	5344(3)	1294(2)	875(2)	49(1)
C(25)	3590(2)	448(1)	1699(1)	33(1)
C(26)	4615(3)	49(2)	2115(2)	45(1)
C(27)	4664(3)	-706(2)	2034(2)	61(1)
C(28)	3700(3)	-1065(2)	1533(2)	63(1)
C(29)	2679(3)	-675(2)	1122(2)	54(1)
C(30)	2620(3)	82(2)	1205(2)	40(1)
C(31)	102(2)	3185(1)	-239(1)	31(1)
C(32)	296(3)	3753(2)	-701(1)	40(1)
C(33)	-136(3)	3692(2)	-1457(2)	46(1)
C(34)	-775(3)	3073(2)	-1759(2)	50(1)
C(35)	-984(3)	2510(2)	-1310(2)	57(1)
C(36)	-533(3)	2554(2)	-551(2)	45(1)
C(37)	-416(2)	878(1)	1218(1)	36(1)
C(38)	-1244(2)	213(2)	1259(2)	39(1)
C(39)	-1298(3)	-319(2)	771(2)	53(1)
C(40)	-1913(3)	189(2)	1889(2)	59(1)
C(41)	-2012(4)	-1040(2)	749(2)	84(1)

Table A5.3 Bond lengths [Å] and angles [°] for (**9**).

Ag(1)-P(1)	2.4099(7)	C(14)-C(15)	1.383(4)
Ag(1)-O(2)	2.430(2)	C(15)-C(16)	1.368(5)
Ag(1)-O(1)	2.436(2)	C(16)-C(17)	1.373(5)
Ag(1)-P(2)	2.4562(8)	C(17)-C(18)	1.376(4)
P(1)-C(1)	1.822(3)	C(19)-C(24)	1.381(4)
P(1)-C(31)	1.825(2)	C(19)-C(20)	1.388(4)
P(1)-C(7)	1.829(3)	C(20)-C(21)	1.381(4)
P(2)-C(13)	1.824(3)	C(21)-C(22)	1.357(5)
P(2)-C(25)	1.826(3)	C(22)-C(23)	1.363(5)
P(2)-C(19)	1.827(3)	C(23)-C(24)	1.395(4)
O(1)-C(37)	1.259(3)	C(25)-C(30)	1.383(4)
O(2)-C(37)	1.253(3)	C(25)-C(26)	1.385(4)
C(1)-C(6)	1.385(4)	C(26)-C(27)	1.380(4)
C(1)-C(2)	1.388(4)	C(27)-C(28)	1.380(5)
C(2)-C(3)	1.389(4)	C(28)-C(29)	1.371(5)
C(3)-C(4)	1.370(5)	C(29)-C(30)	1.385(4)
C(4)-C(5)	1.371(5)	C(31)-C(36)	1.385(4)
C(5)-C(6)	1.377(4)	C(31)-C(32)	1.388(3)
C(7)-C(8)	1.383(4)	C(32)-C(33)	1.382(4)
C(7)-C(12)	1.387(4)	C(33)-C(34)	1.365(4)
C(8)-C(9)	1.386(4)	C(34)-C(35)	1.370(4)
C(9)-C(10)	1.369(4)	C(35)-C(36)	1.387(4)
C(10)-C(11)	1.378(4)	C(37)-C(38)	1.505(4)
C(11)-C(12)	1.381(4)	C(38)-C(39)	1.318(4)

C(13)-C(14)	1.382(4)	C(38)-C(40)	1.504(4)
C(13)-C(18)	1.400(4)	C(39)-C(41)	1.508(4)
P(1)-Ag(1)-O(2)	121.64(5)	C(18)-C(13)-P(2)	124.7(2)
P(1)-Ag(1)-O(1)	112.16(5)	C(13)-C(14)-C(15)	120.8(3)
O(2)-Ag(1)-O(1)	53.86(6)	C(16)-C(15)-C(14)	120.2(3)
P(1)-Ag(1)-P(2)	131.11(2)	C(15)-C(16)-C(17)	120.0(3)
O(2)-Ag(1)-P(2)	101.24(5)	C(16)-C(17)-C(18)	120.3(3)
O(1)-Ag(1)-P(2)	111.77(5)	C(17)-C(18)-C(13)	120.5(3)
C(1)-P(1)-C(31)	106.30(11)	C(24)-C(19)-C(20)	118.0(3)
C(1)-P(1)-C(7)	101.67(11)	C(24)-C(19)-P(2)	120.8(2)
C(31)-P(1)-C(7)	102.61(11)	C(20)-C(19)-P(2)	121.1(2)
C(1)-P(1)-Ag(1)	118.36(8)	C(21)-C(20)-C(19)	120.9(3)
C(31)-P(1)-Ag(1)	110.42(8)	C(22)-C(21)-C(20)	120.2(3)
C(7)-P(1)-Ag(1)	115.88(8)	C(21)-C(22)-C(23)	120.5(3)
C(13)-P(2)-C(25)	105.39(12)	C(22)-C(23)-C(24)	119.9(3)
C(13)-P(2)-C(19)	104.59(12)	C(19)-C(24)-C(23)	120.6(3)
C(25)-P(2)-C(19)	102.57(12)	C(30)-C(25)-C(26)	119.4(2)
C(13)-P(2)-Ag(1)	108.70(9)	C(30)-C(25)-P(2)	118.3(2)
C(25)-P(2)-Ag(1)	114.61(9)	C(26)-C(25)-P(2)	122.1(2)
C(19)-P(2)-Ag(1)	119.70(8)	C(27)-C(26)-C(25)	120.1(3)
C(37)-O(1)-Ag(1)	91.3(2)	C(28)-C(27)-C(26)	120.1(3)
C(37)-O(2)-Ag(1)	91.7(2)	C(29)-C(28)-C(27)	120.3(3)
C(6)-C(1)-C(2)	118.7(2)	C(28)-C(29)-C(30)	119.9(3)
C(6)-C(1)-P(1)	118.0(2)	C(25)-C(30)-C(29)	120.2(3)
C(2)-C(1)-P(1)	123.0(2)	C(36)-C(31)-C(32)	118.6(2)
C(1)-C(2)-C(3)	120.1(3)	C(36)-C(31)-P(1)	118.4(2)
C(4)-C(3)-C(2)	120.3(3)	C(32)-C(31)-P(1)	122.8(2)
C(3)-C(4)-C(5)	119.7(3)	C(33)-C(32)-C(31)	120.7(3)
C(4)-C(5)-C(6)	120.5(3)	C(34)-C(33)-C(32)	120.2(3)
C(5)-C(6)-C(1)	120.5(3)	C(33)-C(34)-C(35)	119.7(3)
C(8)-C(7)-C(12)	118.6(2)	C(34)-C(35)-C(36)	120.9(3)
C(8)-C(7)-P(1)	123.4(2)	C(31)-C(36)-C(35)	119.8(3)
C(12)-C(7)-P(1)	118.0(2)	O(2)-C(37)-O(1)	122.6(2)
C(7)-C(8)-C(9)	120.4(3)	O(2)-C(37)-C(38)	117.9(2)
C(10)-C(9)-C(8)	120.7(3)	O(1)-C(37)-C(38)	119.5(2)
C(9)-C(10)-C(11)	119.4(3)	C(39)-C(38)-C(40)	124.3(3)
C(10)-C(11)-C(12)	120.3(3)	C(39)-C(38)-C(37)	119.1(3)
C(11)-C(12)-C(7)	120.6(3)	C(40)-C(38)-C(37)	116.6(2)
C(14)-C(13)-C(18)	118.2(3)	C(38)-C(39)-C(41)	126.6(3)
C(14)-C(13)-P(2)	117.1(2)		

Table A5.4 Anisotropic displacement parameters ($Å^2$ x 10^3) for (9). The anisotropic displacement factor exponent takes the form: $-2\pi^2[h^2\ a^*\ 2\ U11 + ... + 2\ h\ k\ a^*\ b^*\ U12]$

Atom	U11	U22	U33	U23	U13	U12
Ag(1)	37(1)	31(1)	43(1)	6(1)	7(1)	1(1)
P(1)	32(1)	27(1)	33(1)	2(1)	7(1)	0(1)
P(2)	31(1)	28(1)	36(1)	2(1)	9(1)	0(1)
O(1)	50(1)	47(1)	37(1)	2(1)	14(1)	-10(1)
O(2)	59(1)	60(1)	40(1)	-12(1)	19(1)	-21(1)
C(1)	35(1)	30(1)	39(2)	-2(1)	14(1)	-7(1)
C(2)	40(2)	41(2)	49(2)	6(1)	17(1)	4(1)
C(3)	48(2)	46(2)	86(3)	4(2)	30(2)	8(2)
C(4)	64(2)	57(2)	92(3)	-21(2)	49(2)	-5(2)
C(5)	69(2)	82(3)	53(2)	-21(2)	33(2)	-16(2)

C(6)	49(2)	61(2)	41(2)	-2(2)	15(1)	-2(2)
C(7)	30(1)	32(1)	32(1)	0(1)	3(1)	0(1)
C(8)	37(1)	37(2)	47(2)	-4(1)	10(1)	0(1)
C(9)	48(2)	34(2)	58(2)	-7(1)	5(1)	-6(1)
C(10)	41(2)	50(2)	67(2)	-3(2)	8(2)	-16(1)
C(11)	37(2)	59(2)	84(2)	-9(2)	21(2)	-5(2)
C(12)	42(2)	38(2)	64(2)	-7(1)	17(1)	-1(1)
C(13)	40(2)	29(1)	37(1)	2(1)	11(1)	-2(1)
C(14)	48(2)	70(2)	48(2)	-8(2)	16(1)	-12(2)
C(15)	67(2)	100(3)	52(2)	-19(2)	28(2)	-17(2)
C(16)	82(2)	72(2)	40(2)	-12(2)	16(2)	-25(2)
C(17)	55(2)	45(2)	46(2)	3(1)	-1(1)	-11(2)
C(18)	41(2)	38(2)	47(2)	2(1)	7(1)	2(1)
C(19)	31(1)	36(1)	41(2)	10(1)	8(1)	4(1)
C(20)	50(2)	42(2)	57(2)	5(1)	16(2)	-7(1)
C(21)	48(2)	67(2)	78(2)	17(2)	14(2)	-17(2)
C(22)	46(2)	79(3)	82(3)	34(2)	28(2)	2(2)
C(23)	69(2)	73(2)	67(2)	17(2)	39(2)	19(2)
C(24)	53(2)	48(2)	52(2)	8(1)	23(2)	3(2)
C(25)	35(1)	30(1)	36(1)	4(1)	14(1)	0(1)
C(26)	43(2)	37(2)	53(2)	5(1)	8(1)	2(1)
C(27)	62(2)	41(2)	81(2)	18(2)	20(2)	15(2)
C(28)	79(2)	30(2)	89(3)	-7(2)	35(2)	-2(2)
C(29)	60(2)	41(2)	65(2)	-15(2)	21(2)	-10(2)
C(30)	41(2)	37(2)	43(2)	-3(1)	13(1)	-1(1)
C(31)	30(1)	30(1)	33(1)	1(1)	9(1)	3(1)
C(32)	45(2)	32(1)	41(2)	3(1)	8(1)	-1(1)
C(33)	51(2)	46(2)	41(2)	10(1)	12(1)	3(1)
C(34)	55(2)	61(2)	34(2)	-2(1)	8(1)	-5(2)
C(35)	70(2)	54(2)	46(2)	-13(2)	11(2)	-23(2)
C(36)	53(2)	42(2)	40(2)	-1(1)	14(1)	-14(1)
C(37)	29(1)	39(2)	39(2)	1(1)	10(1)	2(1)
C(38)	34(1)	45(2)	37(1)	3(1)	6(1)	-4(1)
C(39)	58(2)	51(2)	48(2)	-3(2)	9(2)	-14(2)
C(40)	56(2)	67(2)	59(2)	3(2)	24(2)	-12(2)
C(41)	104(3)	57(2)	89(3)	-13(2)	21(2)	-31(2)

Table A5.5 Hydrogen coordinates (x 10^4) and isotropic displacement parameters (Å^2 x 10^3) for (**9**).

Atom	x	y	z	U(eq)
H(2)	-1516(3)	4150(2)	218(2)	51
H(3)	-2793(3)	4874(2)	791(2)	69
H(4)	-2463(3)	4874(2)	2055(2)	79
H(5)	-913(3)	4120(2)	2750(2)	78
H(6)	332(3)	3374(2)	2190(2)	60
H(8)	1164(3)	4765(1)	1169(2)	48
H(9)	2844(3)	5586(2)	1221(2)	57
H(10)	4741(3)	5210(2)	940(2)	64
H(11)	4983(3)	3995(2)	627(2)	70
H(12)	3329(3)	3164(2)	593(2)	57
H(14)	2132(3)	1772(2)	2805(2)	66
H(15)	2573(4)	2107(2)	4032(2)	85
H(16)	4675(4)	2236(2)	4685(2)	77
H(17)	6354(3)	1991(2)	4128(2)	61
H(18)	5937(3)	1652(2)	2906(2)	51
H(20)	5234(3)	2711(2)	1897(2)	59

H(21)	6982(3)	3057(2)	1435(2)	77
H(22)	7710(3)	2308(2)	633(2)	81
H(23)	6674(3)	1220(2)	252(2)	79
H(24)	4934(3)	849(2)	725(2)	59
H(26)	5270(3)	291(2)	2449(2)	54
H(27)	5348(3)	-973(2)	2317(2)	73
H(28)	3742(3)	-1572(2)	1475(2)	76
H(29)	2028(3)	-919(2)	788(2)	65
H(30)	1926(3)	345(2)	928(2)	48
H(32)	721(3)	4179(2)	-500(1)	48
H(33)	9(3)	4074(2)	-1761(2)	55
H(34)	-1068(3)	3033(2)	-2268(2)	60
H(35)	-1435(3)	2093(2)	-1516(2)	69
H(36)	-656(3)	2162(2)	-252(2)	53
H(39)	-803(27)	-252(17)	382(15)	63
H(40A)	-2265(19)	666(4)	1950(8)	88
H(40B)	-1302(6)	53(12)	2333(3)	88
H(40C)	-2599(14)	-167(9)	1784(6)	88
H(41A)	-1973(24)	-1303(7)	307(8)	125
H(41B)	-2899(8)	-946(2)	756(16)	125
H(41C)	-1617(17)	-1331(7)	1171(9)	125

APPENDIX SIX

Crystallographic data for (o-cresolato-*O*) *tris*(triphenylphosphine)silver(I).o-cresol.toluene solvate (17).

A crystal of approximate dimensions 0.35 x 0.35 x 0.3 mm was used for data collection.

Crystal data: $C_{75}H_{68}AgO_2P_3$, M = 1202.07, Triclinic, a = 13.347, b = 14.991, c = 18.012 Å , α = 81.65, β = 74.42, γ = 65.27°, U = 3150.9 Å^3, space group $P\bar{1}$ (No.2), Z = 2, D_c = 1.267 g.cm^{-3}, μ(Mo-K_α) = 0.442 mm^{-1}, F(000) = 1252. Crystallographic measurements were made at 293(2)°K on a CAD4 automatic four-circle diffractometer in the range 2.30<θ<23.92°. Data (10336 reflections) were corrected for Lorentz and polarization but not for absorption.

The asymmetric unit in this crystal structure was seen to contain one molecule of the silver alkoxide complex, one molecule of *ortho*-cresol and one disordered solvent molecule of recrystallisation (toluene). Hydrogen bonding was noted between the alkoxide oxygen (O1) and the phenolic proton H(2A) of the cresol molecule. [O(1)-O(2), 2.565(9); H(2A)-O(1), 1.59(4)Å: O(2)-H(2A)-O(1), 170(10)°]

Solvent disorder was extreme, and difficult to model. However, after exhaustive attempts, the most satisfactory refinement was achieved by 'mopping-up' the solvent electron density as 2 rigid phenyl groups in the occupancy ratio of 52:48 for partial carbons C(69)-C(74) and C(75)-C(80), respectively. Unfortunately, it was impossible to convincingly locate and refine the associated partial methyl carbons of the toluene.

In the final least squares cycles all atoms were allowed to vibrate anisotropically except for the carbons in the solvent region of the electron density map [C(69)-C(80)]. Larger than average thermal motion of the atoms of both cresol fragments may be symptomatic of some positional disorder in these groups. Phenyl rings were treated as rigid hexagons throughout. Hydrogen atoms were included at calculated positions where relevant in the alkoxide and cresol moieties, except for H(2A), which was located in a difference Fourier map based on low Bragg data, and subsequently refined at a distance of 0.98Å from O(2). Because of solvent electron density smearing, hydrogens were not included in this area.

The solution of the structure (SHELX86)[82] and refinement (SHELX93)[83] converged to a conventional [i.e. based on 5532 reflections with $Fo>4\sigma(Fo)$] *R1* = 0.0693 and *wR2* = 0.1457. Goodness of fit = 1.066. The max. and min. residual densities were 0.833 and -0.564eÅ^{-3} respectively. The asymmetric unit (shown in Fig. 3.5), along with the labelling scheme used was produced using ORTEX.[241] Final fractional atomic co-ordinates and isotropic thermal parameters, bond distances and angles are given in Tables A6.2 and A6.3, respectively. Anisotropic temperature factors are given in Table A6.4 and hydrogen coordinates and isotropic temperature factor in Table A.6.5.

Table A6.1 Crystal data and structure refinement for (**17**).

Identification code	97vo3/dae
Empirical formula	$C_{75}H_{68}AgO_2P_3$
Formula weight	1202.07
Temperature	293(2) K
Wavelength	0.70930 Å
Crystal system	Triclinic
Space group	$P\bar{1}$ (No.2)
Unit cell dimensions	a = 13.347Å α= 81.65°
	b = 14.991Å β= 74.42°
	c = 18.012Å γ= 65.27°
Volume	3150.9 Å^3
Z	2
Density (calculated)	1.267 Mg/m^3
Absorption coefficient	0.442 mm^{-1}
F(000)	1252
Crystal size	0.35 x 0.35 x 0.3 mm
Theta range for data collection	2.30 to 23.92 °.
Index ranges	0<=h<=15; -15<=k<=17; -19<=l<=20
Reflections collected	10336
Independent reflections	9853 [R(int) = 0.0412]
Refinement method	Full-matrix least-squares on F^2
Data / restraints / parameters	9816 / 1 / 554
Goodness-of-fit on F^2	1.066
Final R indices [I>2σ(I)]	R1 = 0.0693 wR2 = 0.1457
R indices (all data)	R1 = 0.1606 wR2 = 0.1953
Largest diff. peak and hole	0.833 and -0.564 eÅ^{-3}
Weighting scheme	calc $w=1/[\sigma^2(Fo^2)+(0.0907P)^2+1.9303P]$ where $P=(Fo^2+2Fc^2)/3$
Extinction coefficient	0.0000(5)
Extinction expression	$Fc^*=kFc[1+0.001xFc^2\lambda^3/\sin(2\theta)]^{-1/4}$

Table A6.2 Atomic coordinates (x 10^4) and equivalent isotropic displacement parameters ($Å^2$ x 10^3) for (**17**). U(eq) is defined as one third of the trace of the orthogonalized Uij tensor.

Atom	x	y	z	U(eq)
Ag(1)	2643(1)	7578(1)	7618(1)	48(1)
P(1)	4827(2)	6854(1)	7260(1)	46(1)
P(2)	1899(2)	6988(2)	8962(1)	51(1)
P(3)	1700(2)	7550(1)	6575(1)	47(1)
O(1)	2319(5)	9244(4)	7748(3)	69(2)
O(2)	3483(6)	9729(5)	8414(4)	89(2)
C(1)	5507(5)	6815(5)	8023(3)	61(2)
C(2)	6168(8)	7350(6)	7948(5)	141(6)
C(3)	6669(10)	7316(8)	8541(6)	229(12)
C(4)	6510(9)	6749(8)	9209(5)	155(7)
C(5)	5850(7)	6215(6)	9284(3)	106(4)
C(6)	5348(5)	6248(5)	8691(4)	79(3)
C(7)	5426(4)	7539(3)	6479(3)	49(2)
C(8)	6385(4)	7095(3)	5902(3)	64(2)
C(9)	6810(4)	7669(5)	5342(3)	81(3)
C(10)	6276(5)	8688(4)	5358(3)	80(3)
C(11)	5318(5)	9132(3)	5934(4)	80(3)
C(12)	4893(4)	8557(3)	6495(3)	64(2)
C(13)	5536(4)	5569(3)	6960(3)	52(2)
C(14)	6583(4)	4938(4)	7105(3)	66(2)
C(15)	7065(4)	3967(3)	6886(4)	78(3)
C(16)	6500(5)	3628(3)	6524(4)	82(3)
C(17)	5454(5)	4260(4)	6380(4)	84(3)
C(18)	4972(4)	5231(4)	6598(3)	69(2)
C(19)	2536(5)	7127(4)	9686(3)	59(2)
C(20)	2790(6)	7950(4)	9607(3)	74(2)
C(21)	3239(6)	8122(5)	10158(4)	96(3)
C(22)	3434(6)	7471(6)	10787(4)	107(4)
C(23)	3180(7)	6647(5)	10867(3)	98(3)
C(24)	2731(6)	6475(4)	10316(3)	78(3)
C(25)	375(4)	7540(5)	9405(3)	64(2)
C(26)	-35(6)	7843(6)	10161(3)	102(4)
C(27)	-1196(6)	8293(6)	10461(4)	129(5)
C(28)	-1948(4)	8439(6)	10006(6)	115(4)
C(29)	-1538(5)	8136(6)	9250(5)	123(5)
C(30)	-376(6)	7686(6)	8949(3)	91(3)
C(31)	2210(4)	5665(3)	8993(3)	54(2)
C(32)	1446(4)	5259(4)	9398(3)	79(3)
C(33)	1716(5)	4265(4)	9350(4)	88(3)
C(34)	2748(5)	3676(3)	8896(4)	74(2)
C(35)	3512(4)	4082(4)	8492(3)	79(3)
C(36)	3243(4)	5077(4)	8540(3)	70(2)
C(37)	2156(4)	8122(4)	5654(2)	49(2)
C(38)	3299(4)	7954(4)	5430(3)	64(2)
C(39)	3711(4)	8375(5)	4743(3)	79(3)
C(40)	2980(5)	8965(4)	4279(3)	81(3)
C(41)	1837(5)	9133(4)	4503(3)	86(3)
C(42)	1425(3)	8712(4)	5190(3)	70(2)
C(43)	2078(5)	6292(3)	6322(3)	53(2)
C(44)	2484(6)	6002(4)	5562(2)	82(3)
C(45)	2791(7)	5032(4)	5400(3)	109(4)
C(46)	2691(6)	4351(3)	5996(4)	86(3)

C(47)	2285(5)	4641(3)	6756(3)	74(2)
C(48)	1978(5)	5612(4)	6919(2)	60(2)
C(49)	148(3)	8084(4)	6744(3)	53(2)
C(50)	-458(4)	8904(4)	7195(3)	65(2)
C(51)	-1635(4)	9328(4)	7342(3)	79(3)
C(52)	-2206(3)	8932(5)	7037(4)	83(3)
C(53)	-1600(5)	8112(5)	6586(4)	96(3)
C(54)	-423(5)	7688(4)	6439(3)	80(3)
C(55)	1422(6)	9912(5)	7551(6)	79(3)
C(56)	401(8)	10374(7)	8074(6)	136(6)
C(57)	-525(6)	11072(7)	7812(9)	221(15)
C(58)	-430(9)	11308(6)	7028(10)	203(14)
C(59)	591(11)	10846(7)	6506(7)	219(12)
C(60)	1517(8)	10148(7)	6767(6)	147(7)
C(61)	278(17)	10129(14)	8817(12)	175(8)
C(62)	3816(6)	10444(5)	8037(4)	71(2)
C(63)	3330(6)	11008(6)	7442(4)	95(3)
C(64)	3674(9)	11743(5)	7060(4)	126(5)
C(65)	4503(9)	11915(6)	7273(6)	132(5)
C(66)	4988(6)	11352(7)	7868(6)	120(5)
C(67)	4645(6)	10616(6)	8249(4)	102(3)
C(68)	5174(12)	9975(9)	8853(7)	170(7)
C(69)	9439(7)	4884(8)	6208(6)	138(11)
C(70)	9089(7)	5268(8)	6936(6)	144(12)
C(71)	9432(8)	4663(8)	7560(6)	184(15)
C(72)	10126(8)	3673(8)	7458(6)	214(22)
C(73)	10476(8)	3289(8)	6730(6)	142(11)
C(74)	10132(7)	3894(8)	6106(6)	173(14)
C(75)	9864(8)	3838(8)	8192(6)	148(12)
C(76)	9380(7)	4858(8)	8193(6)	130(11)
C(77)	9158(7)	5401(8)	7519(6)	148(12)
C(78)	9418(7)	4924(8)	6843(6)	115(10)
C(79)	9902(8)	3904(8)	6842(6)	132(11)
C(80)	10125(8)	3361(8)	7516(6)	192(20)

Table A6.3 Bond lengths [Å] and angles [°] for (**17**).

Ag(1)-O(1)	2.386(5)	C(31)-P(2)-Ag(1)	111.3(2)
Ag(1)-P(2)	2.539(2)	C(37)-P(3)-C(43)	103.1(2)
Ag(1)-P(3)	2.540(2)	C(37)-P(3)-C(49)	103.8(2)
Ag(1)-P(1)	2.577(2)	C(43)-P(3)-C(49)	102.6(3)
P(1)-C(1)	1.823(5)	C(37)-P(3)-Ag(1)	113.9(2)
P(1)-C(7)	1.826(4)	C(43)-P(3)-Ag(1)	111.5(2)
P(1)-C(13)	1.842(4)	C(49)-P(3)-Ag(1)	120.1(2)
P(2)-C(19)	1.814(5)	C(55)-O(1)-Ag(1)	116.4(4)
P(2)-C(25)	1.836(5)	C(2)-C(1)-P(1)	121.0(4)
P(2)-C(31)	1.843(4)	C(6)-C(1)-P(1)	119.0(4)
P(3)-C(37)	1.828(4)	C(8)-C(7)-P(1)	123.5(3)
P(3)-C(43)	1.829(4)	C(12)-C(7)-P(1)	116.5(3)
P(3)-C(49)	1.836(4)	C(14)-C(13)-P(1)	122.3(3)
O(1)-C(55)	1.297(8)	C(18)-C(13)-P(1)	117.6(3)
O(2)-C(62)	1.354(8)	C(20)-C(19)-P(2)	117.0(3)
C(56)-C(61)	1.32(2)	C(24)-C(19)-P(2)	123.0(3)
C(67)-C(68)	1.466(12)	C(26)-C(25)-P(2)	122.1(4)
		C(30)-C(25)-P(2)	117.9(4)
O(1)-Ag(1)-P(2)	105.2(2)	C(32)-C(31)-P(2)	123.6(3)
O(1)-Ag(1)-P(3)	107.8(2)	C(36)-C(31)-P(2)	116.3(3)
P(2)-Ag(1)-P(3)	116.41(7)	C(38)-C(37)-P(3)	116.4(3)
O(1)-Ag(1)-P(1)	98.36(14)	C(42)-C(37)-P(3)	123.6(3)

P(2)-Ag(1)-P(1)	111.08(7)	C(44)-C(43)-P(3)	122.0(3)
P(3)-Ag(1)-P(1)	115.73(6)	C(48)-C(43)-P(3)	117.9(3)
C(1)-P(1)-C(7)	102.6(3)	C(50)-C(49)-P(3)	118.1(3)
C(1)-P(1)-C(13)	101.8(3)	C(54)-C(49)-P(3)	121.9(3)
C(7)-P(1)-C(13)	104.8(2)	O(1)-C(55)-C(56)	123.7(8)
C(1)-P(1)-Ag(1)	115.8(2)	O(1)-C(55)-C(60)	116.3(8)
C(7)-P(1)-Ag(1)	113.8(2)	C(61)-C(56)-C(55)	121.0(12)
C(13)-P(1)-Ag(1)	116.2(2)	C(61)-C(56)-C(57)	119.0(12)
C(19)-P(2)-C(25)	102.9(3)	O(2)-C(62)-C(63)	120.4(6)
C(19)-P(2)-C(31)	105.1(3)	O(2)-C(62)-C(67)	119.6(6)
C(25)-P(2)-C(31)	103.2(3)	C(66)-C(67)-C(68)	121.7(9)
C(19)-P(2)-Ag(1)	113.5(2)	C(62)-C(67)-C(68)	118.3(9)
C(25)-P(2)-Ag(1)	119.3(2)		

Table A6.4 Anisotropic displacement parameters ($Å^2$ x 10^3) for (**17**). The anisotropic displacement factor exponent takes the form: $-2\pi^2[h^2 a^* 2 U11 + ... + 2 h k a^* b^* U12]$

Atom	U11	U22	U33	U23	U13	U12
Ag(1)	50(1)	48(1)	46(1)	-2(1)	-9(1)	-20(1)
P(1)	39(1)	46(1)	50(1)	-3(1)	-7(1)	-15(1)
P(2)	51(1)	59(1)	41(1)	-1(1)	-3(1)	-24(1)
P(3)	50(1)	51(1)	46(1)	1(1)	-15(1)	-24(1)
O(1)	63(4)	49(3)	96(4)	-17(3)	-22(3)	-18(3)
O(2)	111(5)	91(5)	80(4)	10(4)	-31(4)	-54(4)
C(1)	68(5)	52(5)	54(5)	-7(4)	-21(4)	-11(4)
C(2)	219(16)	155(12)	137(11)	59(9)	-112(12)	-138(13)
C(3)	395(32)	245(21)	246(21)	126(18)	-265(24)	-246(23)
C(4)	209(18)	156(14)	134(13)	9(10)	-119(13)	-63(13)
C(5)	92(8)	119(9)	62(6)	1(6)	-30(6)	8(7)
C(6)	69(6)	99(7)	58(6)	4(5)	-17(5)	-22(5)
C(7)	44(4)	56(5)	49(4)	-1(3)	-9(3)	-24(4)
C(8)	61(5)	67(5)	66(5)	-13(4)	1(4)	-33(4)
C(9)	73(6)	110(8)	67(6)	-14(5)	10(5)	-54(6)
C(10)	91(7)	91(7)	70(6)	18(5)	-22(6)	-52(6)
C(11)	81(7)	59(5)	98(7)	22(5)	-25(6)	-30(5)
C(12)	55(5)	58(5)	71(5)	9(4)	-8(4)	-23(4)
C(13)	43(4)	52(4)	53(4)	2(3)	3(3)	-20(4)
C(14)	56(5)	50(5)	79(6)	-7(4)	-19(4)	-5(4)
C(15)	69(6)	62(6)	79(6)	-9(5)	-16(5)	-1(5)
C(16)	94(8)	48(5)	81(6)	-15(5)	11(6)	-21(5)
C(17)	75(6)	73(6)	109(8)	-31(6)	-2(6)	-38(5)
C(18)	55(5)	65(6)	90(6)	-7(5)	-18(5)	-26(4)
C(19)	53(5)	65(5)	47(5)	-10(4)	-6(4)	-14(4)
C(20)	86(6)	66(6)	76(6)	-4(5)	-19(5)	-35(5)
C(21)	108(8)	83(7)	109(8)	-24(6)	-40(7)	-33(6)
C(22)	119(9)	115(9)	91(8)	-24(7)	-47(7)	-30(8)
C(23)	116(9)	112(9)	65(6)	8(6)	-38(6)	-38(7)
C(24)	90(7)	86(7)	61(6)	8(5)	-24(5)	-38(6)
C(25)	52(5)	64(5)	69(6)	5(4)	-4(4)	-24(4)
C(26)	67(7)	146(10)	73(7)	-42(7)	11(5)	-26(6)
C(27)	79(8)	149(12)	124(10)	-49(9)	33(8)	-34(8)
C(28)	71(8)	92(8)	143(12)	14(8)	10(8)	-22(6)
C(29)	54(7)	157(12)	146(12)	35(10)	-32(7)	-39(7)
C(30)	71(7)	117(8)	81(7)	10(6)	-23(6)	-33(6)
C(31)	60(5)	64(5)	37(4)	-3(3)	-5(4)	-26(4)

C(32)	65(6)	75(6)	82(6)	-3(5)	11(5)	-31(5)
C(33)	91(7)	72(6)	97(7)	7(5)	0(6)	-46(6)
C(34)	90(7)	68(6)	69(6)	7(5)	-22(5)	-37(5)
C(35)	91(7)	61(6)	69(6)	-9(5)	-2(5)	-23(5)
C(36)	76(6)	65(6)	64(5)	-7(4)	4(5)	-33(5)
C(37)	61(5)	50(4)	46(4)	1(3)	-18(4)	-28(4)
C(38)	54(5)	81(6)	61(5)	7(4)	-20(4)	-29(4)
C(39)	77(6)	102(7)	65(6)	17(5)	-12(5)	-51(6)
C(40)	98(8)	70(6)	67(6)	14(5)	-5(6)	-41(6)
C(41)	89(7)	84(7)	70(6)	29(5)	-27(5)	-23(6)
C(42)	60(5)	78(6)	63(5)	12(5)	-17(4)	-21(5)
C(43)	55(5)	58(5)	49(4)	1(4)	-15(4)	-25(4)
C(44)	137(9)	63(6)	57(5)	1(4)	-17(5)	-53(6)
C(45)	179(12)	87(7)	67(6)	-12(6)	-4(7)	-72(8)
C(46)	117(8)	55(5)	95(7)	-16(5)	-29(6)	-34(6)
C(47)	88(6)	65(6)	86(7)	12(5)	-29(5)	-45(5)
C(48)	68(5)	57(5)	57(5)	0(4)	-15(4)	-26(4)
C(49)	55(5)	66(5)	53(4)	8(4)	-21(4)	-36(4)
C(50)	57(5)	58(5)	79(6)	-7(4)	-12(4)	-24(4)
C(51)	58(6)	71(6)	102(7)	3(5)	-14(5)	-23(5)
C(52)	59(6)	77(7)	109(8)	34(6)	-25(6)	-34(5)
C(53)	63(6)	105(8)	138(10)	-4(7)	-40(6)	-41(6)
C(54)	63(6)	81(6)	104(7)	-15(5)	-27(5)	-29(5)
C(55)	66(6)	39(5)	143(9)	-2(6)	-53(7)	-15(5)
C(56)	79(9)	90(10)	251(20)	-76(12)	-37(12)	-24(8)
C(57)	135(16)	110(13)	442(43)	-121(19)	-130(21)	1(12)
C(58)	99(12)	69(9)	445(44)	-81(16)	-113(18)	13(8)
C(59)	340(33)	106(13)	318(29)	46(16)	-221(29)	-119(18)
C(60)	167(13)	70(8)	265(20)	22(10)	-165(15)	-45(8)
C(61)	168(16)	147(15)	220(20)	-45(15)	10(16)	-93(13)
C(62)	71(6)	65(6)	82(6)	-22(5)	0(5)	-36(5)
C(63)	106(8)	75(7)	95(8)	-14(6)	-8(7)	-33(6)
C(64)	166(13)	96(9)	119(10)	-1(7)	-3(9)	-73(9)
C(65)	143(13)	104(10)	143(13)	-43(9)	38(10)	-76(10)
C(66)	110(10)	111(10)	140(12)	-63(9)	31(9)	-64(9)
C(67)	82(7)	113(9)	107(9)	-41(7)	-5(7)	-34(7)
C(68)	123(12)	240(20)	139(13)	-53(13)	-61(10)	-32(12)

Table A6.5 Hydrogen coordinates (x 10^4) and isotropic displacement parameters (Å^2 x 10^3) for (**17**).

Atom	x	y	z	U(eq)
H(2A)	3120(82)	9489(73)	8128(53)	107
H(2)	6274(12)	7729(9)	7502(6)	169
H(3)	7111(14)	7674(11)	8491(9)	275
H(4)	6846(12)	6727(11)	9606(6)	186
H(5)	5744(10)	5835(8)	9731(4)	128
H(6)	4906(9)	5890(8)	8741(6)	95
H(8)	6741(6)	6413(3)	5892(5)	77
H(9)	7451(6)	7372(6)	4956(4)	97
H(10)	6561(7)	9073(6)	4983(4)	96
H(11)	4961(7)	9814(3)	5945(5)	96
H(12)	4252(5)	8854(4)	6880(4)	77
H(14)	6961(6)	5164(5)	7347(5)	79
H(15)	7765(5)	3545(5)	6983(5)	94
H(16)	6823(7)	2979(3)	6378(5)	99
H(17)	5076(7)	4034(6)	6138(5)	101

H(18)	4271(5)	5653(5)	6502(5)	83
H(20)	2659(8)	8386(5)	9186(4)	89
H(21)	3408(9)	8673(6)	10105(6)	116
H(22)	3734(9)	7586(8)	11156(5)	128
H(23)	3310(9)	6211(7)	11288(4)	117
H(24)	2561(8)	5924(5)	10369(5)	93
H(26)	468(8)	7746(9)	10465(4)	123
H(27)	-1471(9)	8496(9)	10967(5)	154
H(28)	-2725(4)	8740(8)	10207(8)	138
H(29)	-2040(7)	8234(9)	8945(7)	147
H(30)	-101(8)	7483(8)	8444(4)	110
H(32)	755(5)	5653(5)	9701(5)	95
H(33)	1205(6)	3993(6)	9620(5)	105
H(34)	2929(7)	3011(3)	8864(5)	89
H(35)	4203(5)	3688(5)	8188(5)	95
H(36)	3754(5)	5348(5)	8269(4)	84
H(38)	3788(5)	7559(6)	5740(4)	77
H(39)	4476(4)	8263(7)	4593(5)	95
H(40)	3256(7)	9247(6)	3819(3)	97
H(41)	1348(6)	9528(6)	4193(4)	104
H(42)	660(3)	8825(6)	5340(4)	84
H(44)	2551(9)	6457(5)	5163(3)	99
H(45)	3063(10)	4837(6)	4891(3)	130
H(46)	2896(9)	3702(3)	5887(5)	104
H(47)	2218(8)	4186(4)	7155(4)	89
H(48)	1706(7)	5806(5)	7427(2)	72
H(50)	-77(6)	9169(5)	7399(5)	78
H(51)	-2041(6)	9877(5)	7644(5)	95
H(52)	-2994(3)	9216(6)	7135(5)	99
H(53)	-1982(6)	7847(7)	6382(6)	115
H(54)	-17(6)	7139(5)	6138(5)	96
H(57)	-1208(7)	11381(11)	8161(12)	265
H(58)	-1049(12)	11775(8)	6853(13)	243
H(59)	655(16)	11004(11)	5981(8)	263
H(60)	2200(9)	9839(10)	6418(7)	176
H(61A)	-509(25)	10426(97)	9073(19)	263
H(61B)	710(111)	10357(106)	9032(23)	263
H(61C)	543(128)	9428(15)	8886(12)	263
H(63)	2776(8)	10893(8)	7300(6)	114
H(64)	3349(12)	12120(8)	6663(6)	152
H(65)	4732(12)	12407(7)	7018(8)	158
H(66)	5543(8)	11467(10)	8010(8)	144
H(68A)	4827(22)	10296(13)	9336(8)	255
H(68B)	5970(14)	9838(10)	8722(10)	255
H(68C)	5073(8)	9370(13)	8897(8)	255

APPENDIX SEVEN

Crystallographic data for [(monothioacetato)(triphenylphosphine)silver(I)]tetramer. bis(dichloromethane)solvate (22).

A crystal of approximate dimensions 0.4 x 0.4 x 0.4 mm was used for data collection.

Crystal data: C_{82} H_{76} Ag_4 O_4 P_4 S_4 •2(CH_2Cl_2), M = 975.41, Monoclinic, a = 15.494(4), b = 16.782(3), c = 17.694(5) Å, β = 115.55(2)°, U = 4150.9(18) Å^3, space group $P2_1/n$, Z = 2, D_c = 1.561 g.cm^{-3}, μ(Mo-K_α) = 1.284 mm^{-1}, F(000) = 1960. Crystallographic measurements were made at 293(2)°K on a CAD4 automatic four-circle diffractometer in the range $2.31<\theta<23.92°$. Data (6859 reflections) were corrected for Lorentz and polarization but not for absorption.

In the final least squares cycles all atoms were allowed to vibrate anisotropically. Hydrogen atoms were included at calculated positions where relevant.

The asymmetric unit in this structure consists of one half of a tetramer and one molecule of dichloromethane. The remainder of the metal complex is generated via the symmetry operation *1-x,-y,-z.*

The solution of the structure (SHELX86)[82] and refinement (SHELX93)[83] converged to a conventional [i.e. based on 2703 reflections with $Fo>4\sigma(Fo)$] $R1$ = 0.0709 and $wR2$ = 0.1681. Goodness of fit = 0.827. The max. and min. residual densities were 0.868 and -0.490 eÅ^{-3} respectively. The asymmetric unit (shown in Fig. 4.19), along with the labelling scheme used was produced using ORTEX.[241] Final fractional atomic co-ordinates and isotropic thermal parameters, bond distances and angles are given in Tables A7.2 and A7.3, respectively. Anisotropic temperature factors are given in Table A7.4 and hydrogen coordinates and isotropic temperature factor in Table A7.5.

Table A7.1 Crystal data and structure refinement for (**22**).

Identification code	98vo2
Empirical formula	$C_{82}H_{76}Ag_4O_4P_4S_4 \cdot 2(CH_2Cl_2)$
Formula weight	975.41
Temperature	293(2)°K
Wavelength	0.70930 Å
Crystal system	Monoclinic
Space group	$P2_1/n$
Unit cell dimensions	a = 15.494(4)Å b = 16.782(3)Å β = 115.55(2)° c = 17.694(5)Å
Volume	4151(2) $Å^3$
Z	2
Density (calculated)	1.561 Mg/m^3
Absorption coefficient	1.284 mm^{-1}
F(000)	1960
Crystal size	0.4 x 0.4 x 0.4 mm
Theta range for data collection	2.31 to 23.92 °.
Index ranges	0<=h<=17; 0<=k<=19; -20<=l<=18
Reflections collected	6859
Independent reflections	6489 [R(int) = 0.0350]
Refinement method	Full-matrix least-squares on F^2
Data / restraints / parameters	6474 / 0 / 462
Goodness-of-fit on F^2	0.827
Final R indices [I>2σ(I)]	R1 = 0.0709 wR2 = 0.1681
R indices (all data)	R1 = 0.1853 wR2 = 0.2262
Largest diff. peak and hole	0.868 and -0.490 $eÅ^{-3}$
Weighting scheme	calc $w=1/[\sigma^2(Fo^2)+(0.1177P)^2]$ where $P=(Fo^2+2Fc^2)/3$

Table A7.2 Atomic coordinates (x 10^4) and equivalent isotropic displacement parameters ($Å^2$ x 10^3) for (**22**). U(eq) is defined as one third of the trace of the orthogonalized Uij tensor.

Atom	x	y	z	U(eq)
Ag(1)	3556(1)	230(1)	957(1)	66(1)
Ag(2)	5830(1)	-997(1)	574(1)	67(1)
Cl(1)	3311(9)	4706(8)	303(6)	331(7)
Cl(2)	1718(7)	5642(8)	-273(7)	312(6)
P(1)	3188(2)	70(2)	2149(2)	58(1)
P(2)	4958(2)	-2238(2)	361(2)	56(1)
S(1)	5269(2)	198(2)	1086(2)	66(1)
S(2)	2605(2)	748(2)	-517(2)	53(1)
O(1)	2336(11)	1792(6)	442(8)	158(6)
O(2)	6564(7)	-256(7)	2541(6)	109(4)
C(1)	5579(8)	-2978(7)	1158(8)	56(3)
C(2)	5579(9)	-3776(7)	1023(8)	69(4)
C(3)	6054(15)	-4293(11)	1625(13)	118(7)
C(4)	6597(12)	-4032(13)	2405(14)	105(7)
C(5)	6648(11)	-3241(13)	2597(10)	106(6)
C(6)	6155(10)	-2719(9)	1958(10)	87(4)
C(7)	3811(8)	-2122(7)	403(7)	56(3)

C(8)	3513(11)	-2594(8)	876(9)	88(5)
C(9)	2622(13)	-2515(9)	857(11)	108(6)
C(10)	2036(10)	-1924(9)	389(10)	87(4)
C(11)	2341(9)	-1442(8)	-76(8)	73(4)
C(12)	3227(9)	-1536(8)	-62(7)	64(3)
C(13)	4647(9)	-2765(6)	-619(7)	50(3)
C(14)	3775(11)	-3091(8)	-1066(9)	83(4)
C(15)	3591(12)	-3498(8)	-1813(11)	96(5)
C(16)	4288(15)	-3582(10)	-2086(10)	101(5)
C(17)	5139(15)	-3226(11)	-1658(10)	115(6)
C(18)	5347(11)	-2797(9)	-911(8)	86(4)
C(19)	3806(8)	822(7)	2950(7)	55(3)
C(20)	3705(9)	1599(9)	2724(8)	72(4)
C(21)	4177(11)	2210(8)	3280(10)	87(4)
C(22)	4747(11)	2015(11)	4091(10)	94(5)
C(23)	4847(11)	1227(10)	4332(9)	97(5)
C(24)	4372(10)	646(9)	3761(8)	79(4)
C(25)	1937(9)	158(7)	1954(8)	62(3)
C(26)	1670(10)	461(10)	2551(9)	101(5)
C(27)	733(12)	494(12)	2404(10)	114(6)
C(28)	35(12)	168(11)	1703(11)	104(5)
C(29)	263(11)	-173(11)	1107(10)	118(6)
C(30)	1241(10)	-159(10)	1243(7)	100(5)
C(31)	3547(9)	-866(8)	2689(7)	64(3)
C(32)	3102(10)	-1240(9)	3100(9)	88(4)
C(33)	3405(12)	-1977(11)	3485(10)	101(5)
C(34)	4188(15)	-2325(10)	3495(10)	109(6)
C(35)	4662(16)	-1987(12)	3095(11)	141(8)
C(36)	4365(12)	-1221(9)	2704(9)	95(5)
C(37)	2301(9)	1683(7)	-233(9)	70(4)
C(38)	2045(10)	2337(8)	-849(8)	88(4)
C(39)	6038(8)	274(9)	2179(8)	65(4)
C(40)	5985(10)	1040(8)	2573(9)	98(5)
C(41)	2389(20)	5027(24)	-353(18)	366(31)

Table A7.3 Bond lengths [Å] and angles [°] for (**22**).

Ag(1)-P(1)	2.425(3)	C(10)-C(11)	1.38(2)
Ag(1)-S(2)	2.532(3)	C(11)-C(12)	1.37(2)
Ag(1)-S(1)	2.564(3)	C(13)-C(14)	1.35(2)
Ag(2)-P(2)	2.422(3)	C(13)-C(18)	1.39(2)
Ag(2)-S(2)#1	2.505(3)	C(14)-C(15)	1.40(2)
Ag(2)-S(1)	2.506(3)	C(15)-C(16)	1.37(2)
Cl(1)-C(41)	1.50(2)	C(16)-C(17)	1.34(2)
Cl(2)-C(41)	1.51(2)	C(17)-C(18)	1.42(2)
P(1)-C(31)	1.797(14)	C(19)-C(24)	1.35(2)
P(1)-C(25)	1.823(12)	C(19)-C(20)	1.35(2)
P(1)-C(19)	1.830(12)	C(20)-C(21)	1.39(2)
P(2)-C(1)	1.813(12)	C(21)-C(22)	1.36(2)
P(2)-C(13)	1.818(11)	C(22)-C(23)	1.38(2)
P(2)-C(7)	1.821(12)	C(23)-C(24)	1.37(2)
S(1)-C(39)	1.785(13)	C(25)-C(30)	1.36(2)
S(2)-C(37)	1.772(12)	C(25)-C(26)	1.39(2)
S(2)-Ag(2)#1	2.505(3)	C(26)-C(27)	1.36(2)
O(1)-C(37)	1.187(14)	C(27)-C(28)	1.36(2)
O(2)-C(39)	1.189(14)	C(28)-C(29)	1.37(2)
C(1)-C(2)	1.36(2)	C(29)-C(30)	1.43(2)
C(1)-C(6)	1.38(2)	C(31)-C(32)	1.35(2)
C(2)-C(3)	1.32(2)	C(31)-C(36)	1.39(2)

C(3)-C(4)	1.34(2)	C(32)-C(33)	1.39(2)
C(4)-C(5)	1.36(2)	C(33)-C(34)	1.34(2)
C(5)-C(6)	1.37(2)	C(34)-C(35)	1.35(2)
C(7)-C(12)	1.35(2)	C(35)-C(36)	1.44(2)
C(7)-C(8)	1.37(2)	C(37)-C(38)	1.48(2)
C(8)-C(9)	1.37(2)	C(39)-C(40)	1.48(2)
C(9)-C(10)	1.36(2)		

P(1)-Ag(1)-S(2)	133.06(11)	C(14)-C(13)-C(18)	120.7(12)
P(1)-Ag(1)-S(1)	122.88(11)	C(14)-C(13)-P(2)	122.7(10)
S(2)-Ag(1)-S(1)	102.66(10)	C(18)-C(13)-P(2)	116.5(10)
P(2)-Ag(2)-S(2)#1	128.50(11)	C(13)-C(14)-C(15)	119.6(14)
P(2)-Ag(2)-S(1)	119.14(11)	C(16)-C(15)-C(14)	121(2)
S(2)#1-Ag(2)-S(1)	111.93(11)	C(15)-C(16)-C(17)	119(2)
C(31)-P(1)-C(25)	103.4(6)	C(16)-C(17)-C(18)	122(2)
C(31)-P(1)-C(19)	104.6(5)	C(13)-C(18)-C(17)	117.8(14)
C(25)-P(1)-C(19)	104.4(5)	C(24)-C(19)-C(20)	117.6(13)
C(31)-P(1)-Ag(1)	115.2(4)	C(24)-C(19)-P(1)	123.6(10)
C(25)-P(1)-Ag(1)	117.2(4)	C(20)-C(19)-P(1)	118.8(10)
C(19)-P(1)-Ag(1)	110.9(4)	C(19)-C(20)-C(21)	122.9(13)
C(1)-P(2)-C(13)	104.0(6)	C(22)-C(21)-C(20)	118.2(14)
C(1)-P(2)-C(7)	104.0(5)	C(21)-C(22)-C(23)	119.5(14)
C(13)-P(2)-C(7)	103.2(5)	C(24)-C(23)-C(22)	120.1(13)
C(1)-P(2)-Ag(2)	113.3(4)	C(19)-C(24)-C(23)	121.6(14)
C(13)-P(2)-Ag(2)	117.8(4)	C(30)-C(25)-C(26)	118.0(12)
C(7)-P(2)-Ag(2)	113.0(4)	C(30)-C(25)-P(1)	119.7(10)
C(39)-S(1)-Ag(2)	106.0(5)	C(26)-C(25)-P(1)	121.9(10)
C(39)-S(1)-Ag(1)	106.0(4)	C(27)-C(26)-C(25)	120.9(14)
Ag(2)-S(1)-Ag(1)	119.46(14)	C(28)-C(27)-C(26)	121.3(14)
C(37)-S(2)-Ag(2)#1	104.1(4)	C(27)-C(28)-C(29)	120(2)
C(37)-S(2)-Ag(1)	96.9(5)	C(28)-C(29)-C(30)	118.0(14)
Ag(2)#1-S(2)-Ag(1)	87.44(10)	C(25)-C(30)-C(29)	121.4(12)
C(2)-C(1)-C(6)	116.2(12)	C(32)-C(31)-C(36)	117.6(13)
C(2)-C(1)-P(2)	125.4(11)	C(32)-C(31)-P(1)	125.4(12)
C(6)-C(1)-P(2)	118.3(10)	C(36)-C(31)-P(1)	117.0(10)
C(3)-C(2)-C(1)	123(2)	C(31)-C(32)-C(33)	122(2)
C(2)-C(3)-C(4)	120(2)	C(34)-C(33)-C(32)	121(2)
C(3)-C(4)-C(5)	121(2)	C(33)-C(34)-C(35)	120(2)
C(4)-C(5)-C(6)	118(2)	C(34)-C(35)-C(36)	120(2)
C(5)-C(6)-C(1)	122(2)	C(31)-C(36)-C(35)	119(2)
C(12)-C(7)-C(8)	118.7(12)	O(1)-C(37)-C(38)	120.7(12)
C(12)-C(7)-P(2)	117.6(9)	O(1)-C(37)-S(2)	121.3(10)
C(8)-C(7)-P(2)	123.7(10)	C(38)-C(37)-S(2)	118.0(10)
C(7)-C(8)-C(9)	122.0(13)	O(2)-C(39)-C(40)	123.9(12)
C(10)-C(9)-C(8)	119.1(14)	O(2)-C(39)-S(1)	120.9(10)
C(9)-C(10)-C(11)	118.9(13)	C(40)-C(39)-S(1)	115.2(11)
C(10)-C(11)-C(12)	121.4(13)	Cl(1)-C(41)-Cl(2)	130(2)
C(7)-C(12)-C(11)	119.9(12)		

Symmetry transformations used to generate equivalent atoms:

#1 -x+1,-y,-z

Table A7.4 Anisotropic displacement parameters ($Å^2 \times 10^3$) for (**22**). The anisotropic displacement factor exponent takes the form: $-2\pi^2[h^2 a^* 2 U11 + ... + 2 h k a^* b^* U12]$

Atom	U11	U22	U33	U23	U13	U12
Ag(1)	83(1)	72(1)	51(1)	5(1)	36(1)	8(1)
Ag(2)	70(1)	56(1)	85(1)	-1(1)	44(1)	-6(1)
Cl(1)	343(13)	446(18)	176(8)	-13(9)	84(8)	186(13)
Cl(2)	228(9)	335(14)	361(14)	-94(12)	116(10)	34(9)
P(1)	59(2)	72(2)	48(2)	7(2)	27(2)	2(2)
P(2)	59(2)	50(2)	62(2)	4(2)	29(2)	-2(2)
S(1)	68(2)	82(2)	53(2)	13(2)	31(2)	23(2)
S(2)	55(2)	59(2)	48(2)	1(2)	25(2)	1(2)
O(1)	323(18)	93(8)	135(10)	18(8)	173(12)	68(10)
O(2)	74(7)	137(10)	77(7)	6(7)	-4(6)	41(7)
C(1)	63(8)	50(8)	75(9)	19(7)	49(8)	7(6)
C(2)	78(9)	46(8)	76(9)	20(7)	25(8)	20(7)
C(3)	159(19)	96(14)	125(15)	38(14)	85(15)	58(14)
C(4)	79(12)	120(16)	148(18)	93(16)	79(13)	67(12)
C(5)	97(13)	150(17)	64(10)	47(13)	28(9)	19(12)
C(6)	81(10)	94(11)	87(11)	10(10)	37(9)	-9(9)
C(7)	68(8)	51(8)	50(7)	13(6)	26(7)	-4(7)
C(8)	107(11)	90(11)	103(11)	33(9)	80(10)	27(9)
C(9)	132(15)	77(11)	166(17)	30(11)	112(14)	14(11)
C(10)	60(9)	78(11)	124(13)	-4(10)	40(9)	-5(9)
C(11)	69(10)	64(9)	85(10)	17(7)	32(8)	-5(7)
C(12)	69(9)	71(9)	60(8)	-9(7)	36(7)	-18(8)
C(13)	60(7)	50(7)	39(7)	0(6)	22(6)	-8(6)
C(14)	98(12)	61(9)	79(10)	-14(8)	28(9)	4(8)
C(15)	114(13)	55(9)	109(14)	-4(9)	40(11)	-4(9)
C(16)	147(17)	89(12)	71(11)	1(9)	52(12)	20(12)
C(17)	156(18)	135(16)	82(12)	-13(11)	79(13)	-9(14)
C(18)	103(11)	110(12)	63(9)	-7(9)	53(9)	-3(9)
C(19)	71(8)	49(8)	58(8)	12(6)	38(7)	6(6)
C(20)	71(9)	95(12)	63(9)	-6(9)	42(7)	-9(8)
C(21)	114(12)	66(9)	84(12)	-20(9)	46(10)	-16(9)
C(22)	105(12)	113(14)	65(11)	-42(10)	38(10)	-43(11)
C(23)	106(12)	96(13)	49(9)	-14(9)	-6(8)	-11(10)
C(24)	91(10)	104(11)	43(8)	14(9)	30(8)	-10(9)
C(25)	64(8)	71(8)	52(7)	4(7)	25(7)	8(7)
C(26)	75(11)	138(14)	103(12)	-48(11)	50(10)	-13(10)
C(27)	74(11)	197(20)	81(11)	-33(12)	43(10)	9(12)
C(28)	80(12)	139(15)	110(13)	31(12)	58(12)	27(11)
C(29)	57(10)	188(19)	84(12)	-12(12)	7(9)	15(11)
C(30)	80(10)	196(17)	34(7)	1(9)	34(8)	26(11)
C(31)	54(8)	83(10)	54(8)	-6(7)	22(7)	-21(7)
C(32)	85(10)	85(11)	95(11)	14(9)	40(9)	-14(9)
C(33)	102(13)	104(14)	94(12)	25(11)	39(11)	-13(11)
C(34)	157(18)	68(11)	85(12)	8(9)	35(13)	18(12)
C(35)	245(24)	115(16)	111(15)	35(12)	123(17)	72(16)
C(36)	133(14)	79(11)	92(11)	26(9)	68(11)	12(10)
C(37)	91(10)	54(8)	94(11)	14(8)	66(9)	15(7)
C(38)	103(11)	75(10)	88(10)	9(9)	43(9)	30(9)
C(39)	26(7)	92(10)	71(9)	-20(8)	14(7)	-8(7)
C(40)	110(12)	85(11)	117(12)	-48(10)	66(10)	-1(9)
C(41)	204(29)	493(61)	213(30)	-216(35)	-86(23)	200(36)

Table A7.5 Hydrogen coordinates (x 10^4) and isotropic displacement parameters ($Å^2$ x 10^3) for (**22**).

Atom	x	y	z	U(eq)
H(2)	5229(9)	-3967(7)	482(8)	83
H(3)	6010(15)	-4836(11)	1509(13)	142
H(4)	6946(12)	-4396(13)	2821(14)	126
H(5)	7004(11)	-3062(13)	3141(10)	128
H(6)	6210(10)	-2175(9)	2069(10)	105
H(8)	3928(11)	-2979(8)	1221(9)	105
H(9)	2422(13)	-2861(9)	1160(11)	130
H(10)	1439(10)	-1847(9)	383(10)	105
H(11)	1939(9)	-1043(8)	-406(8)	88
H(12)	3424(9)	-1197(8)	-373(7)	76
H(14)	3301(11)	-3046(8)	-879(9)	99
H(15)	2988(12)	-3714(8)	-2125(11)	115
H(16)	4174(15)	-3881(10)	-2562(10)	121
H(17)	5603(15)	-3264(11)	-1858(10)	138
H(18)	5933(11)	-2544(9)	-625(8)	103
H(20)	3303(9)	1730(9)	2172(8)	86
H(21)	4104(11)	2738(8)	3103(10)	104
H(22)	5068(11)	2411(11)	4479(10)	113
H(23)	5237(11)	1089(10)	4885(9)	117
H(24)	4440(10)	117(9)	3934(8)	95
H(26)	2138(10)	644(10)	3058(9)	121
H(27)	567(12)	745(12)	2791(10)	137
H(28)	-598(12)	175(11)	1627(11)	125
H(29)	-205(11)	-406(11)	629(10)	142
H(30)	1407(10)	-370(10)	838(7)	120
H(32)	2576(10)	-996(9)	3126(9)	106
H(33)	3062(12)	-2229(11)	3736(10)	122
H(34)	4405(15)	-2803(10)	3781(10)	131
H(35)	5180(16)	-2248(12)	3072(11)	169
H(36)	4717(12)	-966(9)	2462(9)	114
H(38A)	1375(17)	2307(32)	-1219(35)	132
H(38B)	2410(47)	2289(31)	-1168(39)	132
H(38C)	2181(59)	2839(8)	-562(9)	132
H(40A)	6474(46)	1393(22)	2575(56)	147
H(40B)	6079(69)	945(11)	3138(21)	147
H(40C)	5369(27)	1278(29)	2261(36)	147
H(41A)	1993(20)	4561(24)	-587(18)	439
H(41B)	2548(20)	5229(24)	-790(18)	439

APPENDIX EIGHT

Instrumentation

Microanalysis.

Analyses for carbon, hydrogen and nitrogen were carried out using a Carlo-Erba Strumentazione E.A. model 1106 microanalyser operating at 500°C. Results were calibrated against an acetanilide [$PhNHC(O)CH_3$] standard.

Infrared Spectroscopy.

Infrared spectra were recorded as nujol (liquid paraffin) mulls or liquid films between NaCl plates. Measurements were taken using a Nicolet 510P Fourier Transform spectrometer within the range 4000-600 cm^{-1} with a medium slit width and peak resolution of 4.0 cm^{-1}. All bands are sharp unless otherwise stated.

^{1}H, $^{13}C\{1H\}$ Nuclear Magnetic Resonance spectroscopy.

Proton and carbon-13 NMR spectra were recorded using either Jeol JNM-GX-270FT (270 MHz) or Jeol EX-400 (400 MHz) Fourier Transform spectrometers using tetramethylsilane ($SiMe_4$) as an internal reference.

^{31}P Nuclear Magnetic Resonance spectroscopy.

Phosphorus NMR spectra were recorded using either Jeol JNM-GX-270FT (270 MHz) or Jeol EX-400 (400 MHz) Fourier Transform spectrometers. Chemical shifts [$\delta(^{31}P)$] for the phosphorus spectra are relative to 85 % H_3PO_4.

FAB (LSIMS) Mass spectrometry.

The EPSRC Mass Spectrometry Service at the University College of Swansea carried out Fast Atom Bombardment (Liquid Secondary Ion Mass Spectrometry) and

electrospray experiments. FAB (LSIMS) spectra were carried out on a VG AutoSpec instrument using a caesium ion bombardment at 25 kV. Samples were dissolved in a 3-nitrobenzyl alcohol (NOBA) matrix typically with the aid of a CH_2Cl_2 co-solvent.

Thermogravimetric Analysis (TGA).

TGA experiments were carried out at atmospheric pressure in a helium-purged atmosphere, from room temperature to 450°C at a ramp rate of 25°C.min^{-1}, using a TA instrument 2100 Thermal Analysis.

Scanning Electron Microscopy.

SEM was carried out using a JEOL JSM T330 scanning electron microscope operating at an accelerating voltage of 15 kV. Coatings under investigation were not sputter-coated although a path to ground was provided by means of silver dag or electrically conducting putty.

Energy Dispersive X-Ray Spectrometry.

Film thickness estimates using EDXS techniques were performed on a Jeol Superprobe instrument operating at an accelerating voltage of 5kV or 10 kV with a beam current of 5×10^{-8}A or 5×10^{-9}A. X-ray counts (100 or 200 seconds) from sample films were compared against a solid silver standard.

Conductivity measurements.

Sheet resistances of films were measured over a 25 mm square. Silver "dag" busbar contacts were painted on the sample and the resistance measured using a digital voltmeter.

Reflectance measurements.

Reflection spectra at near-normal incidence were measured on a Hitachi U-3410 spectrophotometer over the range 295-2600 nm in 5 nm steps. Calibration was against

rhodium standard mirrors. The assessment area was a rectangle of approximately 11 by 4 mm.

APPENDIX NINE

CVD Reactor

The CVD apparatus used in this study has been assembled as a general screening rig for the use in this and other related projects. The system consists of a horizontal cold wall reactor with associated gas lines and electrical heater controls. The reactor contains two separate systems, a heated bubbler assembly and an ultrasonic nebuliser equipment. Screening tests for this study have exclusively used the ultrasonic nebuliser. A schematic of the relevant apparatus is shown in Figure A9.1.

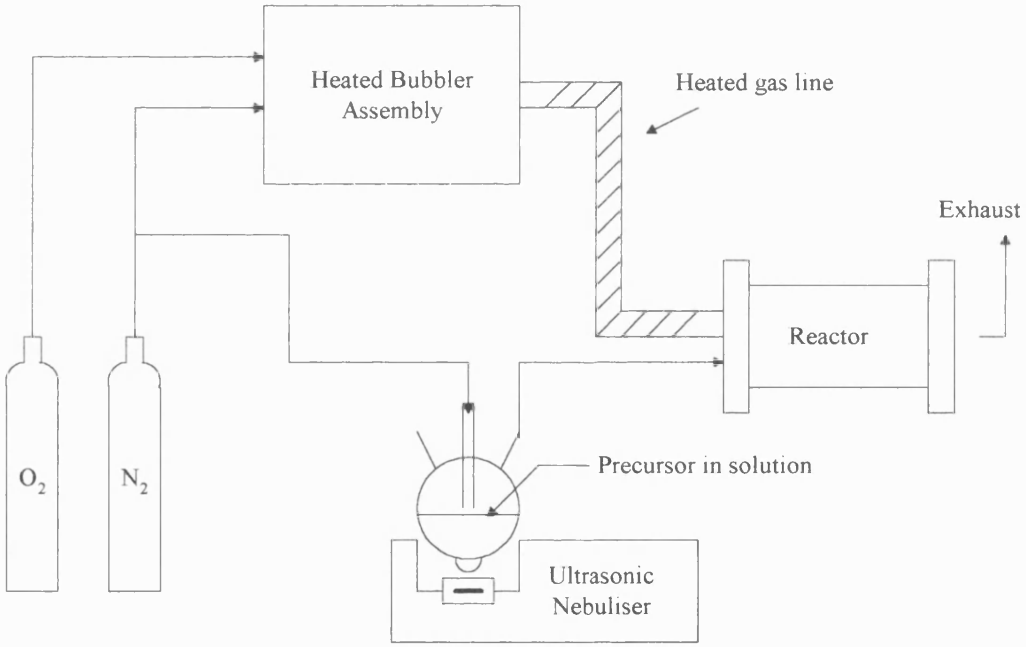

Figure A9.1 Schematic representation of the CVD system.

The ultrasonic nebuliser used is an ultrasonic humidifier from Pifco Health (model No 1077) bought in Argos. The piezoelectric transducer, situated in the reservoir containing water, transmits ultrasound through the water and the glass of the flask into the solution to be nebulised. The distance between the piezoelectric transducer and the flask is approximately 3-4 cm. The water in the reservoir is replaced every 30 minutes in order to cool the transducer.

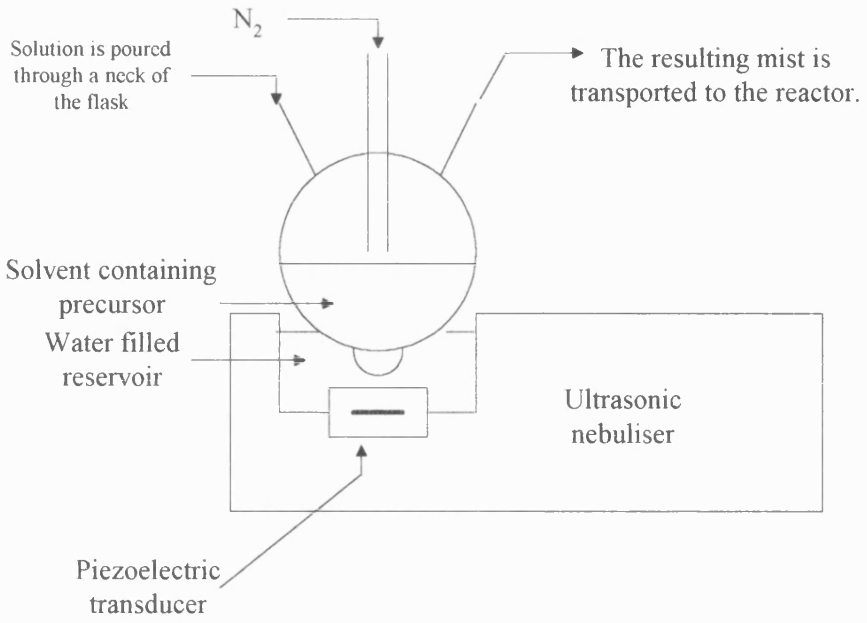

Figure A9.2 Schematic representation of the nebuliser equipment.

A solution of the precursor is poured into the three neck round-bottomed flask and placed on the nebuliser. When the power is switched on, the solution in the flask fountains to generate an aerosol of fine droplets of the solution (droplet size: 0.2-5 microns). The mist can be controlled via two controls, the mist output (MO) and the humidity level (HL). For a solution in THF, the efficiency of the nebuliser is 1.2 $cm^3.min^{-1}$ when the MO button is in position 1/2 or 3/4 of its full power and the HL button is in position 3/4 of its full power.

This aerosol is simply swept out of the flask by a flow of nitrogen gas and transported to a horizontal cold wall CVD reactor. Before the mist reaches the reactor, it is passed through a baffle to promote laminar flow. A schematic representation of the CVD reactor is represented in Figure A9.3. After passing through the baffle, the mist passes directly into the reactor chamber (8 mm high, 40 mm wide and 300 mm long). The ceiling tile and walls of the reactor are constructed from silica. The glass substrate is positioned upon a large graphite support, which is heated by three Watlow firewood cartridge heaters. A Watlow series 9965 controller, which monitors the temperature by means of thermocouples positioned inside the block, maintains the temperature of the graphite block. The graphite support is held inside a large silica tube (330 mm long, 100 mm diameter) suspended between stainless steel flanges upon which many of the electrical and gas line fittings are fixed. Airtight seals are provided by "Viton" O-rings.

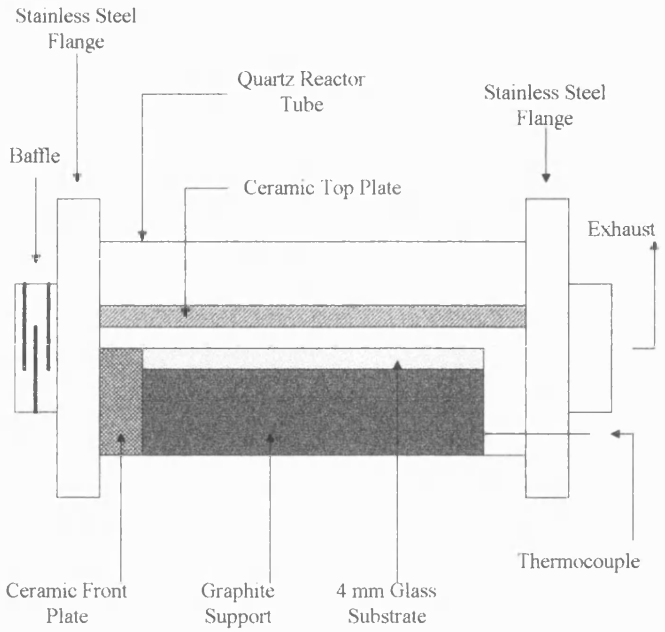

Figure A9.3 Schematic representation of the CVD reactor chamber.

Substrate Preparation Procedure

All the glass substrates were cleaned in an identical way prior to use. The cleaning routine was as follows:

1. The glass was washed thoroughly with tap water and detergent.
2. The glass was then washed thoroughly with copious amounts of distilled water.
3. Then finally washed with a generous amount of isopropyl alcohol (IPA) and allowed to drain.

The glass was always prepared immediately before a deposition experiment to ensure a clean surface. The glass was handled very carefully, the deposition area not being touched.

After the completion of screening of each precursor, the flask and the pipework were cleaned in order to prevent contamination of the next deposition.

References

REFERENCES

1. R. Harker, Ph.D.Thesis, University of Bath, 1996.
2. 'Deposition Technologies for Films and Coatings: Development and Applications', Edited by R.F. Bunshah, pub. Noyes, New Jersey, 1982.
3. 'Thin Film Processes', J.L. Vossen, W. Kern, pub. Academic Press, London, 1978.
4. A.F. Rubira, J.D. Rancourt, M.L. Caplan, A.K. St. Clair, L.T. Taylor, *Chem. Mater.*, 1994, **6**, 2351.
5. R.E. Southward, D.S. Thompson, D.W. Thompson, M.L. Caplan, A.K. St. Clair, *Chem. Mater.*, 1995, **7**, 2171.
6. G. Grolig, K.H. Kochem, *Adv. Mater.*, 1992, **4**, 179.
7. Chem. Abs. 1994, **121**, 41212r. R Latz, B. Ocker, R. Schneider, Ger. Offen. DE 4,239,355.
8. Chem. Abs.1995, **122**, 185520c. S. Koch, V. Rondeau, J.P. Brochot, O. Guiselin, Eur. Pat. Appl. EP 611,213, August 1994.
9. Chem. Abs.1995, **122**, 194970x. O. Guiselin, J. Brochot, P. Petit, Eur. Pat. Appl. EP 638,528.
10. 'The Chemistry of Metal CVD', T.T. Kodas, M.J. Hampden-Smith, pub.VCH, Weinheim, 1994.
11. S.F. Wang, J.P. Dougherty, W. Huebner, I.G. Pepin, *J. Amer. Ceram. Soc.*, 1994, **77**, 3051.
12. M.J. Shapiro, W.J. Lackey, J.A. Hanigofsky, D.N. Hill, W.B. Carter, E.K. Barefield, *J. Alloys and Compounds*, 1992, **187**, 331.
13. P. M. Jeffries, S.R. Wilson, G.S. Girolami, *J. Organometal. Chem.*, 1993, **449**, 203.
14. J.H. Miller, S.L. Holder, J.D. Hunn, G.N. Holder, *Appl.Phys. Lett.*, 1989, **54**, 2256.
15. J.A. Deluca, P.L. Karas, J.E. Tkaczyk, P.J. Bednarczyk, M.F. Garbauskas, C.L. Briant, D.B. Sorensen, *Physica C*, 1993, **205**, 21.
16. C.L. Briant, J.A. Deluca, P.L. Karas, M.F. Garbauskas, J.A. Sutcliff, A. Goyal, D. Kroeger, *J. Mater. Research*, 1995, **10**, 823.
17. J.M. Zhang, B.W. Wessels, L.M. Tonge, T.J. Marks, *Appl. Phys. Lett.*, 1990, **56**, 976.
18. R. Yufang, Z. Zuotao, M. Jian, H. Ping, *Solid State Commun.*, 1990, **75**, 625.
19. D. Wu, R.A. Outlaw, R.L. Ash, *J. Appl. Phys.*, 1993, **74**, 4990.

20. Z.Y. Li, H. Maeda, K. Kusakabe, S. Morooka, H. Anzai, S. Akiyama, *J. Membrane Sci.*, 1993, **78**, 247.
21. J.T. Spencer, *Progr. in Inorg. Chem.*, 1994, **41**, 145.
22. K.F. Jensen, W. Kern, *Thin film processes II*, 1991, 283.
23. M.J. Hampden-Smith, T.T. Kodas, *Chem.Vap. Deposition*, 1995, **1**, 8.
24. M.J. Hampden-Smith, T.T. Kodas, *Chem.Vap. Deposition*, 1995, **1**, 39.
25. 'Deposition Technologies for Films and Coatings: Development and Applications', Edited by R.F. Bunshah, pub. Noyes, New Jersey 1982.Chapter 4.
26. 'Deposition Technologies for Films and Coatings: Development and Applications', Edited by R.F. Bunshah, pub. Noyes, New Jersey 1982. Chapter 5.
27. 'Thin Film Processes', J.L. Vossen, W. Kern, Part II 'Physical methods of film deposition' various authors, pub. Academic Press, New York, 1978.
28. 'The Chemistry of Metal CVD' Eds. T.T. Kodas, H.J. Hampden-Smith, pub. VCH, Weinheim, 1994. Chapter 7.
29. 'The Chemistry of Metal CVD' Eds. T.T. Kodas, H.J. Hampden-Smith, pub. VCH, Weinheim, 1994. Chapter 6.
30. 'Deposition Technologies for Films and Coatings: Development and Applications', Edited by R.F. Bunshah, pub. Noyes, New Jersey 1982. Chapter 9.
31. V. Bhaskaran, M.J. Hampden-Smith, T.T. Kodas, *Chem. Vap. Deposition*, 1997, **3**, 85.
32. C. Xu, M.J. Hampden-Smith, T.T. Kodas, E.N. Duesler, A.L. Rheingold, G. Yap, *Inorg. Chem.*, 1995, **34**, 4767.
33. A. Gurav, T. Kodas, T. Pluym, Y. Xiong, *Aerosol Science and Technology*, 1993, **19**, 411.
34. C. Roger, T.S. Corbitt, M.J. Hampden-Smith, T.T. Kodas, *Appl. Phys. Lett.*, 1994, **65**, 1021.
35. C. Xu, M.J. Hampden-Smith, T.T. Kodas, *Adv. Mater.*, 1994, **6**, 746.
36. C. Xu, M.J. Hampden-Smith, T.T. Kodas, *Chem. Mater.*, 1995, **7**, 1539.
37. G. Shang, M.J. Hampden-Smith, E.N. Duesler, *J. Chem. Soc. Chem. Commun.*, 1996, 1733.
38. M. Nyman, M.J. Hampden-Smith, E.N. Duesler, *Chem. Vap. Deposition*, 1996, **2**, 171.
39. M. Nyman, K. Jenkins, M.J. Hampden-Smith, T.T. Kodas, E.N. Duesler, A.L. Rheingold, M.L. Liable-Sands, *Chem. Mater.*, 1998, **10**, 914.

40. R.J.H. Voorhoeve, J.W. Merewether, *J. Electrochem. Soc.: Solid-State Science and Technology*, 1972, **119**, 364.
41. Anonymous, *Research Disclosure*, 26343, March 1986.
42. T.H. Baum, C.E. Larson, U.S. Pat. 5,096,737, March 1992.
43. K.M. Chi, K.H. Chen, S.M. Peng, G.H. Lee, *Organometallics*, 1996, **15**, 2575.
44. N.H. Dryden, J.J. Vittal, R.J. Puddephatt, *Chem. Mater.*, 1993, **5**, 765.
45. W. Lin, T.H. Warren, R.G. Nuzzo, G.S. Girolami, *J. Am. Chem. Soc.*, 1993, **115**, 11644.
46. Z. Yuan, N.H. Dryden, J.J. Vittal, R.J. Puddephatt, *Chem. Mater.*, 1995, **7**, 1696.
47. Z. Yuan, N.H. Dryden, X. Li, J.J. Vittal, R.J. Puddephatt, *J. Mater. Chem.*, 1995, **5**, 303.
48. K.M. Chi, C.T. Lin, S.M. Peng, G.H. Lee, *Organometallics*, 1996, **15**, 2660.
49. A. Erbil, U.S. Pat. 4,880,670, November 1989.
50. C.Oehr, H. Suhr, *Appl. Phys.*, 1989, **A49**, 691.
51. P. Sorbe, J. Grannec, J. Portier, P. Hagenmuller, *Compt. Rend.*, 1977, **284**, 231.
52. H.N. Po, *Coord. Chem. Rev.*, 1976, **20**, 171.
53. W. Levason, M.D. Spicer, *Coord. Chem. Rev.*, 1987, **76**, 45.
54. B. Standke, M. Jansen, *Angew. Chem. Int. Ed. Engl.*, 1985, **24**, 118.
55. B. Standke, M. Jansen, *Angew. Chem. Int. Ed. Engl.*, 1986, **25**, 77.
56. 'Comprehensive Coordination Chemistry', Eds. G. Willkinson, R.D. Gillard, J.A. McCleverty, Volume 5, Chapter 54'Silver' by R.J. Lancashire, pub. Pergamon Press, Oxford, 1987.
57. Y. Shu-Yan, L. Qin-Hui, S. Meng-Chang, H. Xiao-Yun, *Inorg. Chem*, 1994, **33**, 1251.
58. R. Eujen, B. Hoge, D.J. Brauer, *Inorg. Chem.*, 1997, **36**, 3160.
59. R. Eujen, B. Hoge, D.J. Brauer, *Inorg. Chem.*, 1997, **36**, 1464.
60. 'Advanced Inorganic Chemistry' 5th edition, F.A. Cotton and G. Willkinson, pub. Wiley-Interscience, New York, 1988.
61. L.J. Baker, G.A. Bowmaker, D. Camp, Effendy, P.C. Healy, H. Schmidbaur, O. Steigelmann, A.H. White, *Inorg. Chem.* 1992, **31**, 3656.
62. D. Venkataraman, S. Lee, J.S. Moore, P. Zhang, K.A. Hirsch, G.B. Gardner, A.C. Covey, C.L. Prentice, *Chem. Mater.* 1996, **8**, 2030.
63. M. Hong, D.Wu, H. Lui, T.C.W. Mak, Z. Zhou, D. Wu, S. Li, *Polyhedron*, 1997, **16**, 1957.

64. D.I. Arnold, F.A. Cotton, J.H. Matonic, C.A. Murillo, *Polyhedron*, 1997, **16**, 1837.

65. B.K. Teo, J.C. Calabrese, *J. Am. Chem. Soc.*, 1975, **97**, 1256.

66. G.A. Bowmaker, Effendy, J.V. Hanna, P.C. Healy, B.W. Skelton, A.H. White, *J. Chem. Soc. Dalton Trans.*, 1993, 1387.

67. S.P. Neo, T.S.A. Hor, Z.Y. Zhou, T.C.W. Mak, *J. Organometal. Chem.*, 1994, **464**, 113.

68. G.A. Bowmaker, Effendy, P.J. Harvey, P.C. Healy, B.W. Skelton, A.H. White, *J. Chem. Soc. Dalton Trans.*, 1996, 2449.

69. M.C. Gimeno, P.G. Jones, A. Laguna, C. Sarroca, *J. Chem. Soc. Dalton Trans.*, 1995, 1473.

70. B.K. Teo, J.C. Calabrese, *J. Chem. Soc. Chem. Commun.*, 1976, 185.

71. E.C. Constable, A.J. Edwards, G.R. Haire, M.J. Hannon, P.R. Raithby, *Polyhedron*, 1998, **17**, 243.

72. D. Affandi, S.J. Bernes-Price, Effendy, P.J. Harvey, P.C. Healy, B.E. Ruch, A.H. White, *J. Chem. Soc. Dalton Trans.*, 1997, 1411.

73. J.A. Darr, M. Poliakoff, W.S. Li. A.J. Blake, *J. Chem. Soc. Dalton Trans.*, 1997, 2869.

74. Y. Fu, J. Sun, Q. Li, Y. Chen, W. Dai, D. Wang, T.C.W. Mak, W. Tang, H. Hu, *J. Chem. Soc. Dalton Trans.*, 1996, 2309.

75. A.J. Blake, G. Reid, M. Schröder, *J. Chem. Soc. Chem. Comm.*, 1992, 1074.

76. H.J. Drexler, H. Reinke, H.J. Holdt, *Chem. Ber.*, 1996, **129**, 807.

77. S.P. Crabtree, A.S. Batsanov, J.A.K. Howard, M. Kilner, *Polyhedron*, 1998, **17**, 367.

78. F. Caruso, M. Camalli, H. Rimml, L.M. Venanzi, *Inorg. Chem.*, 1995, **34**, 673.

79. E.C. Constable, M.G.B. Drew, G. Forsyth, M.D. Ward, *J. Chem. Soc. Chem. Commun.*, 1988, 1450.

80. A.S. Craig, R. Kataky, R.C. Matthews, D. Parker, G. Ferguson, A. Lough, H. Adams, N. Bailey, H. Schneider, *J. Chem. Soc. Perkin Trans. 2*, 1990, 1523.

81. M.N.I. Khan, R.J. Staples, C. King, J.P. Fackler, R.E.P. Winpenny, *Inorg. Chem.*, 1993, **32**, 5800.

82. G.M. Sheldrick, *Acta Cryst.*, 1990, **A46**, 467.

83. G.M. Sheldrick, SHELXL, a computer program for crystal structure refinement, 1995, University of Göttingen.

84. 'NMR in Chemistry: A Multinuclear Introduction', W. Kemp, pub. Macmillan, London, 1986.

85. E.L. Muetterties, C.W. Alegranti, *J. Am. Chem. Soc.*, 1972, **94**, 6386.

86. 'NMR 16: Basic Principles and Progress. ^{31}P and ^{13}C NMR of Transition Metal Phosphine Complexes', P.S. Pregosin, R.W. Kunz, pub. Springer-Verlag, Berlin, 1979.

87. G. Smith, D.E. Lynch, C.H.L. Kennard, *Inorg. Chem.*, 1996, **35**, 2711.

88. 'Metal Carboxylates', R.C. Mehrotra, R. Bohra, pub. Academic Press, London, 1983.

89. X.M. Chen, T.C.W. Mak, *Polyhedron*, 1991, **10**, 1723.

90. B.T. Usubaliev, E.M. Movsumov, I.R. Amiraslanov, A.I. Akhmedov, A.A. Musaev, Kh.S. Mamedov, *Zh. Strukt. Khim.*, 1981, **22**, 98.

91. T.C.W. Mak, W.H. Yip, C.H.L. Kennard, G. Smith, E.J. O'Reilly, *Aust. J. Chem.*, 1988, **41**, 683.

92. G. Smith, A.N. Reddy, K.A. Byriel, C.H.L. Kennard, *Polyhedron*, 1994, **13**, 2425.

93. D.W. Hartley, G. Smith, D.S. Sagatys, C.H.L. Kennard, *J. Chem. Soc. Dalton Trans.*, 1991, 2735.

94. T.C.W. Mak, W.H. Yip, C.H.L. Kennard, G. Smith, E.J. O'Reilly, *Aust. J. Chem.*, 1986, **39**, 541.

95. G. Smith, D.S. Sagatys, C. Dahlgren, D.E. Lynch, R.C. Bott, K.A. Byriel, C.H.L. Kennard, *Z. Kristallogr.*, 1995, **210**, 44.

96. D.A. Edwards, M.F. Mahon, T.J. Paget, *Polyhedron*, 1997, **16**, 25.

97. D.Y. Naumov, A.V. Virovets, N.V. Podberezskaya, E.V. Boldyreva, *Acta Cryst.*, 1995, **C51**, 60.

98. G. Smith, A.N. Reddy, K.A. Byriel, C.H.L. Kennard, *Aust. J. Chem.*, 1994, **47**, 1179.

99. A.E. Blakeslee, J.L. Hoard, *J. Am. Chem. Soc.*, 1956, **78**, 3029.

100. W.Y. Huang, L. Lü, X.M. Chen, T.C.W. Mak, *Polyhedron*, 1991, **10**, 2687.

101. D.S. Sagatys, G. Smith, R.C. Bott, D.E. Lynch, C.H.L. Kennard, *Polyhedron*, 1993, **12**, 709.

102. F. Charbonnier, R. Faure, H. Loiseleur, *Rev. Chim. Minérale*, 1981, **18**, 245.

103. G.W. Hunt, T.C. Lee, E.L. Amma, *Inorg. Nucl. Chem. Letters*, 1974, **10**, 909.

104. V.M. Hedrich, H. Hartl, *Acta Cryst.*, 1983, **C39**, 533.

105. G. Smith, D.S. Sagatys, C.A. Campbell, D.E. Lynch, C.H.L. Kennard, *Aust. J. Chem.*, 1990, **43**, 1707.

106. F. Charbonnier, M. Petit-Ramel, R. Faure, H. Loiseleur, *Rev. Chim. Minérale*, 1984, **21**, 601.

107. L. Eriksson, M. Kritikos, *Acta Cryst.*, 1995, **C51**, 1508.

108. A. Michaelides, S. Skoulika, V. Kiritsis, A. Aubry, *J. Chem. Soc. Chem. Commun.*, 1995, 1415.

109. R.G. Griffin, J.D. Ellett, M. Mehring, J.G. Bullitt, J.S. Waugh, *J. Chem. Physics*, 1972, **57**, 2147.

110. T.C.W. Mak, W.H. Yip, C.H.L. Kennard, G. Smith, E.J. O'Reilly, *J. Chem. Soc. Dalton Trans.*, 1988, 2353.

111. D.D. Wu, T.C.W. Mak, *J. Chem. Soc. Dalton Trans.*, 1995, 2671.

112. P.R. Wei, Q. Li, B.M. Wu, T.C.W. Mak, *Polyhedron*, 1997, **16**, 153.

113. F. Jaber, F. Charbonnier, R. Faure , K. Gebicki, *Acta Cryst.*, 1994, **C50**, 1444.

114. F. Charbonnier, R. Faure, M. Petit-Ramel, *Eur. J. Solid State Inorg. Chem.*, 1992, **29**, 93.

115. F. Charbonnier, R. Faure, M. Petit-Ramel, *Z. Kristallogr*, 1994, **209**, 536.

116. G. Smith, A.N. Reddy, K.A. Byriel, C.H.L. Kennard, *J. Chem. Soc. Dalton Trans.*, 1995, 3565.

117. W.H. Chan, T.C.W. Mak, W.H. Yip, C.H.L. Kennard, G. Smith, E.J. O'Reilly, *Aust. J. Chem.*, 1987, **40**, 1161.

118. D.R. Whitcomb, R.D. Rogers, *Inorg. Chim. Acta*, 1997, **256**, 263.

119. F. Jaber, F. Charbonnier, R. Faure, *Eur. J. Solid State Inorg. Chem.*, 1995, **32**, 25.

120. P. Coggon, T. McPhail, *J. Chem. Soc. Chem. Commun.*, 1972, 91.

121. F. Jaber, F. Charbonnier, R. Faure, *Polyhedron*, 1996, **15**, 2909.

122. M.N. Tahir, D. Üklü, E.M. Muvsumov, *Acta Cryst.*, 1996, **C52**, 593.

123. P.R. Wei, D.D. Wu, T.C.W. Mak, *Inorg. Chim. Acta*, 1996, **249**, 169.

124. S. Weng Ng, *Acta Cryst.*, 1998, **C54**, 743.

125. T.S.A. Hor, S.P. Neo, C.S. Tan, T.C.W. Mak, K.W.P. Leung, R.J. Wang, *Inorg. Chem.*, 1992, **31**, 4510.

126. S.P. Noe, Z.Y. Zhou, T.C.W. Mak, T.S.A. Hor, *Inorg. Chem.*, 1995, **34**, 520.

127. E.T. Blues, M.G.B. Drew, B. Femi-Onadeko, *Acta Cryst.*, 1977, **B33**, 3965.

128. G.A. Bowmaker, Effendy, J.V. Hanna, P.C. Healy, G.J. Millar, B.W. Skelton, A.H. White, *J. Phys. Chem.*, 1995, **99**, 3909.

129. S. Weng Ng, A.H. Othman, *Acta Cryst.*, 1997, **C53**, 1396.
130. D.R. Whitcomb, R.D. Rogers, *Polyhedron*, 1997, **16**, 863.
131. A.F.M.J.van der Ploeg, G. van Koten, A.L. Spek, *Inorg. Chem.*, 1979, **18**, 1052.
132. G. Ferguson, R. McCrindle, M. Parvez, *Acta Cryst.*, 1984, **C40**, 354.
133. P. Schulte, U. Behrens, *J. Organometal. Chem.*, 1998, **563**, 235.
134. J. Powell, M.J. Horvath, A. Lough, A. Phillips, J. Brunet, *J. Chem. Soc. Dalton Trans.*, 1998, 637.
135. J. Powell, M.J. Horvath, A. Lough, *J. Organometal. Chem.*, 1993, **456**, C27.
136. S.K. Adams, D.A. Edwards, R. Richards, *Inorg. Chim. Acta*, 1975, **12**, 163.
137. G.B. Deacon, R.J. Phillips, *Coord. Chem. Rev.*, 1980, **33**, 227.
138. B. Milani, E. Alessio, G. Mestroni, A. Sommazzi, F. Garbassi, E. Zangrando, N. Bresciani-Pahor, L. Randaccio, *J. Chem. Soc. Dalton Trans.*, 1994, 1903.
139. X.M. Chen, Z.T. Xu, T.C.W. Mak, *Polyhedron*, 1994, **13**, 3329.
140. D.A. Edwards, R.N. Hayward, *Can. J. Chem.*, 1968, **46**, 3443.
141. B.J. Edmondson, A.B.P. Lever, *Inorg. Chem.*, 1965, **4**, 1608.
142. P.F. Barron, J.C. Dyason, P.C. Healy, L.M. Engelhardt, B.W. Skelton, A.H. White, *J. Chem. Soc. Dalton Trans.*, 1986, 1965.
143. C.W. Liu, H. Pan, J.P. Fackler, G. Wu, R.E. Wasylishen, M. Shang, *J. Chem. Soc. Dalton Trans.*, 1995, 3691.
144. J.M. Miller, *Adv. Inorg. Chem. Radiochem.*, 1984, **28**, 1.
145. S.A. Martin, C.E. Costello, K. Blemann, *Anal. Chem.*, 1982, **54**, 2362.
146. C. Fenselau, R.J. Cotter, *Chem. Rev.*, 1987, **87**, 501.
147. 'Mass Spectrometry of Organic Compounds' Eds. H. Budzikiewicz, C. Djerassi, D.H. Williams, pub. Holden-Day, inc, 1967.
148. G.D. Roberts, E.V. White, *Org. Mass Spectr.*, 1981, **16**, 546.
149. L.D. Detter, R.G. Cooks, R.A. Walton, *Inorg. Chim. Acta*, 1986, **115**, 55.
150. M.I. Bruce, M.J. Liddell, *J. Organometal. Chem.*, 1992, **427**, 263.
151. A.J. Canty, R. Colton, *Inorg. Chim. Acta*, 1994, **220**, 99.
152. W. Clegg, J.T. Cressey, D.R. Harbron, B.P. Straughan, *J. Chem. Crystallogr.*, 1994, **24**, 211.
153. P. Starynowicz, *Acta Cryst.*, 1993, **C49**, 1621.
154. T. Nakamoto, M. Katada, S. Kawata, S. Kitagawa, K. Kikuchi, I. Ikemoto, K. Endo, H. Sano, *Chem. Letters*, 1993, 1463.
155. M.L. Post, J. Trotter, *J. Chem. Soc. Dalton Trans.*, 1974, 285.

156. D.J. Darensbourg, E.M. Longridge, M.W. Holtcamp, K.K. Klausmeyer, J.H. Reibenspies, *J. Am. Chem. Soc.*, 1993, **115**, 8839.

157. D.J. Darensbourg, E.M. Longridge, E.V. Atnip, J.H. Reibenspies, *Inorg. Chem.*, 1991, **30**, 357.

158. M.G.B. Drew, A.H. Othman, D.A. Edwards, R. Richards, *Acta Cryst.*, 1975, **B31**, 2695.

159. M.T. Ashby, M.A. Khan, J. Halpern, *Organometallics*, 1991, **10**, 2011.

160. I. Łakomska, A. Grodzicki, E. Szłyk, *Thermochim. Acta*, 1997, **303**, 41.

161. 'Transport Phenomena in CVD Reactors' ed. C. Keijn, 1991.

162. Personal Communication from Dr D. Sheel, Pilkington Plc.

163. J.R. Creighton, J.E. Parmeter, *Critical Reviews in Solid State and Materials Science*, 1993, **18**, 175.

164. 'Metal Alkoxides', D.C. Bradley, R.C. Mehrotra, D.P. Gaur, pub. Academic Press, London, 1978.

165. D.C. Bradley, *Chem. Rev.*, 1989, **89**, 1317.

166. J.E. Stanley, PhD thesis, University of Bath, 1997.

167. P.M. Jeffries, G.S. Girolami, *Chem. Mater.*, 1989, **1**, 8.

168. P.M. Jeffries, L.H. Dubois, G.S. Girolami, *Chem. Mater.*, 1992, **4**, 1169.

169. M.J. Hampden-Smith, T.T. Kodas, M.F. Paffett, J.D. Farr, H.K. Shin, *Chem. Mater.*, 1990, **2**, 636.

170. R.C. Mehrotra, A. Singh, *Progr. Inorg. Chem.*, 1997, **46**, 239.

171. H.E. Bryndza, W. Tam, *Chem. Rev.*, 1988, **88**, 1163.

172. W.A. Hermann, N.W. Huber, O. Runte, *Angew. Chem. Int. Ed. Engl.* 1995, **34**, 2187.

173. R.S. Macomber, J.C. Ford, J.H. Wenzel, *Syn. React. Inorg. Metal-Org. Chem.*, 1977, **7**, 111.

174. G. Smith, E.J. O'Reilly, B.J. Reynolds, C.H.L. Kennard, T.C.W. Mak, *J. Organometal. Chem.*, 1987, **331**, 275.

175. G. Wulfsberg, D. Jackson, W. Ilsley, S. Dou, A. Weiss, J. Gagliardi, *Z. Naturforsch., Teil A*, 1992, **47**, 75.

176. N. Galesić, M. Herceg, D. Sevdić, *Acta Cryst.*, 1988, **C44**, 1405.

177. A.H. Othman, S.C. Goh, H.K. Fun, K. Sivakumar, *Acta Cryst.*, 1996, **C52**, 2760.

178. D. Sevdević, L. Fekete, L. Meider, *J. Inorg. Nucl. Chem.*, 1980, **42**, 885.

179. T. Tsuda, T. Hashimoto, T. Saegusa, *J. Am. Chem. Soc.*, 1972, **94**, 658.

180. A.P. Purdy, C.F. George, J.H. Callahan, *Inorg. Chem.*, 1991, **30**, 2812.

181. S.P. Abraham, N. Narasimhamurthy, M. Nethaji, A.G. Samuelson, *Inorg. Chem.*, 1993, **32**, 1739.

182. D.A. Atwood, A.H. Cowley, R.D. Schluter, M.R. Bond, C.J. Carrano, *Inorg. Chem.*, 1995, **34**, 2186.

183. M. Kubota, A. Yamamoto, *Bull. Chem. Soc. Japan*, 1978, **51**, 2909.

184. M.R. Colsman, T.D. Newbound, L.J. Marschall, M.D. Noirot, M.M. Miller, G.P. Wulfsberg, J.S. Frye, O.P. Anderson, S.H. Strauss, *J. Am. Chem. Soc.*, 1990, **112**, 2349.

185. 'Organic Chemistry', R.T. Morrison, R.N. Boyd, 6th Edition, pub. Prentice Hall International Inc, 1992.

186. T. Sone, M. Iwata, N. Kasuga, S. Komiya, *Chem. Letters*, 1991, 1949.

187. 'Spectroscopic Methods in Organic Chemistry', D.H. Williams, I. Fleming, 4th Edition, pub. McGraw-Hill Book Company (UK) Limited, 1987.

188. M. Camilli, F. Caruso, *Inorg. Chim. Acta*, 1987, **127**, 209.

189. L.M. Engelhardt, P.C. Healy, V.A. Patrick, A.H. White, *Aust. J. Chem.*, 1987, **40**, 1873.

190. S.E. Kegley, C.J. Schaverien, J.H. Freudenberger, R.G. Bergman, *J. Am. Chem. Soc.*, 1987, **109**, 6563.

191. S.H. Strauss, K.D. Abney, O.P. Anderson, *Inorg. Chem.* 1986, **25**, 2806.

192. M.D. Janssen, D.M. Grove, G. van Koten, *Progr. Inorg. Chem.*, 1997, **46**, 97.

193. A.M. Mannoti Lanfredi, F. Ugozzoli, A. Camus, N. Marsich, *J. Chem. Cryst.*, 1995, **25**, 37.

194. G. Shang, K. Klunze, M.J. Hampden-Smith, E.N. Duesler, *Chem. Vap. Deposition*, 1996, **2**, 242.

195. S.W. Maggata, M.A. Malik, M. Motevalli, P. O'Brien, J.C. Knowles, *Chem. Mater.*, 1995, **7**, 716.

196. K. Kunze, L. Birhy, P. Atanosova, M.J. Hampden-Smith, E.N. Duesler, *Chem. Vap. Deposition*, 1996, **2**, 105.

197. D. Coucouvanis, *Progr. Inorg. Chem.*, 1970, **11** 233.

198. H. Yamagchi, A. Kido, T. Vechi, K. Yasukouchi, *Bull. Chem. Soc. Japan*, 1976, **49**, 1271.

199. K. Tang, M. Aslam, E. Block, T. Nicholson, J. Zubieta, *Inorg. Chem.*, 1987, **26**, 1488.

200. E. Block, M. Gernon, H. Kang, G. Ofori-Okai, J. Zubieta, *Inorg. Chem.*, 1989, **28**, 1263.

201. W. Wojnowski, M. Wojnowski, K. Peters, E.M. Peters, H.G. von Schnering, *Z. Anorg. Allg. Chem.*, 1985, **530**, 79.

202. L.S. Ahmed, J.R. Dilworth, J.R. Miller, N. Whealtley, *Inorg. Chim. Acta*, 1998, **278**, 229.

203. I. Casals, P. Gonzalez-Duarte, J. Sola, J. Vives, M. Font-Bardia, X. Solans, *Polyhedron*, 1990, **9**, 769.

204. I.G. Dance, *Polyhedron*, 1986, **5**, 1037.

205. I.G. Dance, *Aust. J. Chem.*, 1978, **31**, 2195.

206. E. Block, D. Macherone, S.N. Shaikh, J. Zubieta, *Polyhedron*, 1990, **9**, 1429.

207. I.G. Dance, L.J. Fitzpatrick, M.L. Scudder, *Inorg. Chem.*, 1984, **23**, 2276.

208. I.G. Dance, *Inorg. Chem.*, 1981, **20**, 1487.

209. I.G. Dance, L.J. Fitzpatrick, D.C. Craig, M.L. Scudder, *Inorg. Chem.*, 1989, **28**, 1853.

210. I.G. Dance, L. Fitzpatrick, M. Scudder, D Craig, *J. Chem. Soc. Chem. Commun.*, 1984, 17.

211. I.G. Dance, *Inorg. Chim. Acta*, 1977, **25**, L17.

212. H. Nöth, W. Beck, K. Burger, *Eur. J. Inorg. Chem.*, 1998, 93.

213. P. Gonzalez-Duarte, J. Sola, J. Vives, X. Solans, *J. Chem. Soc. Chem Commun.*, 1987, 1641.

214. S.H. Hong, Å. Olin, R. Hesse, *Acta Chem. Scand.*, 1975, **A29**, 583.

215. I.G. Dance, L.J. Fitzpatrick, A.D. Rae, M.L. Scudder, *Inorg., Chem.*, 1983, **22**, 3785.

216. K. Tang, J. Yang, Q. Yang, Y. Tang, *J. Chem. Soc. Dalton Trans.*, 1989, 2297.

217. H.G. Fijolek, J.R. Grohal, J.L. Sample, M.J. Natan, *Inorg. Chem.*, 1997, **36**, 622.

218. H.G. Fijolek, P. Gonzalez-Duarte, S.H. Park, S.L. Suik, M.J. Natan, *Inorg. Chem.*, 1997, **36**, 5299.

219. I.G. Dance, K.J. Fischer, R.M.H. Banda, M.L. Scudder, *Inorg. Chem.*, 1991, **30**, 183.

220. W. Su, R. Cao, M. Hong, J. Chen, J. Lu, *J. Chem. Soc. Chem. Commun.*, 1998, 1389.

221. P. Jennische, R. Hesse, *Acta Chem. Scand.*, 1971, **25**, 423.

222. L. Golič, N. Bulc, W. Dietzsch, *Polyhedron*, 1983, **2**, 1201.

223. P. Strauch, W. Dietzsch, L. Golič, J. Sieler, A. Franke, I. Münzberg, K. Trübenbach, R. Kirmse, J. Reinhold, E. Hoyer, *Inorg. Chem.*, 1995, **34**, 763.
224. J.A. Schuerman, F.R. Fronczek, J. Selbin, *Inorg. Chim. Acta*, 1989, **160**, 43.
225. P.J.M.W.L. Birker, G.C. Verschoor, *J. Chem. Soc. Chem. Commun.*, 1981, 322.
226. H. Dietrich, W. Storck, G. Manecke, *J. Chem. Soc. Chem. Commun.*, 1982, 1036.
227. A.M. Mannotti Lanfredi, F. Ugozzoli, F. Asaro, G. Pollizer, N. Marsich, A. Camus, *Inorg. Chim. Acta*, 1991, **190**, 71.
228. R. Hesse, L. Nilson, *Acta Chem. Scand.*, 1969, **23**, 825.
229. O. Crespo, M.C. Gimeno, P.G. Jones, A. Laguna, C. Sarroca, *J. Chem. Soc. Chem. Comm.*, 1998, 1481.
230. A.H. Athman, H.K. Fun, K. Sivakumar, *Acta Cryst.*, 1996, **C52**, 843.
231. H. Otto, H. Werner, *Chem. Ber.*, 1987, **120**, 97.
232. R.W. Bost, O.L Shealy, *J. Am. Chem. Soc.*, 1951, **73**, 24.
233. R.W. Bost, W.J. Mattox, *J. Am. Chem. Soc.*, 1930, **52**, 332.
234. P. Singh, S. Bhattacharya, V.D. Gupta, H. Nöth, *Chem. Ber.*, 1996, **129**, 1093.
235. S. Kato, Y. Kawahara, H. Kageyama, R. Yamada, O. Niyomura, T. Murai, T. Kanda, *J. Am. Chem. Soc.*, 1996, **118**, 1262.
236. H.A. Jenkins, S.J. Loeb, A. Malats i Riera, *Inorg. Chim. Acta*, 1996, **246**, 207.
237. I.G. Dance, M.L. Scudder, L.J. Fitzpatrick, *Inorg. Chem.*, 1985, **24**, 2547.
238. M.D. Nyman, M.J. Hampden-Smith, E.N. Duesler, *Inorg. Chem.*, 1997, **36**, 2218.
239. N.Kuhn, H. Schumann, *J. Organometal. Chem.*, 1986, **315**, 93.
240. N. Walker, D. Stewart, *Acta Cryst.*, 1983, **A39**, 158.
241. P. McArdle, *J. Appl. Phys.*, 1994, **27**, 438.

LIST OF COMPOUNDS

[$Ag(O_2CCH_2CN)$] (**1**)

[$Ag(O_2CCH_2CN)(PPh_3)_2$] (**2**)

[$Ag(O_2CCH{=}CH_2)$] (**3**)

[$Ag(O_2CCH{=}CH_2)(PPh_3)_2$] (**4**)

[$Ag\{O_2C(CH_2)_2CH{=}CH_2\}$] (**5**)

[$Ag\{O_2C(CH_2)_2CH{=}CH_2\}(PPh_3)_2$] (**6**)

[$Ag\{O_2C(CH_2)_2CH{=}CH_2\}(PhSC_2H_4SPh)_2$] (**7**)

[$Ag\{O_2C(CH_3)C{=}CHCH_3\}$] (**8**)

[$Ag\{O_2C(CH_3)C{=}CHCH_3\}(PPh_3)_2$] (**9**)

[$Ag\{O_2C(CH_3)C{=}CHCH_3\}(PhSC_2H_4SPh)_2$] (**10**)

[$Ag(O_2CCH{=}CHPh)$] (**11**)

[$Ag(O_2CCH{=}CHPh)(PPh_3)_2$] (**12**)

[$Ag(OC_6H_2Cl_3\text{-}2,4,6)(PPh_3)_2$] (**13**)

[$Ag(OC_6H_5)(PPh_3)_3]\cdot C_6H_5OH$ (**14**)

[$Ag\{OC_6H_2(CH_2NMe_2)_3\text{-}2,4,6\}(PPh_3)_2$] (**15**)

[$Ag(OC_6H_4Me\text{-}2)(PPh_3)_2$] (**16**)

[$Ag(OC_6H_4Me\text{-}2)(PPh_3)_3]\cdot(HOC_6H_4Me\text{-}2)\cdot C_6H_5CH_3$ (**17**)

[$Ag(OCMe_3)(PPh_3)_3$] (**18**)

[$Ag(SCH_2CH_2CH_3)$] (**19**)

[$Ag\{S(CH_2)_{11}CH_3\}$] (**20**)

[$Ag(SOCCH_3)(PPh_3)]_4\cdot 2CH_2Cl_2$ (**22**)

[$Ag(SOCCH_3)(PPh_3)_2$] (**23**)

[$Ag(SOCPh)$] (**24**)

[$Ag(SOCPh)(PPh_3)_2$] (**25**)

[$Ag(S_2CNEt_2)(PPh_3)_2$] (**26**)